JAERI-M
8560

VERIFICATION STUDY OF LOCA ANALYSIS CODE THYDE-P

(Sample Calculation Run 10)

November 1979

Yoshiro ASAHI and Masashi HIRANO

日本原子力研究所
Japan Atomic Energy Research Institute

この報告書は，日本原子力研究所がJAERI-Mレポートとして，不定期に刊行している研究報告書です．入手，複製などのお問合わせは，日本原子力研究所技術情報部（茨城県那珂郡東海村）あて，お申しこしください．

JAERI-M reports, issued irregularly, describe the results of research works carried out in JAERI. Inquiries about the availability of reports and their reproduction should be addressed to Division of Technical Information, Japan Atomic Energy Research Institute, Tokai-mura, Naka-gun, Ibaraki-ken, Japan.

JAERI-M 8560

Verification Study of LOCA Analysis Code THYDE-P (Sample Calculation Run 10)

Yoshiro ASAHI and Masashi HIRANO

Division of Reactor Safety Evaluation,
Tokai Research Establishment, JAERI

(Received October 22, 1979)

THYDE-P is a code to analyze loss-of-coolant accidents (LOCA) of the pressurized water reactor (PWR). In this report, the blowdown portion of THYDE-P sample calculation Run 10 is presented along with THYDE-P inputs requirements. Run 10 forms a portion of a series of THYDE-P sample salculations to be performed by the evaluation model option on a specified plant design and is characterized by a simple nodalization such as a single active core node and discharge coefficient 0.6.

Keywords: LOCA, PWR, THYDE-P Code, Code Verification, Sample Calculation.

JAERI－M 8560

冷却材喪失事故解析用コード THYDE－P の検証
（ サンプル計算 Run 10）

日本原子力研究所東海研究所安全解析部
朝 日 義 郎・平 野 雅 司

（1979 年 10 月 22 日受理）

THYDE－P は加圧水圧原子炉の冷却材喪失事故を解析するコードである。本報告書には，THYDE－P インプット法と伴に，THYDE－P サンプル計算 Run 10 のブローダウン部分が載せてある。Run 10 は，ある特定のプラントに関しての評価モデルによる一連の THYDE－P サンプル計算の一部をなす。Run 10 は，単一熱源炉心ノードのような単純なノーディングと，放出系数 0.6 とによって特徴づけられる。

TABLE OF CONTENTS

目　　次

List of Figures

1. Introduction

THYDE-P[1] is a computer code to analyze the transient thermal-hydraulic responses of a PWR plant to a postulated LOCA (loss-of-coolant accident). The present status of THYDE-P may be considered to be at the stage of verification so that what is needed at present for the THYDE-P development may be to conduct a systematic study by sample calulations. Thus far, three series (10, 20 and 30) have been started for sample calculations by THYDE-P. This document presents the sample calculation Run 10 which is the first of the series 10.

These calculations are hoped to become the bases for the future safety calculations by the THYDE-P code. It is expected, however, that in order to meet the objective, at least several runs are needed for each of the series, until the true base cases will be established. They will be performed by the EM (evaluation model) option on a specified plant design, a typical 4-loop PWR. The inputs and assumptions for these sample calculations are almost identical with those of the "base case" calculation[2] of WREM[3] scrutinized by Reactor Safety Evaluation Laboratory, JAERI or those of sample problem 5 in RELAP 4 (mod 5) tape acquired through NEA CPL. Series 10 are characterized by a simple nodalization such as a single active core node and discharge coefficient 0.6.

In section 2, a brief description of the specified PWR plant is given for which the sample calculations will be conducted. In section 3, the THYDE-P representation of the PWR plant is presented along with Run 10 nodalization. In section 4, remarks are made on the steady state adjustment of the primary loop pressure distribution. In section 5, the time step width control of Run 10 is described. In section 6, some of the modifications implemented after publication of Ref.(1) are explained. In section 7, the calculated results of Run 10 are presented in order. In section 8, code modifications yet to be made, which have been found necessary in the course of this work or after publication of Ref.(1) are described (as of Oct.15, 1979, items (1), (2) and (7) cited in section 8 have been resolved.).

2. PWR Description

A typical 4-loop, 1,100 MWe PWR was selected for the THYDE-P sample calculations.

The reactor is a vertical cylinder 12 feet high (active fuel length) and approximately 12 feet in diameter. The core is made up of 193 fuel assemblies. Each fuel assembly contains a 15 × 15 array of rods. A fuel rod consists of UO_2 fuel pellets clad with zircaloy-4 tubing.

Light water coolant (and moderator) flows up through the core to the upper plenum of the reactor vessel and into the four coolant loops. Each coolant loop consists of a heat exchanger, a pump, and the connecting piping. The heat exchangers are an inverted U-tube design with steam generation on the shell side of the tubes. Primary coolant flows from the upper plenum of the reactor vessel to the inlet plenum of the heat exchanger. The inlet plenum water flows into the heat exchanger tubing and back to the outlet plenum of the heat exchanger. The water then goes to the centrifugal pump and back to the annulus of the reactor vessel. The water flows down the annulus to the lower plenum of the reactor vessel and then flows up through the core.

3. THYDE-P Plant Representation

The Run 10 nodalization of the 4-loop PWR system is shown in Fig.3.1, where numbering of nodes and junctions are made according to the rules given in section A.1 of Appendix A. Run 10 is characterized by a simple nodalization such as a single active core node. The main inputs and assumptions for Run 10 are presented below. In the next section, we give a brief remark on the steady state adjustment of the primary loop pressure distribution. The complete list of the input data is given in Appendix B.

(1) The double-ended break was assumed to occur at junction 8. And the pressure at the break was assumed to drop exponentially with time constant 0.4 sec.

(2) In the steady state adjustment, THYDE-P requires G and h at one point of the primary coolant network. They were selected to be;

$$G = 9.0 \times 10^3 \ kg/m^2sec$$

2. PWR Description

A typical 4-loop, 1,100 MWe PWR was selected for the THYDE-P sample calculations.

The reactor is a vertical cylinder 12 feet high (active fuel length) and approximately 12 feet in diameter. The core is made up of 193 fuel assemblies. Each fuel assembly contains a 15 × 15 array of rods. A fuel rod consists of UO_2 fuel pellets clad with zircaloy-4 tubing.

Light water coolant (and moderator) flows up through the core to the upper plenum of the reactor vessel and into the four coolant loops. Each coolant loop consists of a heat exchanger, a pump, and the connecting piping. The heat exchangers are an inverted U-tube design with steam generation on the shell side of the tubes. Primary coolant flows from the upper plenum of the reactor vessel to the inlet plenum of the heat exchanger. The inlet plenum water flows into the heat exchanger tubing and back to the outlet plenum of the heat exchanger. The water then goes to the centrifugal pump and back to the annulus of the reactor vessel. The water flows down the annulus to the lower plenum of the reactor vessel and then flows up through the core.

3. THYDE-P Plant Representation

The Run 10 nodalization of the 4-loop PWR system is shown in Fig.3.1, where numbering of nodes and junctions are made according to the rules given in section A.1 of Appendix A. Run 10 is characterized by a simple nodalization such as a single active core node. The main inputs and assumptions for Run 10 are presented below. In the next section, we give a brief remark on the steady state adjustment of the primary loop pressure distribution. The complete list of the input data is given in Appendix B.

(1) The double-ended break was assumed to occur at junction 8. And the pressure at the break was assumed to drop exponentially with time constant 0.4 sec.

(2) In the steady state adjustment, THYDE-P requires G and h at one point of the primary coolant network. They were selected to be;

$$G = 9.0 \times 10^3 \ kg/m^2sec$$

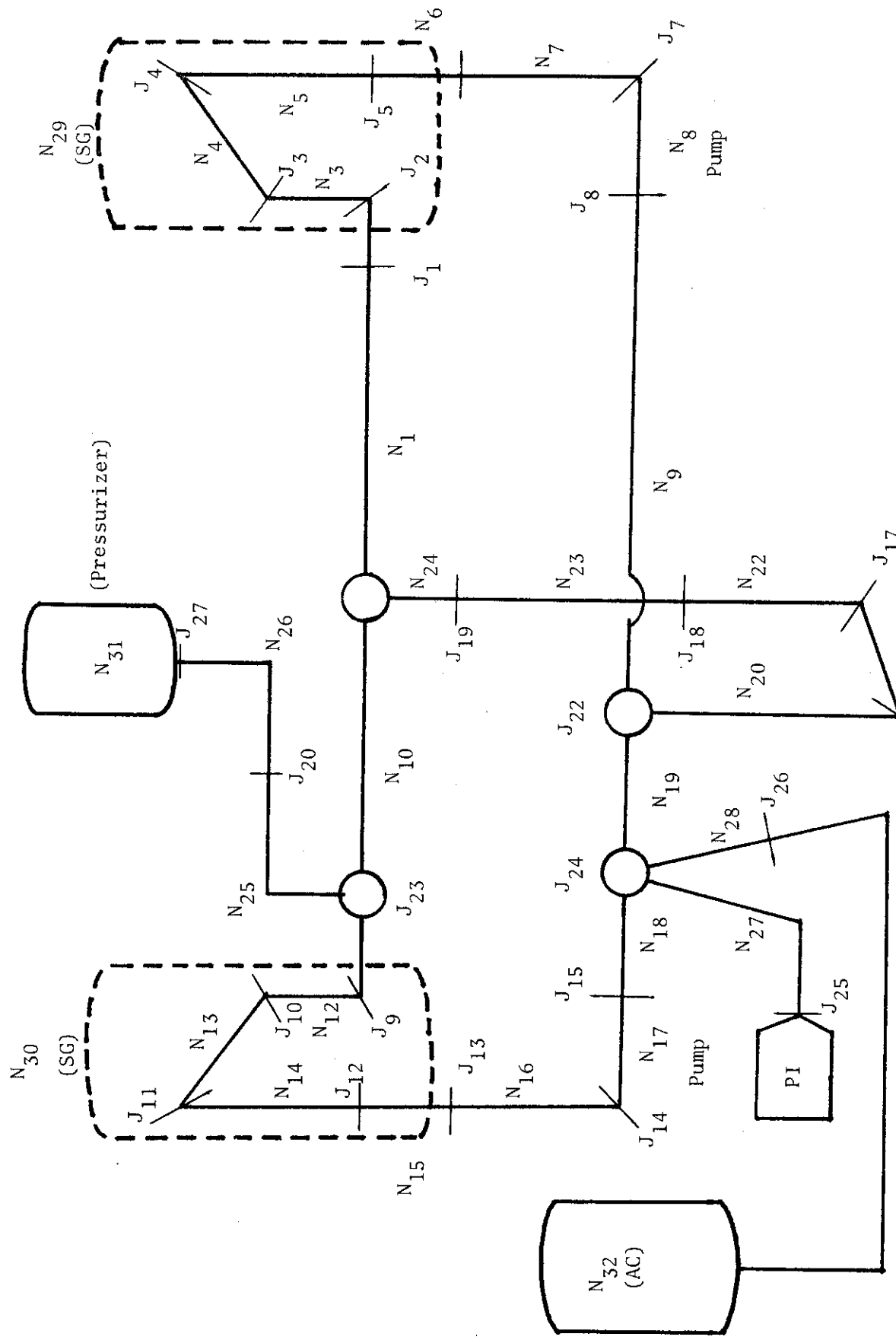

Fig.3-1 Run 10 Nodalization

and

$$h = 360 \text{ kcal/kg}$$

at point A of normal node 1.

(3) SG (Steam generator);

secondary system pressure	45 ata
shut-off time of feedwater and steam flows	0.4 sec
specific enthalpy of feedwater	140 kcal/kg
set point of relief valve	80 ata
U-tube outer radius	0.0111 m
U-tube pitch	0.030 m
number of U-tubes of one unit	4,000
subcooled water level	4 m

initial heat flux (relative value)

node	ϕ(-)
3	60
4	65
5	70
12	60
13	65
14	70

(4) Core;

reactor thermal power	3,479 MWt

initial heat flux

node	ϕ(kcal/m^2/sec)
22	0.0
23	208.0
24	0.0

number of fuel rods	40,000
active fuel length	3.66 m
plenum gas volume	1.229×10^{-5} m^3
clad outer radius	5.36×10^{-3} m
clad thickness	6.20×10^{-3} m
pellet radius	4.62×10^{-2} m
fuel rod pitch	1.42×10^{-2} m

(The last six values are those at the initial operating condition.)

(5) Pressurizer;

cross-sectional area	3.58 m^2
height	15.56 m
initial water level	9.0 m

(6) Accumulator;

initial water volume	70 m^3
initial nitrogen volume	30 m^3
specific enthalpy of water	50.9 kcal/kg
initial pressure	40.0 ata

(7) Pumped injection;

specific enthalpy of water	50.0 kcal/kg
mass flow rate	600 kg/sec

(8) No structural heat source or sink was assumed.

(9) No particular model for the container was provided except the temporal behavior of the container pressure which was an input function of time, i.e.,

time (sec)	0.0	7.5	15.0	1000.0
press. (ata)	1.0	2.7	3.0	3.0

(10) The rotor of the centrifugal pump was assumed to be locked at time = 0.1 sec.

(11) The discharge coefficient was selected to be 0.6.

(12) The loss coefficients for the linkage nodes are;

$$k_{25} = k_{26} = 1.0$$

$$k_{27} = k_{28} = 10.0$$

4. Steady State Adjustment of Primary Loop Pressure Distribution

THYDE-P is capable of setting up the steady state not only of the primary loop, but also of all the other plant elements such that it is the exact solution of the equations governing the transients. These steady state adjustments are straightforward, except for the primary loop pressure distribution.

The steady state adjustment of the primary loop pressure distribution may need a good deal of experience, since if the input pressure distribution is not proper, some of the resulting loss coefficients may turn out to be either negative or unrealistically large. In the following, we will give a

(5) Pressurizer;

cross-sectional area	3.58 m^2
height	15.56 m
initial water level	9.0 m

(6) Accumulator;

initial water volume	70 m^3
initial nitrogen volume	30 m^3
specific enthalpy of water	50.9 kcal/kg
initial pressure	40.0 ata

(7) Pumped injection;

specific enthalpy of water	50.0 kcal/kg
mass flow rate	600 kg/sec

(8) No structural heat source or sink was assumed.

(9) No particular model for the container was provided except the temporal behavior of the container pressure which was an input function of time, i.e.,

time (sec)	0.0	7.5	15.0	1000.0
press. (ata)	1.0	2.7	3.0	3.0

(10) The rotor of the centrifugal pump was assumed to be locked at time = 0.1 sec.

(11) The discharge coefficient was selected to be 0.6.

(12) The loss coefficients for the linkage nodes are;

$$k_{25} = k_{26} = 1.0$$

$$k_{27} = k_{28} = 10.0$$

4. Steady State Adjustment of Primary Loop Pressure Distribution

THYDE-P is capable of setting up the steady state not only of the primary loop, but also of all the other plant elements such that it is the exact solution of the equations governing the transients. These steady state adjustments are straightforward, except for the primary loop pressure distribution.

The steady state adjustment of the primary loop pressure distribution may need a good deal of experience, since if the input pressure distribution is not proper, some of the resulting loss coefficients may turn out to be either negative or unrealistically large. In the following, we will give a

recipe for steady state adjustment of primary loop pressure distribution.

We will have to put the THYDE-P code on a computer for a short computer time at least several times by changing the primary loop pressure distribution until we obtain a set of realistic loss coefficients. In view of the quantities printed out on the output list for each run, we may modify the input pressure distribution so that we can obtain realistic loss coefficients. We note that the steady state pressure distribution has nothing to do with the enthalpy and mass velocity distributions and hence that a small variation in the input pressure distribution only gives rise to a small perturbation in the flow properties other than the loss coefficients.

Suppose that the loss coefficient of node n resulted in an unrealistic value and thus try to obtain a suitable value for it by changing the pressure at point A of the adjacent node n'. To this end, we will obtain a relationship among p_n^A, $p_{n'}^A$, and k_n.

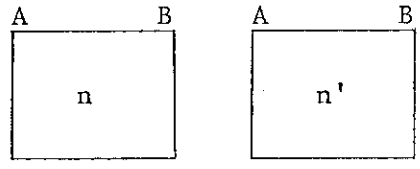

From Eq.(2-1-22) of Ref.(1), we obtain

$$p_n^E - p_{n'}^A = \frac{1}{2}\left(\frac{G_{n'}^{A\,2}}{\rho_{n'}^A} - \frac{G_n^{E\,2}}{\rho_n^E}\right) \tag{1}$$

since a steady state of a PWR is subcooled throughout the primary loop. From Eq.(2-1-16) of Ref.(1), we obtain

$$0 = p_n^A - p_n^E + \frac{G_n^{A\,2}}{\rho_n^A} - \frac{G_n^E}{\rho_n^E} - \frac{1}{2}\left(k_n + \frac{f_n L_n}{D_n}\right)\frac{G_n^2}{\rho_n} + \rho_n g L_{Hn} \tag{2}$$

Eliminating p_n^E from Eqs.(1) and (2), we obtain

$$p_{n'}^A = p_n^A - \zeta_n k_n + \xi_{nn'} \tag{3}$$

where

$$\xi_{nn'} = -\frac{1}{2}\left(\frac{G_{n'}^2}{\rho_{n'}^A} + \frac{G_n^2}{\rho_n^E}\right) + \frac{G_n^2}{\rho_n^A} - \frac{1}{2}\frac{f_n L_n}{D_n}\frac{G_n^2}{\rho_n} + \rho_n g L_{Hn}$$

and

$$\zeta_n = G_n^2 / \rho_n$$

It is assumed that the value obtained for k_n has been found inappropriate which satisfies Eq.(3) with inputs p_n^A, and p_n^A. We note that ζ_n and $\xi_{nn'}$, can be evaluated by the various values printed out on the output list and that they do not change much with p_n^A and p_n^A,. Thus, choosing any desired value for k_n, we can obtain a new candidate for p_n^A, from Eq.(3) with the help of ζ_n and $\xi_{nn'}$, evaluated from the last calculation provided that the resultant p_n^A, is sufficiently close to the original one.

We can repeat this procedure from one node after another, for example, up to a pump node.

5. Time Step Width Control

THYDE-P has an option which allows automatic time step width control. We define a relative increment R of quantity χ in the interval t (old) and $t + \Delta t$ (new) as

$$R = \frac{|\chi^{new} - \chi^{old}|}{\frac{|\chi^{new}| + |\chi^{old}|}{2} + E_3} \qquad (4)$$

where E_3 is an input value. If any R is greater than E_1 (an input value), the time step width will be halved and the calculation is to be done over again. If all R's are less than E_1E_2 (E_2: an input value), then the calculation proceeds to the next time step which will have twice as large a width as the last. It all R's are less than E_1 and, moreover, any R is in between E_1 and E_1E_2, then the calculation proceeds to the next time step with the same width as the last. In Run 10, we sellected E_1, E_2 and E_3 as

$$\begin{pmatrix} E_1 \\ E_2 \\ E_3 \end{pmatrix} = \begin{pmatrix} 0.2 \\ 0.2 \\ 100.0\ \mathrm{kg/m^2/sec} \end{pmatrix} \quad \text{for G} \qquad (5)$$

$$\xi_{nn'} = -\frac{1}{2}\left(\frac{G_{n'}^2}{\rho_{n'}^A} + \frac{G_n^2}{\rho_n^E}\right) + \frac{G_n^2}{\rho_n^A} - \frac{1}{2}\frac{f_n L_n}{D_n}\frac{G_n^2}{\rho_n} + \rho_n g L_{Hn}$$

and

$$\zeta_n = G_n^2 / \rho_n$$

It is assumed that the value obtained for k_n has been found inappropriate which satisfies Eq.(3) with inputs p_n^A, and p_n^A. We note that ζ_n and $\xi_{nn'}$ can be evaluated by the various values printed out on the output list and that they do not change much with p_n^A and $p_{n'}^A$. Thus, choosing any desired value for k_n, we can obtain a new candidate for p_n^A, from Eq.(3) with the help of ζ_n and $\xi_{nn'}$ evaluated from the last calculation provided that the resultant $p_{n'}^A$ is sufficiently close to the original one.

We can repeat this procedure from one node after another, for example, up to a pump node.

5. Time Step Width Control

THYDE-P has an option which allows automatic time step width control. We define a relative increment R of quantity χ in the interval t (old) and $t + \Delta t$ (new) as

$$R = \frac{|\chi^{new} - \chi^{old}|}{\frac{|\chi^{new}| + |\chi^{old}|}{2} + E_3} \qquad (4)$$

where E_3 is an input value. If any R is greater than E_1 (an input value), the time step width will be halved and the calculation is to be done over again. If all R's are less than E_1E_2 (E_2: an input value), then the calculation proceeds to the next time step which will have twice as large a width as the last. It all R's are less than E_1 and, moreover, any R is in between E_1 and E_1E_2, then the calculation proceeds to the next time step with the same width as the last. In Run 10, we sellected E_1, E_2 and E_3 as

$$\begin{pmatrix} E_1 \\ E_2 \\ E_3 \end{pmatrix} = \begin{pmatrix} 0.2 \\ 0.2 \\ 100.0\ \text{kg/m}^2\text{/sec} \end{pmatrix} \quad \text{for G} \qquad (5)$$

and

$$\begin{pmatrix} E_1 \\ E_2 \\ E_3 \end{pmatrix} = \begin{pmatrix} 0.1 \\ 0.2 \\ 0.001 \end{pmatrix} \quad \text{for the others} \tag{6}$$

In the present version of THYDE-P, all the time step control parameters E_1, E_2 and E_3 are set in subroutines TSCHK and TSCHK2, except E_1(EPSMX) for variables other than G and DELTMAX (the maximum allowable time step width) which are specified by input data block BB03. For Run 10, we chose

$$\begin{pmatrix} \text{DELTMX} \\ \text{EPSMX} \end{pmatrix} = \begin{pmatrix} 4 \times 10^{-3} \text{ sec} \\ 0.1 \end{pmatrix} \tag{7}$$

We should note that the time step control parameters (5), (6) and (7) are only tentative and that there should be better choices for them since the computer time critically depends on them.

Finally, we did not apply in Run 10 the time step width control to the linkage nodes.

6. Code Modifications

6.1 Node Equations

The node equations described in section 2.1.3 of Ref.(1) has undergone several modifications which are explained below. The notations are the same as in Ref.(1). The quantities with a bar on top should be interpreted as the average values defined in the following.

As mass and energy equations, we have

$$L \frac{d\bar{\rho}}{dt} = G_A - G_E \tag{8}$$

and

$$L \frac{d\bar{\rho}\bar{h}}{dt} = G_A h_A - G_E h_E + I_A - I_E + Q'''L \tag{9}$$

where

$$I = x\rho_{fs} u_{gj} h_{fg} \quad .$$

and

$$\begin{pmatrix} E_1 \\ E_2 \\ E_3 \end{pmatrix} = \begin{pmatrix} 0.1 \\ 0.2 \\ 0.001 \end{pmatrix} \quad \text{for the others} \tag{6}$$

In the present version of THYDE-P, all the time step control parameters E_1, E_2 and E_3 are set in subroutines TSCHK and TSCHK2, except E_1(EPSMX) for variables other than G and DELTMAX (the maximum allowable time step width) which are specified by input data block BB03. For Run 10, we chose

$$\begin{pmatrix} \text{DELTMX} \\ \text{EPSMX} \end{pmatrix} = \begin{pmatrix} 4 \times 10^{-3} \text{ sec} \\ 0.1 \end{pmatrix} \tag{7}$$

We should note that the time step control parameters (5), (6) and (7) are only tentative and that there should be better choices for them since the computer time critically depends on them.

Finally, we did not apply in Run 10 the time step width control to the linkage nodes.

6. Code Modifications

6.1 Node Equations

The node equations described in section 2.1.3 of Ref.(1) has undergone several modifications which are explained below. The notations are the same as in Ref.(1). The quantities with a bar on top should be interpreted as the average values defined in the following.

As mass and energy equations, we have

$$L \frac{d\bar{\rho}}{dt} = G_A - G_E \tag{8}$$

and

$$L \frac{d\bar{\rho}\bar{h}}{dt} = G_A h_A - G_E h_E + I_A - I_E + Q'''L \tag{9}$$

where

$$I = x\rho_{fs} u_{gj} h_{fg} \quad .$$

Since

$$\frac{d\bar{\rho}}{dt} = \frac{\partial\bar{\rho}}{\partial\bar{h}} \frac{\partial\bar{h}}{dt} + \frac{\partial\bar{\rho}}{\partial p} \frac{d\bar{p}}{dt} \tag{10}$$

we obtain, from Eq.(8) and (9), Eqs.(2-1-14) and (2-1-15) in Ref.(1), i.e.,

$$\dot{\bar{h}} = \frac{1}{\bar{\rho}L} \{G_A h_A - G_E h_E - \bar{h}(G_A - G_E) + I_A - I_E + Q''' L\} \tag{11}$$

and

$$\{1 + a_d(h_A - \bar{h})\}G_A - \{1 + a_d(h_E - \bar{h})\}G_E + b - L \frac{d\bar{\rho}}{dp} \dot{P} = 0 \tag{12}$$

where

$$a_d = - \frac{1}{\bar{\rho}} \frac{d\bar{\rho}}{d\bar{h}}$$

$$b = a_d \ (I_A - I_E + Q''' L)$$

We now define an average $\bar{f}$ of quantity f(p,h) as

$$\bar{f} = f(\bar{p},\bar{h}) \quad . \tag{13}$$

where

$$\bar{p} = (p_A + p_E) \ / \ 2$$

and $\bar{h}$ is the solution of Eq.(11). Eqs.(11) and (12) contain h_A and h_E, which will be expressed in terms of $\bar{h}$ as follows.

In order to ensure smooth change in enthalpy with flow direction change, we introduce parameters η_A and η_E for each node such that

$$\frac{d\eta_i}{dt} = \frac{SS_i - \eta_i}{\tau} \qquad (i = A \text{ or } E) \tag{14}$$

where

$$SS_i = \begin{cases} 1 & G_i < 0 \\ 0 & G_i \geq 0 \end{cases}$$

With the help of η_A and η_E, we define h_A and h_E as

$$h_A^{new} = h_{from}\ (1-\eta_A) + \bar{h}^{new}\ \eta_A \tag{15}$$

and

$$h_E^{new} = \bar{h}^{new}\ (1-\eta_E) + h_{to}\ \eta_E \tag{16}$$

where h_{from} and h_{to} are the enthalpies just outside points A and E of the node in question, respectively, as shown in Table1.

adjacent volume	h_{from}	h_{to}
normal node	$\bar{h}^{new}$ of from-node	$\bar{h}^{new}$ of to-node
mixing junction	h^{+new}	h^{+new}
container (break)	$0.1h_{gs}(Pref)+0.9h_{fs}(Pref)$	$0.1h_{gs}(Pref)+0.9h_{fs}(Pref)$
AC or PZR or PI	(not defined)	enthalpy of AC or PZR or PI

Table 1. h_{from} and h_{to}

For Run 10, we used τ = 15 ms for enthalpy smoothing for flow direction change.

6.2 Smoothing of Heat Transfer Coefficients

One of the characteristics of THYDE-P code is the automatic time step width control which requires, for example, complete steady state adjustment so that the initial state is the exact solution of the equations governing the following transients. It also requires continuity of various parameters such as those appearing in Eqs.(11) and (12), which could have discontinuity with various mode changes. Discontinuity in h_A and h_E with flow direction change, for example, is avoided by introducing the delay parameters η_A and η_E (see section 6.1). Discontinuity in thermodynamic properties which could take place with phase change is circumvented in terms of another kind of delay parameters η in Eq.(A-2) in Ref.(1).

There is still another kind of mode changes, which may introduce large discontinuities leading to numerical instabilities i.e., the mode changes in heat transfer. Since there are so many heat transfer modes involved in LOCA analysis, we introduced another smoothing technique to ensure continuous transition of heat transfer coefficient with the mode change. Thus, we consider

$$\frac{d\, h_{tr}^{eff}}{dt} = \frac{h_{tr}^{c} - h_{tr}^{eff}}{\tau} \qquad (17)$$

where h_{tr}^{c} is the heat transfer coefficient calculated from the correlations. We will make use of the "effective" heat transfer coefficient h_{tr}^{eff} obtained from Eq.(17), in order to evaluate the heat input to the coolant flow. For Run 10, we selected τ = 160 msec for Eq.(17).

7. Calculated Results

7.1 CPU Time

The CPU time depends on various factors, especially on (1) the time step width control parameters and (2) the iteration method for obtaining the solution of the hydraulic network equations. The parameters E_1, E_2, E_3, DELTMX and EPSMX for Run 10 are given by Eqs.(5) to (7), which are only tentatively chosen. Therefore, it is very likely that other sets of values for these parameters could yield shorter CPU times.

We note that the THYDE-P solution technique for the primary loop flow is a nonlinear implicit technique which invariably requires an iterative method. Normally, 5 or 6 iterations are needed to obtain the solution for the primary loop flow. If we relax the criterion for convergence of the iteration, the computer time will of course be reduced. We note that if we adopt a linear implicit technique such as those in RELAP[3] or FLASH[4], we can considerably reduce the computer time, since it is equivalent to performing no iteration for the loop flow.

The CPU time required for Run 10 by a FACOM 230-75 computer was about 7 hours.

7.2 Steady State Adjustment

Fig.7.1 shows the distribution of the average pressure $\bar{p} = (p_A+p_E)/2$ in the primary loop which was obtained following the procedure described in section 4.

$$\frac{d\, h_{tr}^{eff}}{dt} = \frac{h_{tr}^{c} - h_{tr}^{eff}}{\tau} \qquad (17)$$

where h_{tr}^{c} is the heat transfer coefficient calculated from the correlations. We will make use of the "effective" heat transfer coefficient h_{tr}^{eff} obtained from Eq.(17), in order to evaluate the heat input to the coolant flow. For Run 10, we selected τ = 160 msec for Eq.(17).

7. Calculated Results

7.1 CPU Time

The CPU time depends on various factors, especially on (1) the time step width control parameters and (2) the iteration method for obtaining the solution of the hydraulic network equations. The parameters E_1, E_2, E_3, DELTMX and EPSMX for Run 10 are given by Eqs.(5) to (7), which are only tentatively chosen. Therefore, it is very likely that other sets of values for these parameters could yield shorter CPU times.

We note that the THYDE-P solution technique for the primary loop flow is a nonlinear implicit technique which invariably requires an iterative method. Normally, 5 or 6 iterations are needed to obtain the solution for the primary loop flow. If we relax the criterion for convergence of the iteration, the computer time will of course be reduced. We note that if we adopt a linear implicit technique such as those in RELAP[3] or FLASH[4], we can considerably reduce the computer time, since it is equivalent to performing no iteration for the loop flow.

The CPU time required for Run 10 by a FACOM 230-75 computer was about 7 hours.

7.2 Steady State Adjustment

Fig.7.1 shows the distribution of the average pressure $\bar{p} = (p_A + p_E)/2$ in the primary loop which was obtained following the procedure described in section 4.

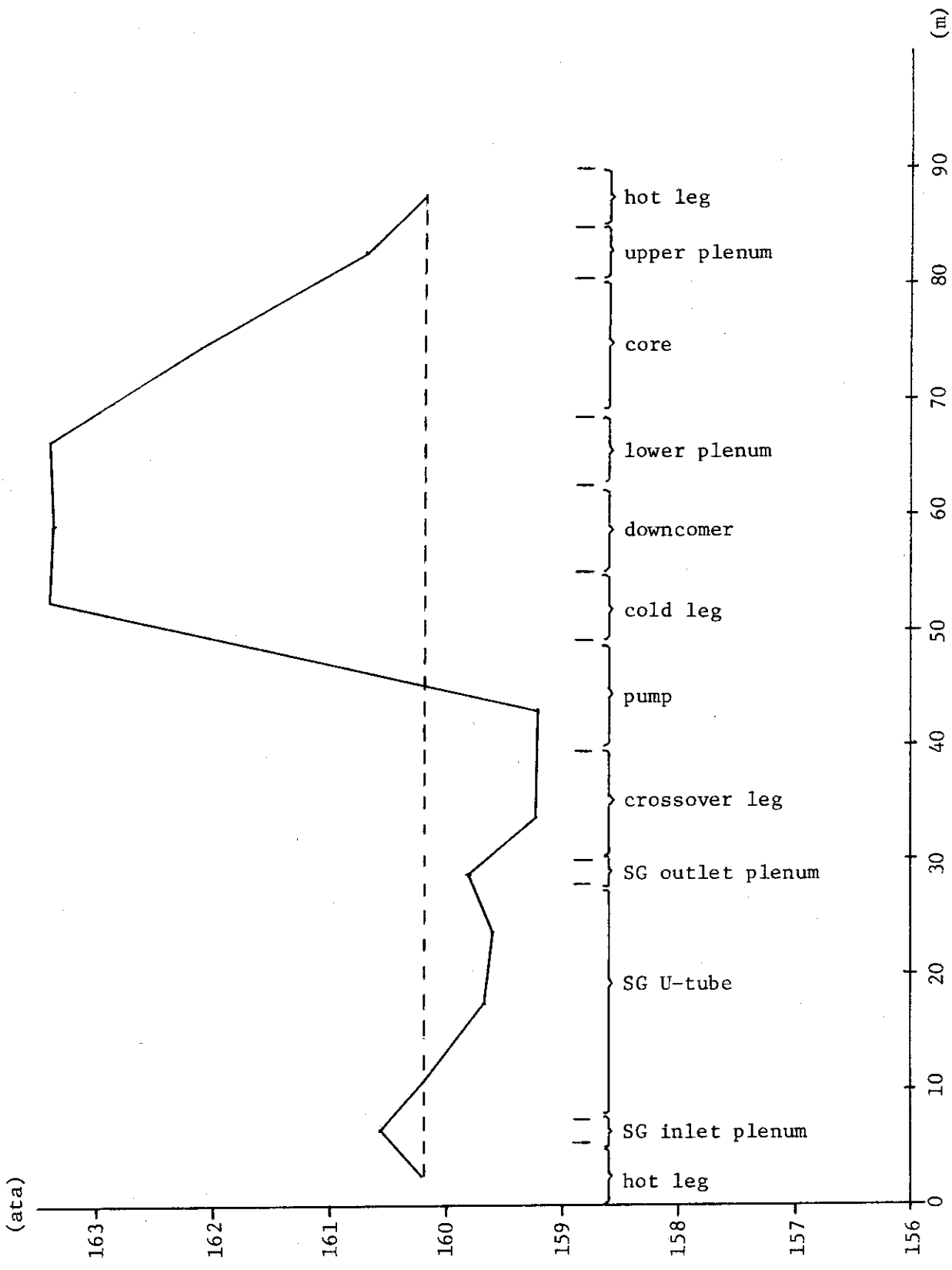

Fig.7-1 Distribution of Steady State Pressure $p = (p^A + p^E)/2$

It was found that the steady state adjustment for the SG secondary system is not adequate. The input value of the SG secondary system pressure for Run 10 is chosen to be 45 ata, for which a solution was found to exist. The actual value of the SG secondary system pressure is about 65 ata, for which, however, the present steady state adjustment failed to obtain a solution for the U-tube wall temperatures. The reason why the present adjustment failed for 65 ata and succeeded for 45 ata has not entirely been clarified. There might be two reasons conceivable for it. One is the fact that the steam table of THYDE-P is so crude in the neighborhood of 65 ata that the bulk temperatures of the secondary coolant become too close to those of the primary coolant. The second possibility is that the numerical technique to obtain the U-tube wall temperatures is not able to cope with some of the heat transfer mode changes during iteration. Finally, we note that at the primary nodes corresponding to the SG subcooled water level there may be a discrepancy between the initially uniformly assumed heat input and the resultant non-uniform heat input to the secondary system. In order to obtain consistency, we will have to resort to an iterative technique. In Run 10, the calculated SG feedwater flow rate is

$$m_{feed} = \frac{Q_{II}}{h_{fs} - h_{feed}} \qquad (18)$$

$$= 982 \quad \text{kg/s}$$

at 45 ata for the input water level 9.0 m. The actual value of m_{feed} is about 470 kg/s, while Eq.(18) for 65 ata gives 899 kg/sec. The actual initial subcooled water level seems to be much lower than 9.0 m.

In order to obtain a realistic value for the initial value of m_{feed}, in addition to giving a realistic value for the initial subcooled water level, we will have to implement an overall iterative technique stated above.

7.3 Plant Transient Behaviors

Division of the primary loop into 5 sections, as shown in Fig.7-2 may help us to classify the various calculated results:

A ; flow path composed of the intact loop SG, hot legs, broken loop SG and broken loop pump

B ; flow path in the intact loop composed of the SG, crossover leg, cold leg down to mixing junction 24

C ; flow path composed of the rest of the intact loop cold leg, downcomer top and broken loop cold leg

D ; flow path composed of the downcomer, lower plenum and core

E ; the ECC ducts and the pressurizer duct

The positive direction of a flow is taken to be that of the initial steady state. State of a node is represented by various quantities at the entrance and exit of the node, designated by A and E, respectively.

7.3.1 Pressures

The asymptotic behaviors of the pressure throughout the primary loop are almost identical except their amplitudes. Figs.7-3 to 7-5 show some of the calculated results for pressures. The rate of depressurization of the system is closely related to the value of the discharge coefficient which is 0.6 in this sample calculation.

7.3.2 Mass fluxes

Figs.7-6 to 7-19 show the calculated results for mass fluxes at various points in the primary loop. The positive direction of a flow coincides with that at the initial steady state. By examining these figures, we can find that the flows in each of paths A, B, C and D have common features so that the figures may be classified into the groups designated by A, B, C, D and E corresponding with the respective flow paths:

A ; Figs.7-6 to 7-9

B ; Figs.7-11 and 7-12

C ; Figs.7-13 and 7-14

D ; Figs. 7-15 and 7-16

E ; Figs.7-17 to 7-19

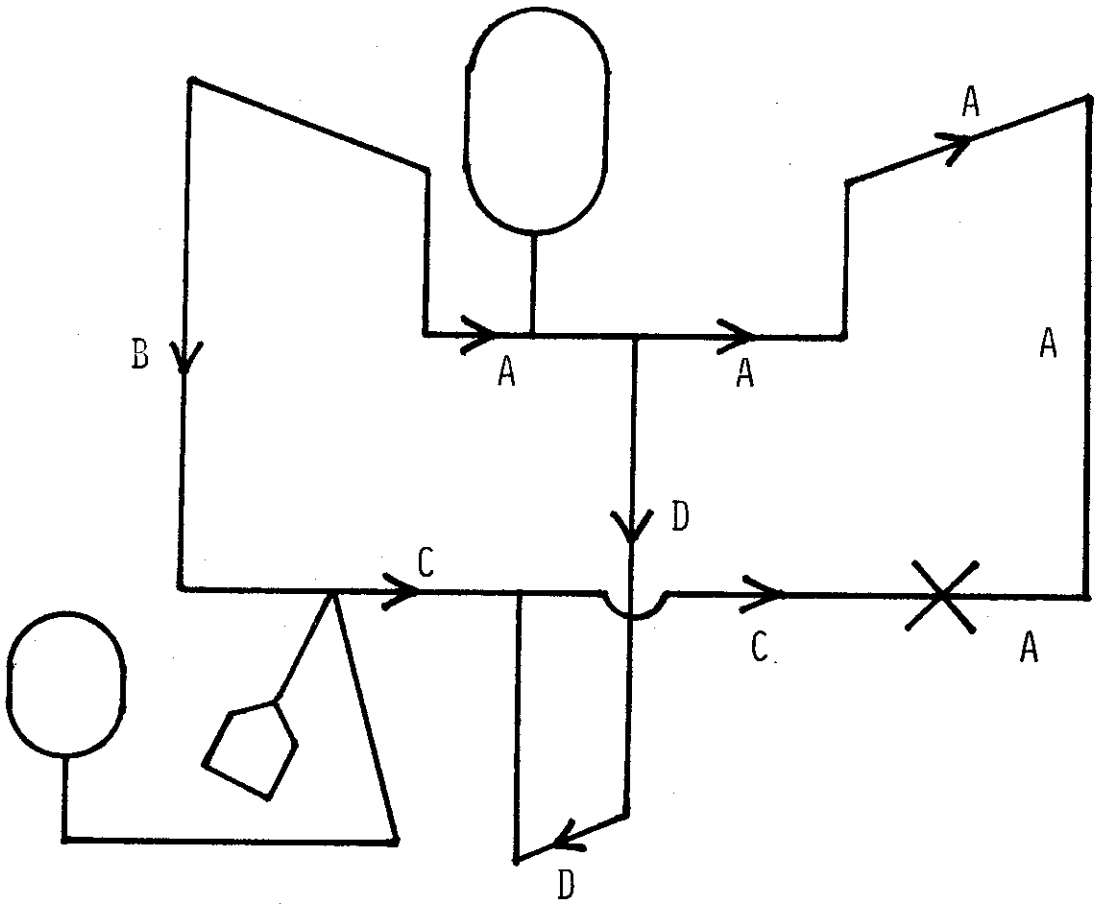

Fig.7-2 Flow Paths

Fig.7-10 shows that G^{E}_{13} first belongs to group B, but later to group A. The asymptotic difference in magnitude between G^{E}_{18} (Fig.7-12) and G^{E}_{19} (Fig.7-13) is due to ECC injections (see Fig.7-18 and 7-19).

The asymptotic flows in paths A, B and C are composed of two main streams, one which starts at the SG of the intact loop, passes through the upper plenum and goes out of the primary loop as the break flow and the other that starts at the SG of the intact loop with the oposite direction, passes through the downcomer top and goes out of the primary loop as the other break flow. The flow resistances for the two streams through A and B plus C may be considered identical.

It is interesting to note that the core flow mostly flowed downward and tended to be stagnant.

Fig.7-17 shows G^{A}_{27} which increased at 28 sec. when the pumped injection was initiated. Figs.7-18 and 7-19 show the flows out of the pressurizer and accumulator, respectively.

7.3.3 Enthalpies

Figs.7-20 to 7-32 show the calculated results for specific enthalpies which also can be divided into the groups associated with paths A, B, C, D and E:

A ; Figs.7-20 to 7-23

B ; Figs.7-24 and 7-25

C ; Figs.7-26 and 7-27

D ; Figs.7-28 and 7-29

E ; Figs.7-30 and 7-32

Looking over Figs.7-20 to 7-25, we can find that the specific enthalpies in paths A and B were almost constant till the flows became superheated steam. It is interesting to note that paths A and B became superheated steam almost at the same time. Specific enthalpies at 9A and 19A shown in Figs.7-27 and 7-26, respectively, started to decrease when the accumulator was actuated at 19.6 sec and decreased more rapidly after the initiation of the pumped injection at 28.0 sec.

Figs.7-28 and 7-29 show the specific enthalpies of the downcomer inlet and the core inlet, respectively. The oscillation till 16.5 sec. correspondes with the flow oscillation in Fig.7-15 or 7-16 which shows that the direction of the flow alternated. Therefore, the specific enthalpies in path D oscillated between the saturated enthalpy of the

downcomer top and the superheated steam enthalpy of the core. Then, as shown in Figs.7-28 and 7-29, after 20A or 23A became superheated steam at 16.5 sec., the enthalpies first decreased and then again increased. This can be explained as follows. The flow in path D remained negative and didn't change its direction after 16.5 sec. (see Figs.7-15 and 7-16) so that the coolant did not have enough time to heat itself up inside the core. Later, however, after 25 sec., the specific enthalpies of the hot legs gradually increased (see Fig.2-21 and 2-22) to become as large as 600 kcal/kg so that heat transferred to the coolant inside the core was large enough to make it superheated steam. The influence of ECC on 20A is seen in Fig.7-28 after 28 sec, but not yet in Fig.29.

7.3.4 Qualities

Figs.7-33 to 7-48 show the calculated results for qualities which also can be classified into the groups associated with paths A, B, C, D and E:

A ; Figs.7-33 to 7-38
B ; Figs.7-39 and 7-40
C ; Figs.7-41 and 7-42
D ; Figs.7-43 to 7-45
E ; Figs.7-46 to 7-48

The quality behaviors are directly related to the behaviors of the specific enthalpies. The figures of qualities, however, clearly show the phase transition during the transients. Path A except the hot legs became superheated steam at about 30 sec, while path B became superheated steam later at about 40 sec. It is interesting to note that the hot legs remained saturated during the blowdown. The effect of ECC is clearly shown in Figs.7-41, 7-42 and 7-43. Figs.7-47 and 7-48 show the qualities of the ECC injection ducts.

7.3.5 Temperatures

As we have seen in 7.3.4, the hot legs did not become superheated steam. This is in agreement with Figs.7-49 and 7-50, in which the temperatures were monotone decreasing. In path B and the rest of path A, the temperatures gradually decreased until coolant became superheated steam. Temperatures in path C also decreased and the temperature of node 19 decreased more rapidly after 29 sec due to ECC water, while the effect

of ECC on the temperature of the cold leg of the broken loop was yet to be seen.

The lower envelope of each of Figures for paths A, B and D is equal to the saturation temperature of the pressure whose asymptotic behavior was observed in 7.3.1 to be identical throughout the system.

Figs.7-58 to 7-62 show the temperatures in path D, whose behaviors should be understood in light of the discussions in 7.3.3 and 7.3.4.

7.3.6 Densities

Figs.7-63 to 7-75 are the densities which can be classified as

A ; Figs.7-63 to 7-66

B ; Figs.7-67 and 7-68

C ; Figs.7-70 and 7-71

D ; Figs.7-72 to 7-75

The crossover legs and the cold legs remained subcooled longer since the initial steady state subcoolings were large. Therefore, the densities of the crossover legs and the cold legs also remained large for a considerably long time. The density at 13E (see Fig.7-69) may be considered as an intermediate of the densities of the hot leg and crossover leg. Figs.7-70 and 7-71 show the densities in path C, which first decreased like the others, but later increased due to ECC water. The effect of ECC water can also be seen in Fig.7-72, which shows the density of the downcomer. Figs.7-74 and 7-75 show that the density at the core inlet (23A) was mostly lower than that at the core outlet (23E), especially in the range of 16.5~30.0 sec. This can be explained in the light of the discussions in 7.3.2 to 7.3.4.

7.3.7 Pressurizer Behavior

Fig.7-76 shows the temporal variation of mass in region 2 (lower region) which decreased rapidly till 13 sec, with depressurization of the primary loop. Fig.7-78 shows the temporal variation of the level of region 2. After 13 sec., mass in region 1 instead of region 2 flowed out of the pressurizer (see Fig.7-77) and as a result the pressure in the pressurizer decreased more slowly (see Fig.7-78). Figs.7-80 and 7-81 show the specific enthalpies of regions 1 and 2, respectively. Fig.7-82 shows the density of the flow out of the pressurizer. Figs.7-18, 7-31, and 7-46 show the temporal variations of the mass flux, specific enthalpy and

quality at 25A, respectively.

7.3.8 Accumulator Behavior

The calculated results for the accumulator are shown in Figs.7-83 and 7-84. The specific enthalpy of the accumulator water remained 50 kcal/kg. At 19.5 sec. when the pressure at node 28 decreased below the initial accumulator pressure 40 ata, the accumulator started to discharge water to the primary loop. The discharge flow is shown in Fig.7-19. As the discharge of water proceeded, the accumulator pressure decreased (see Fig.7-83) and instead the nitrogen gas volume increased (see Fig.7-84).

7.3.9 Pump Behavior

The rotor of the centrifugal pump was assumed to be locked at 0.1 sec. Figs.7-85 and 7-86 show the heads of the centrifugal pumps of the broken and intact loops, respectively.

7.3.10 SG behavior

In the present version of THYDE-P, the rates of the feed water, turbine flow and mass transfer at the region interface are assumed to be identical. Therefore, mass in each region of the SG secondary systems did not change after the container isolation (see Fig.7-87, 7-88 and 7-89).

Figs.7-90, 7-91 and 7-92 show the temporal variations of the pressure and the specific enthalpies of the upper and lower regions, respectively, for the SG secondary system of the intact loop. Figs.7-92, 7-93 and 7-94 show the corresponding quantities of the broken loop.

Figs.7-96 to 7-107 show the heat transfer coefficients of the SG's. After the initiation of the LOCA, first the temperature of the SG secondary system is lower than that of the primary coolant in the U-tubes. Later, however, the relationship reverses so that the SG secondary coolant becomes a heat source to the primary loop flow. This transition occured at 25.4, 8.0, 18.6, 25.9, 9.9 and 19.9 sec. for nodes 3, 4, 5, 12, 13, 14, respectively. This transition is most clearly shown in Figs.7-98 and 7-99 for node 4 and Figs.104 and 105 for node 13. Sufficiently after the secondary system became a heat source to the primary flow, the heat transfer coefficient for the primary side decreased two orders of magnitude due to a transition of coolant state from saturated mixture to superheated steam.

7.3.11 Core Behaviors

Fig.7-108 shows the heat generation inside the fuel rod. Fig.7-109 shows the temporal variation of the heat transfer coefficient at the core node obtained directly from the various heat transfer correlations. Fig.7-110 shows the effective heat transfer coefficient h_{tr}^{eff} obtained from Eq.(17). Fig.7-112 and 7-113 show the temporal variations of the fuel center and surface temperatures. Since only one active node is set for the core, the peak of the rod surface temperature during the blowdown turned out to be 540 °C which should be understood to be the maximum of the temperature averaged over the fuel rod length.

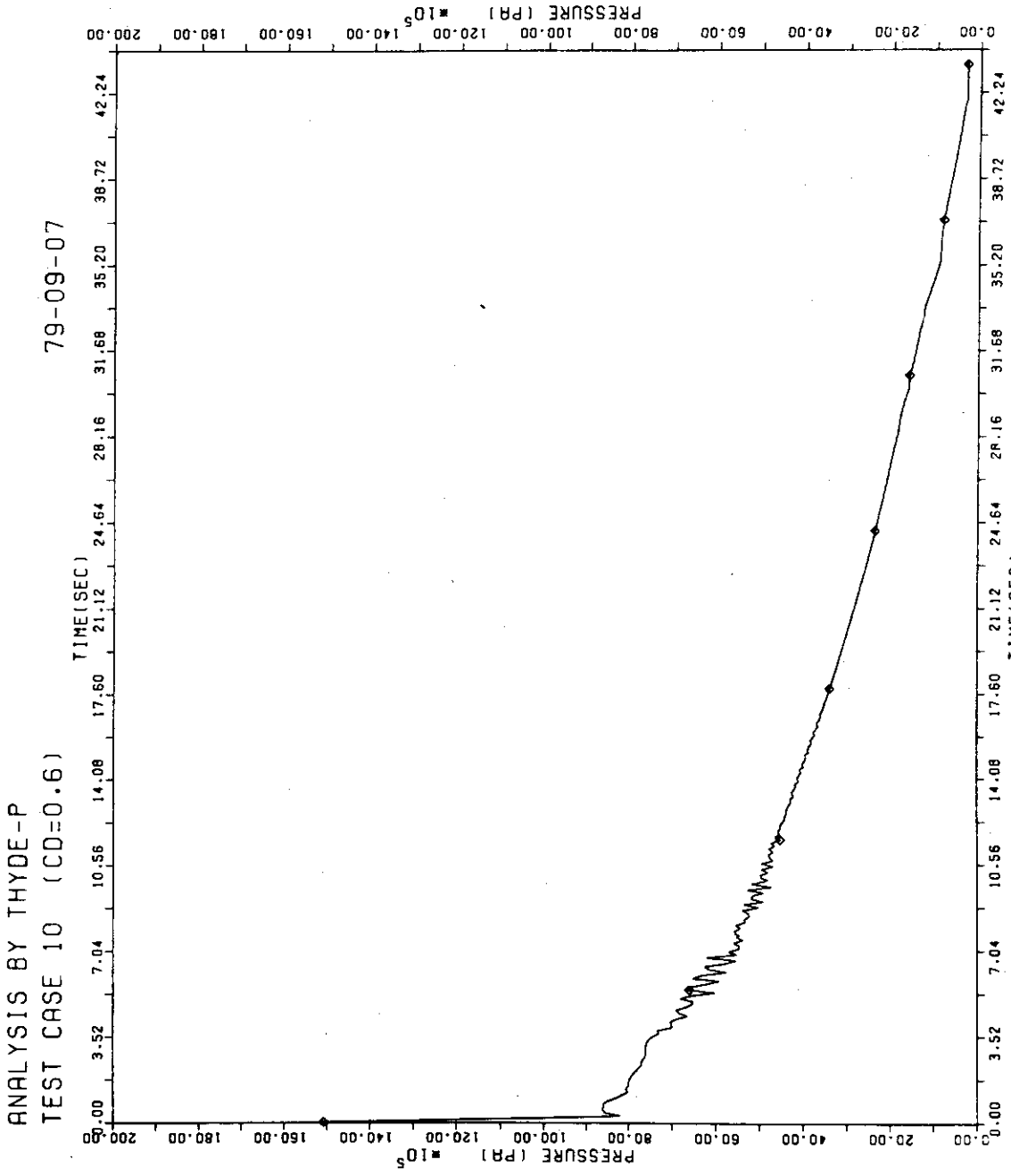

FIG. 7-3 PRESSURE AT 8E

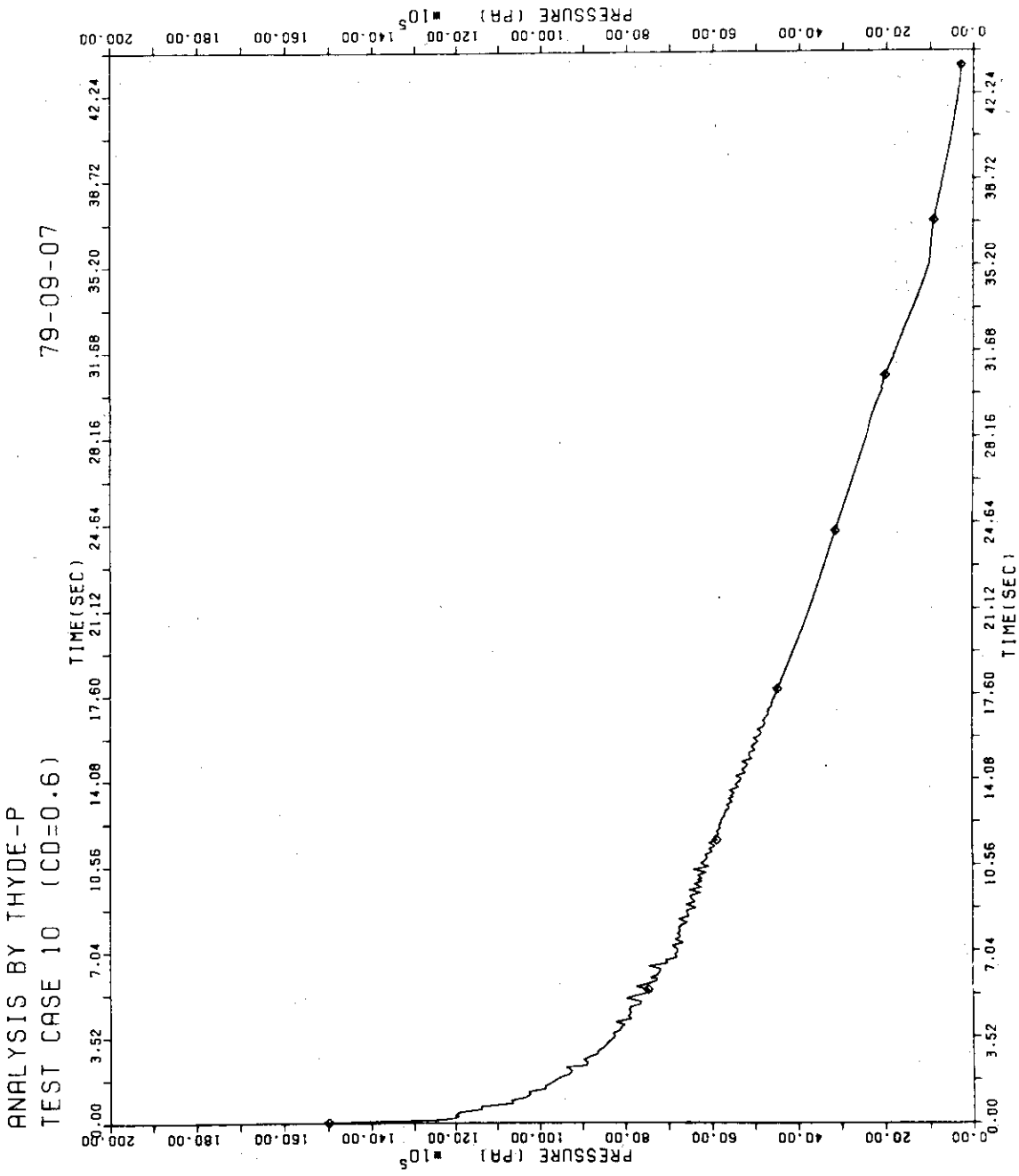

FIG. 7-4 PRESSURE AT 10A

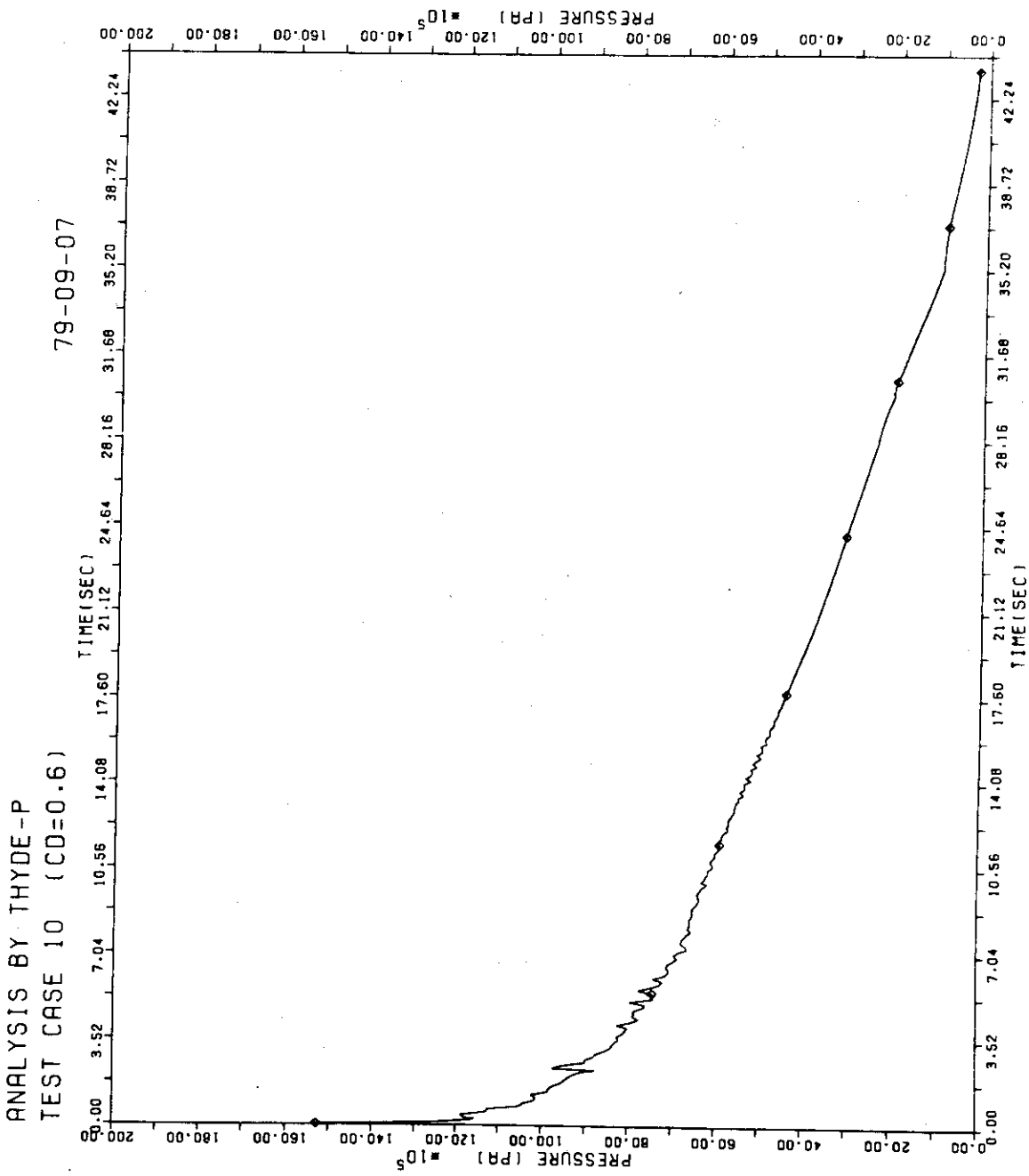

FIG. 7-5 PRESSURE AT 19A

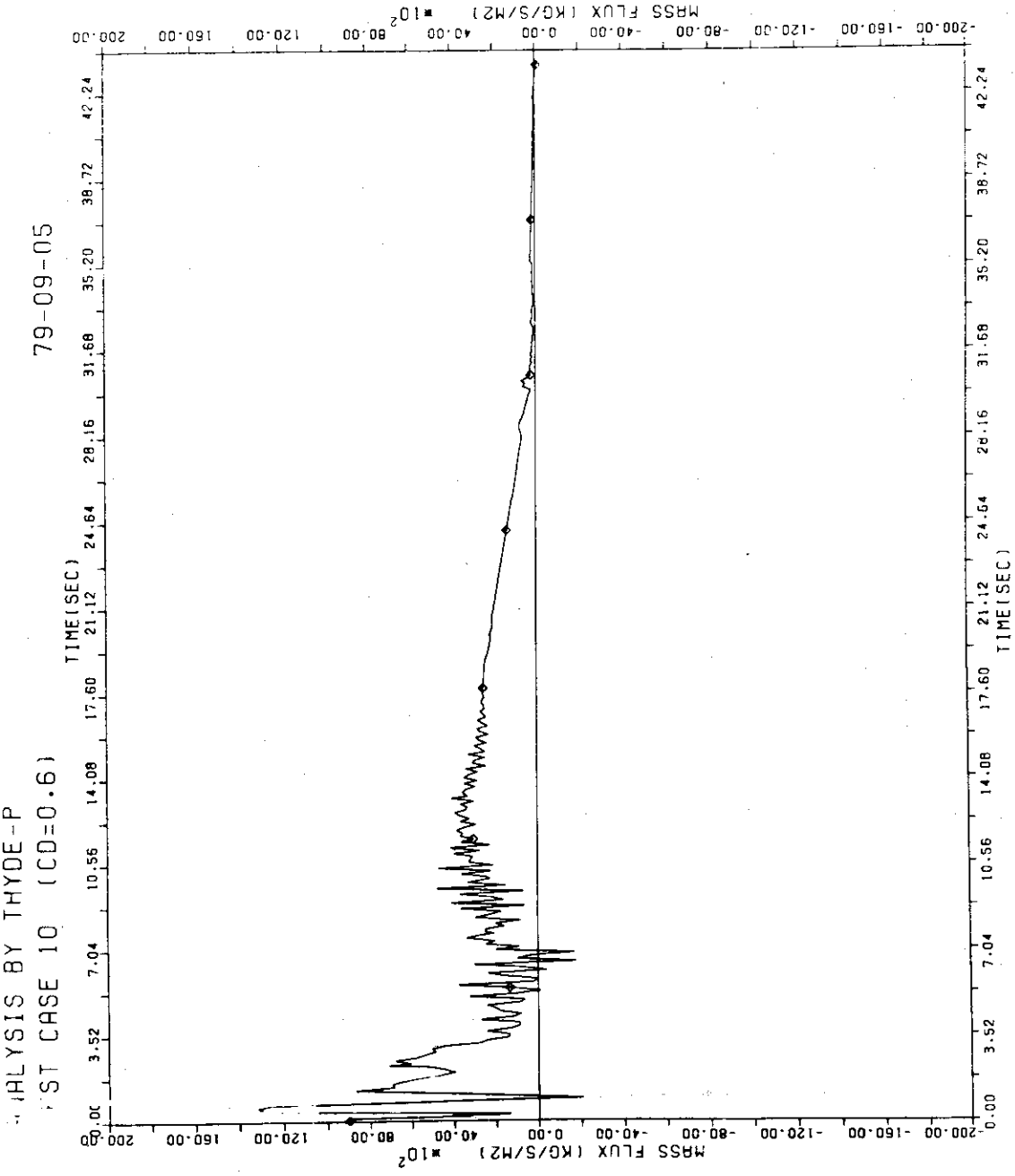

FIG. 7-6 MASS FLUX AT 1A

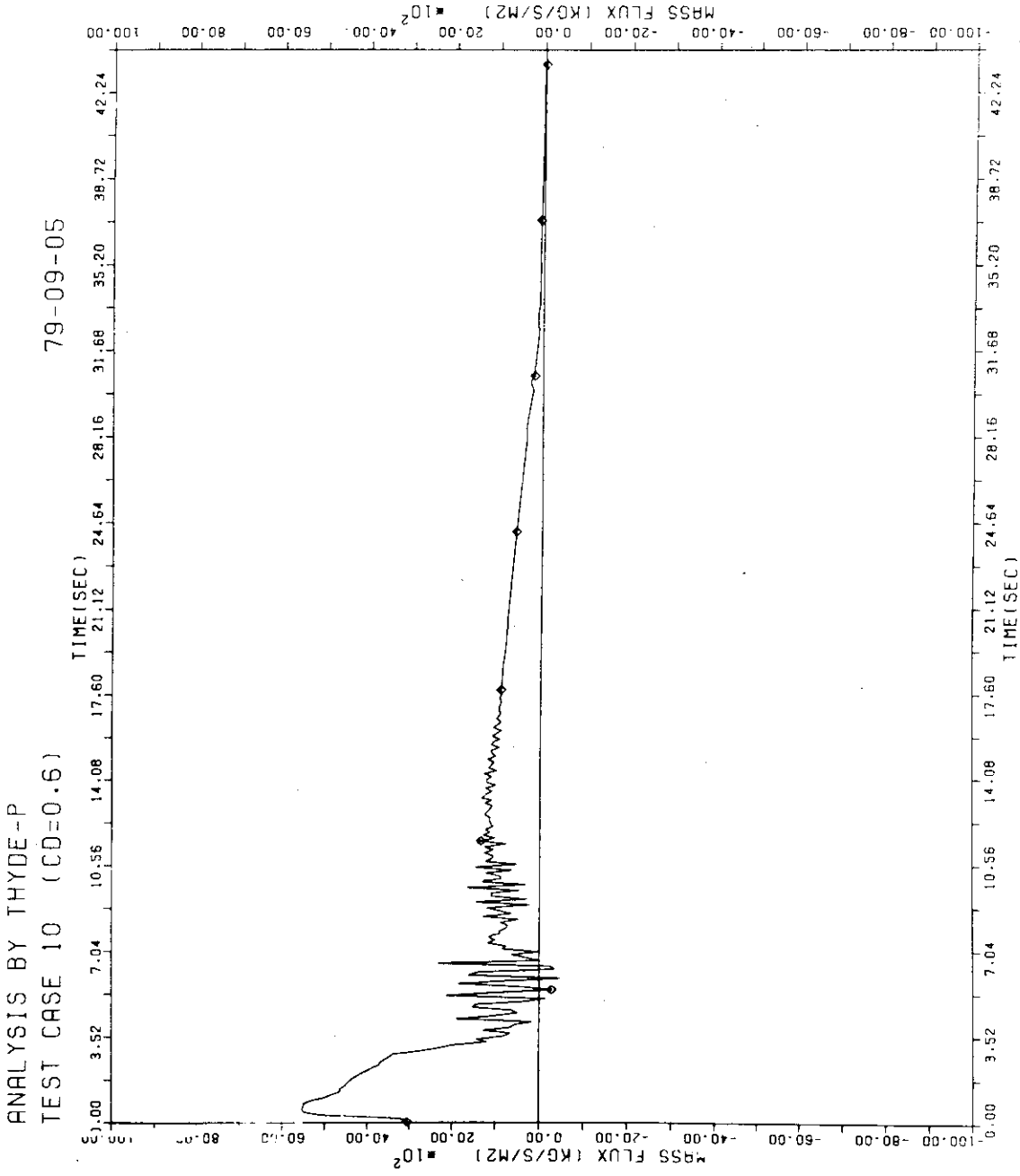

FIG. 7-7 MASS FLUX AT 4E

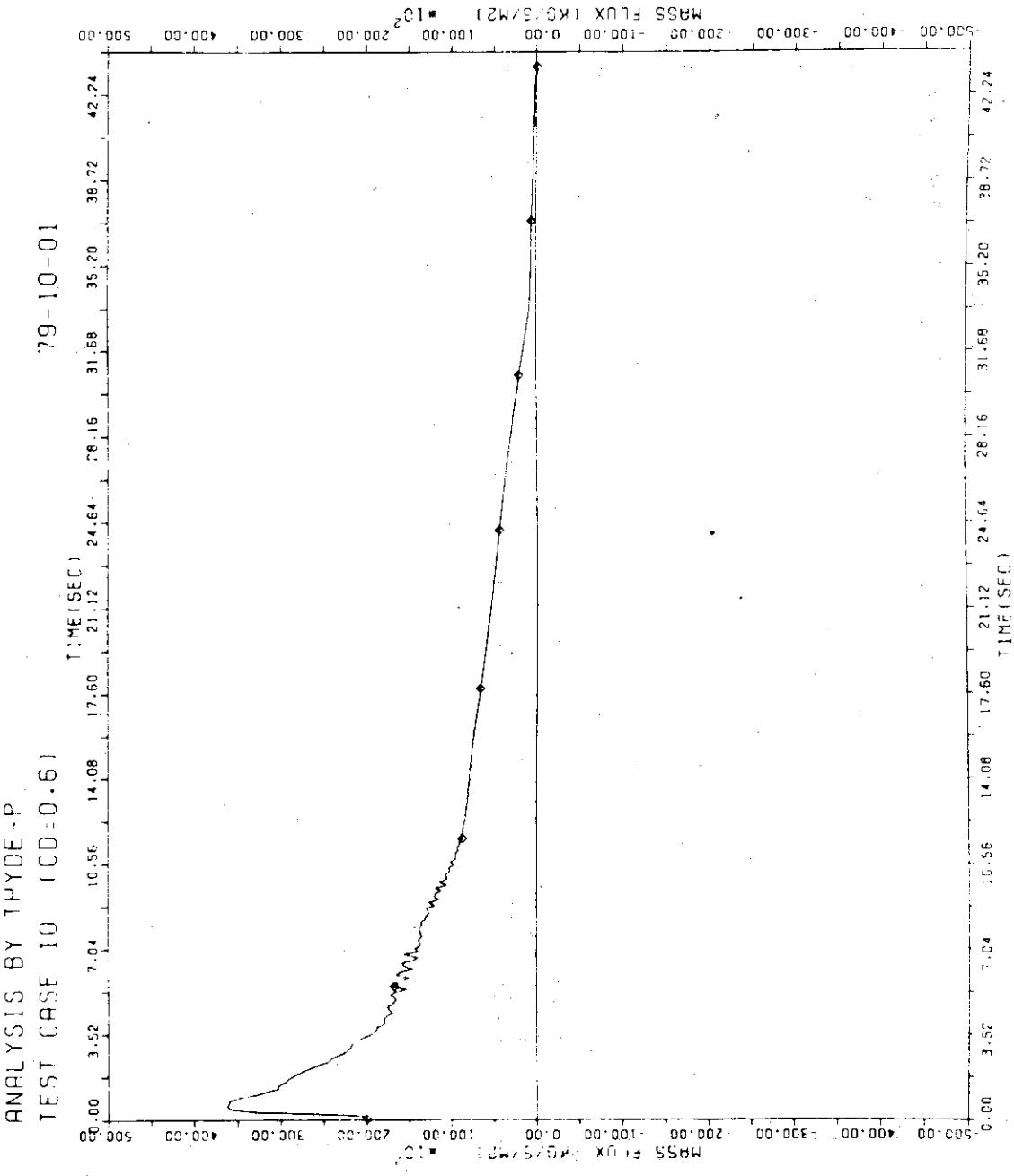

FIG. 7.8 MASS FLUX AT 8F

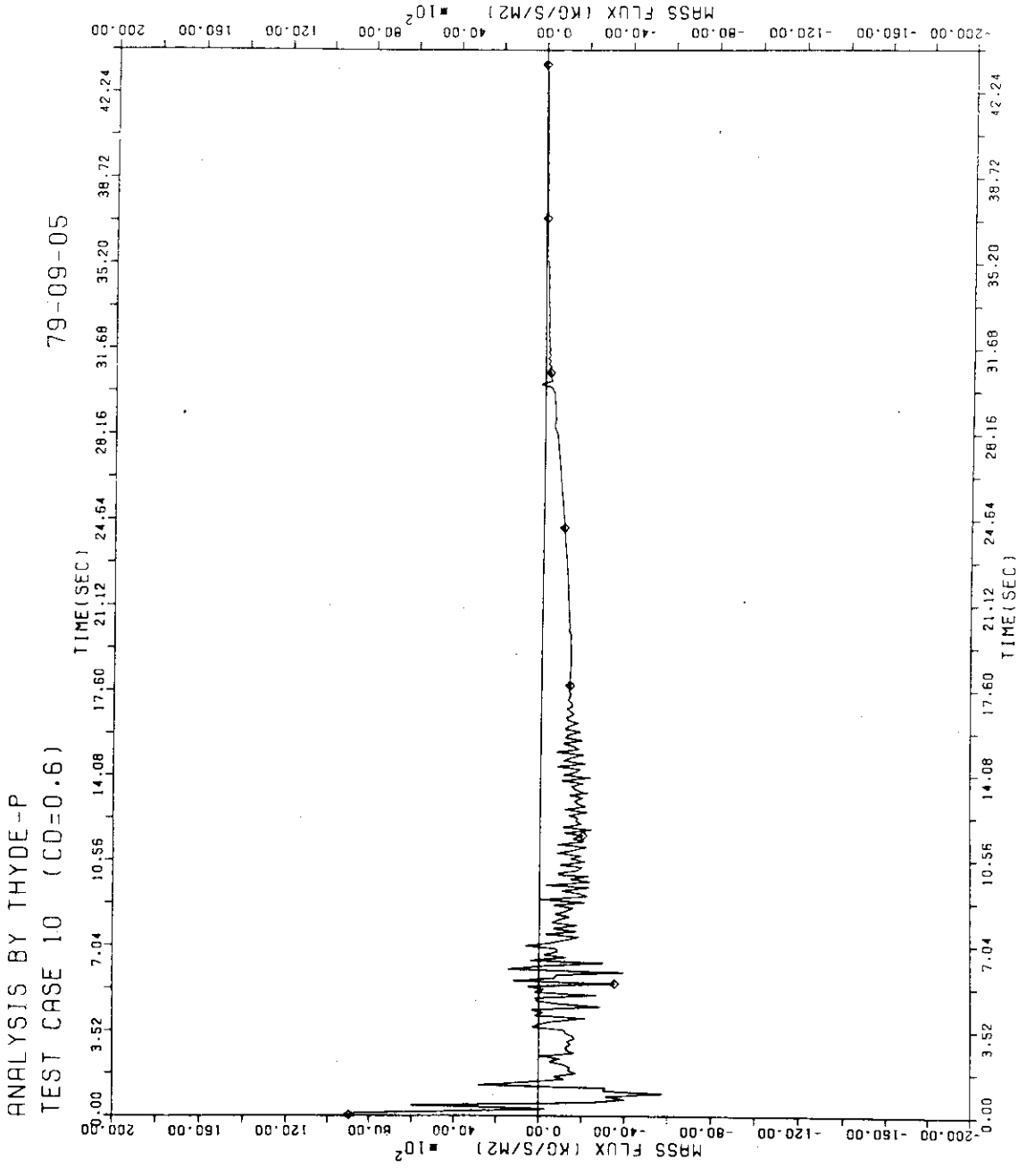

FIG. 7-9 MASS FLUX AT 10A

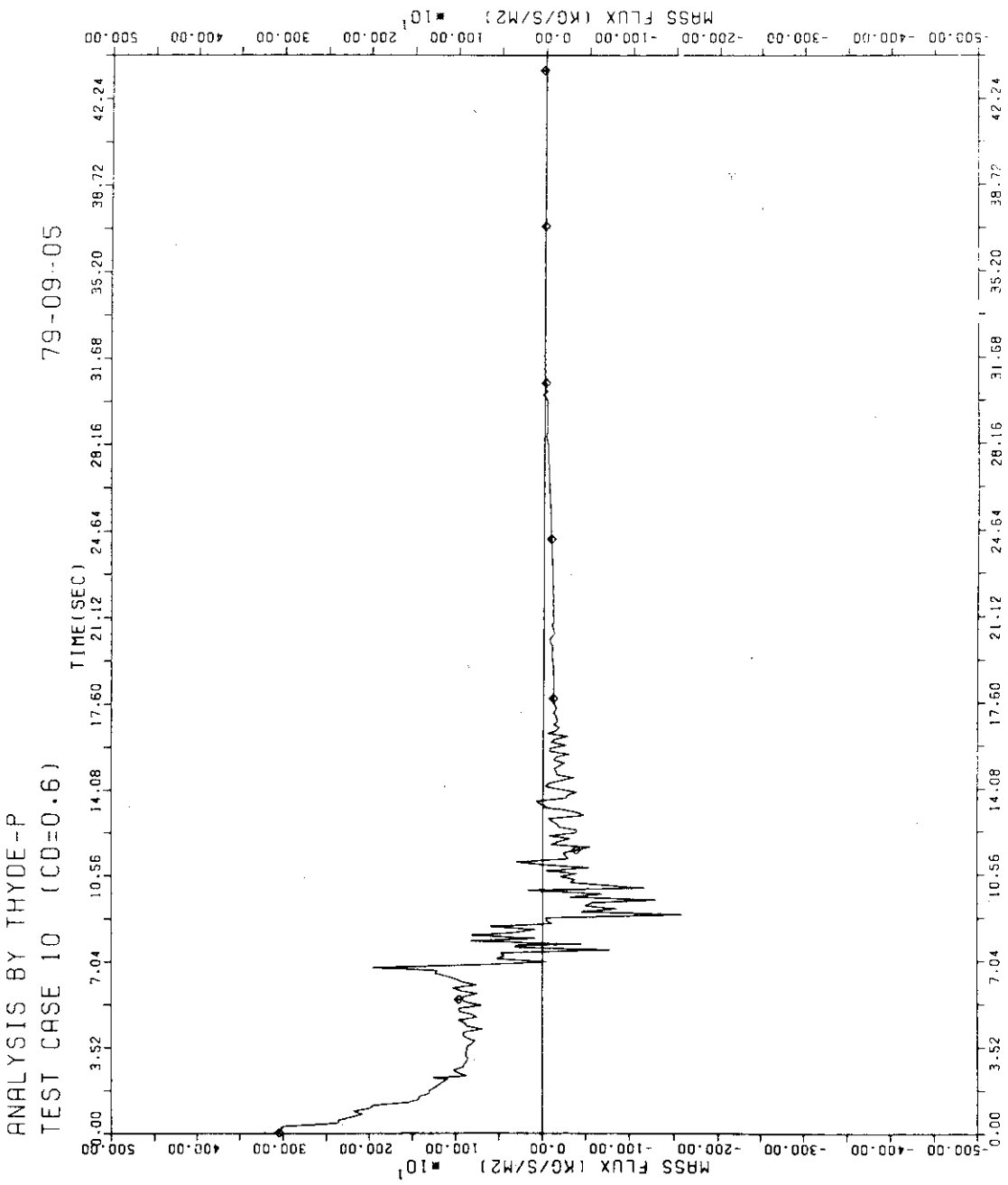

FIG. 7-10 MASS FLUX AT 13E

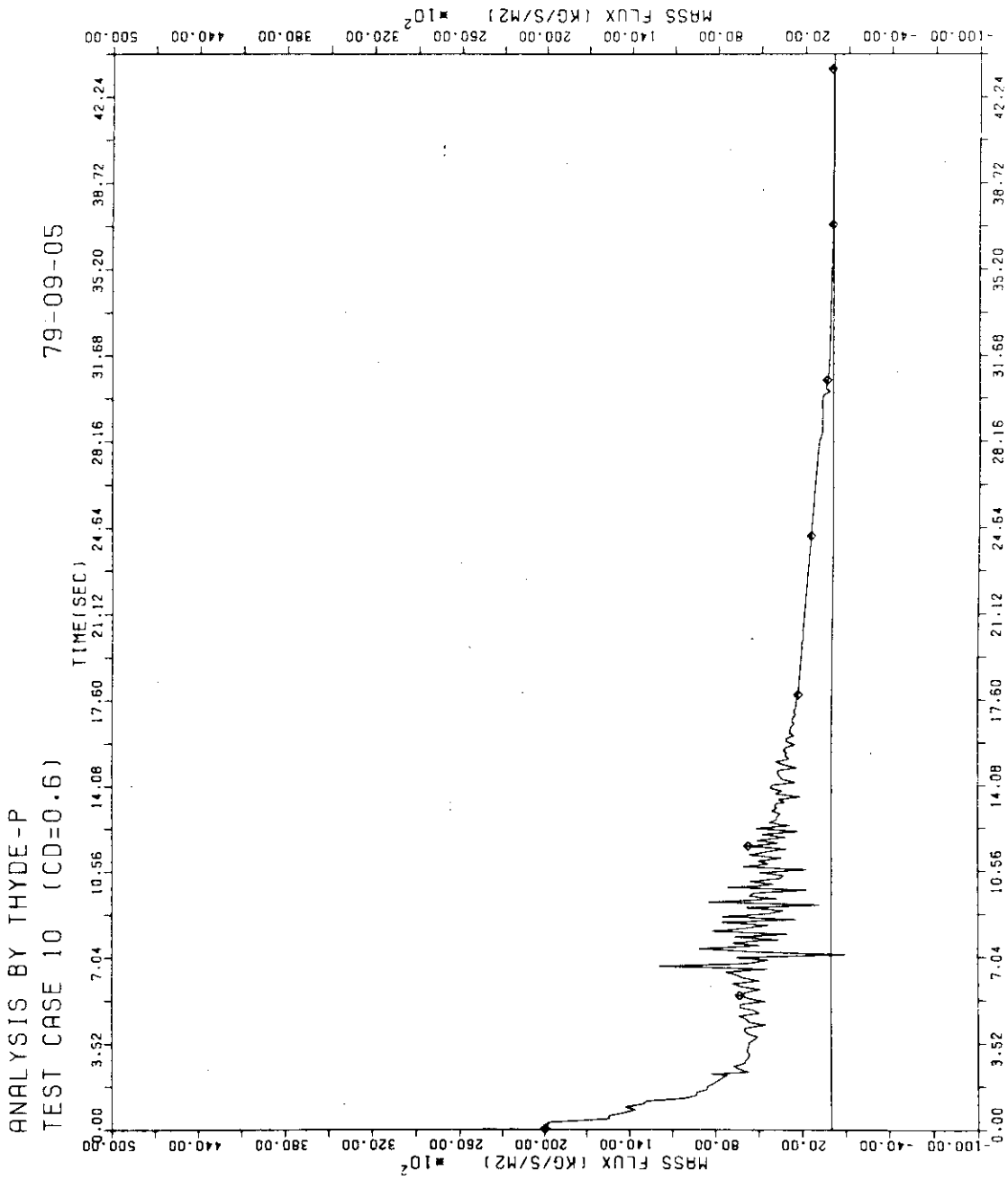

FIG. 7 - 11 MASS FLUX AT 17A

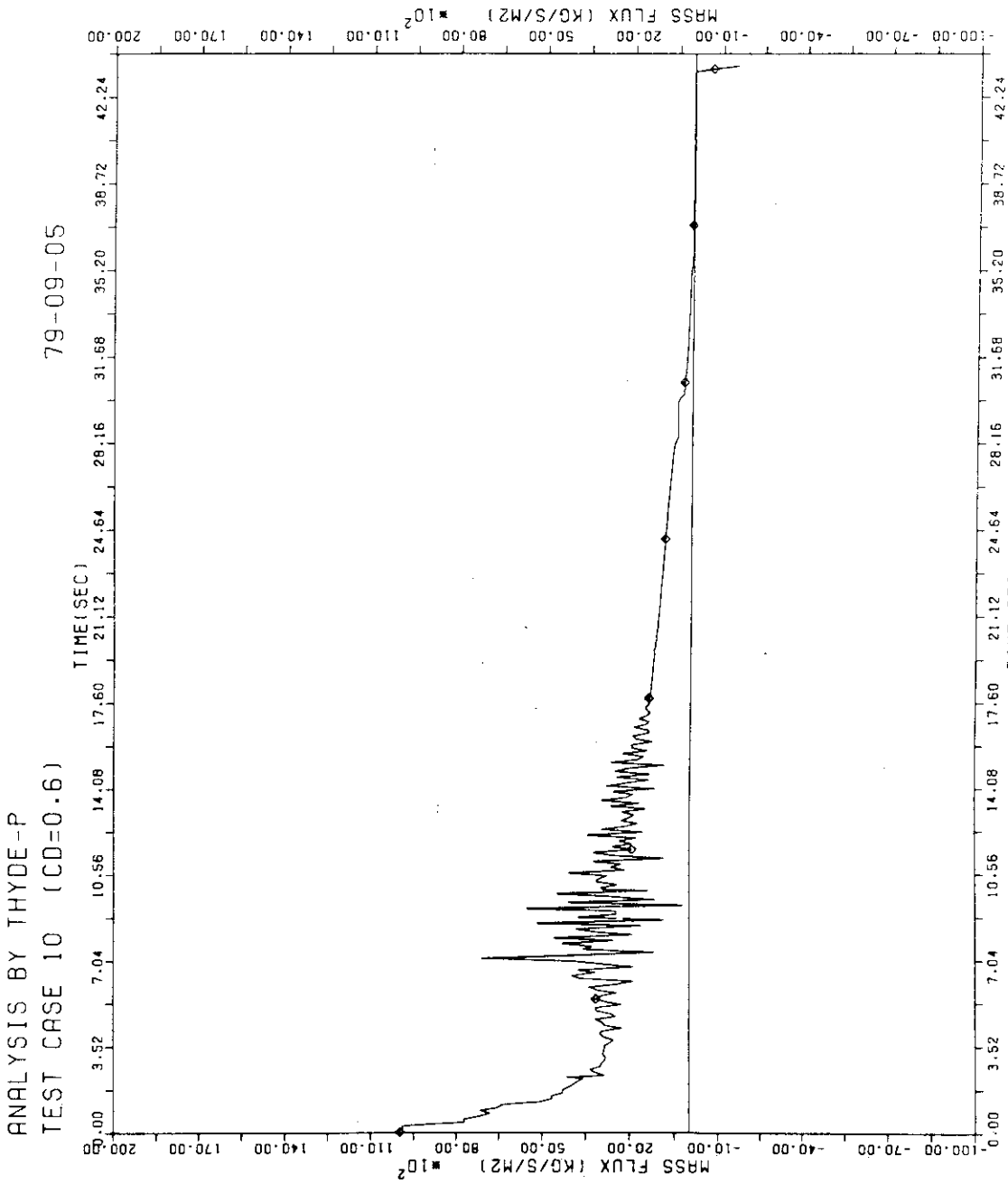

FIG. 7-12 MASS FLUX AT 18E

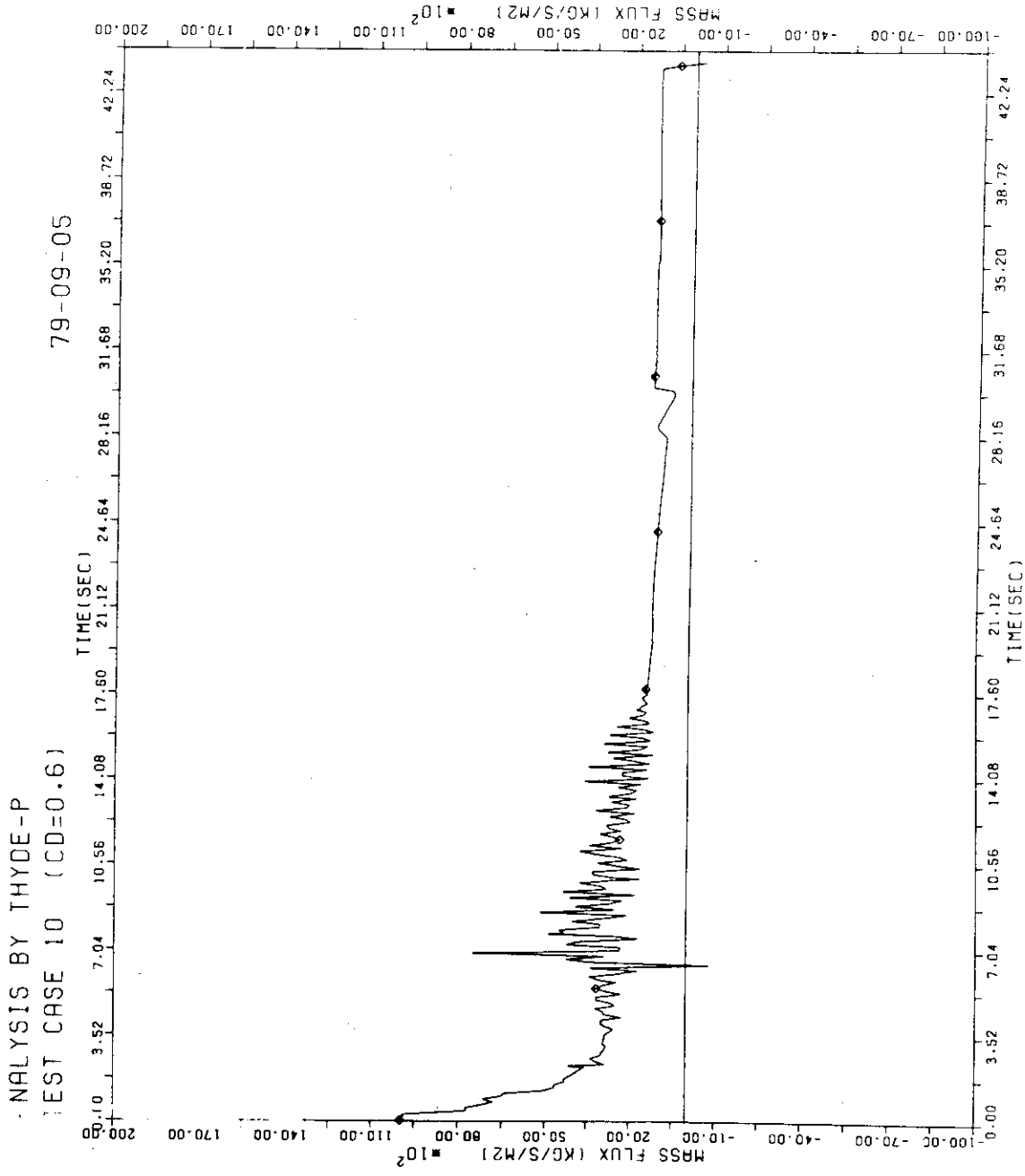

FIG. 7 - 13 MASS FLUX AT 19E

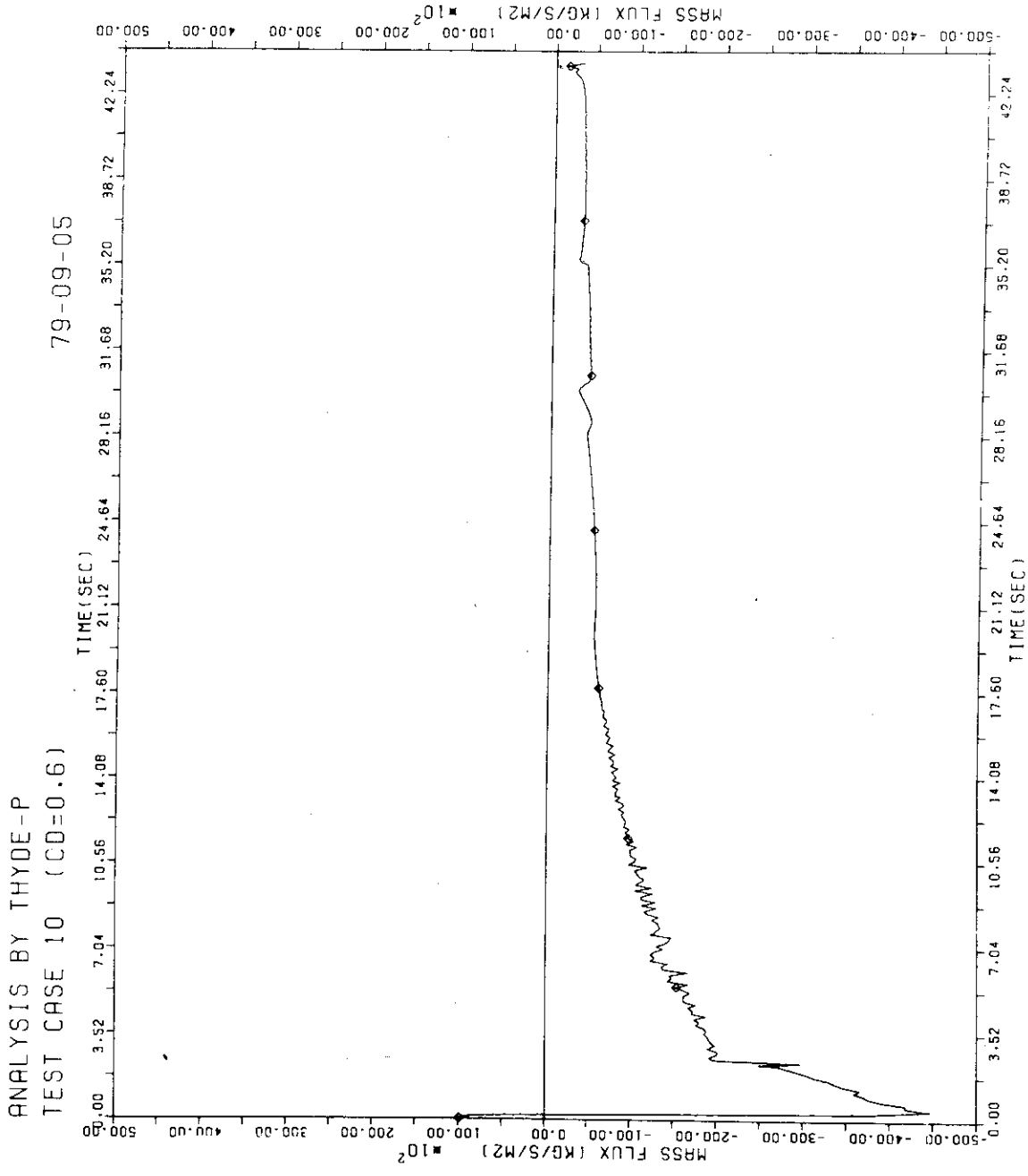

FIG. 7-14 MASS FLUX AT 9A

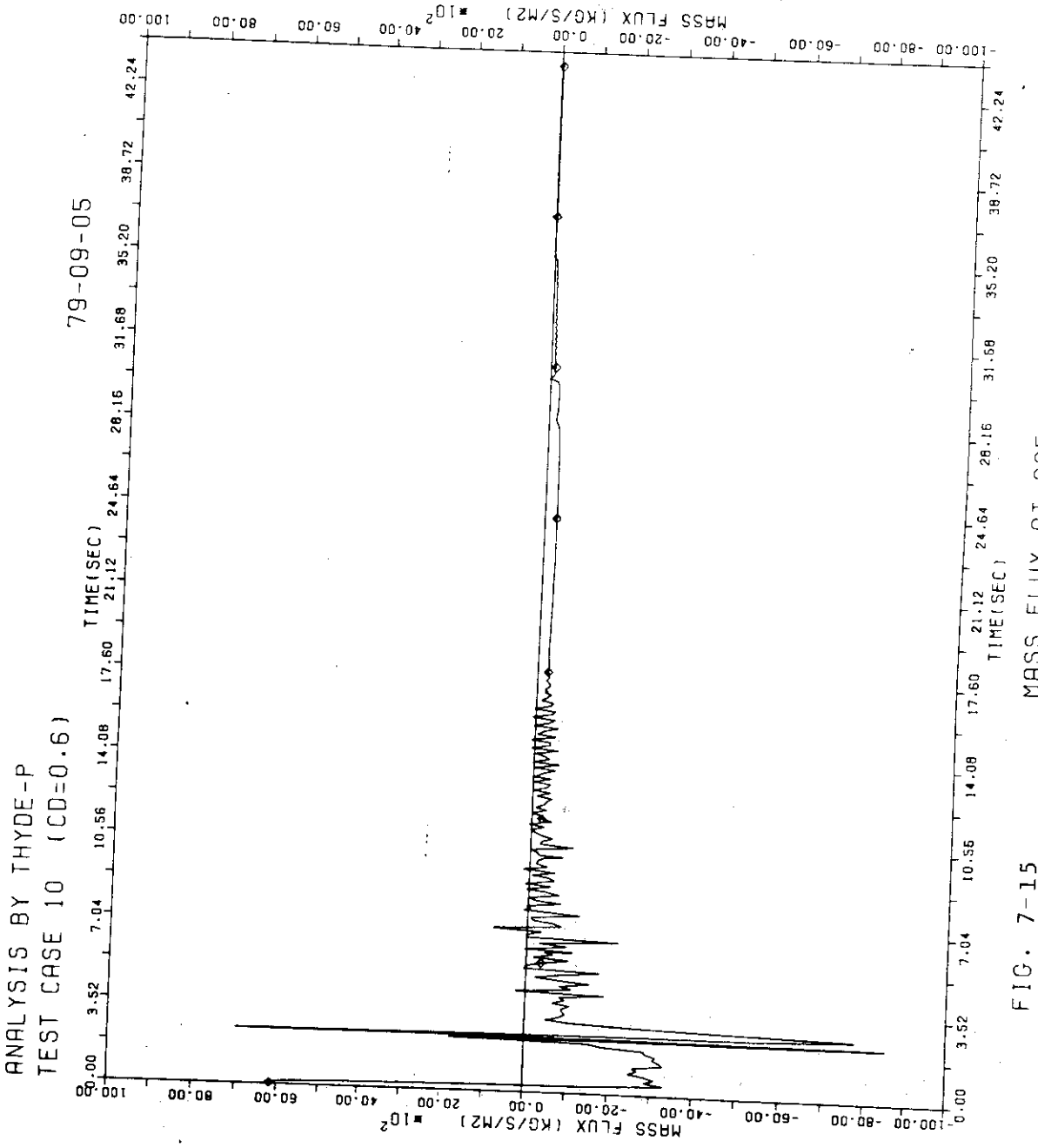

FIG. 7-15 MASS FLUX AT 20E

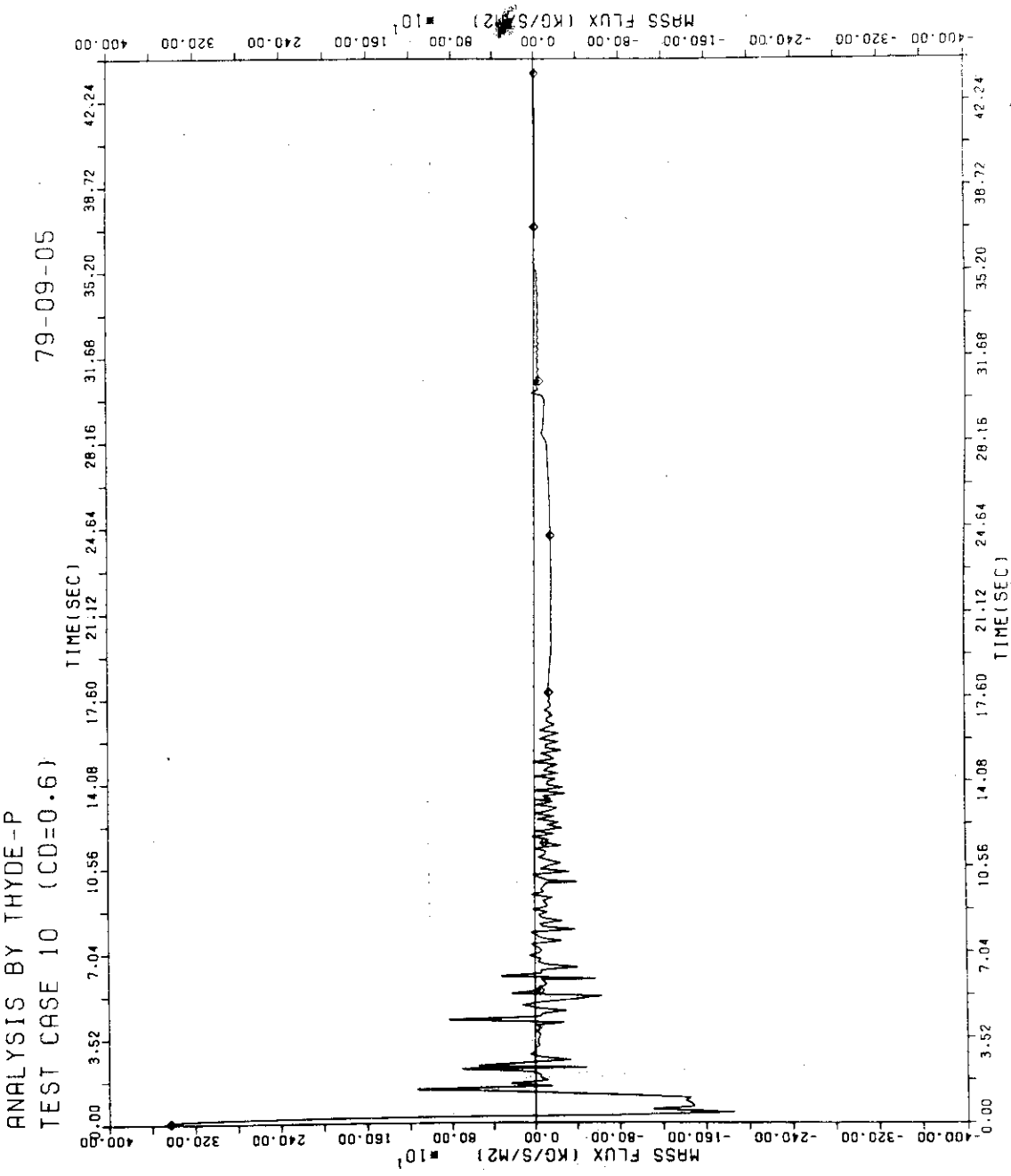

FIG. 7-16 MASS FLUX AT 23A

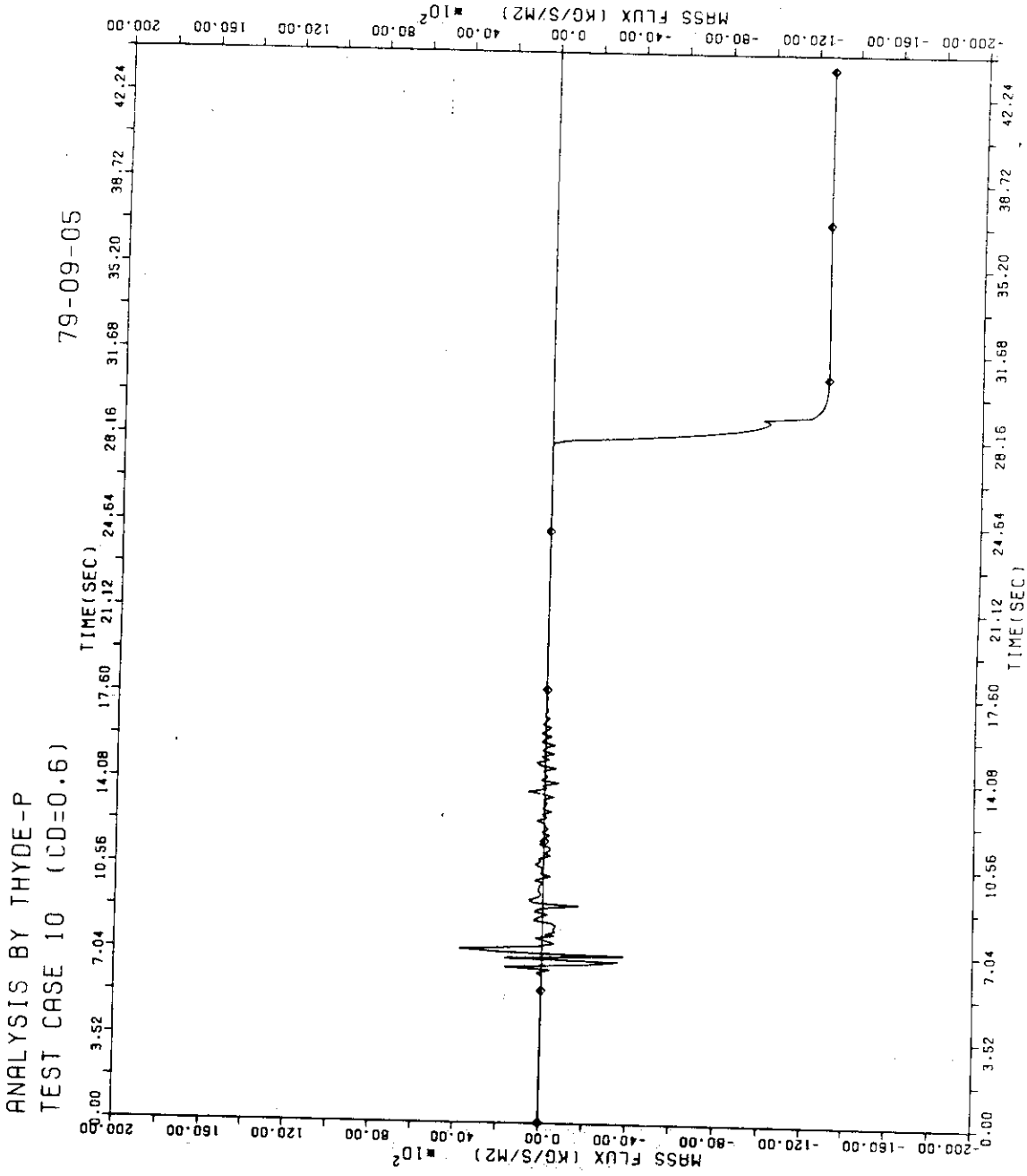

FIG. 7-17 MASS FLUX AT 27A

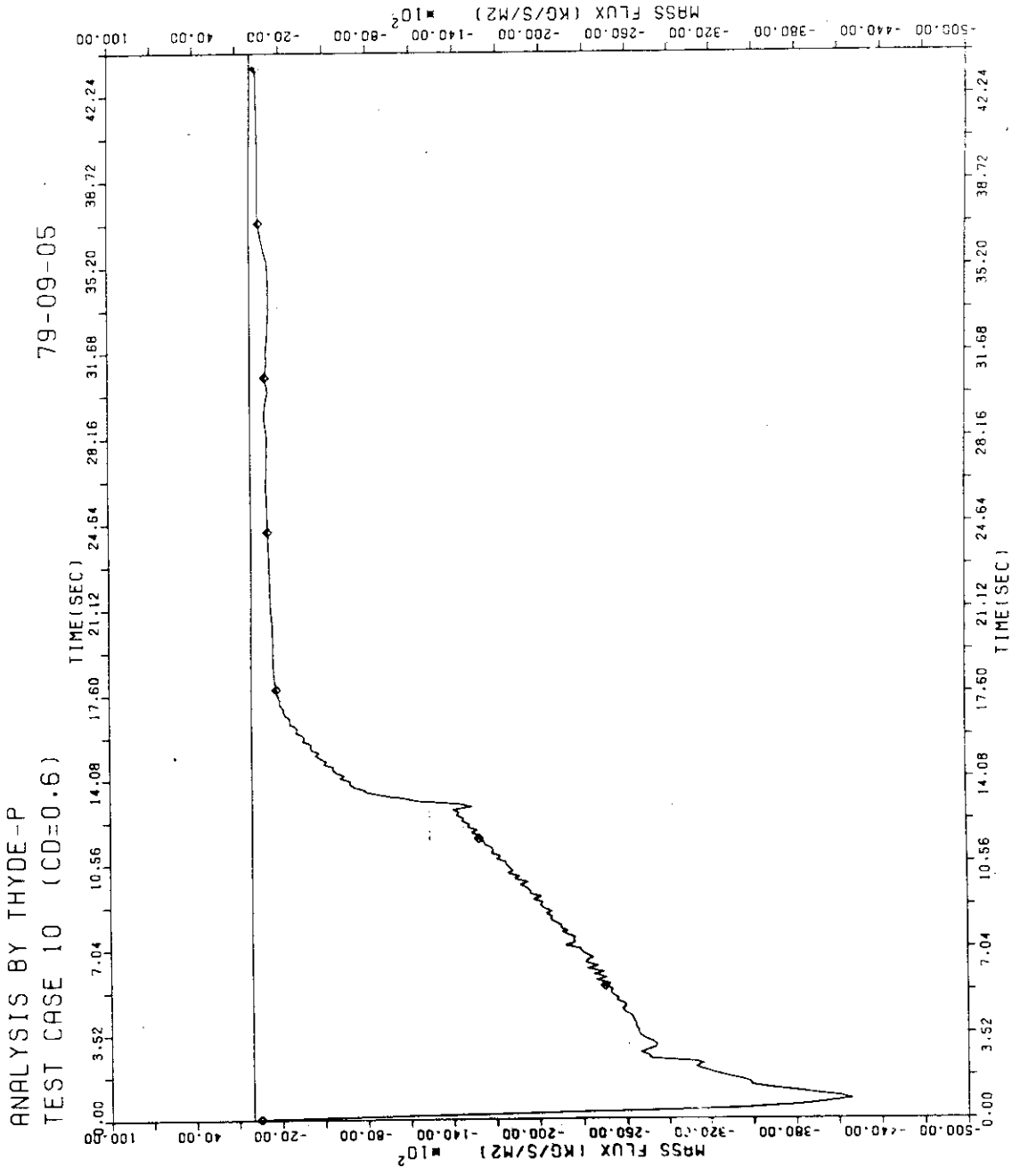

FIG. 7-18 MASS FLUX AT 25A

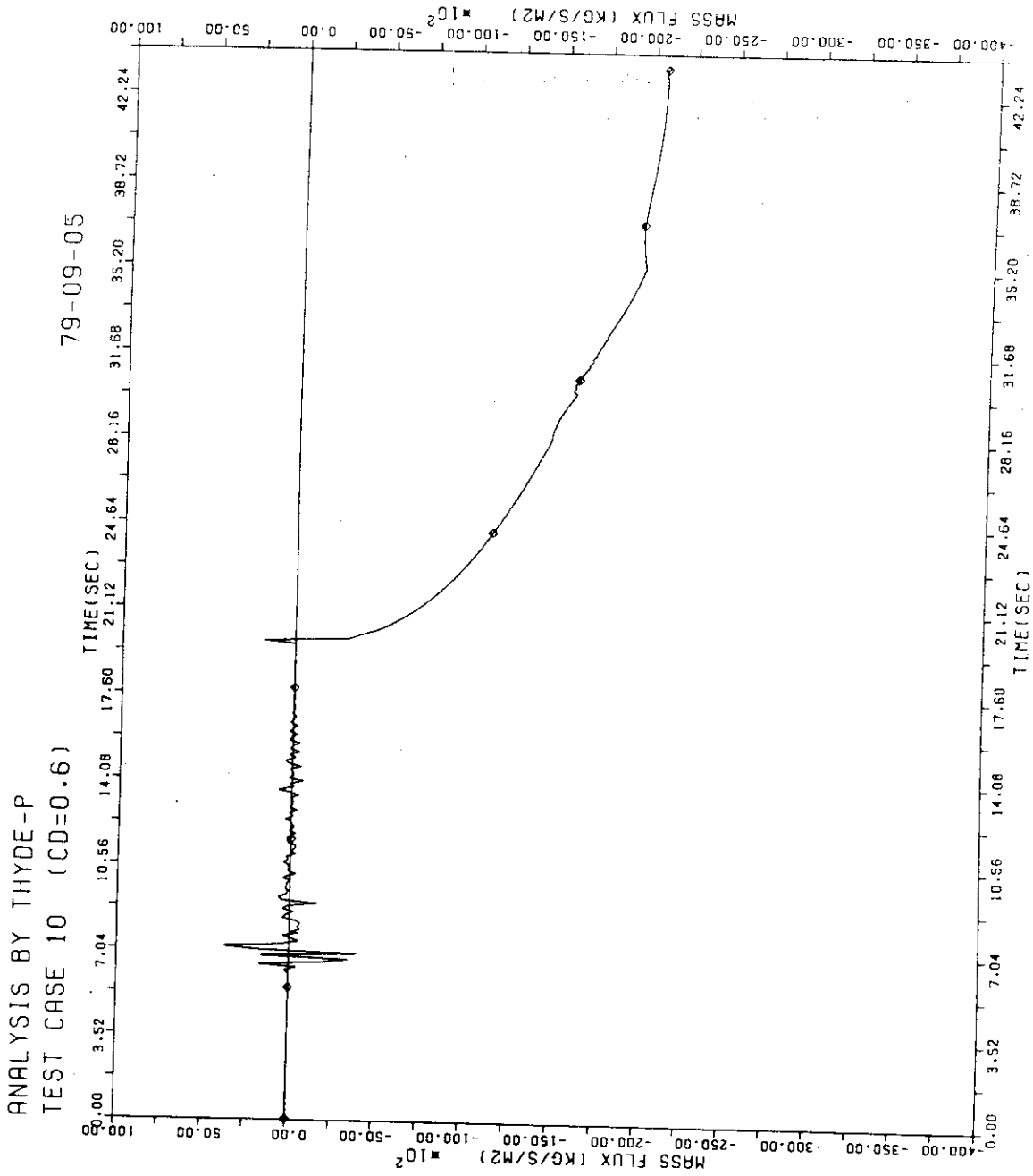

FIG. 7-19 MASS FLUX AT 28A

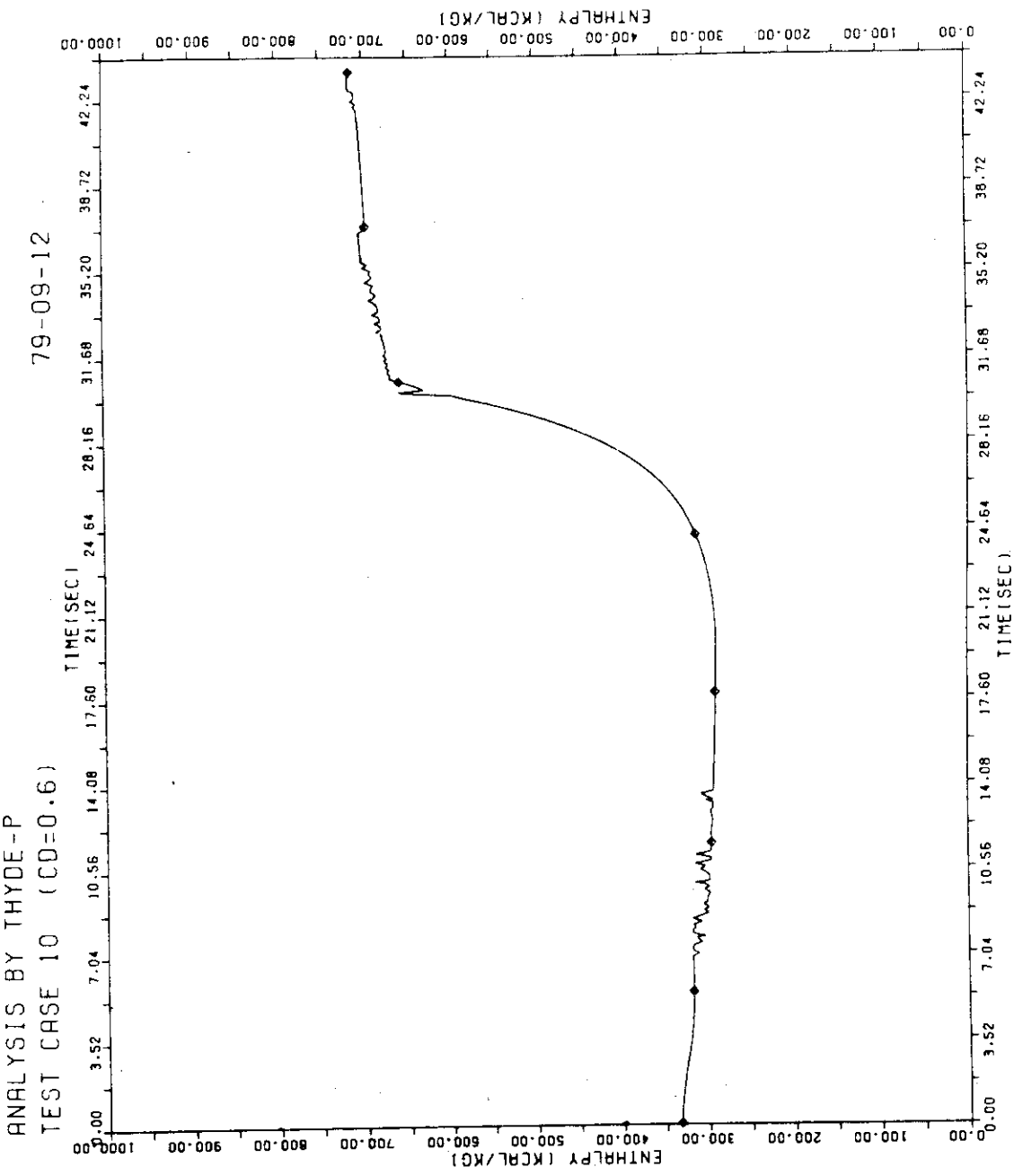

FIG. 7 - 20 ENTHALPY AT 13E

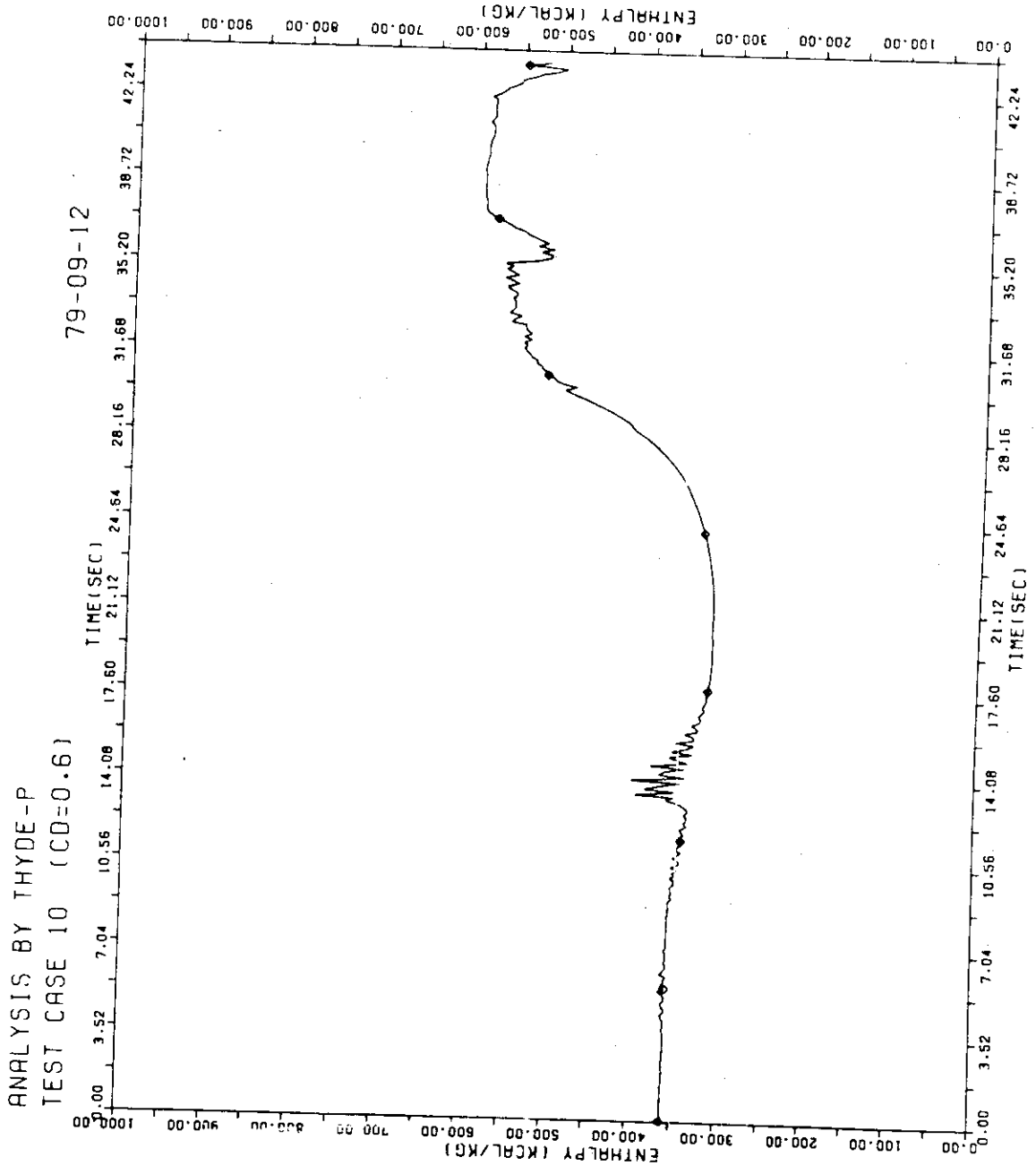

FIG. 7-21 ENTHALPY AT 10E

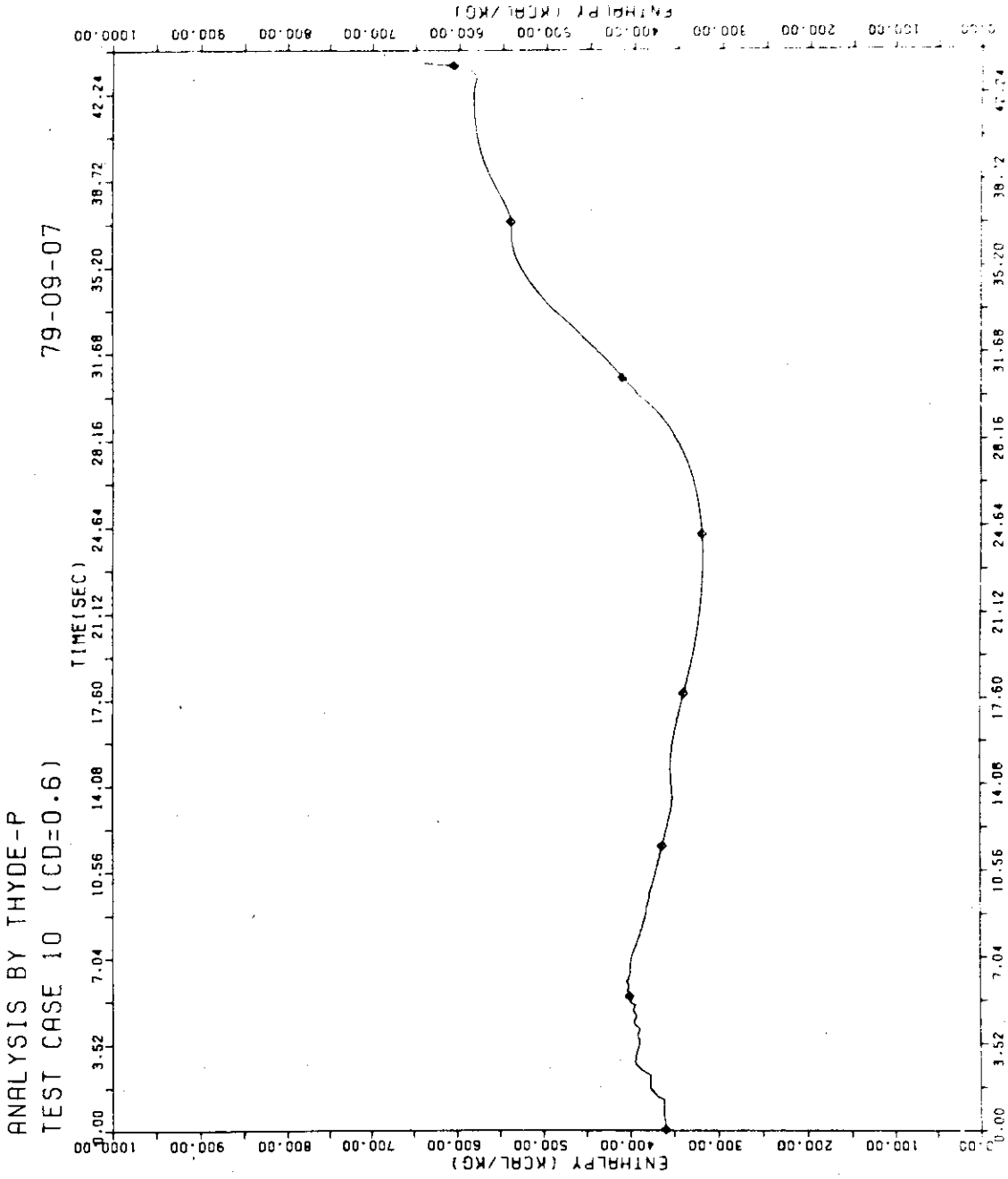

FIG. 7-22 ENTHALPY AT 1A

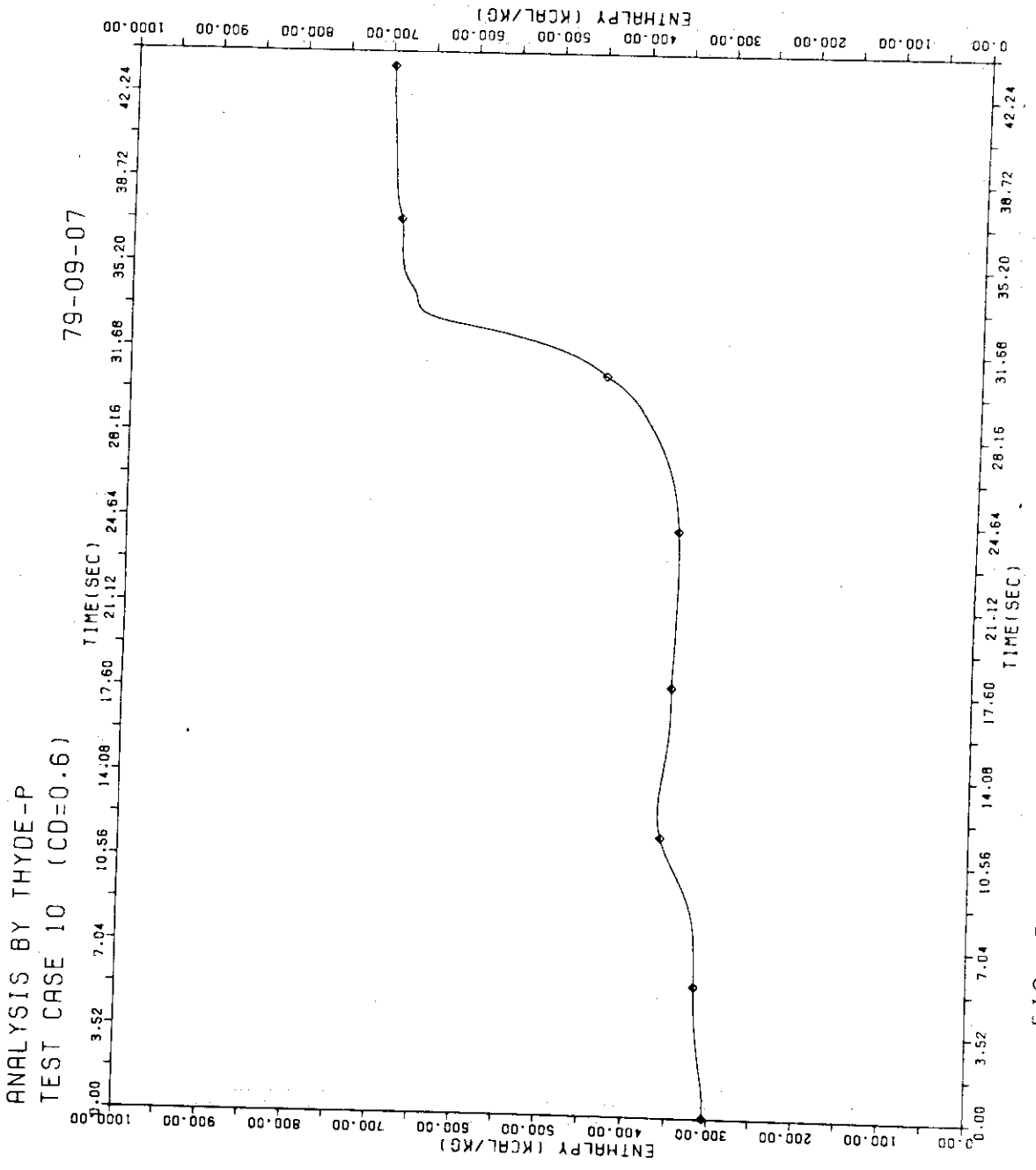

FIG. 7-23 ENTHALPY AT 8E

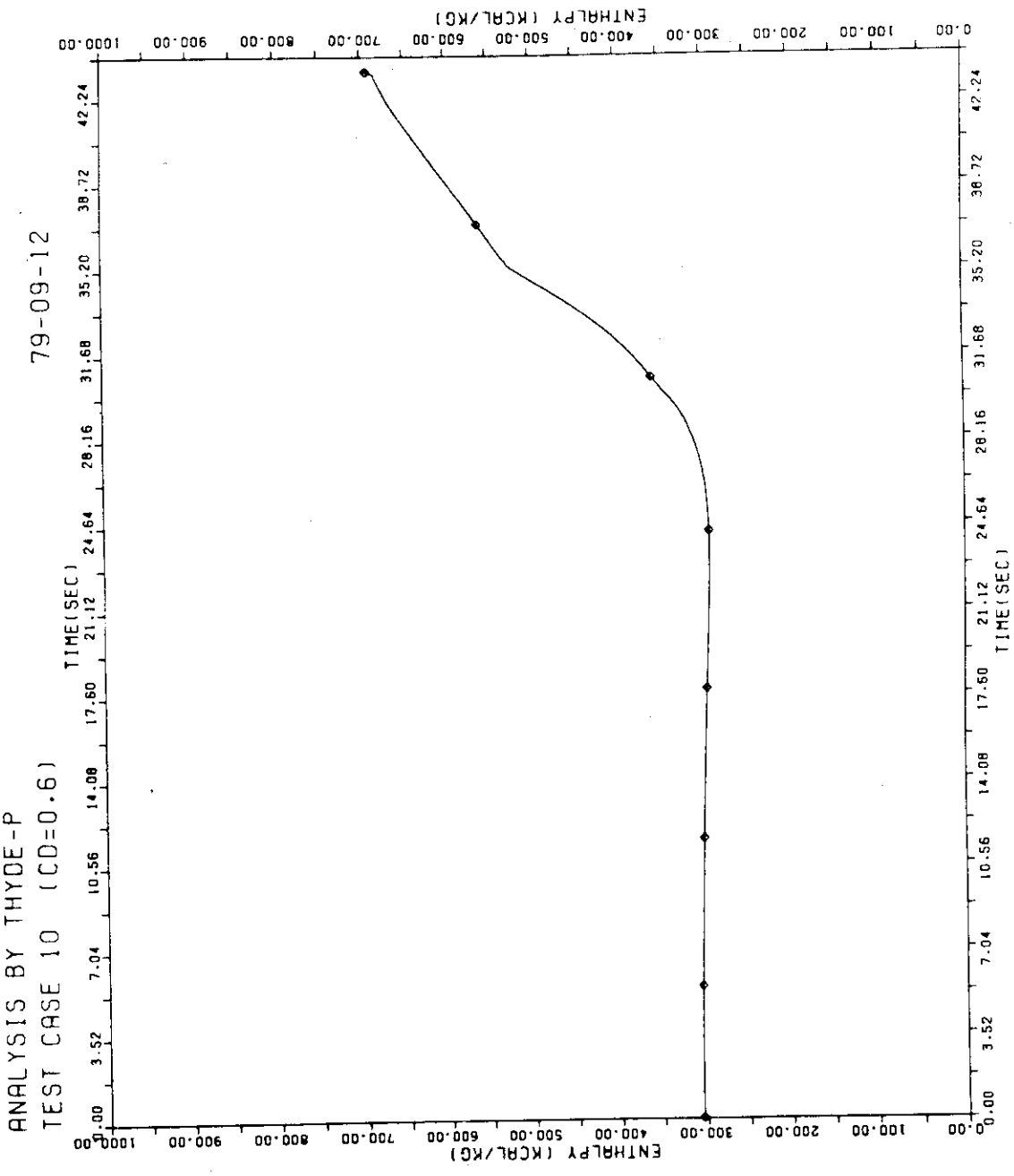

FIG. 7-24 ENTHALPY AT 17E

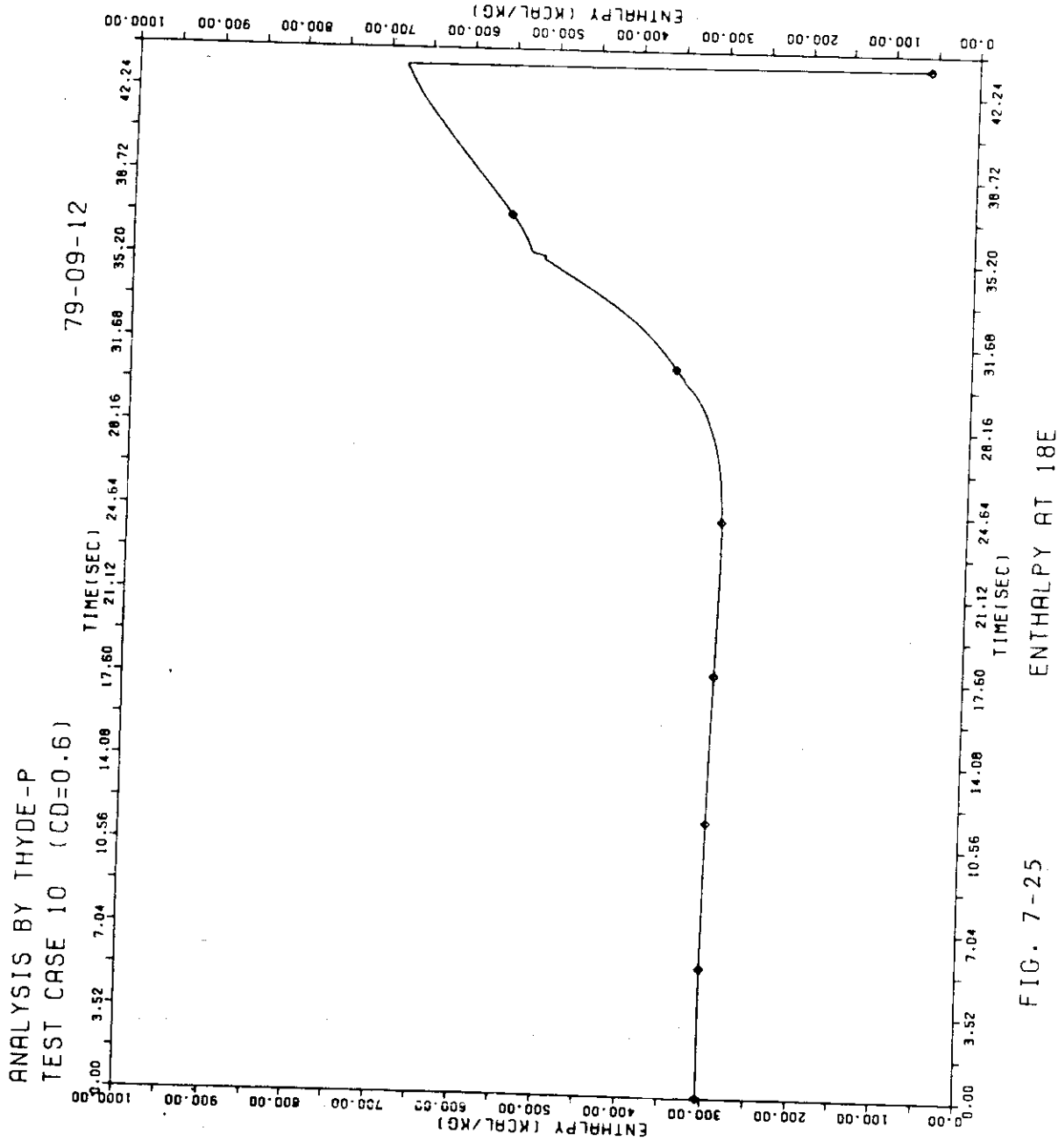

FIG. 7-25 ENTHALPY AT 18E

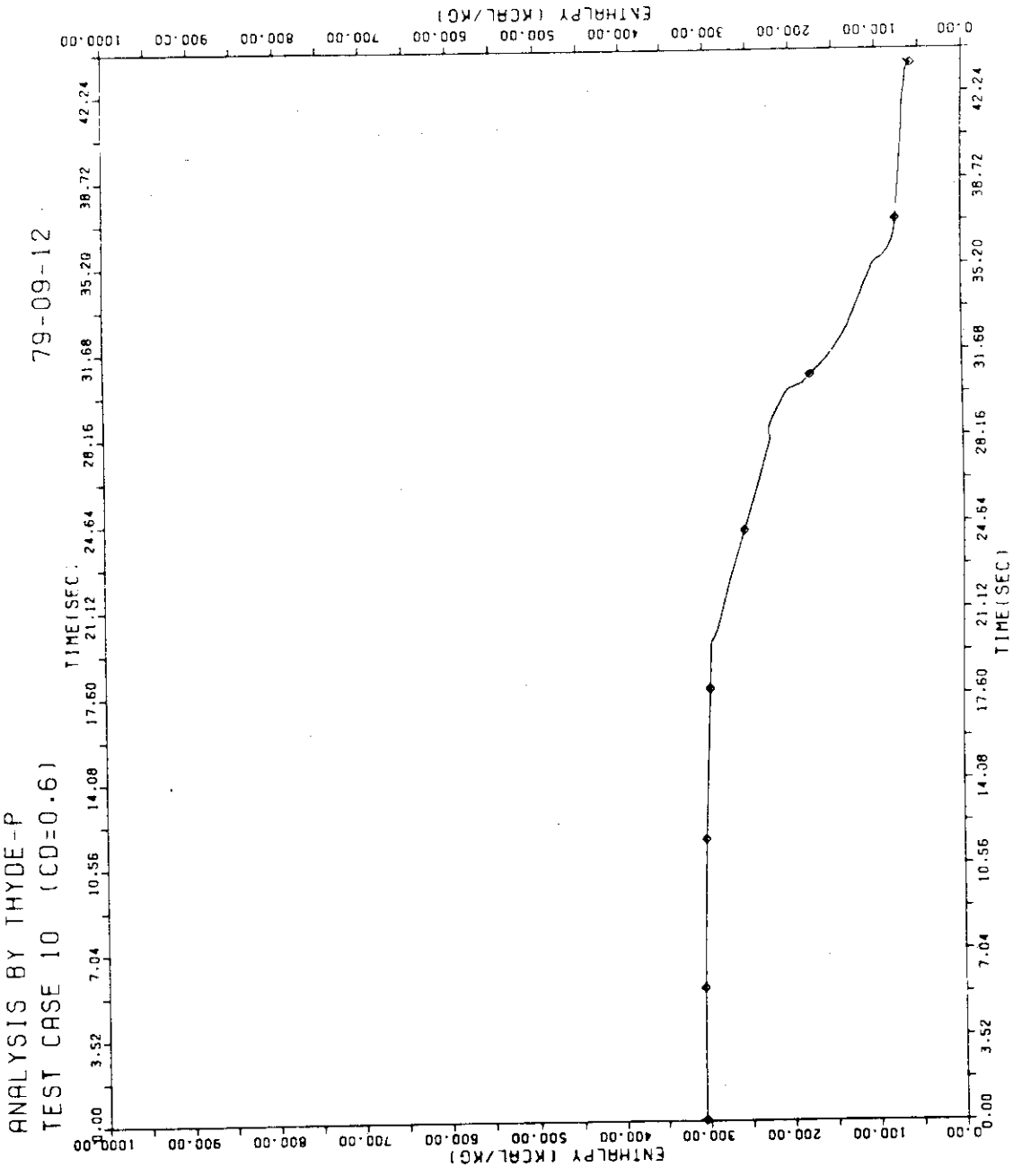

FIG. 7-26 ENTHALPY AT 19A

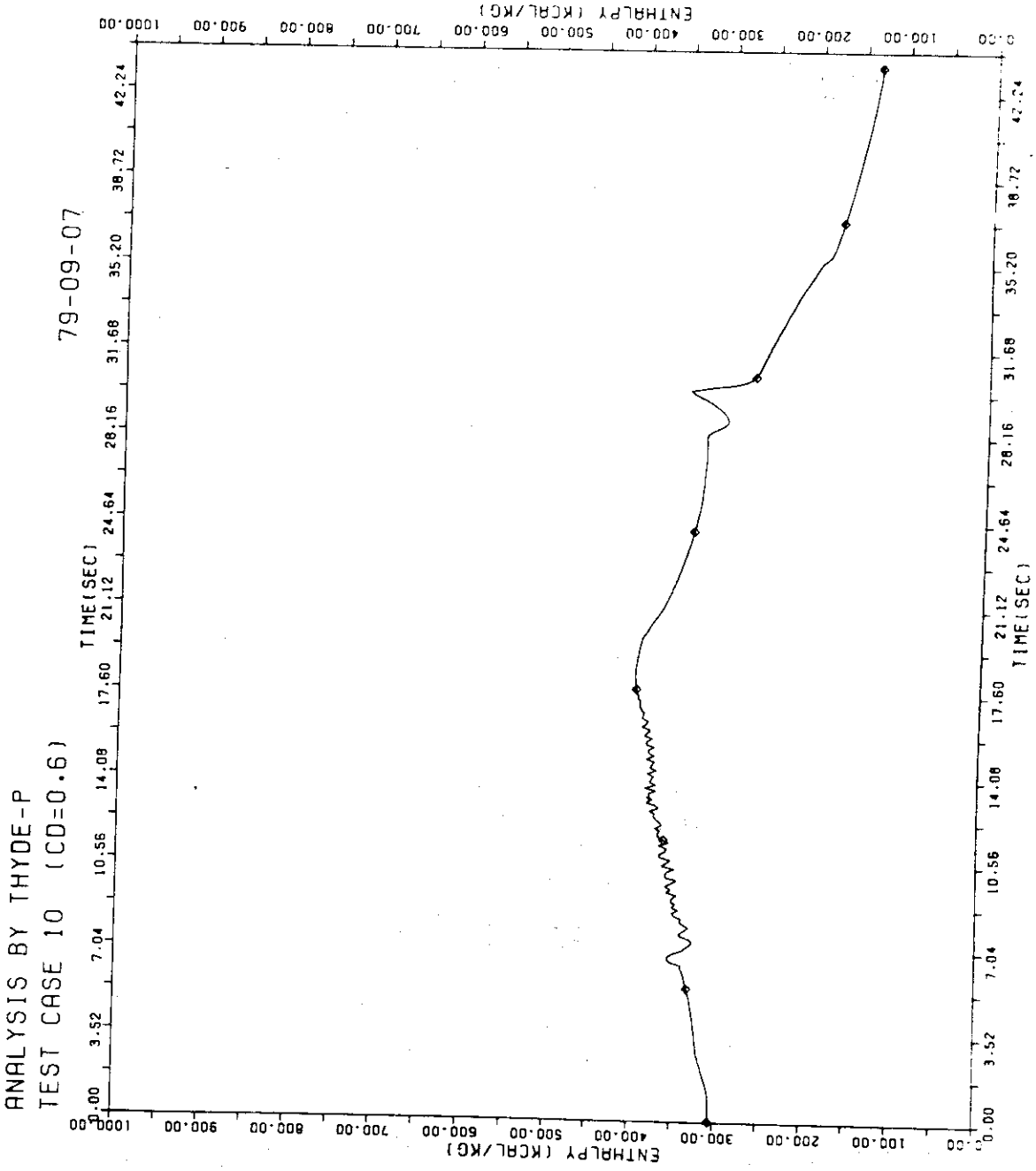

FIG. 7.27 ENTHALPY AT 9A

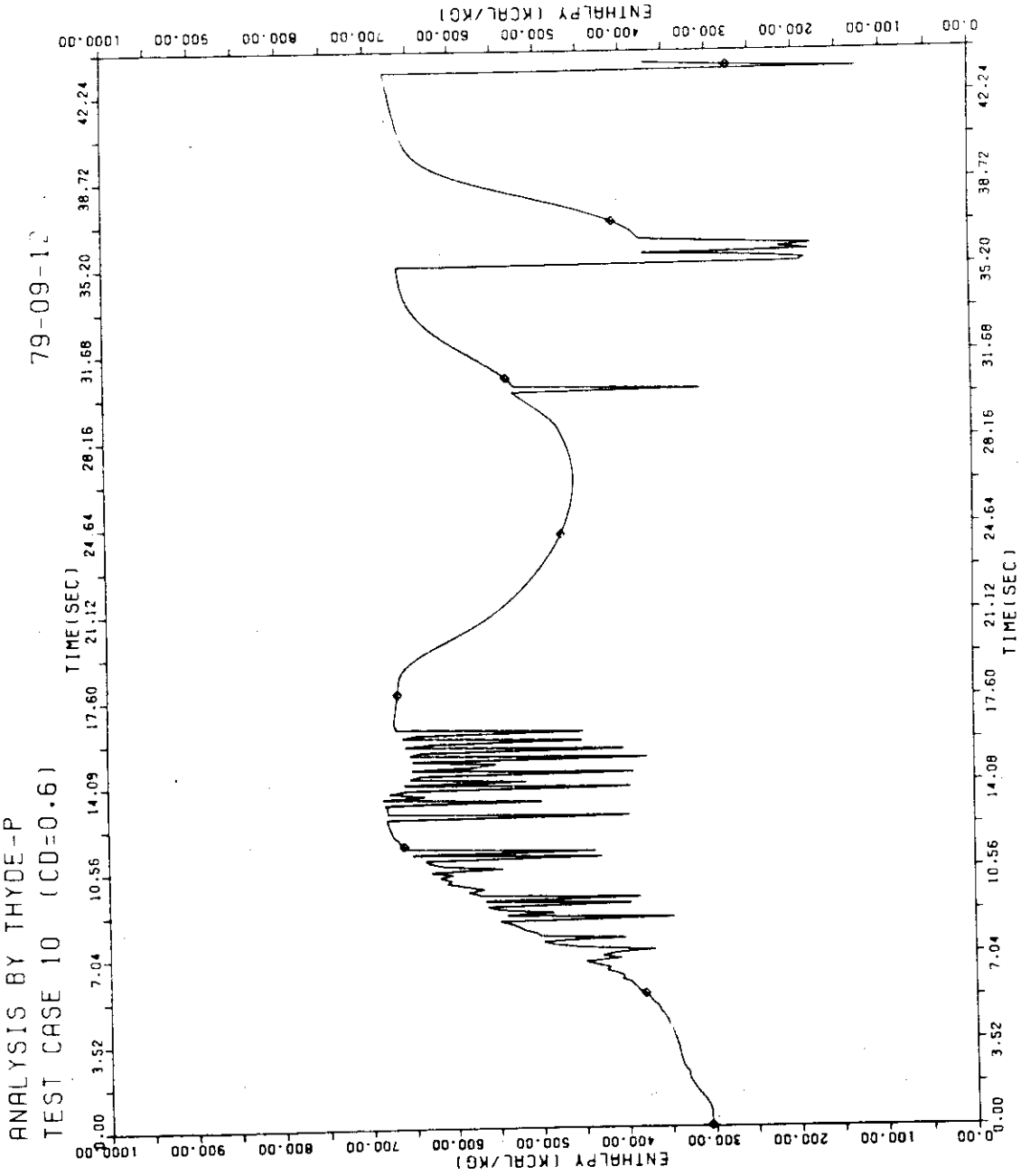

FIG. 7-28 ENTHALPY AT 20A

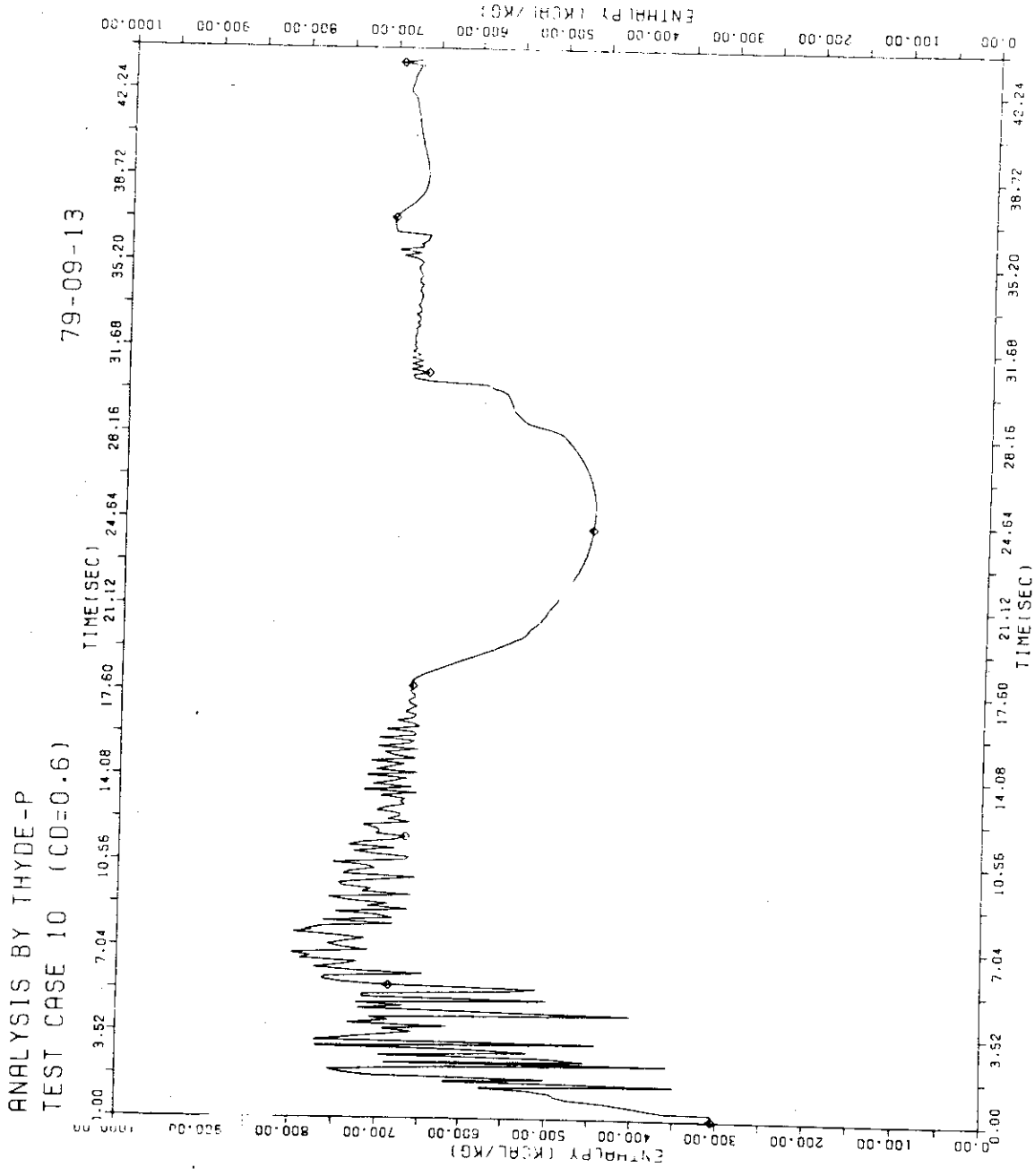

FIG. 7-29 ENTHALPY AT 23A

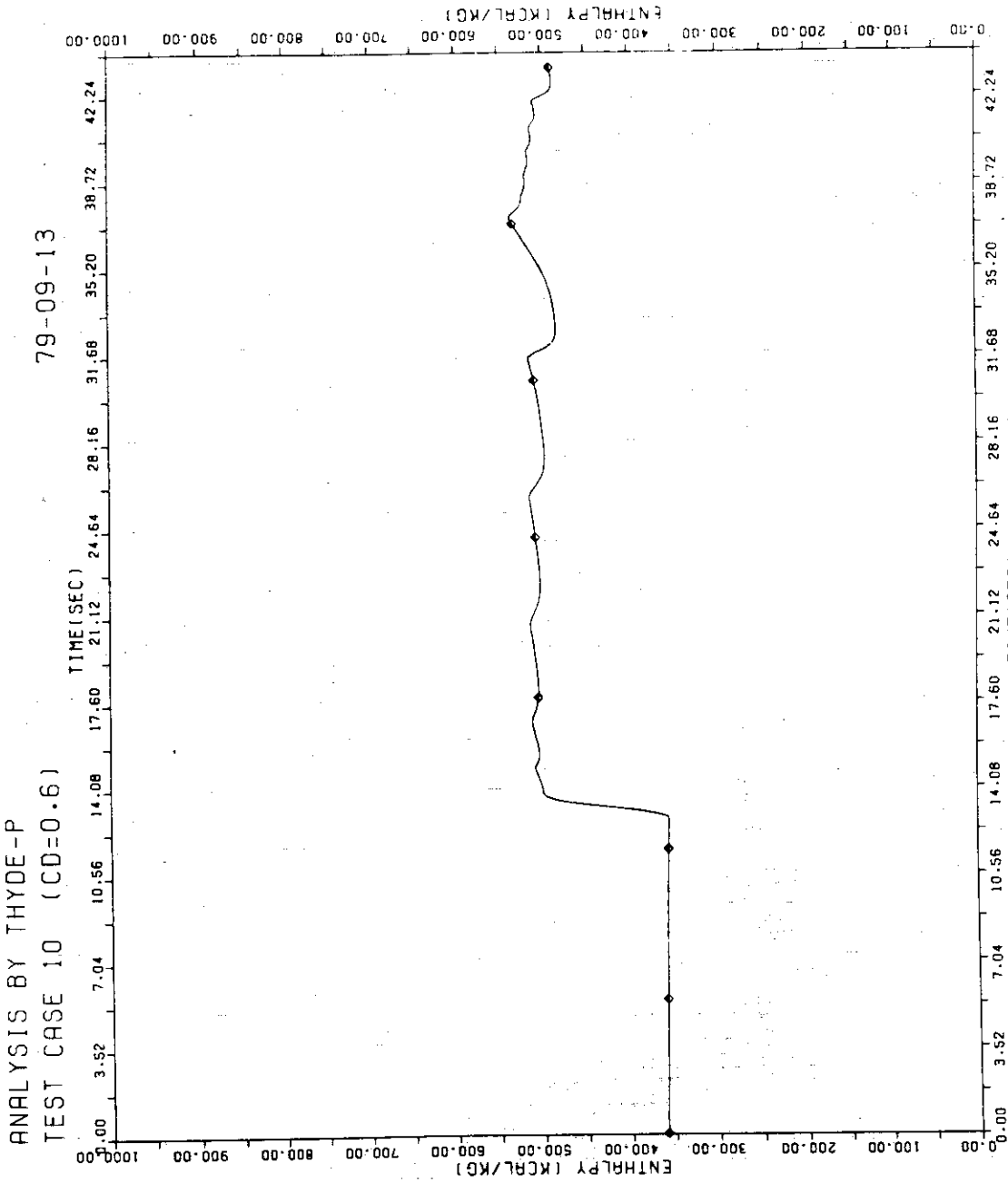

FIG. 7 - 30 ENTHALPY AT 25A

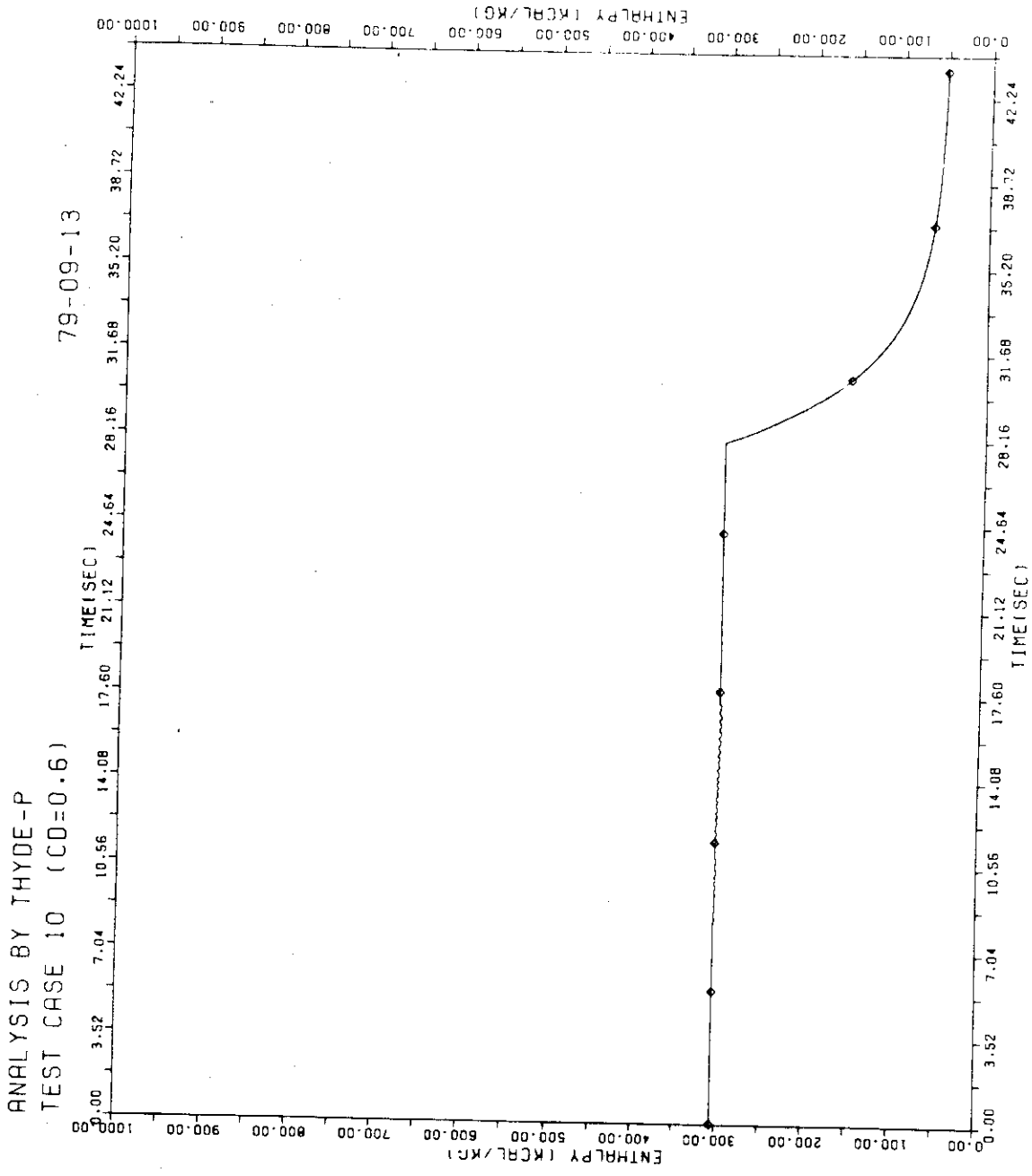

FIG. 7-31 ENTHALPY AT 27A

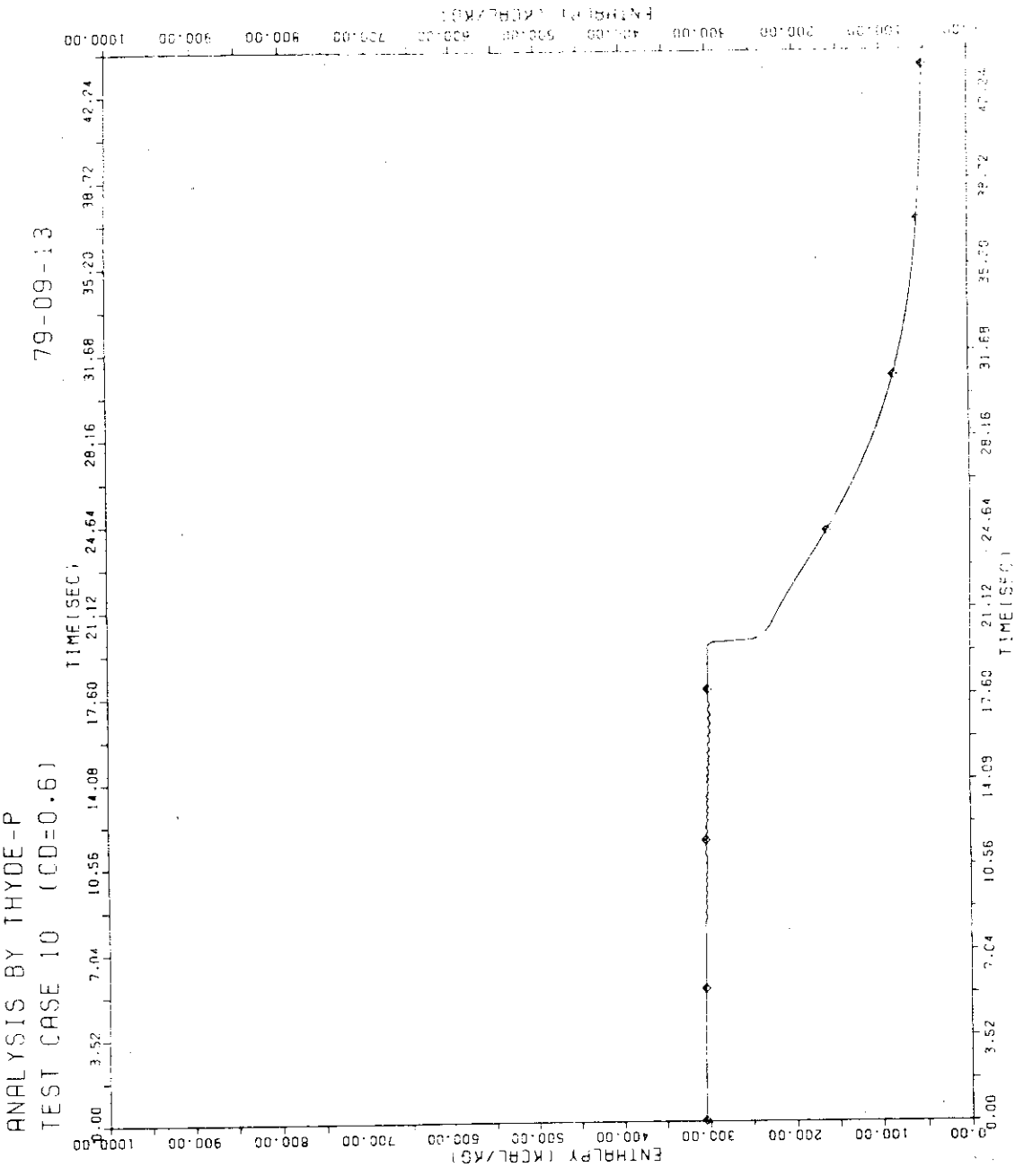

FIG. 7-32 ENTHALPY AT 28Q

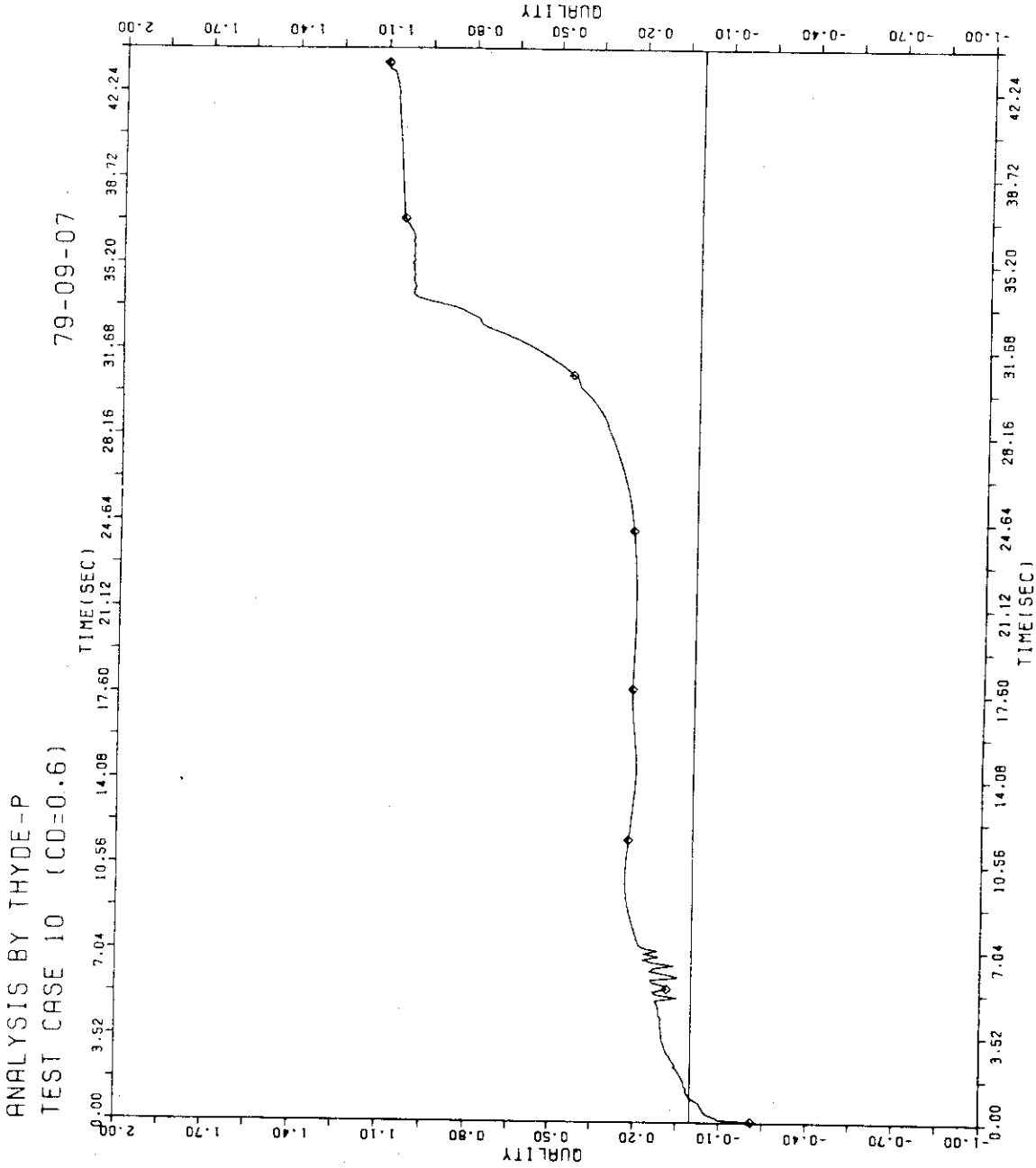

FIG. 7-33 QUALITY AT 4E

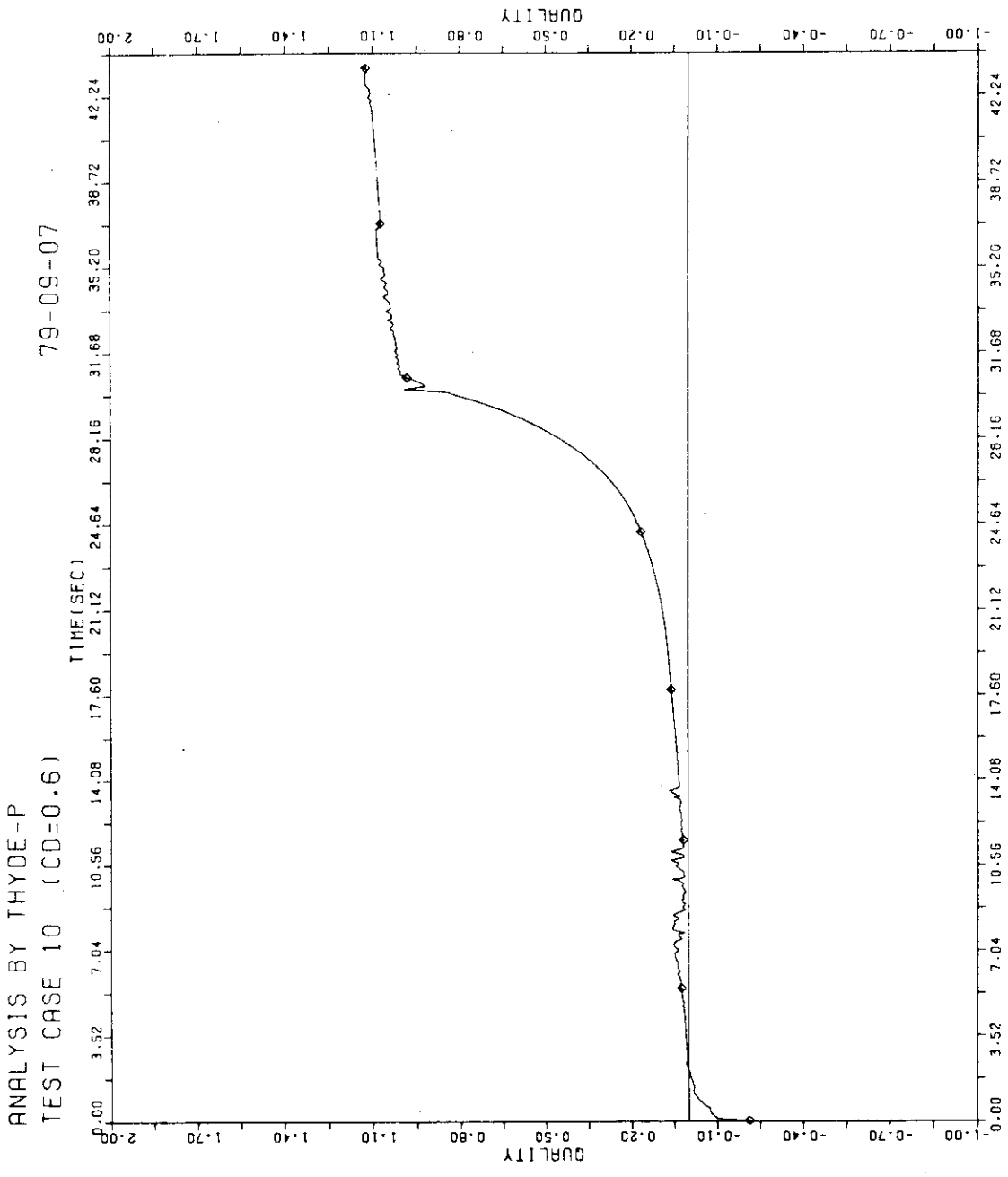

FIG. 7-34 QUALITY AT 1?F

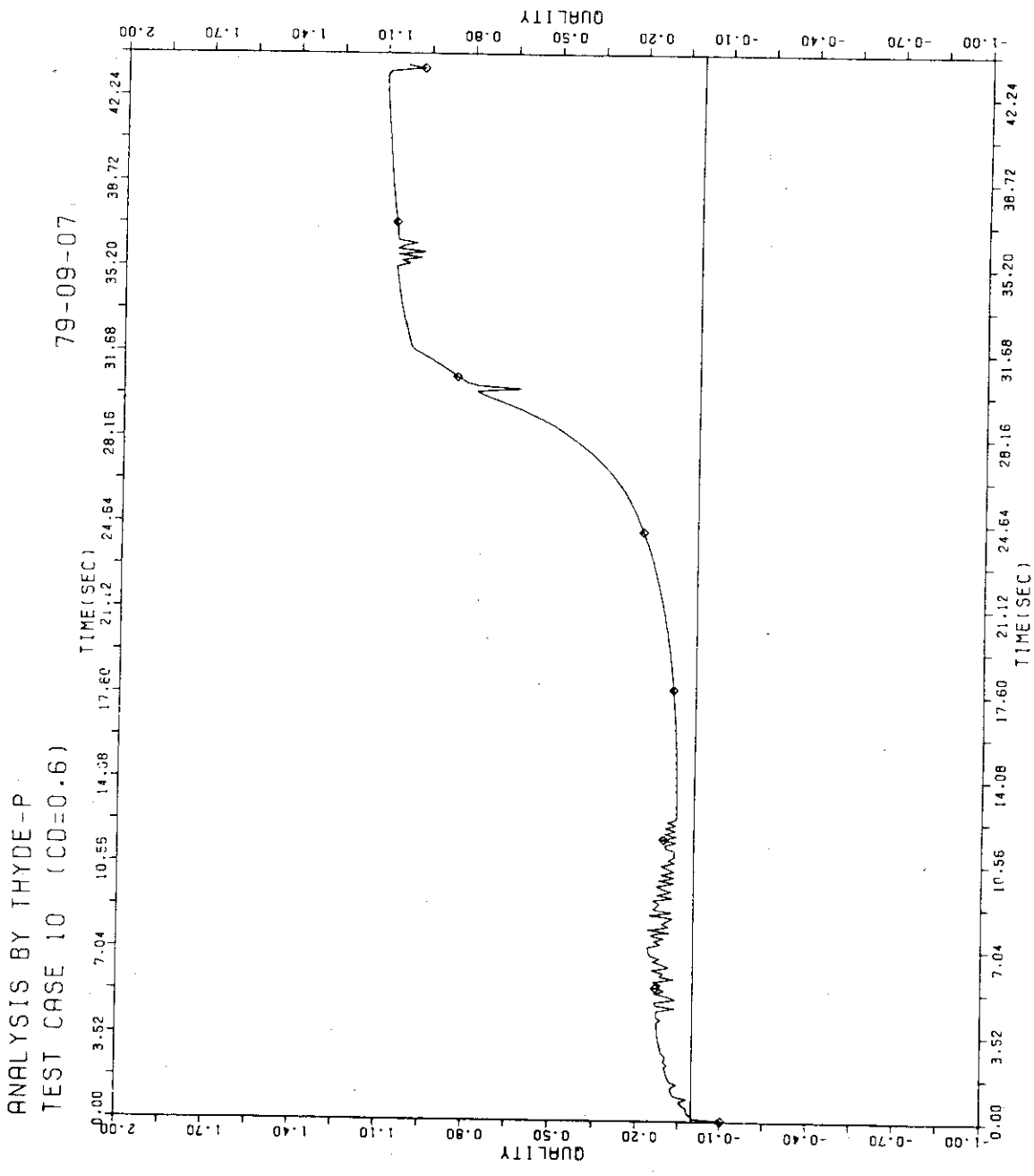

FIG. 7-35 QUALITY AT 11E

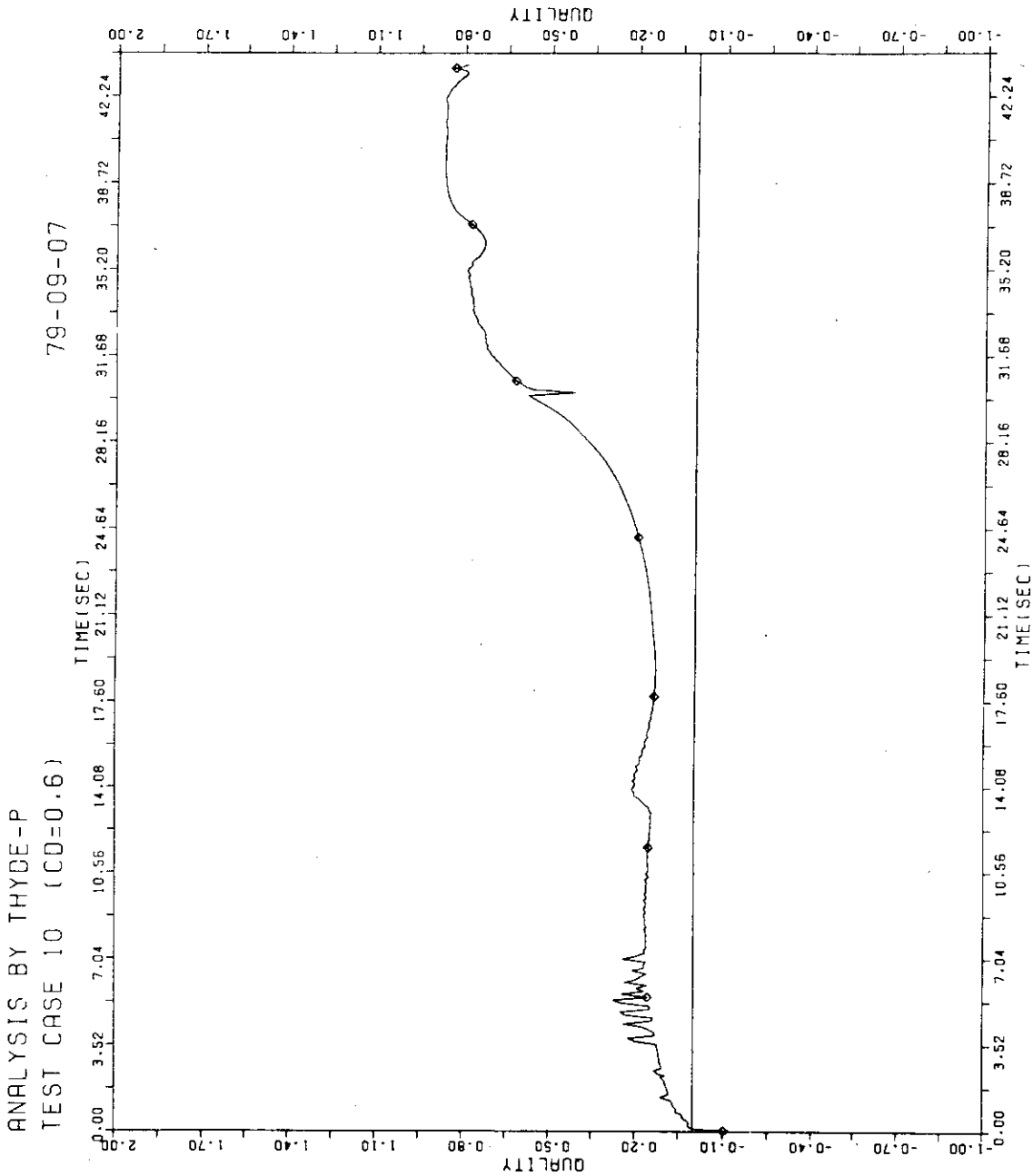

FIG. 7-36 QUALITY AT 10A

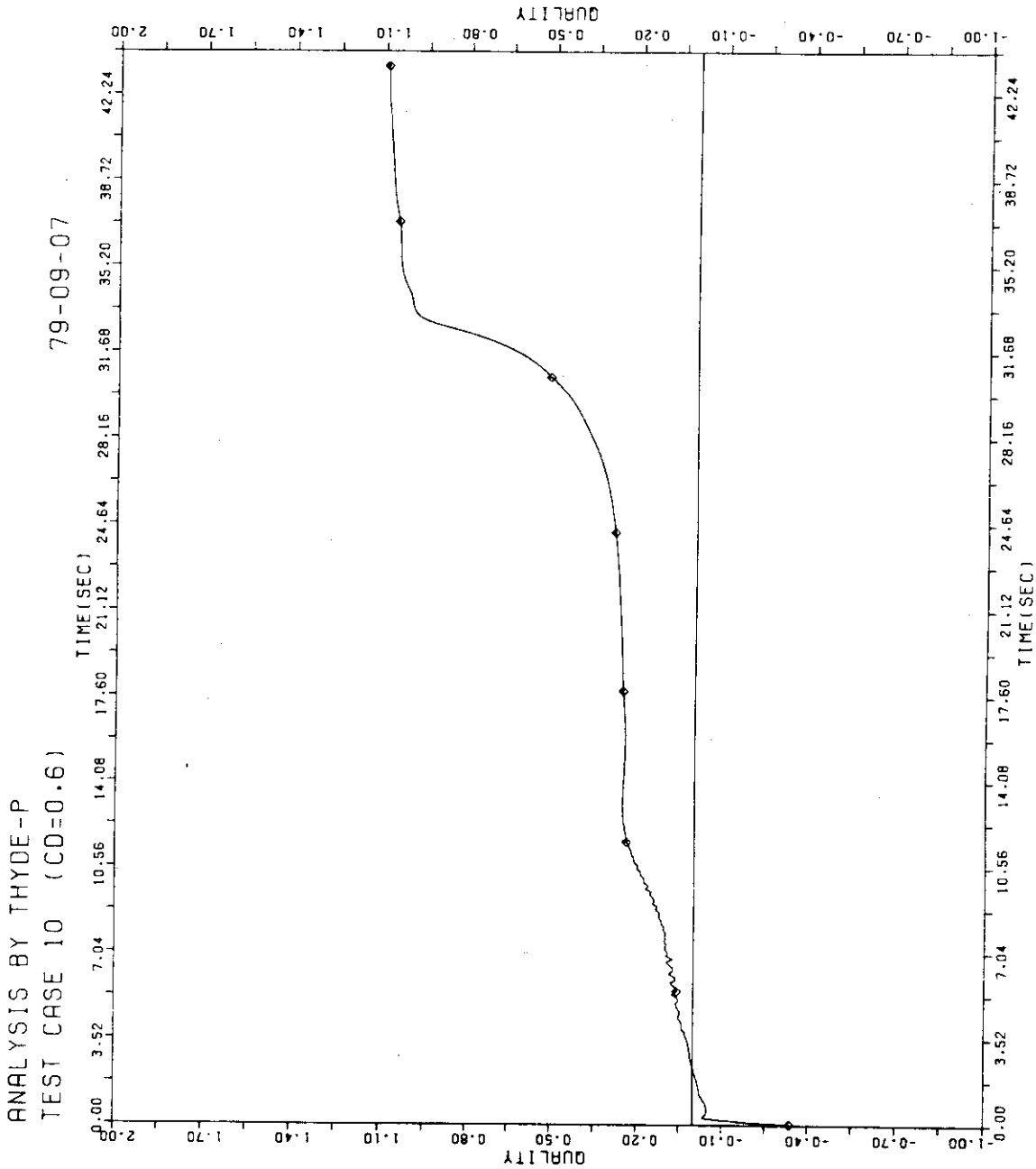

FIG. 7-37 QUALITY AT 8E

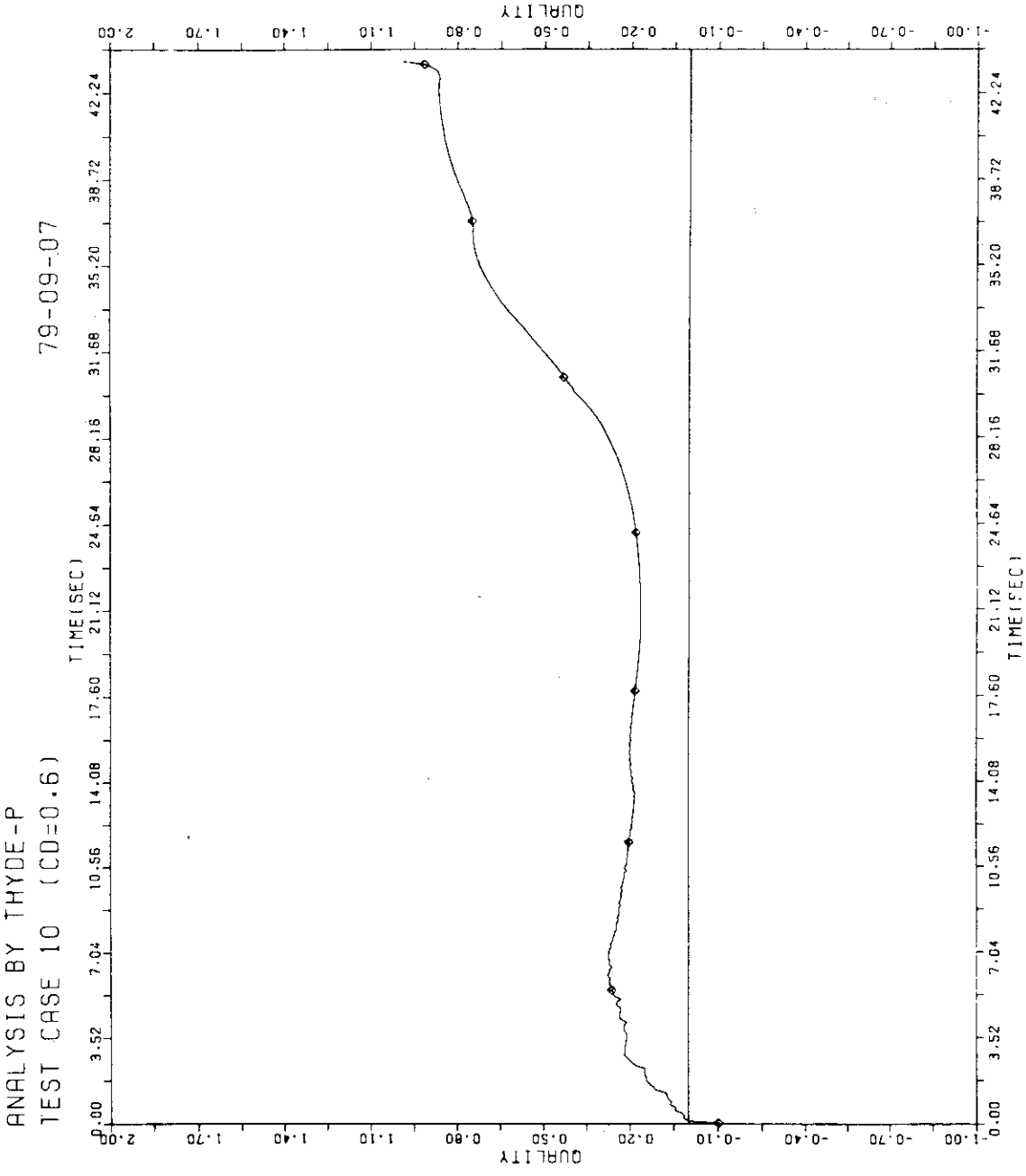

FIG. 7 - 38 QUALITY AT 1A

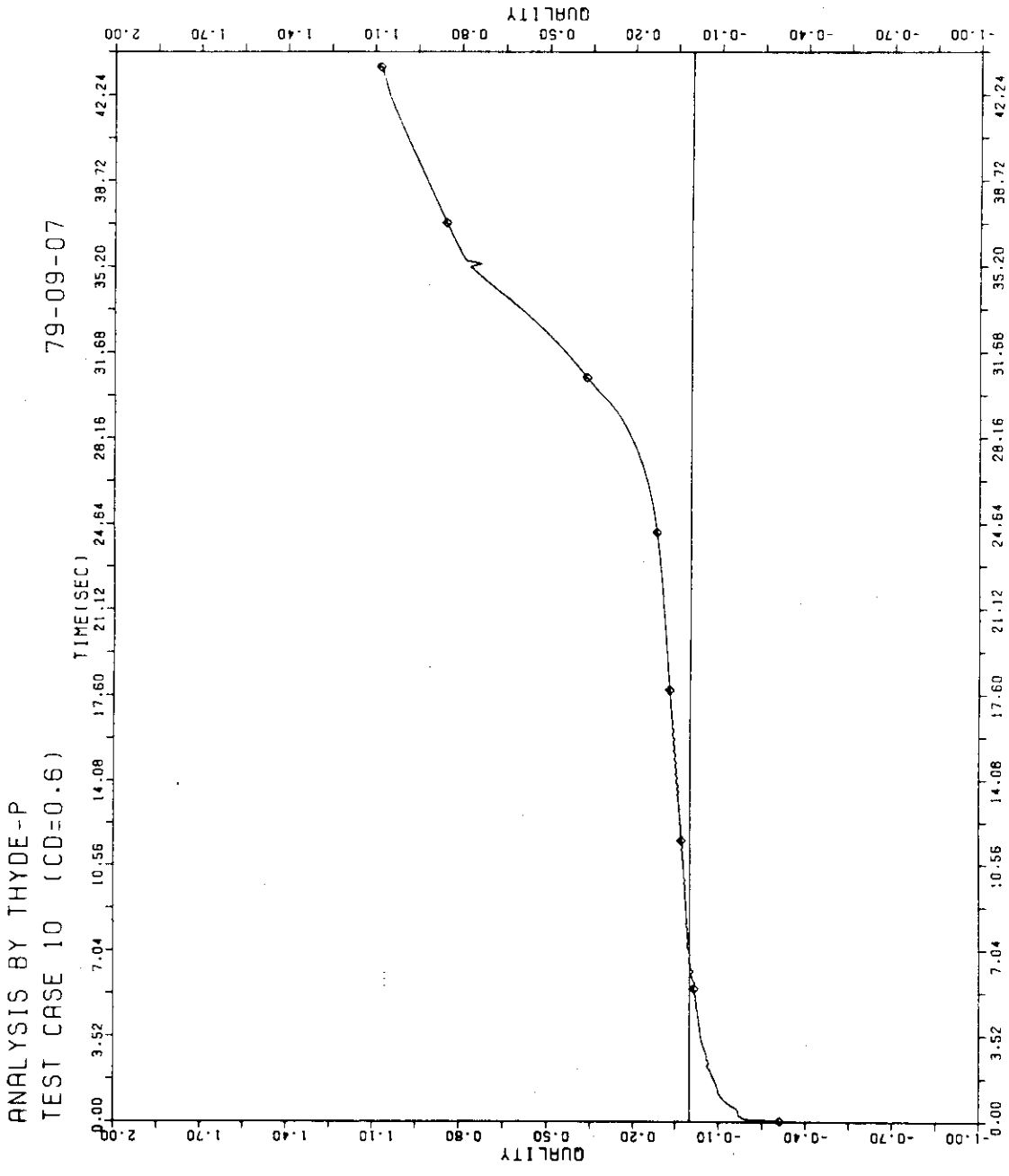

FIG. 7-39 QUALITY AT 17A

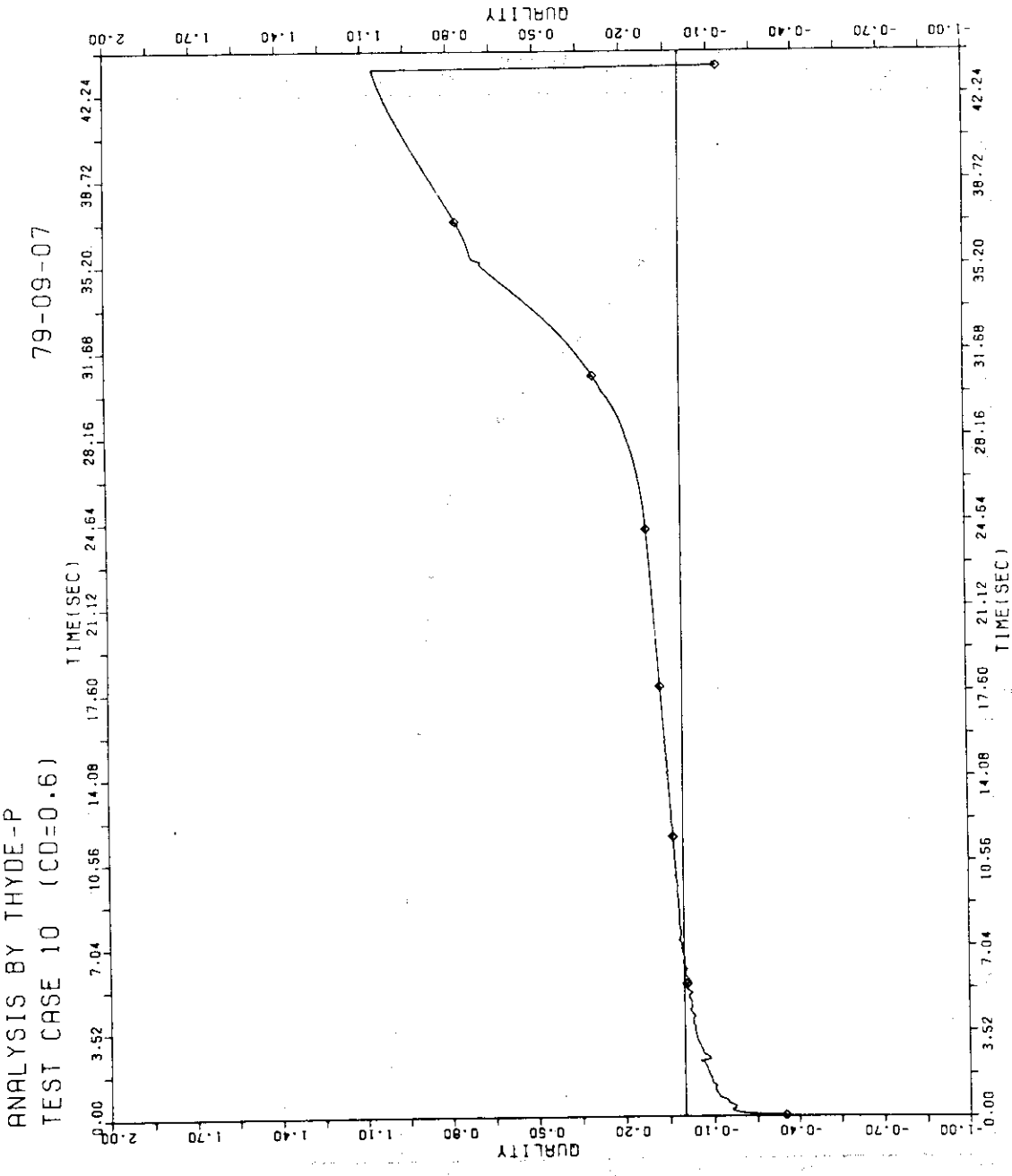

FIG. 7-40 QUALITY AT 18E

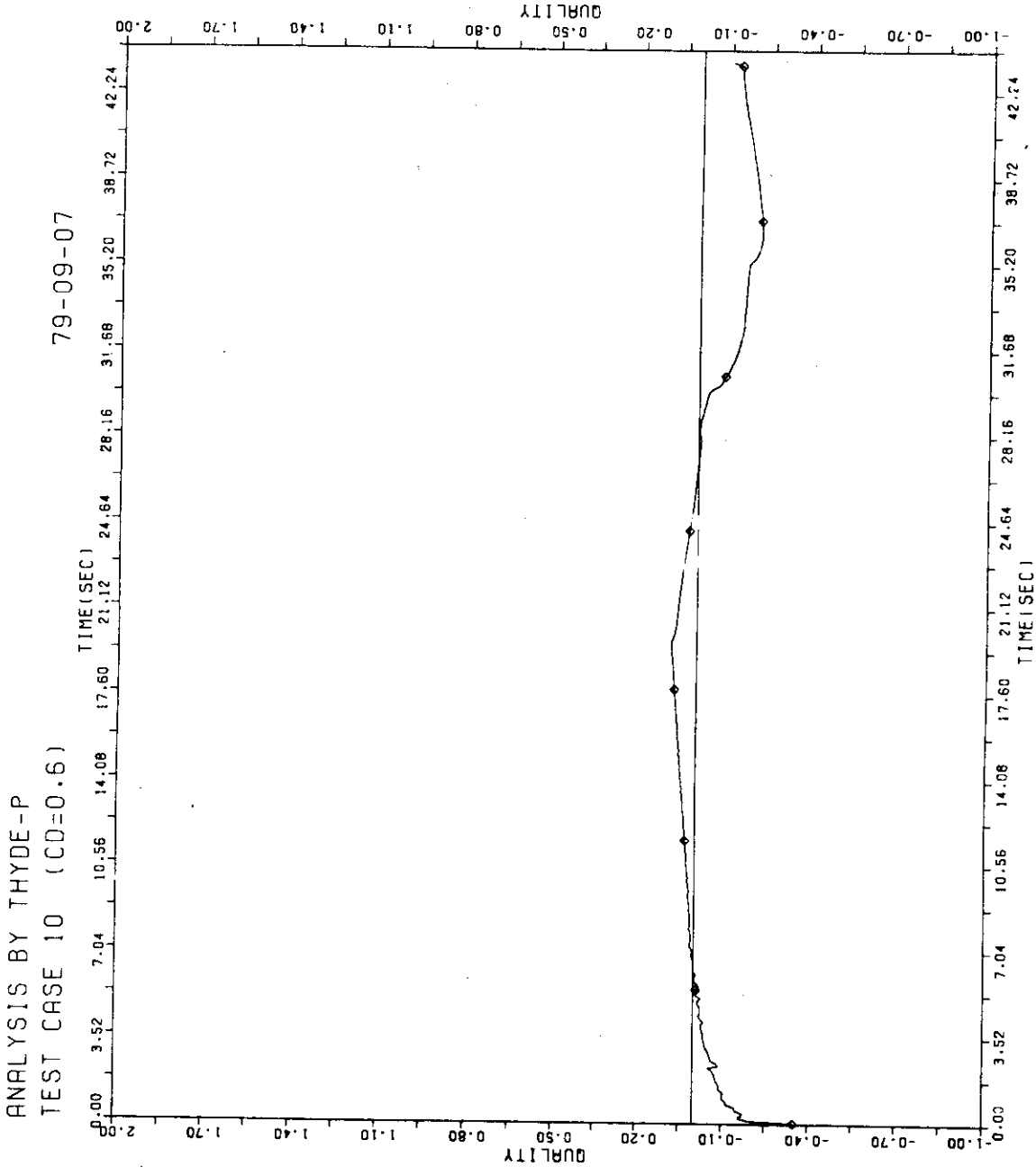

FIG. 7 - 41 QUALITY AT 19A

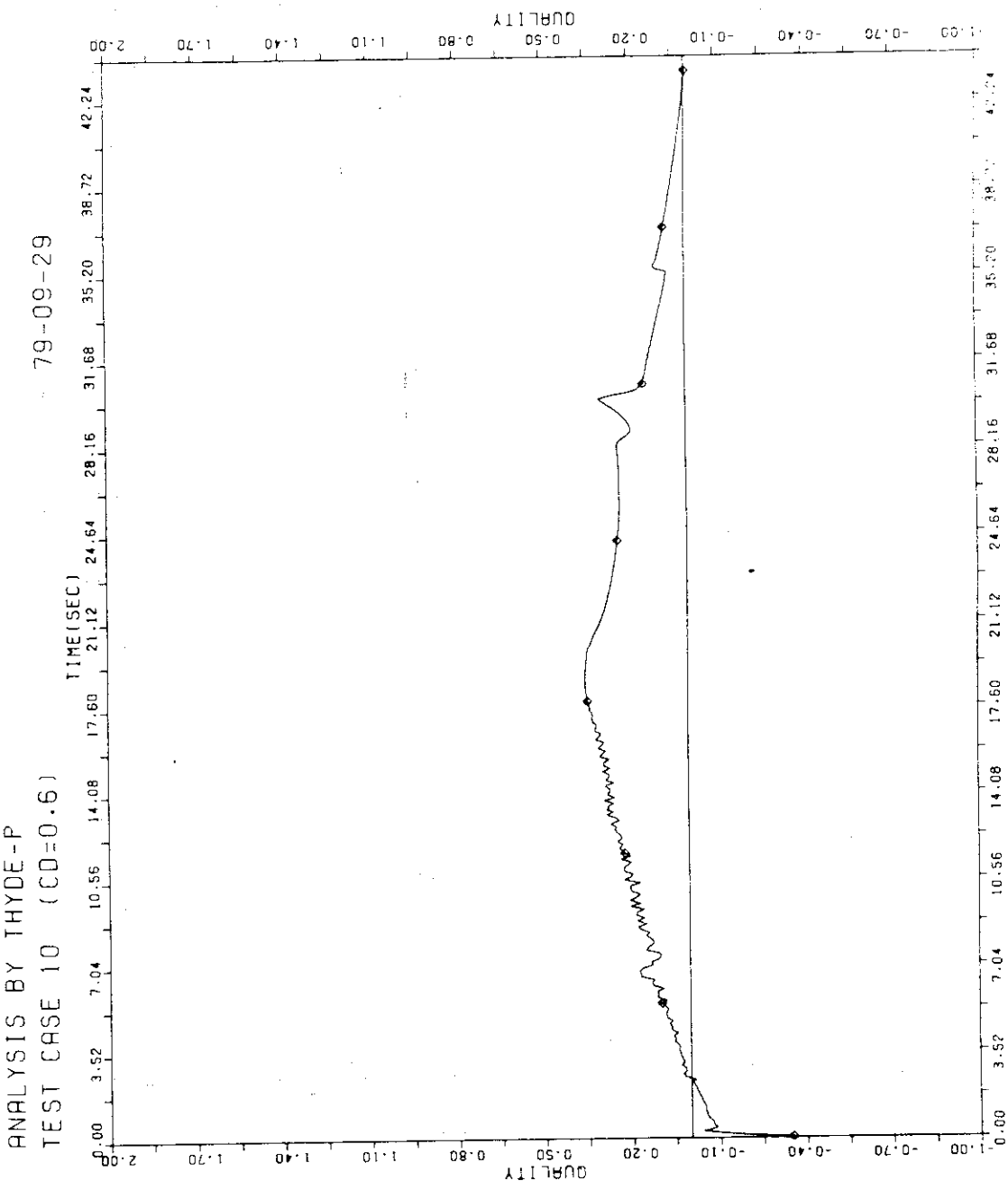

FIG. 7-42 QUALITY AT 9A

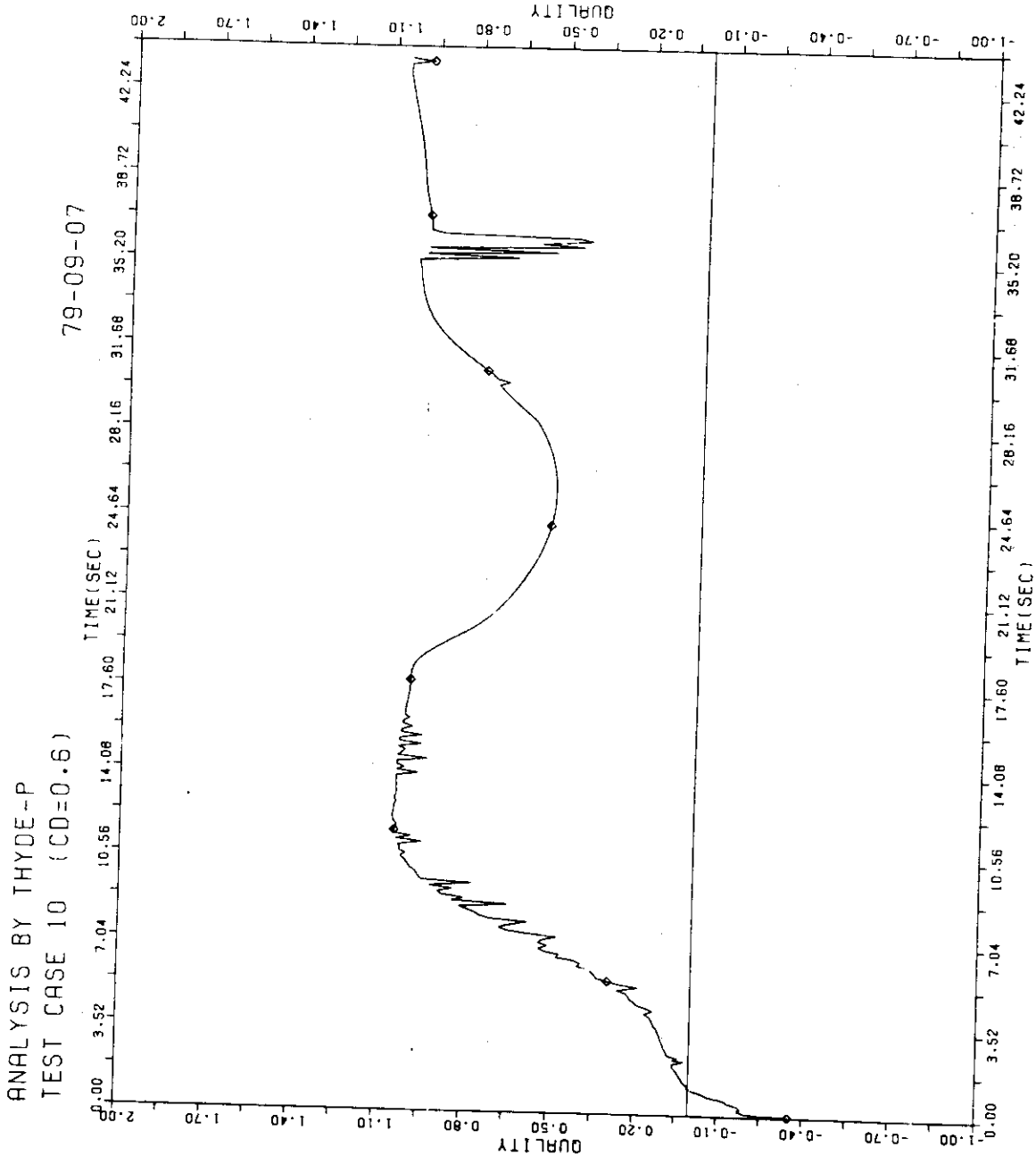

FIG. 7-43 QUALITY AT 21A

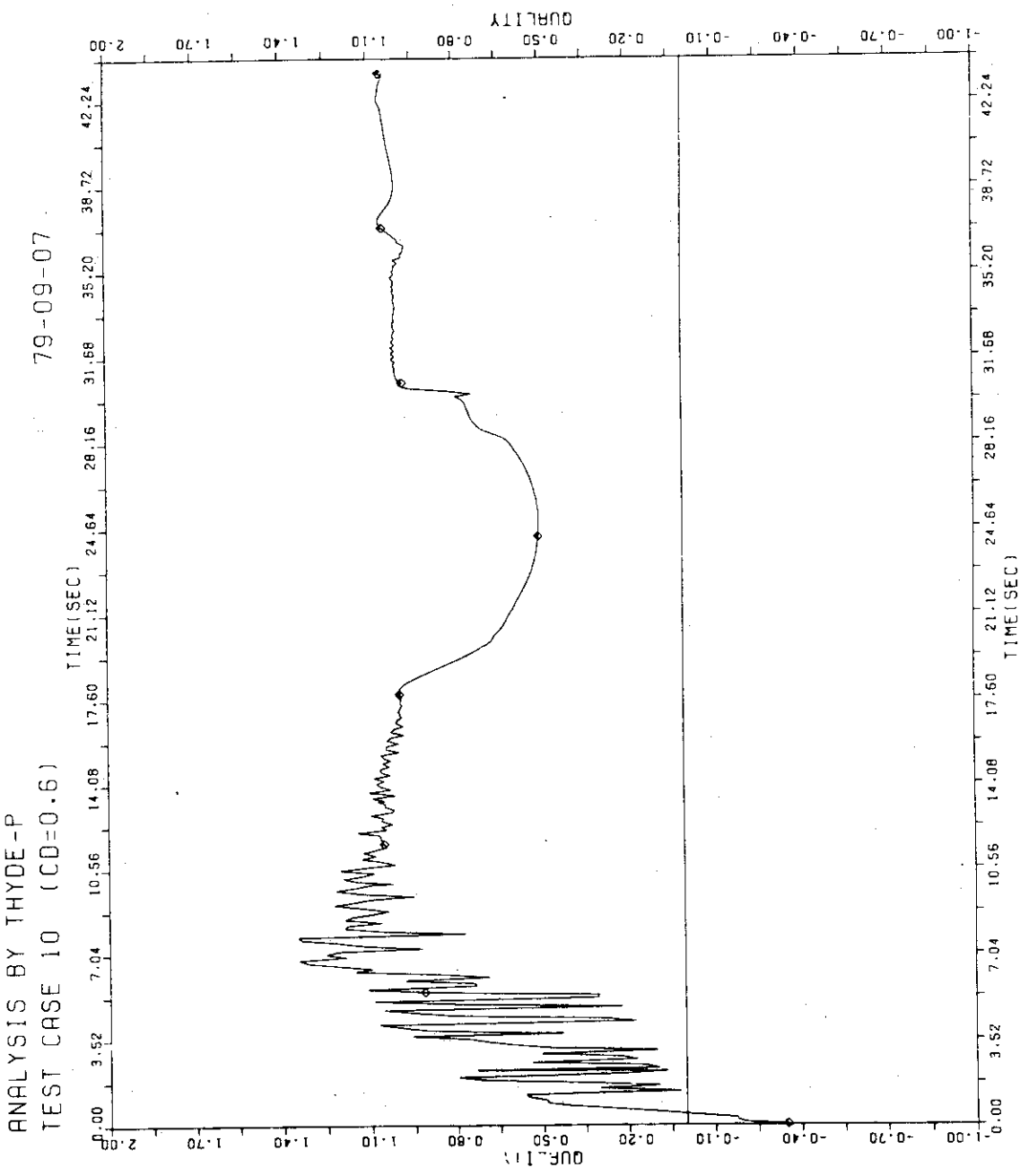

FIG. 7-44 QUALITY AT 22A

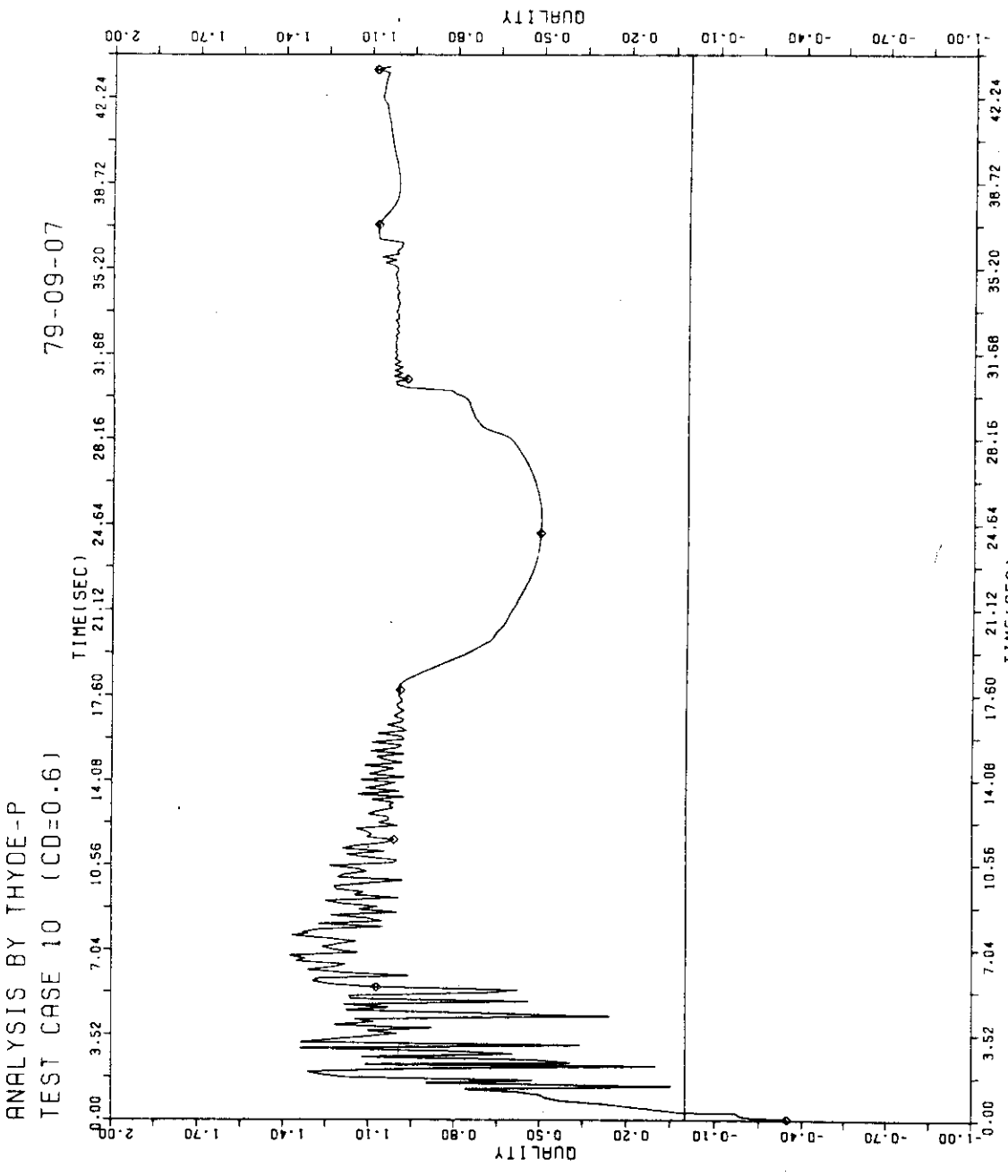

FIG. 7-45 QUALITY AT 23A

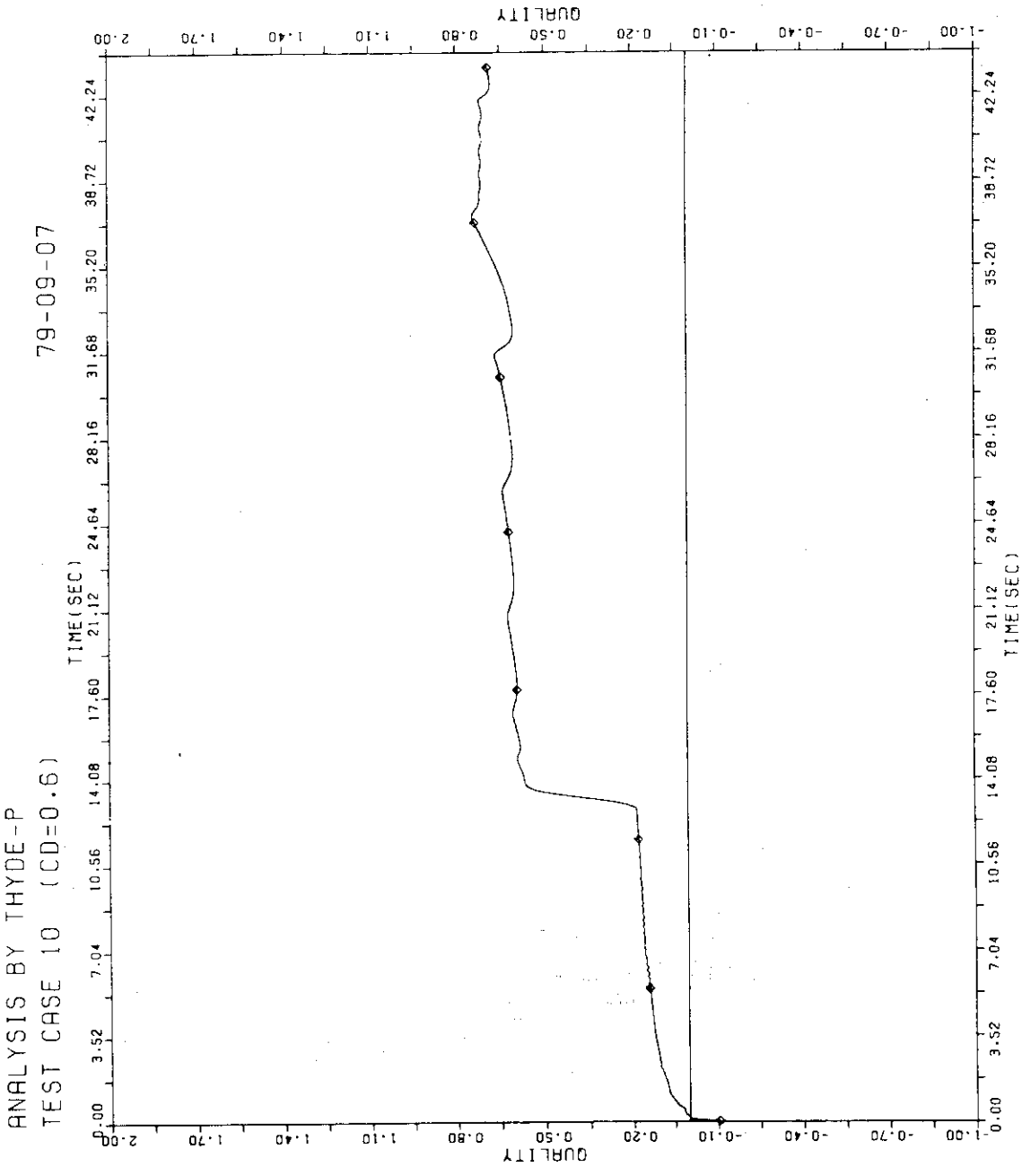

FIG. 7 - 46 QUALITY AT 25A

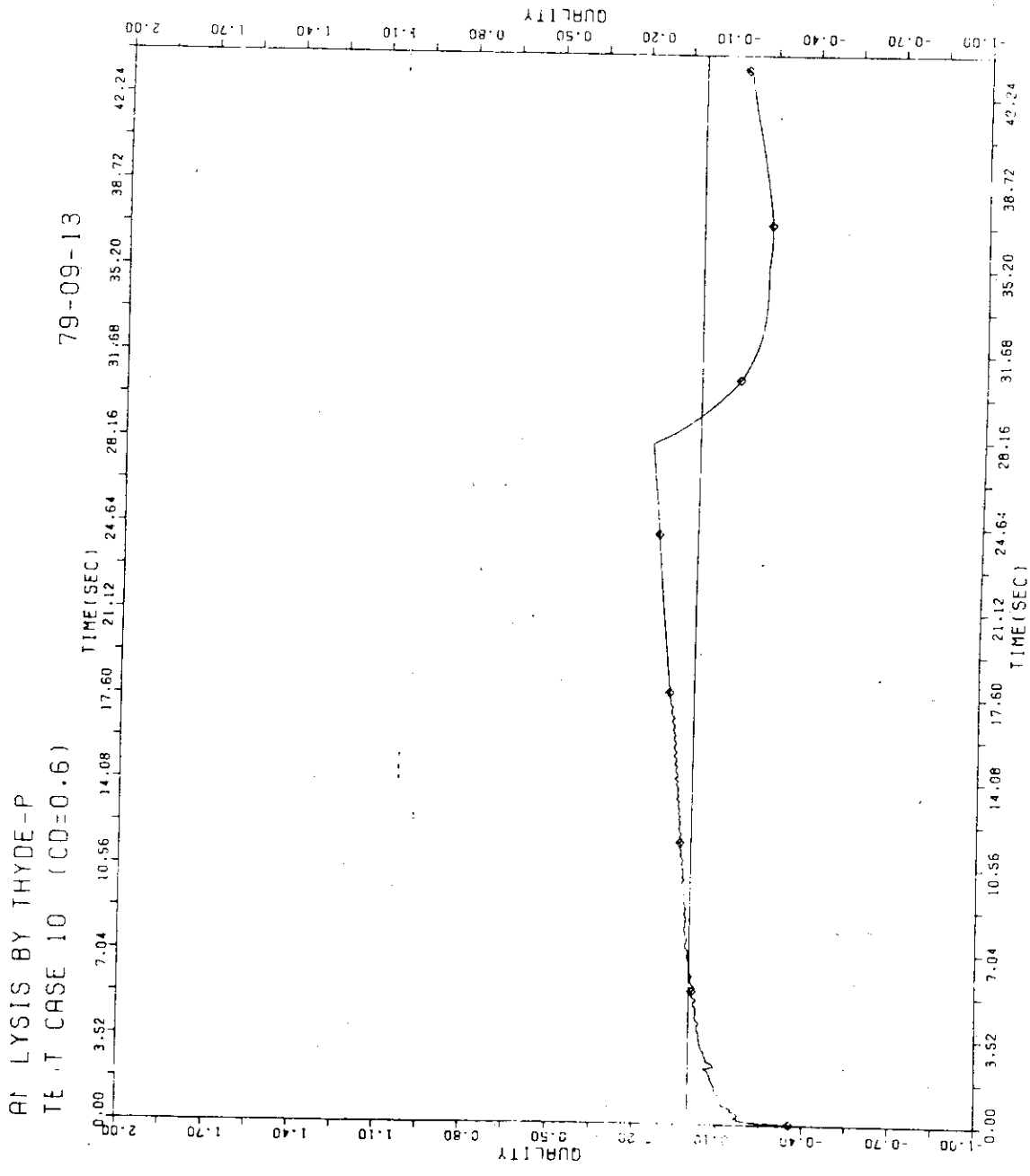

FIG. 7-47 QUALITY AT 27A

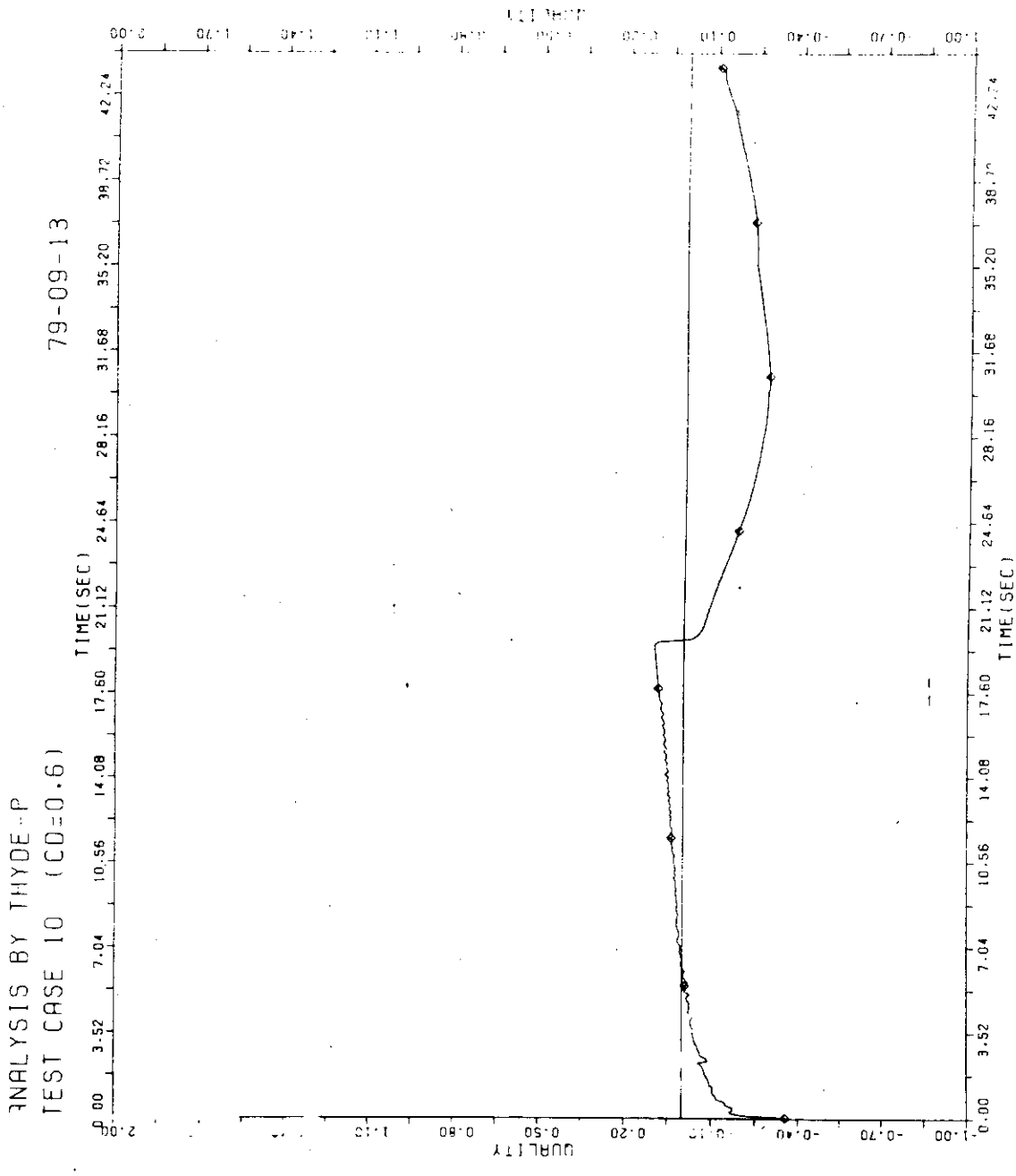
ANALYSIS BY THYDE-P
TEST CASE 10 (CD=0.6)
79-09-13
TIME(SEC)
QUALITY AT 28A

FIG. 7-48

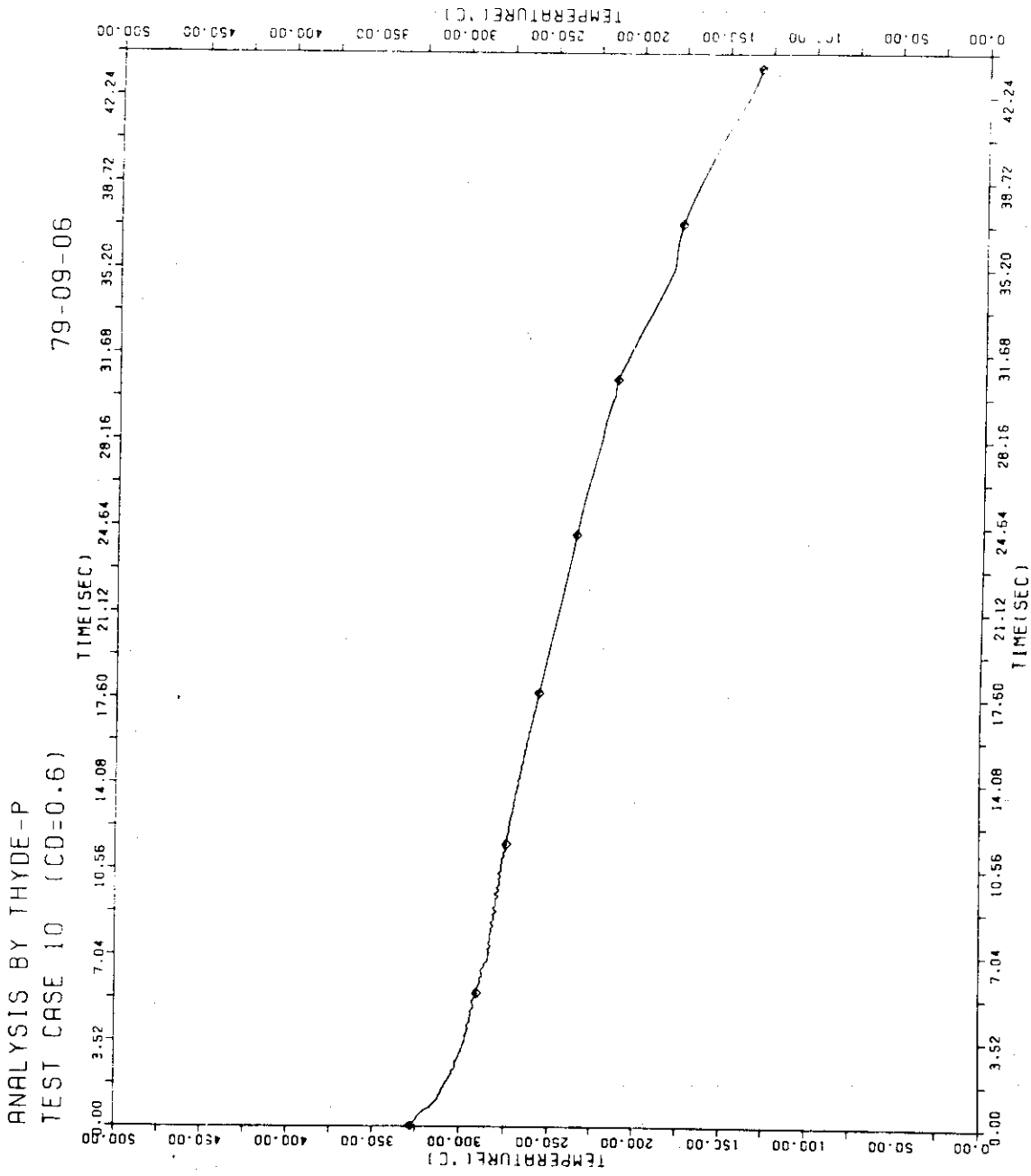

FIG. 7-49 TEMPERATURE AT NODE 10

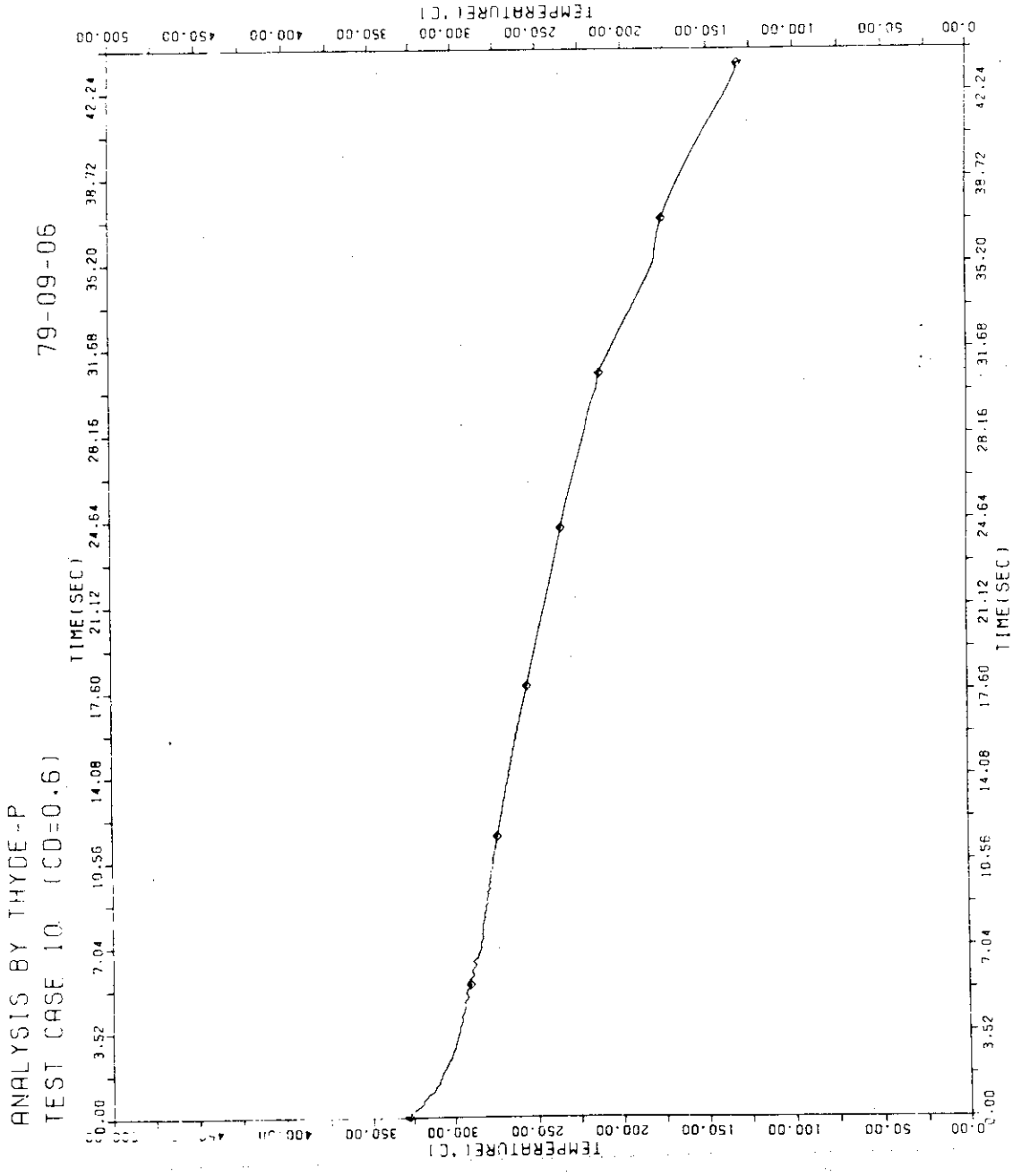

FIG. 7-50 TEMPERATURE AT NODE 1

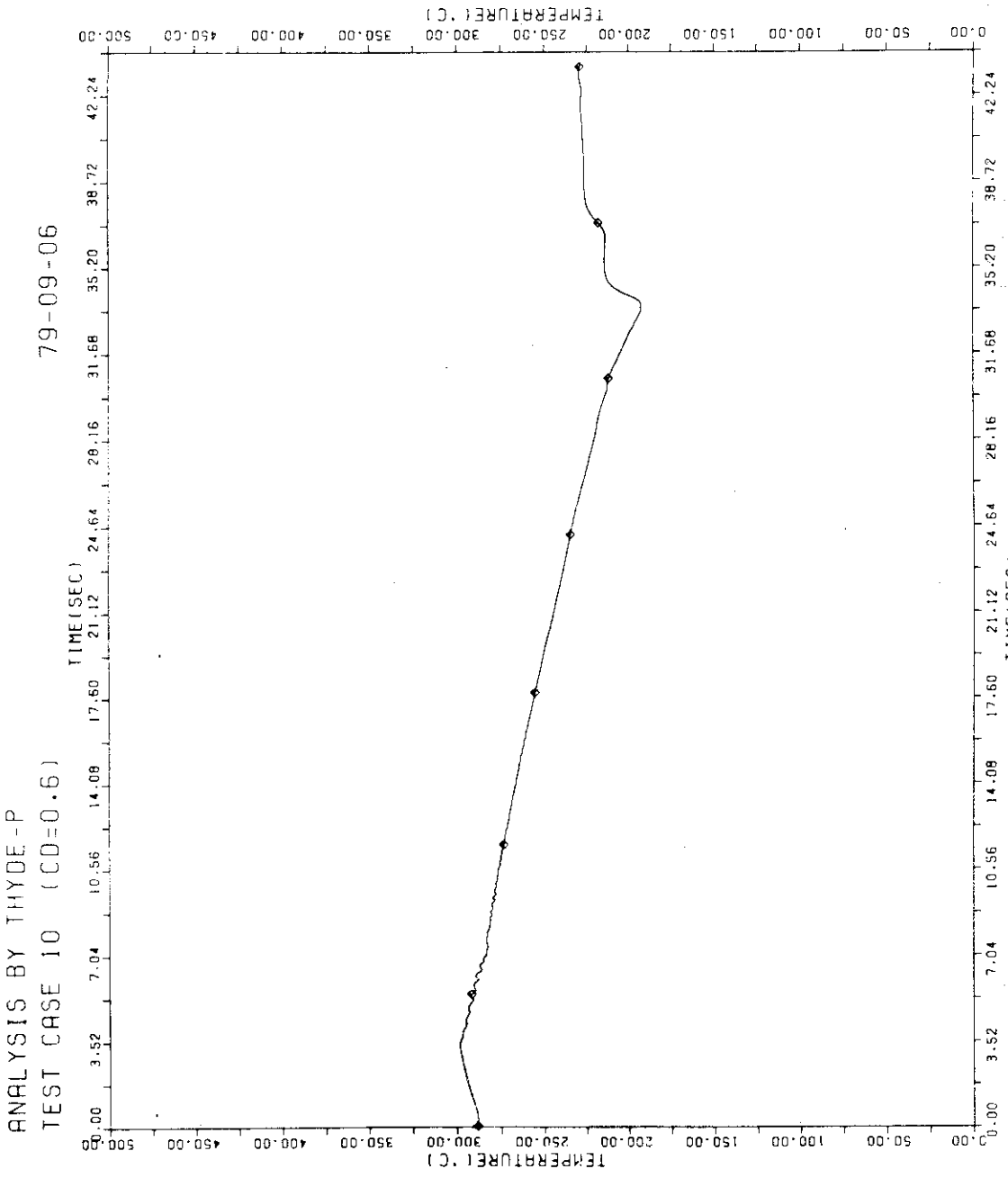

FIG. 7- 51 TEMPERATURE AT NODE 6

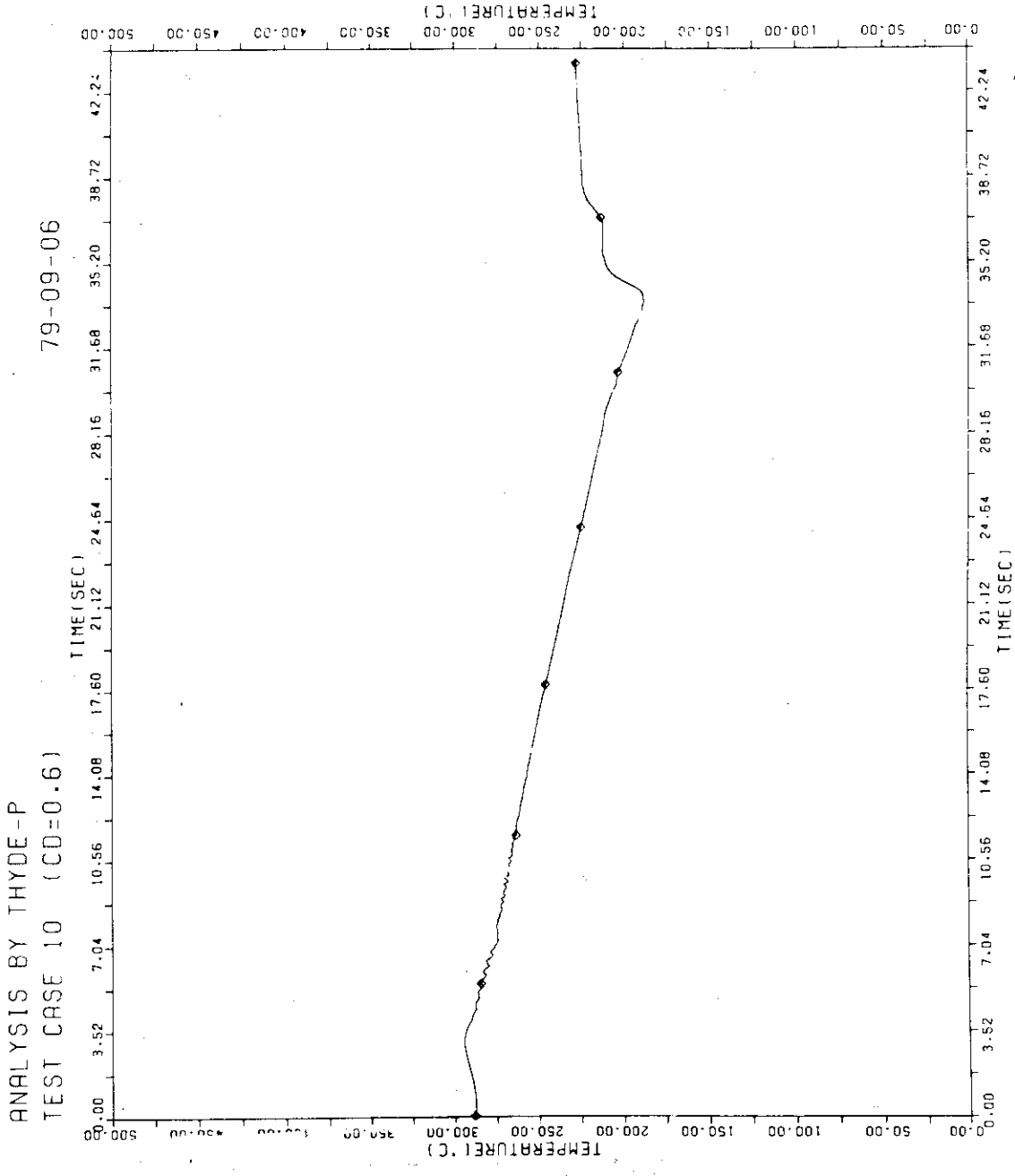

FIG. 7-52 TEMPERATURE AT NODE 8

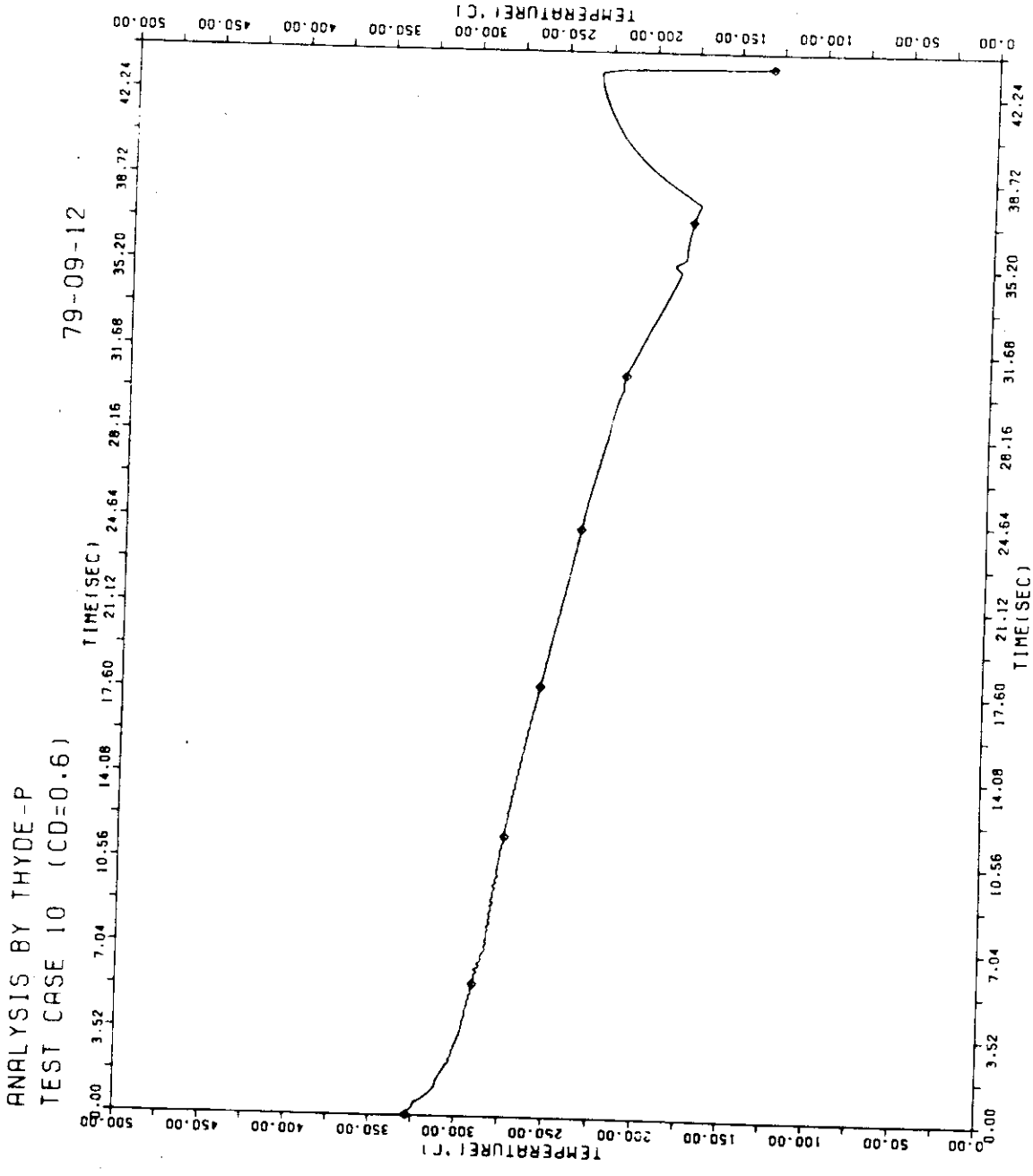

FIG. 7 - 53 TEMPERATURE AT NODE 11

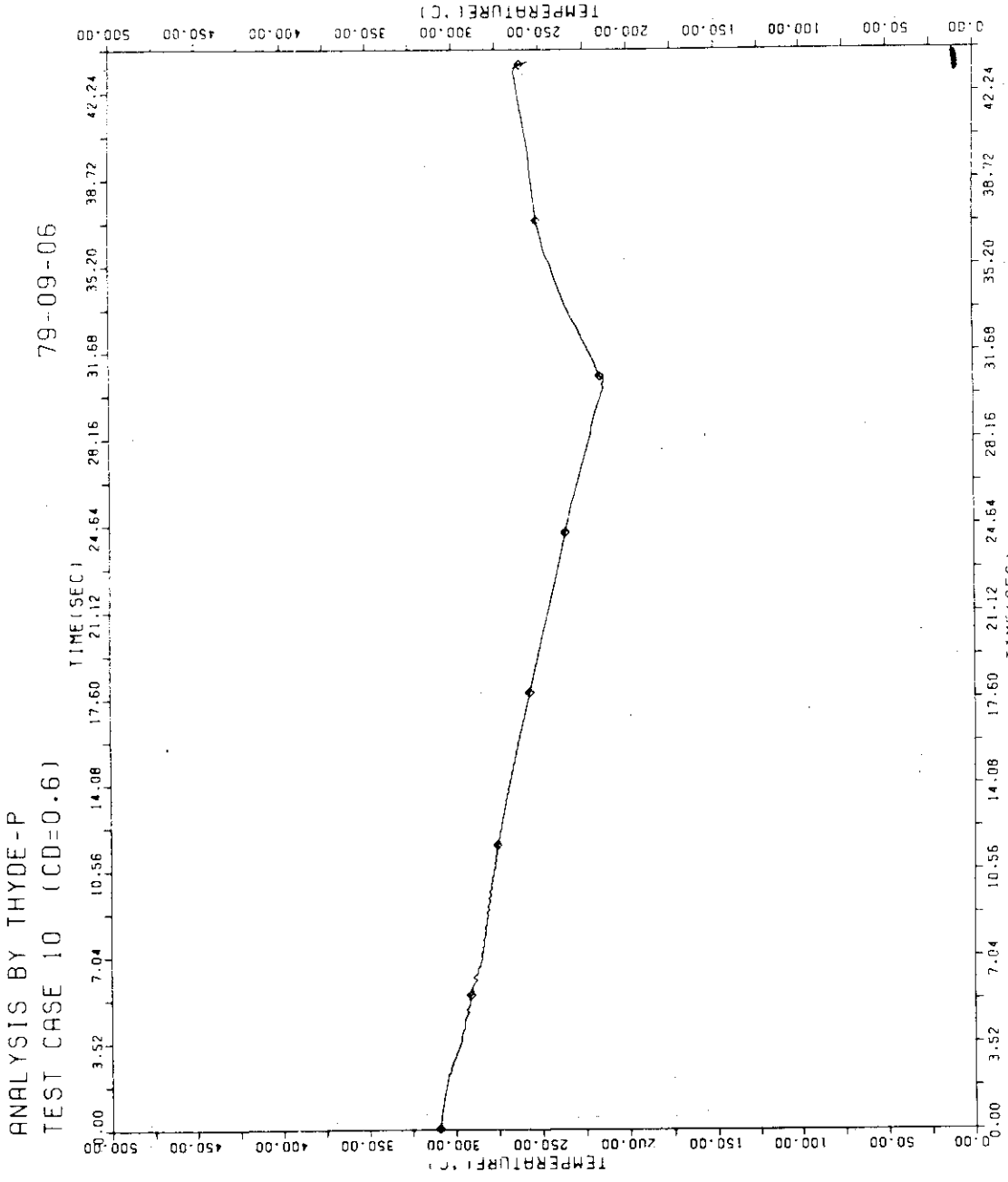

FIG. 7 - 54 TEMPERATURE AT NODE 13

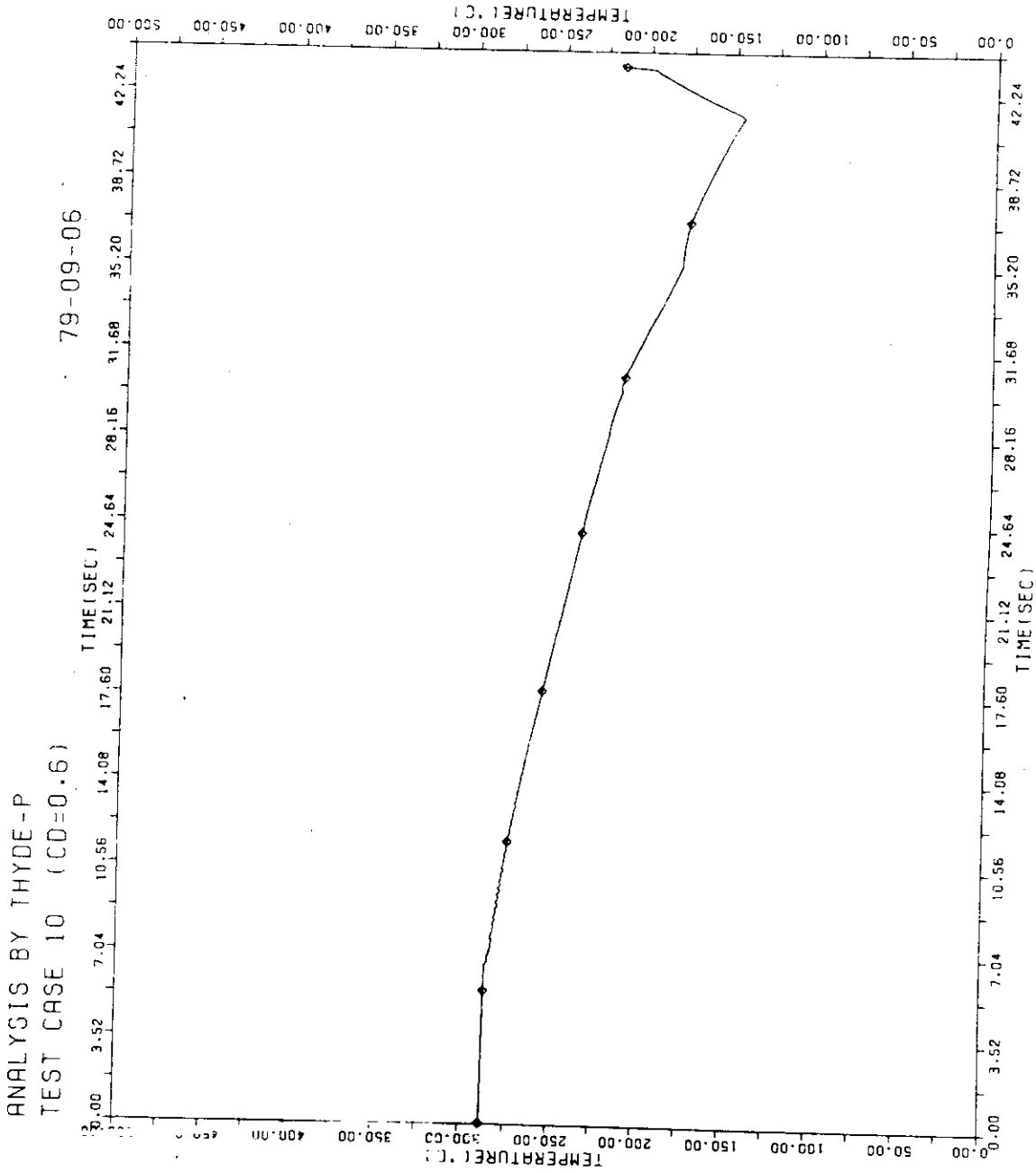

FIG. 7-55 TEMPERATURE AT NODE 17

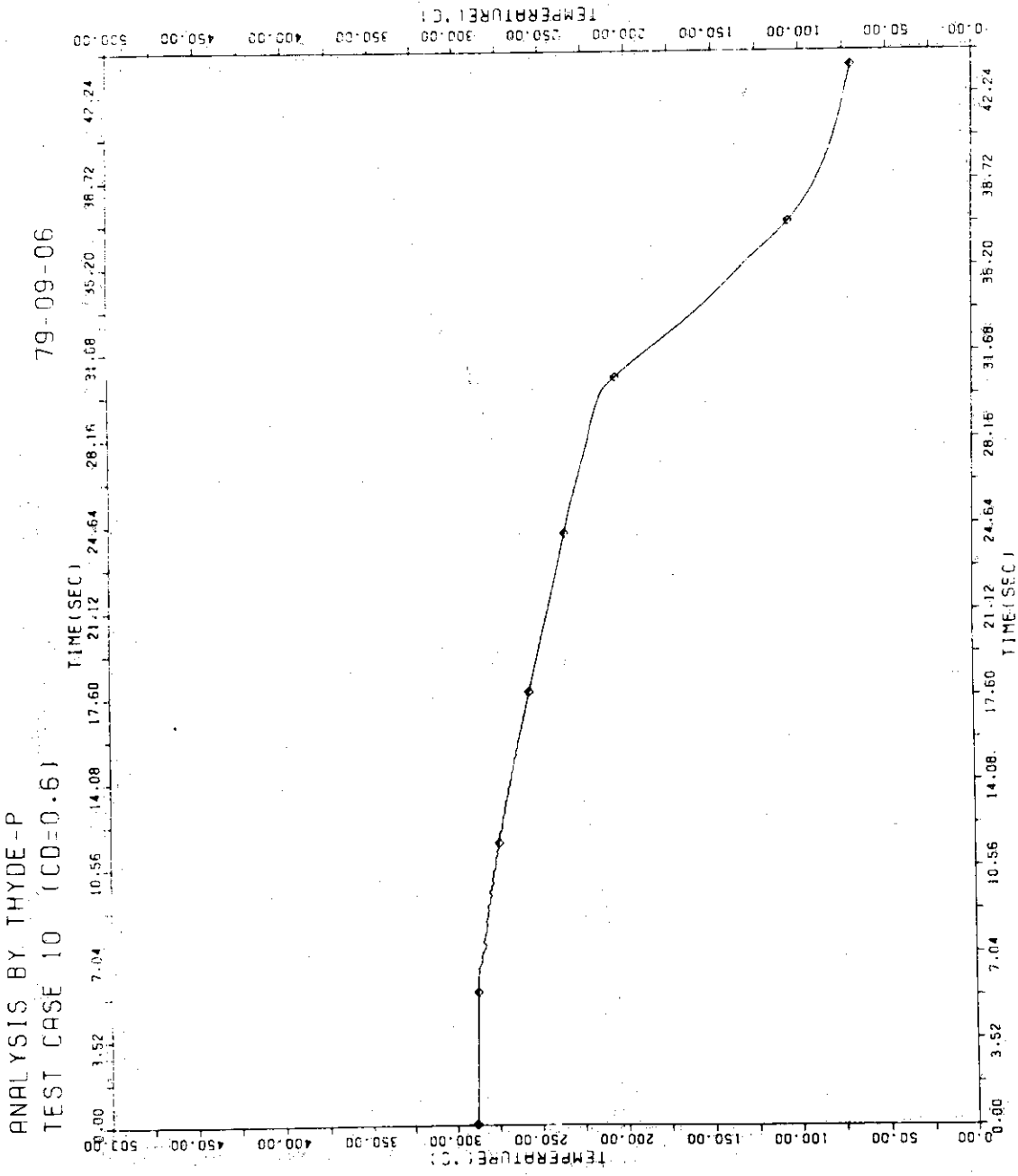

FIG. 7-56 TEMPERATURE AT NODE 19

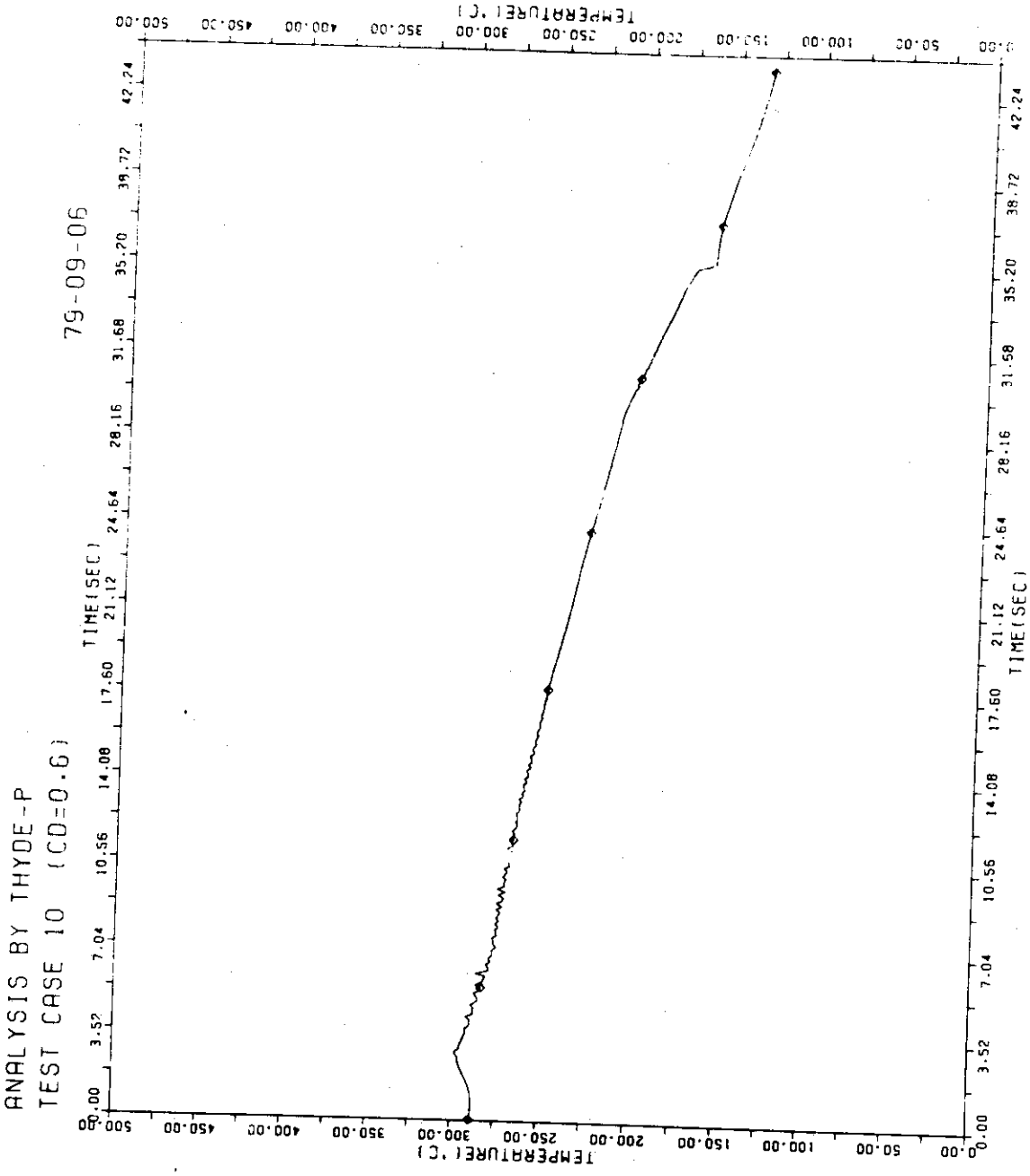

FIG. 7 - 57 TEMPERATURE AT NODE 9

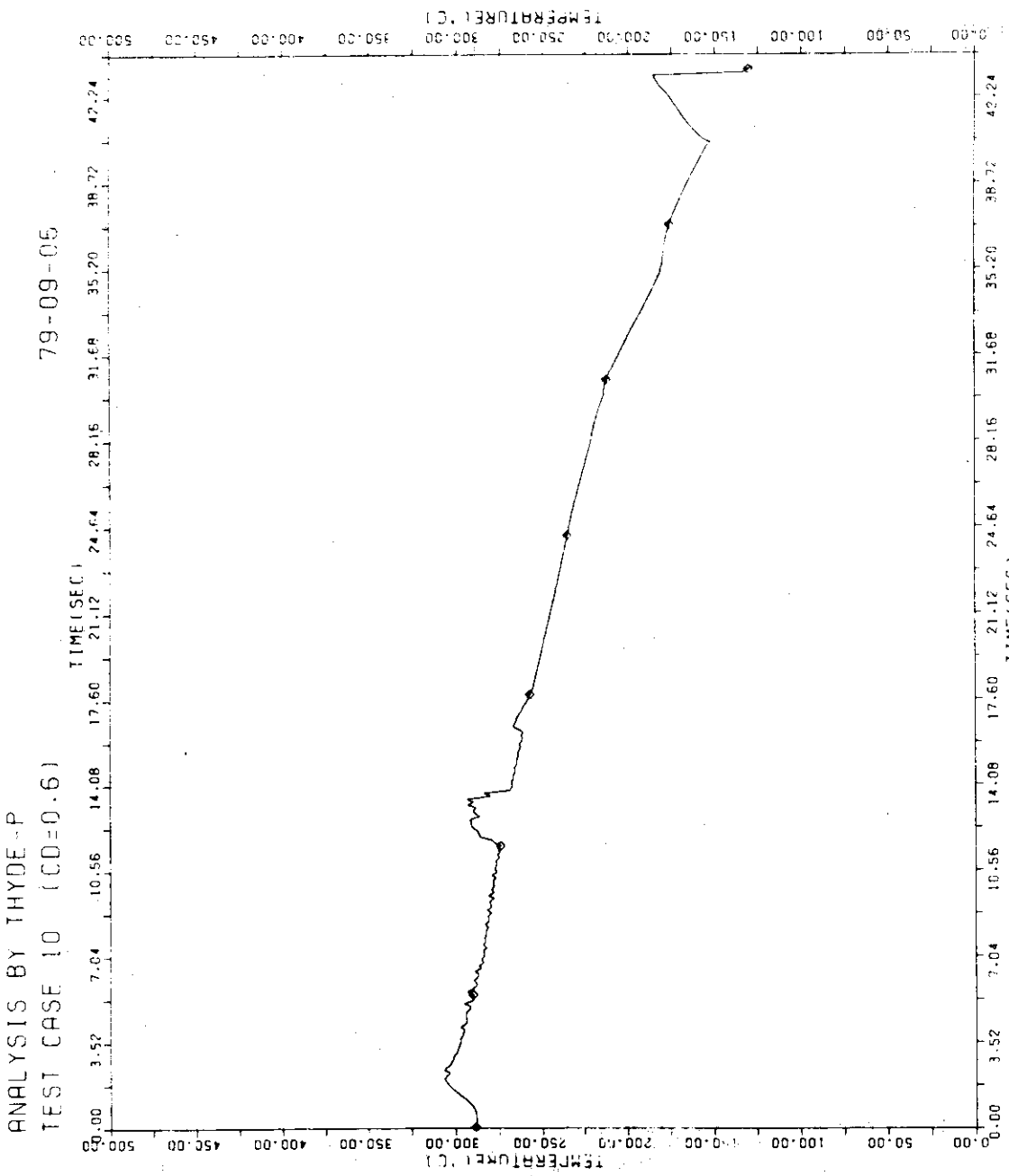

FIG. 7 - 58 TEMPERATURE AT NODE 20

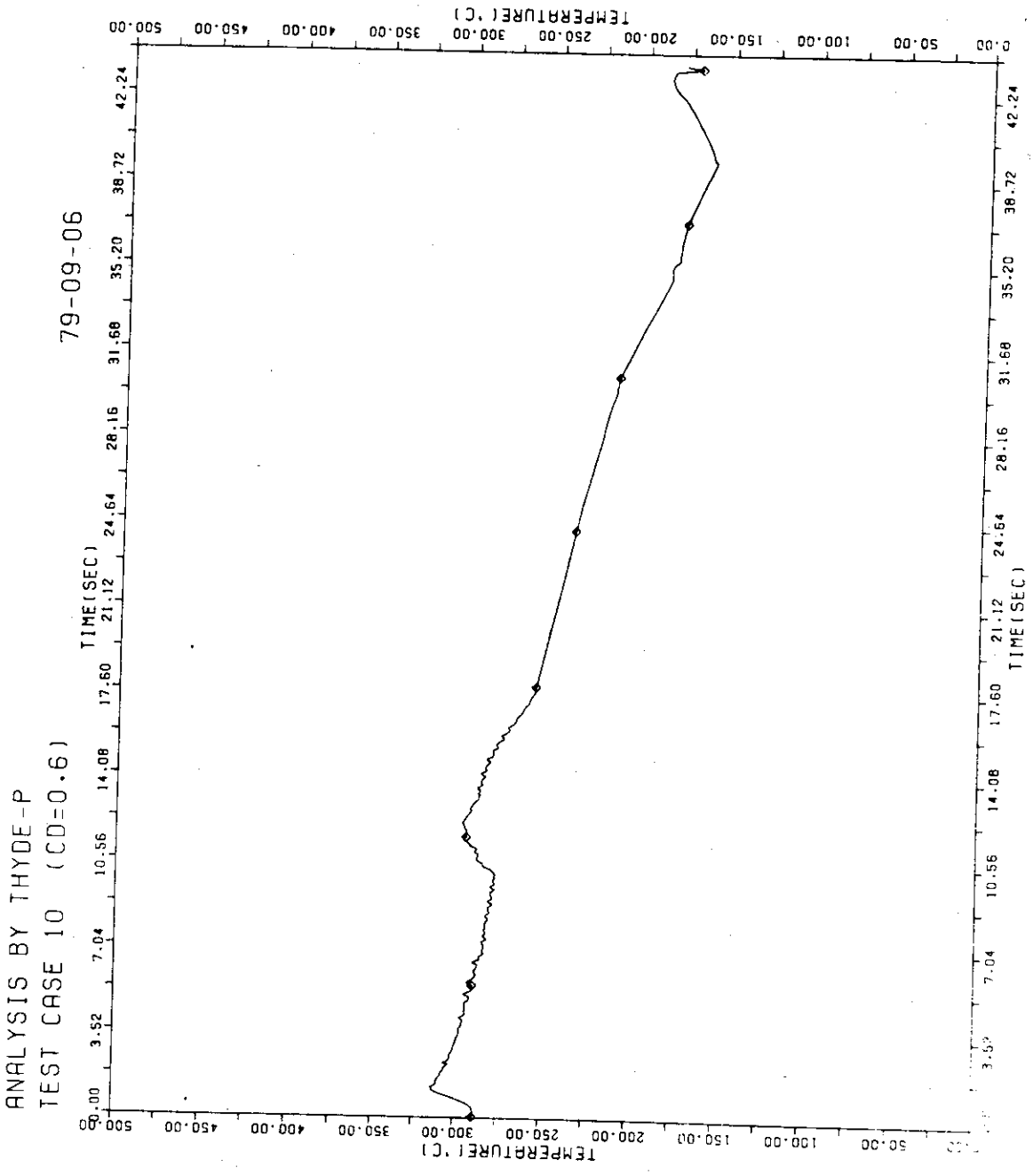

FIG. 7-59 TEMPERATURE AT NODE 21

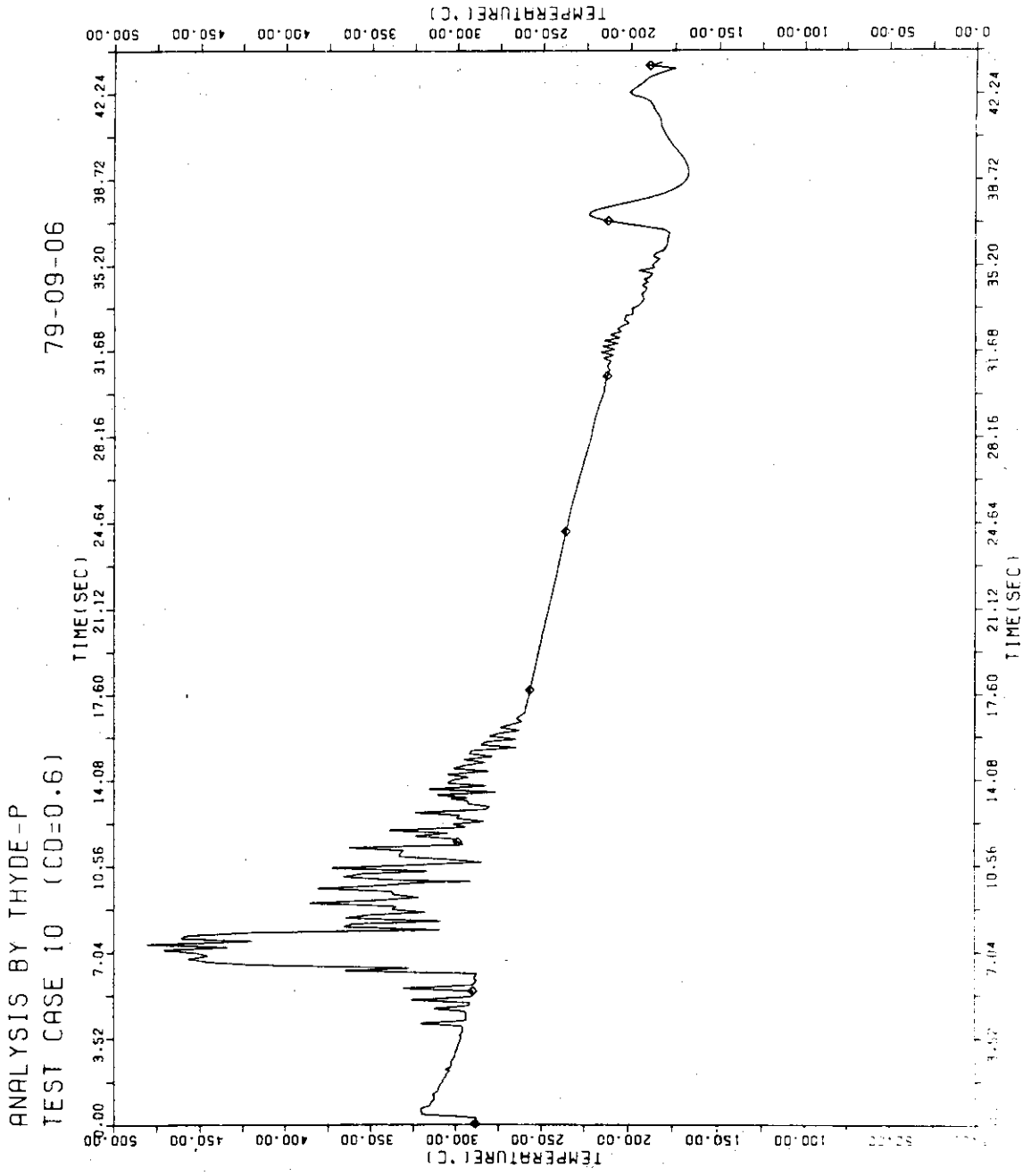

FIG. 7 60 TEMPERATURE AT NODE 22

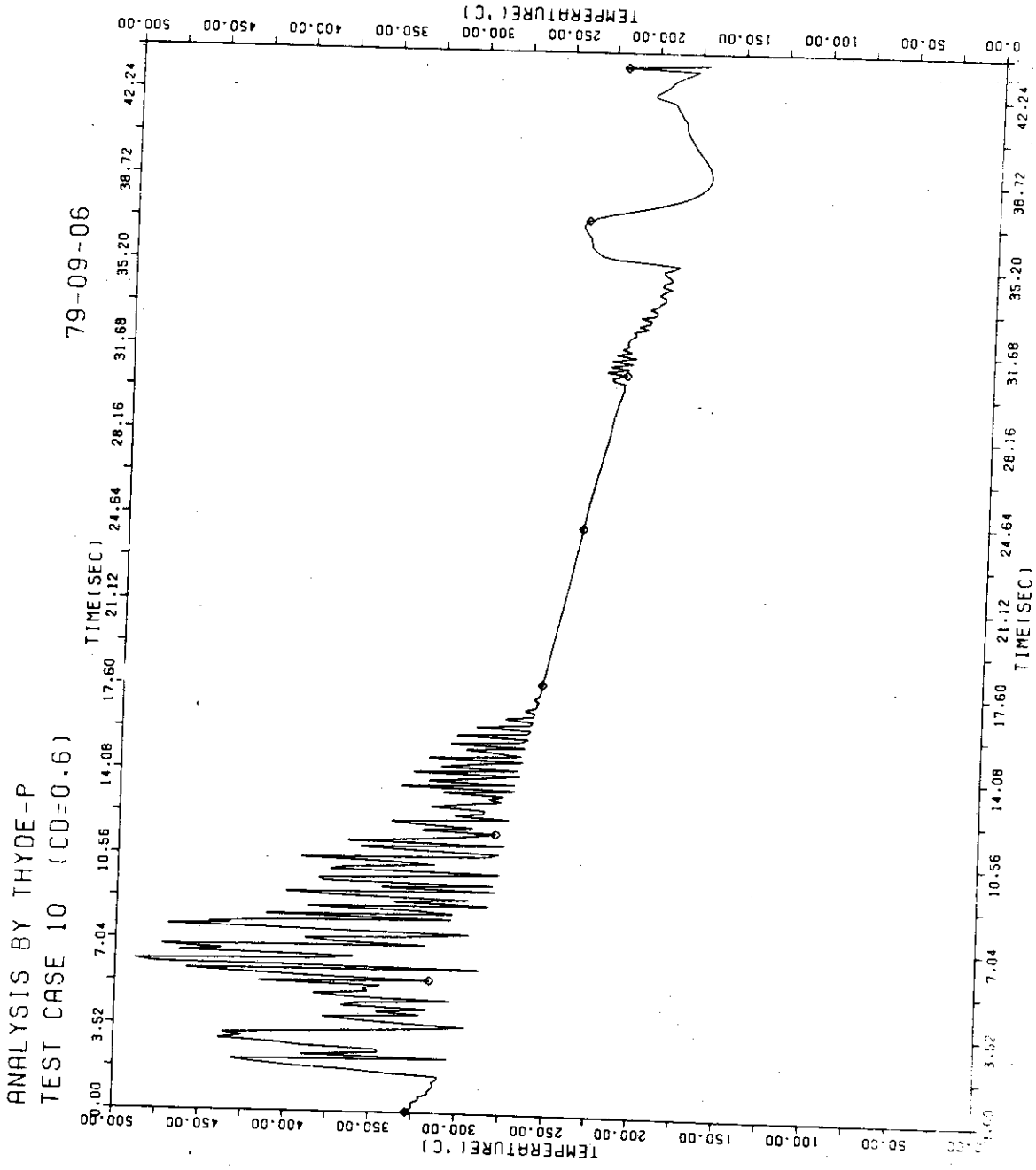

FIG. 7-61 TEMPERATURE AT NODE 23

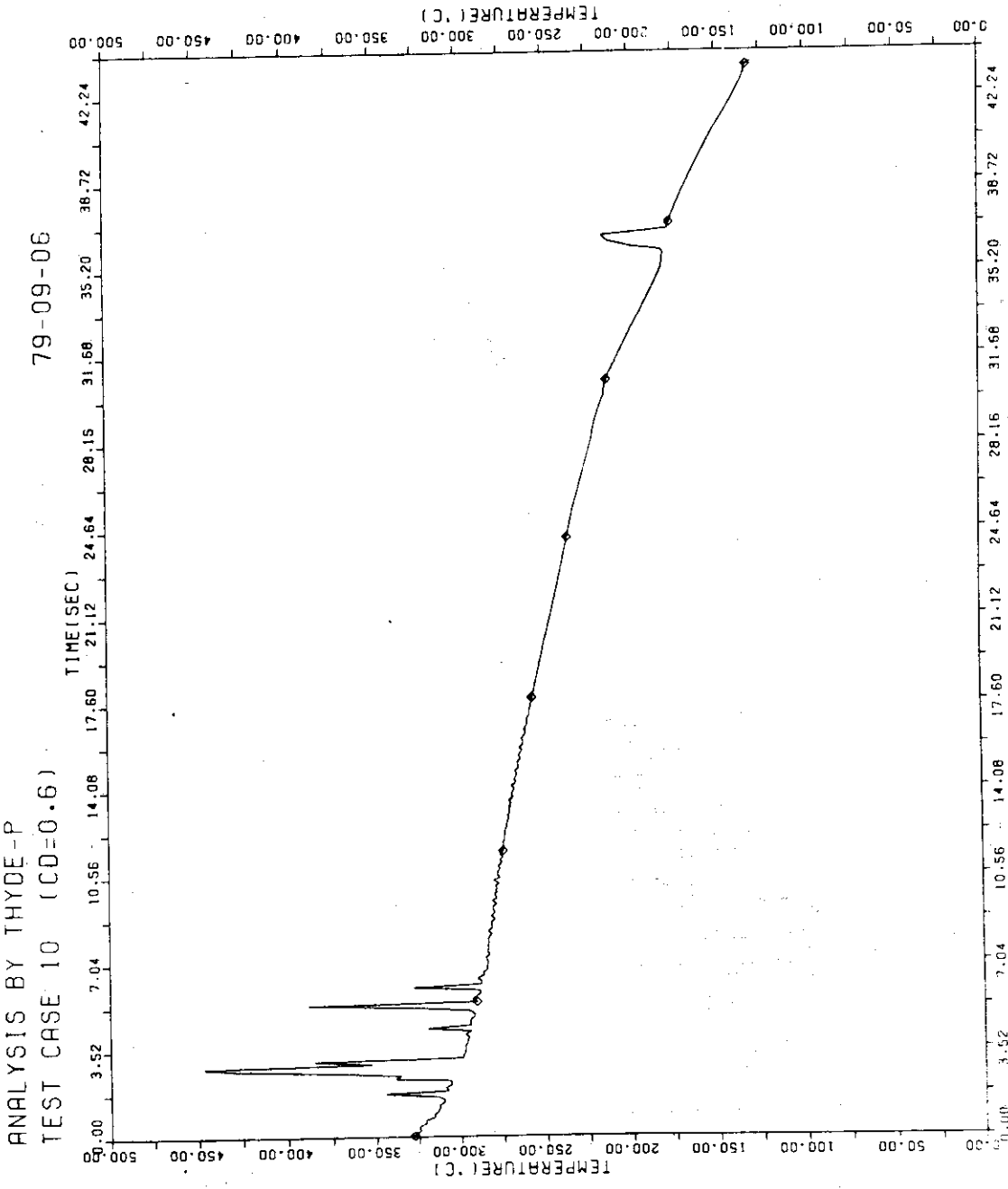

FIG. 7-62 TEMPERATURE AT NODE 24

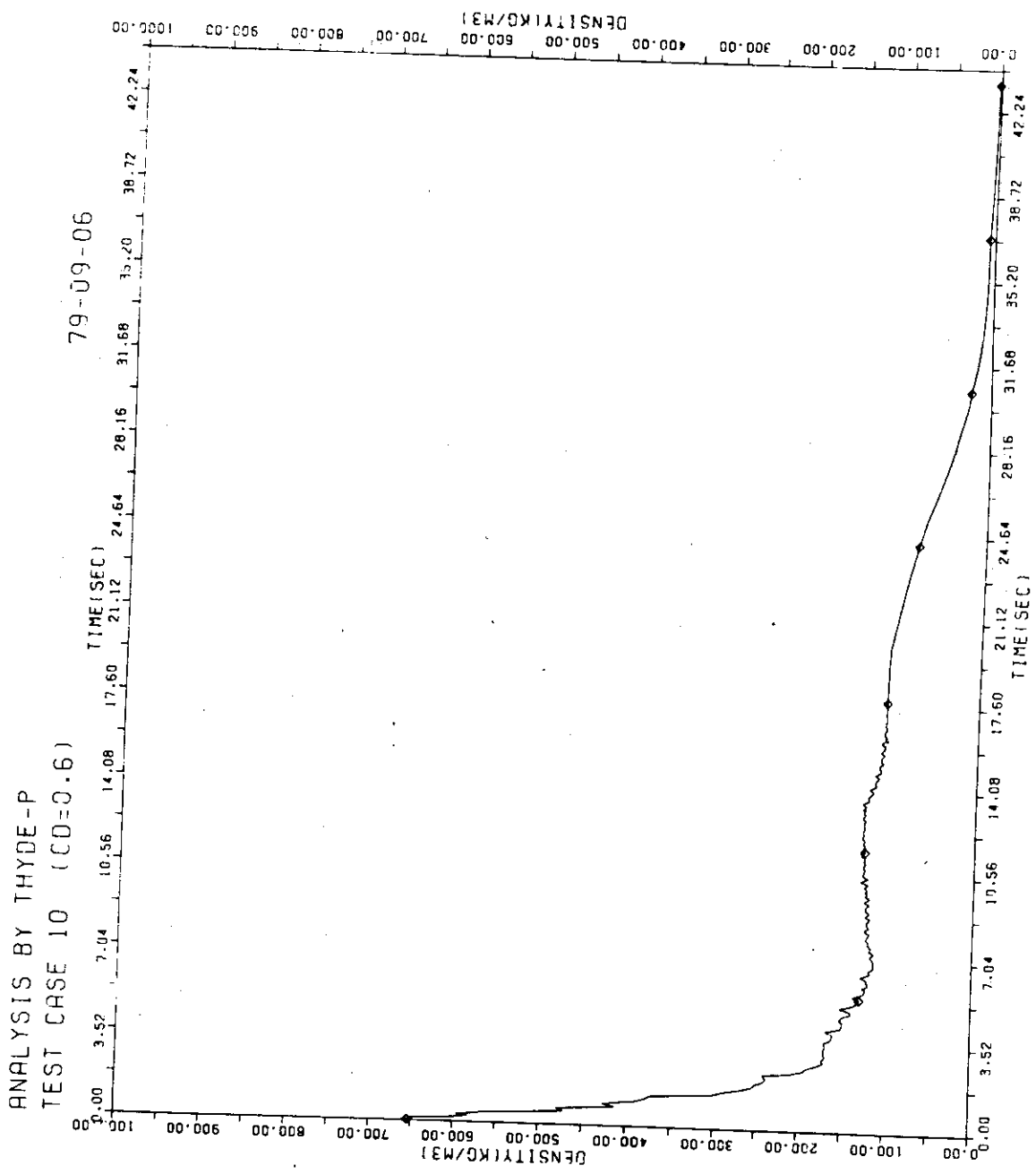
ANALYSIS BY THYDE-P
TEST CASE 10 (CD=0.6)
79-09-06
DENSITY AT 1A
TIME(SEC)
0.00
3.52
7.04
10.56
14.08
17.60
21.12
24.64
28.16
31.68
35.20
38.72
42.24
DENSITY(KG/M3)
0.0
100.00
200.00
300.00
400.00
500.00
600.00
700.00
800.00
900.00
1000.00

FIG. 7 - 63

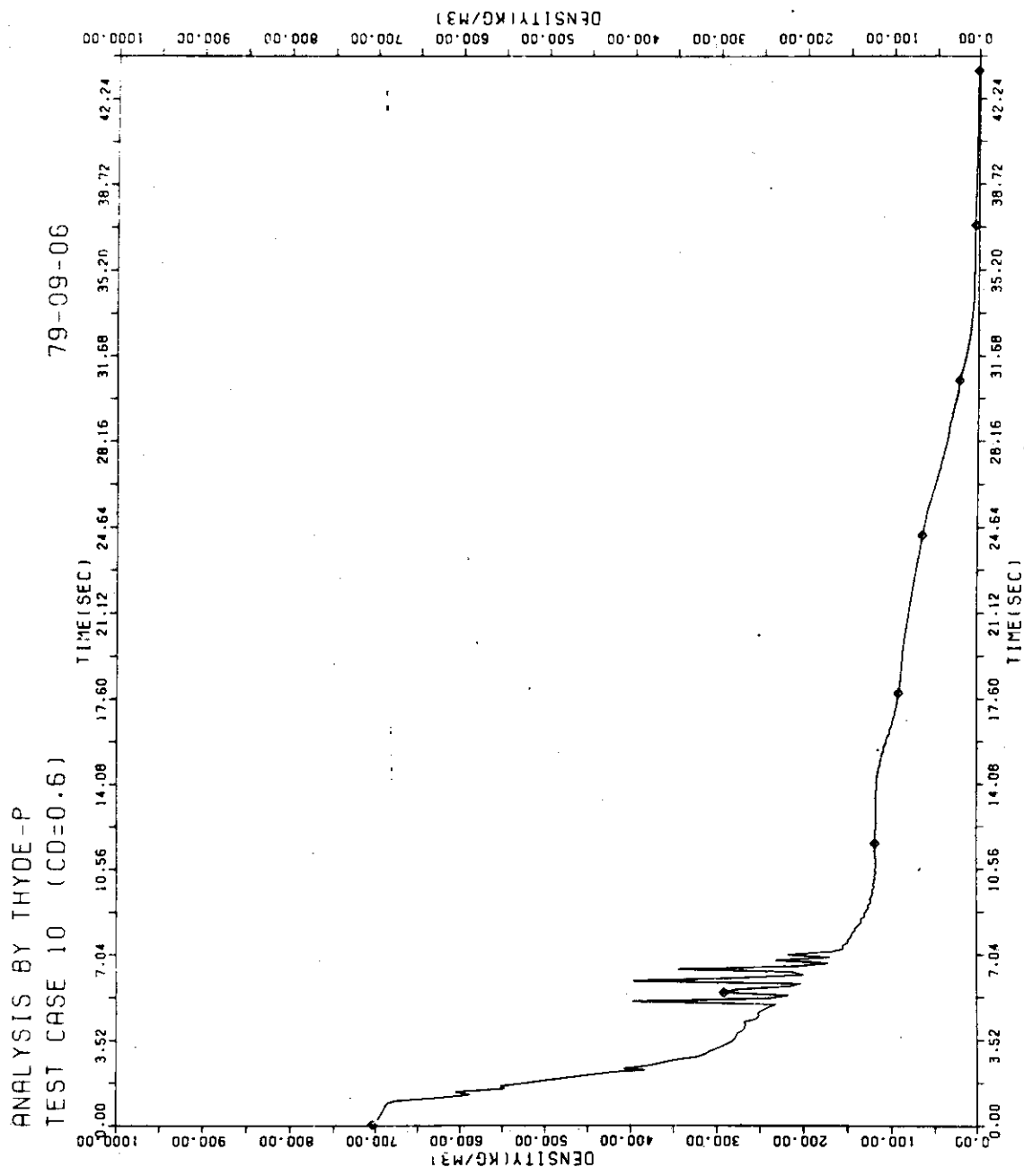

FIG. 7-64 DENSITY AT 4E

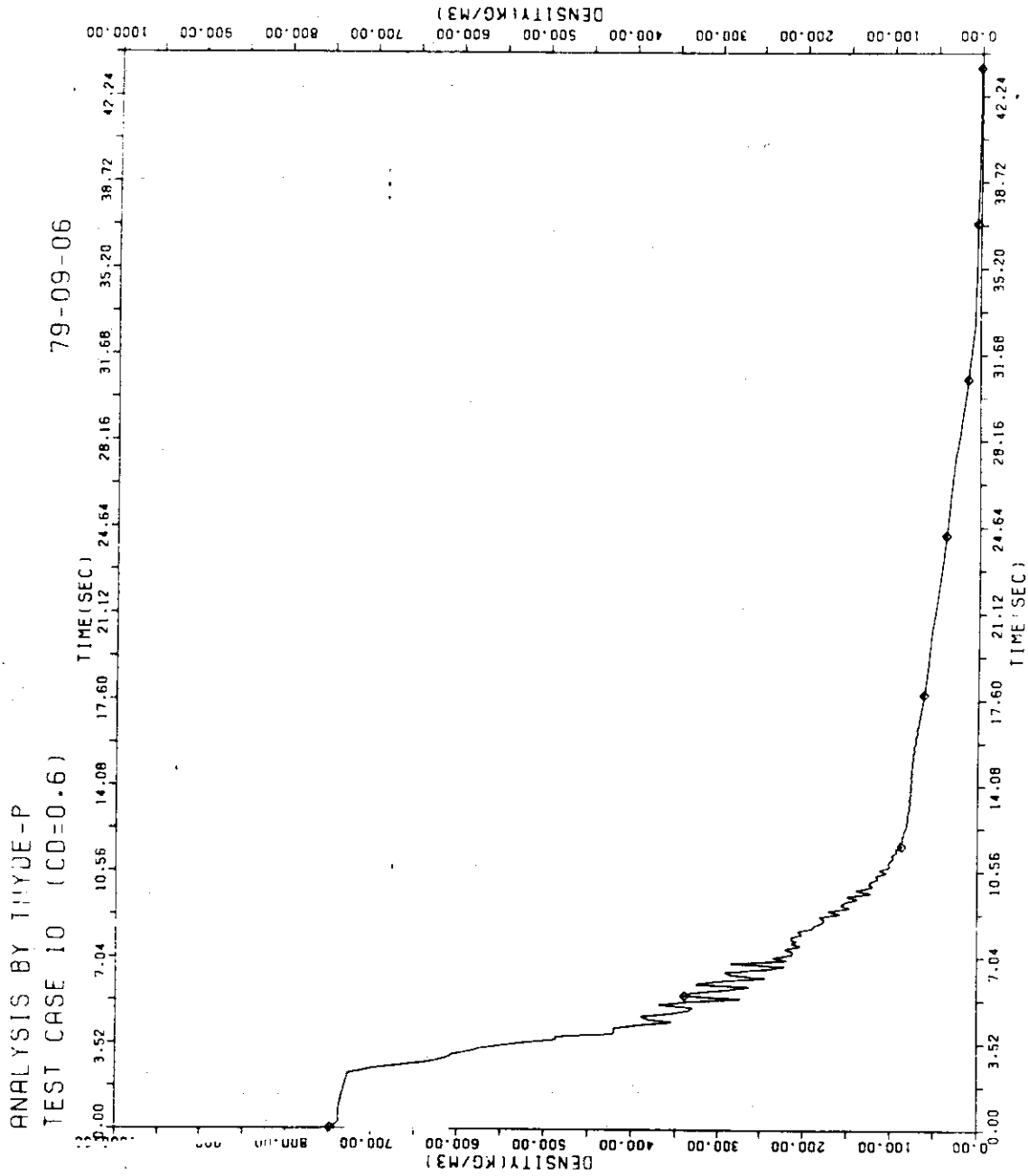

FIG. 7 - 65 DENSITY AT 8E

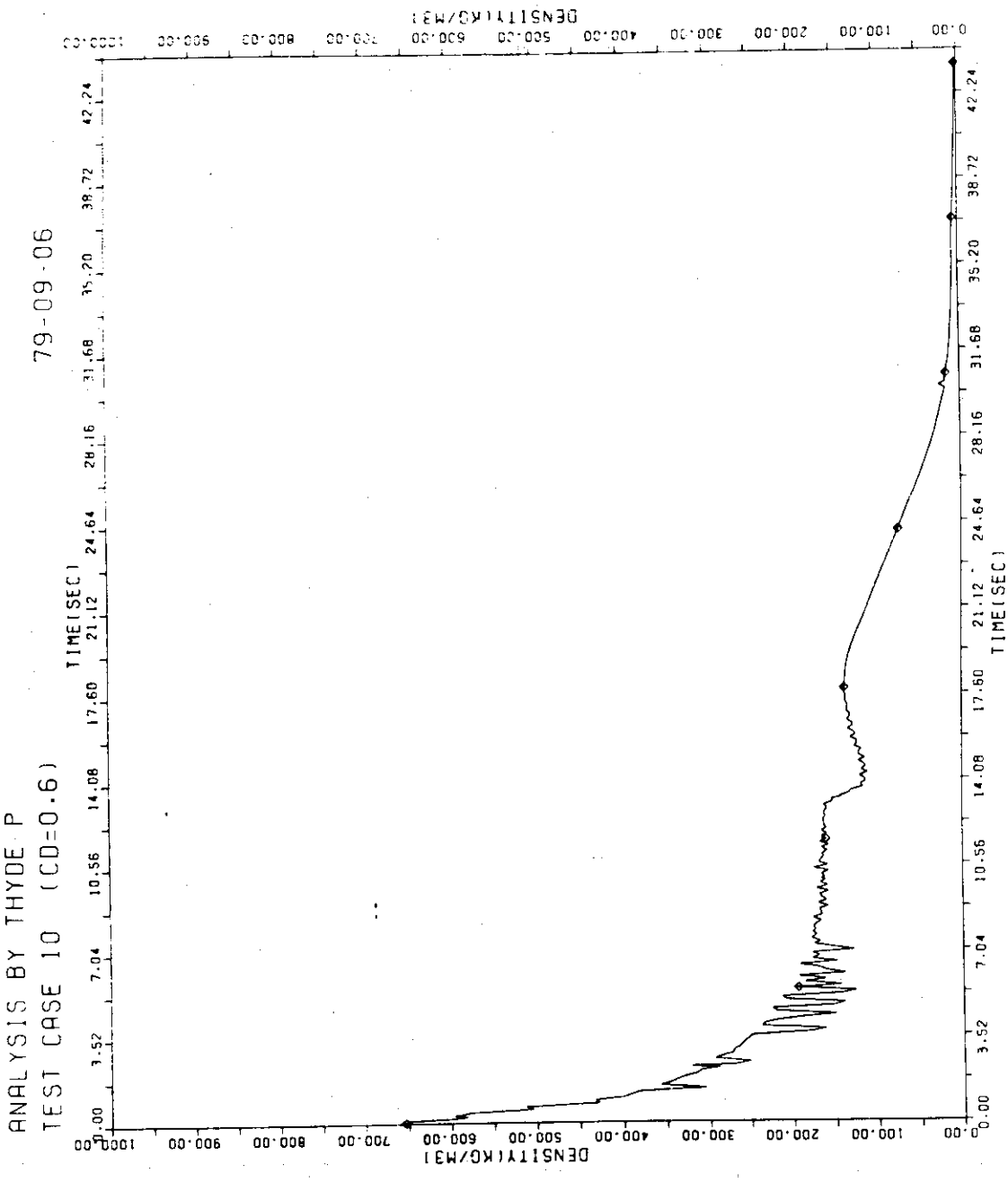
ANALYSIS BY THYDE P
TEST CASE 10 (CD=0.6)
79-09-06
DENSITY AT 10A
TIME(SEC)
DENSITY(KG/M3)
0.00
3.52
7.04
10.56
14.08
17.60
21.12
24.64
28.16
31.68
35.20
38.72
42.24
0.0
100.00
200.00
300.00
400.00
500.00
600.00
700.00
800.00
900.00
1000.00

FIG. 7 - 66

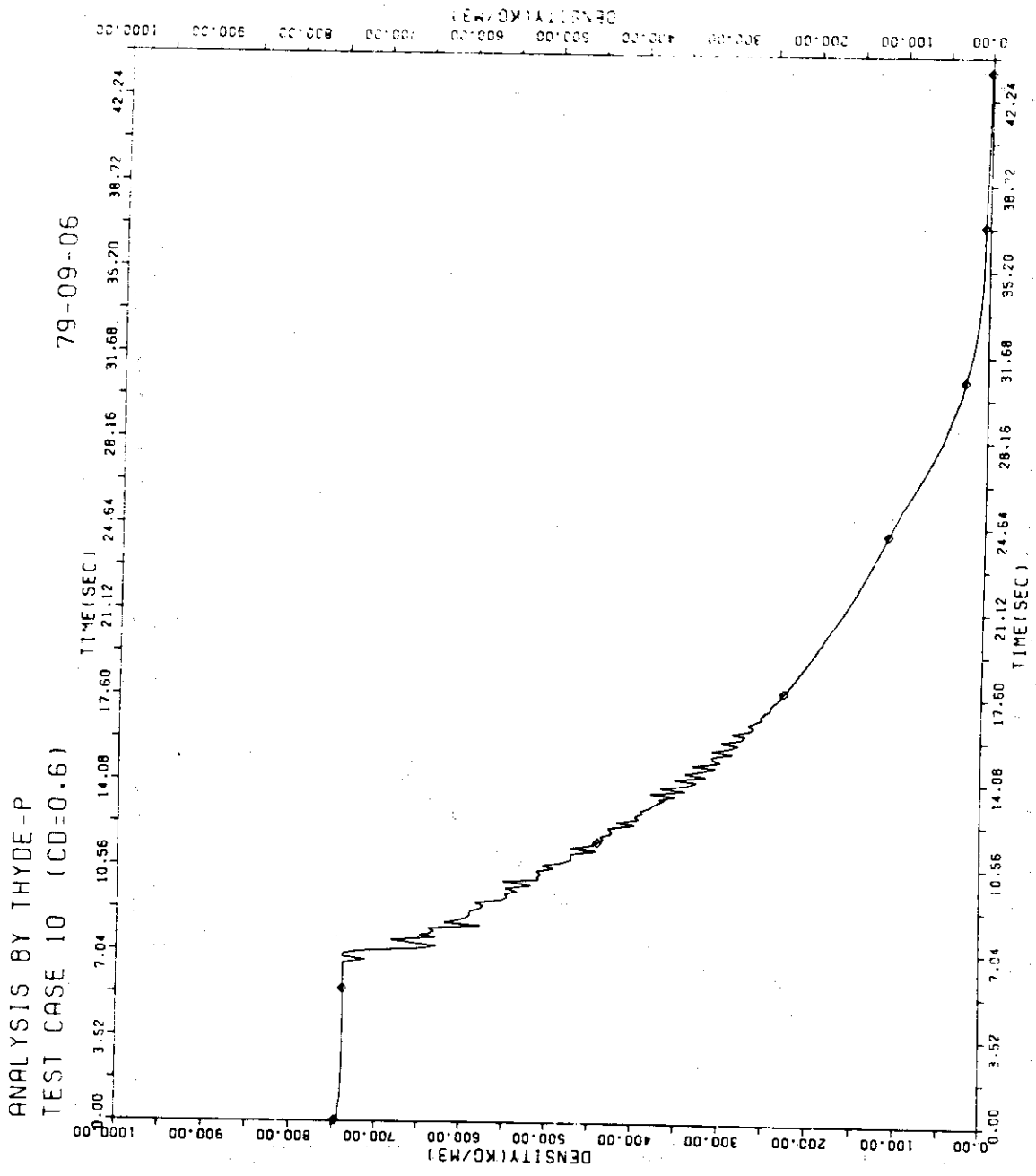

FIG. 7-67 DENSITY AT 17A

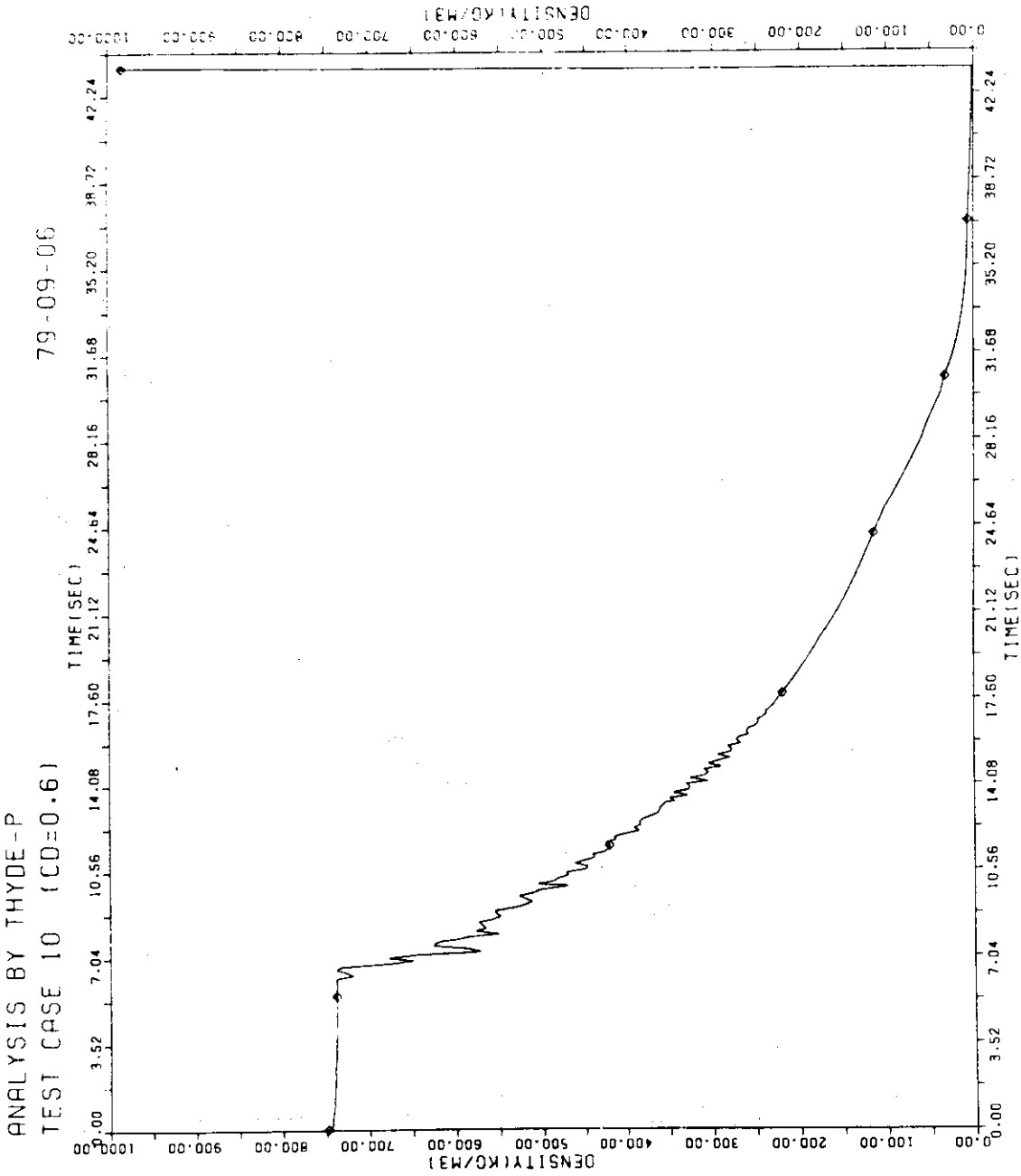

FIG. 7-68 DENSITY AT 18E

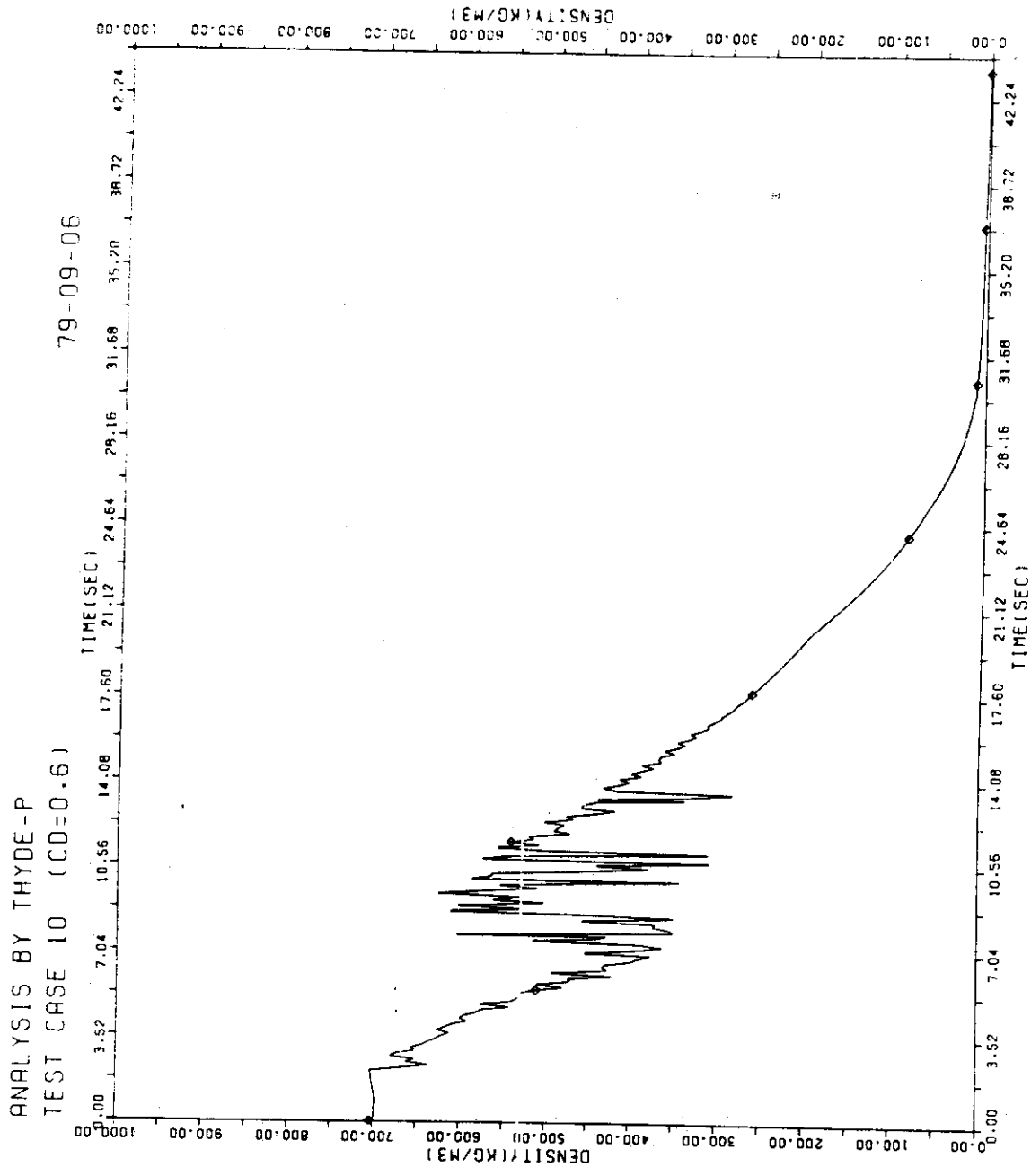
ANALYSIS BY THYDE-P
TEST CASE 10 (CD=0.6)
79-09-06
DENSITY AT 13E
DENSITY(KG/M3)
TIME(SEC)
0.00
3.52
7.04
10.56
14.08
17.60
21.12
24.64
28.16
31.68
35.20
38.72
42.24
0.0
100.00
200.00
300.00
400.00
500.00
600.00
700.00
800.00
900.00
1000.00

FIG. 7-69

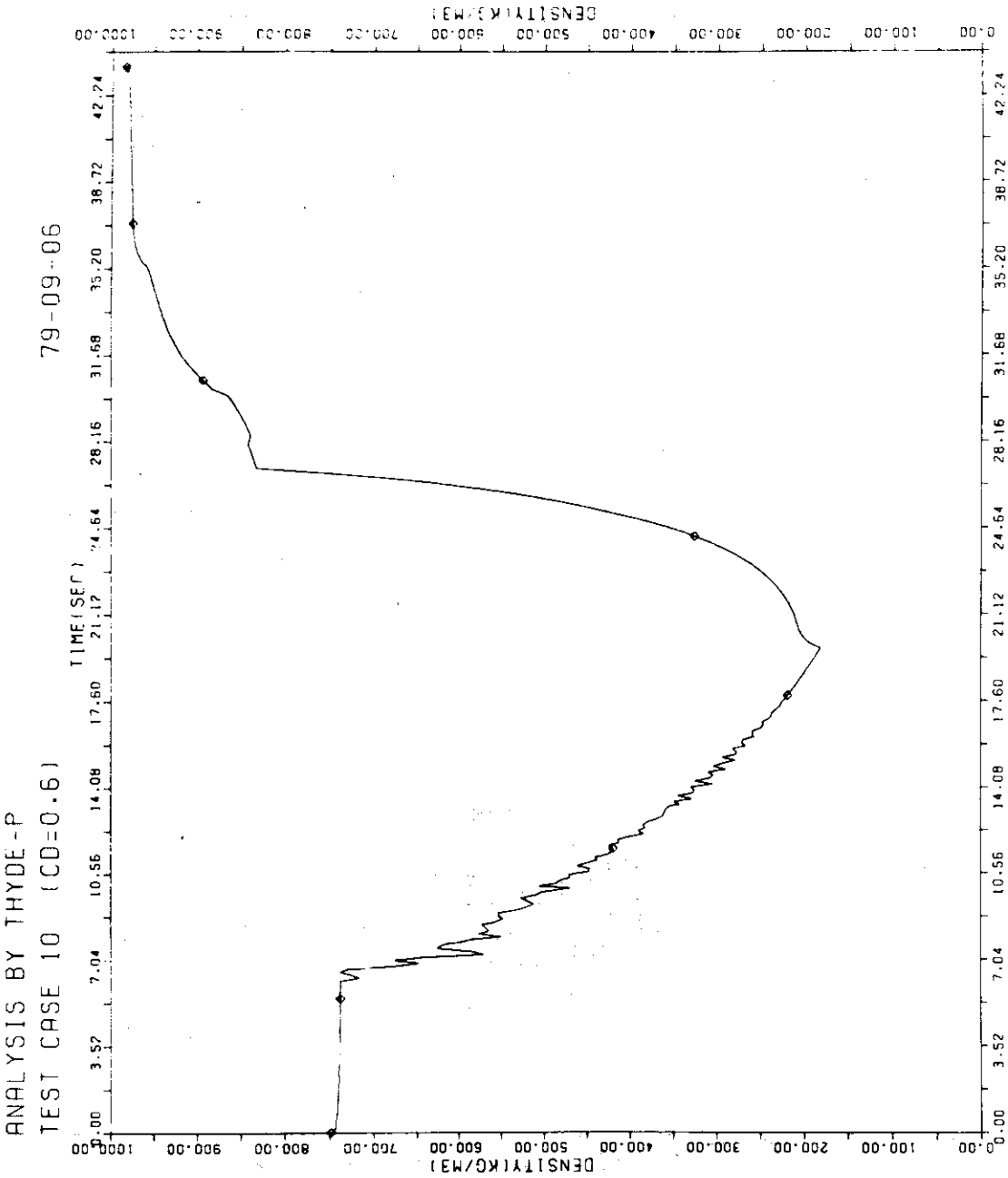

FIG. 7 - 70 DENSITY AT 19A

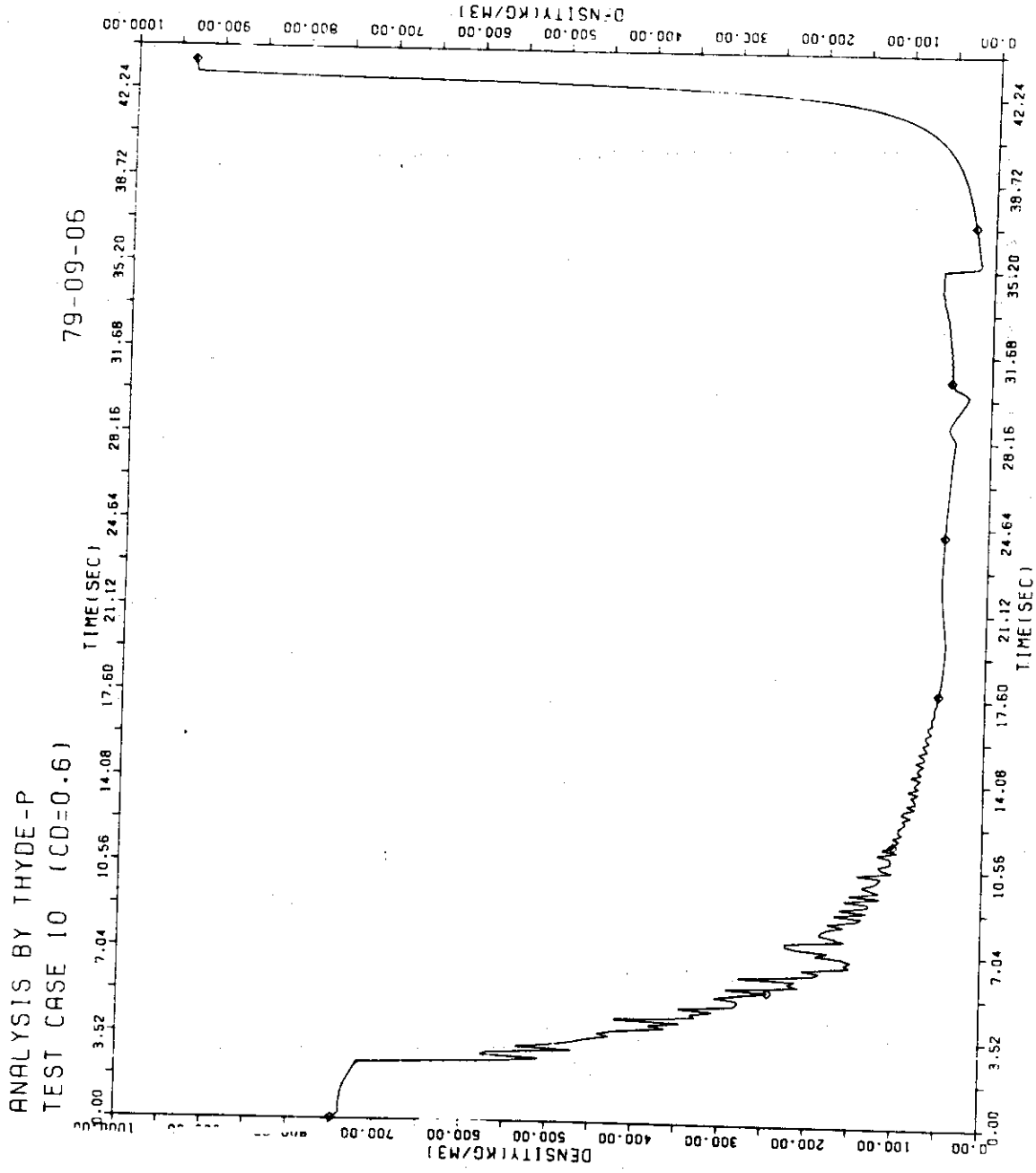

FIG. 7-71 DENSITY AT 9A

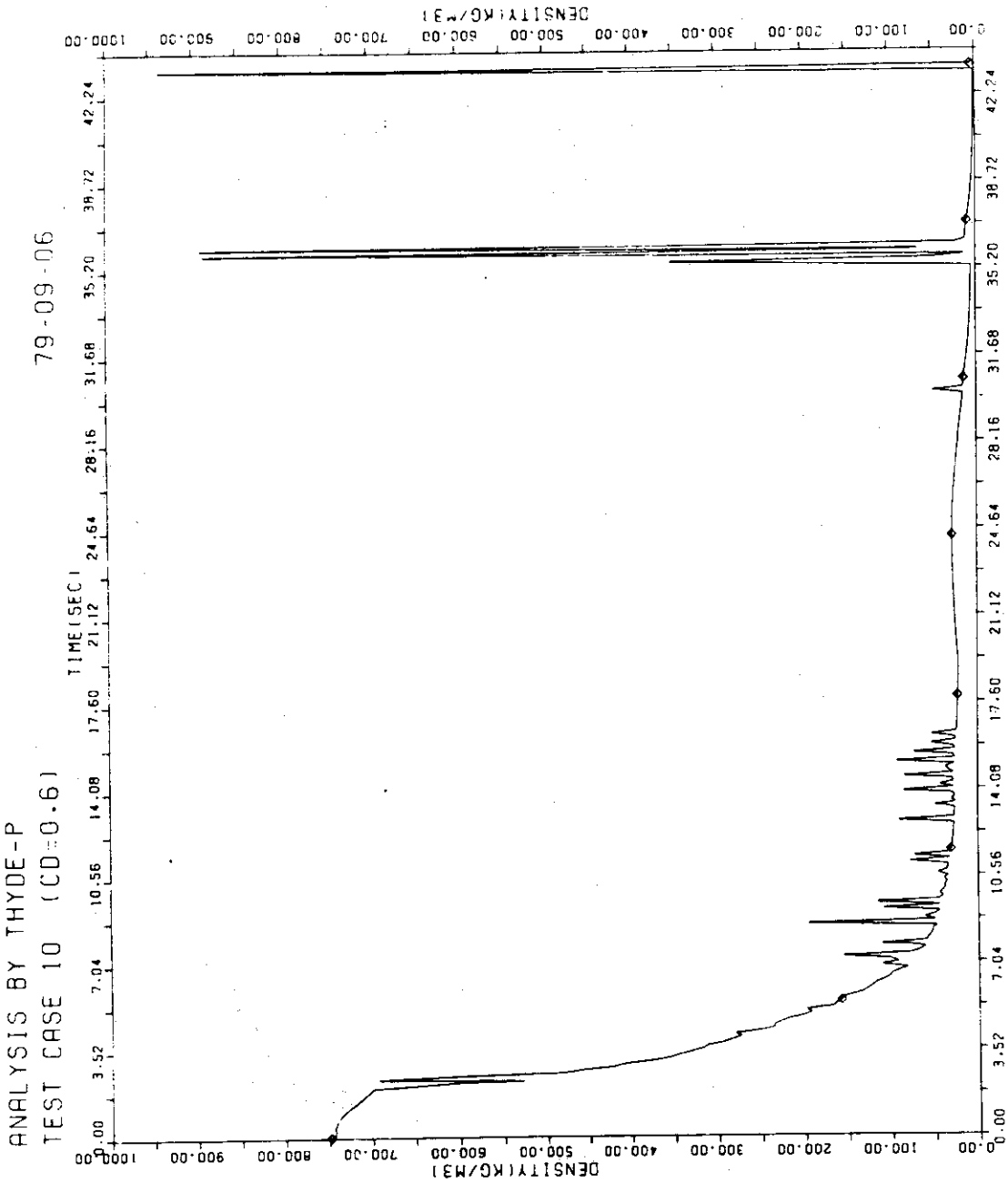

FIG. 7-72 DENSITY AT 20A

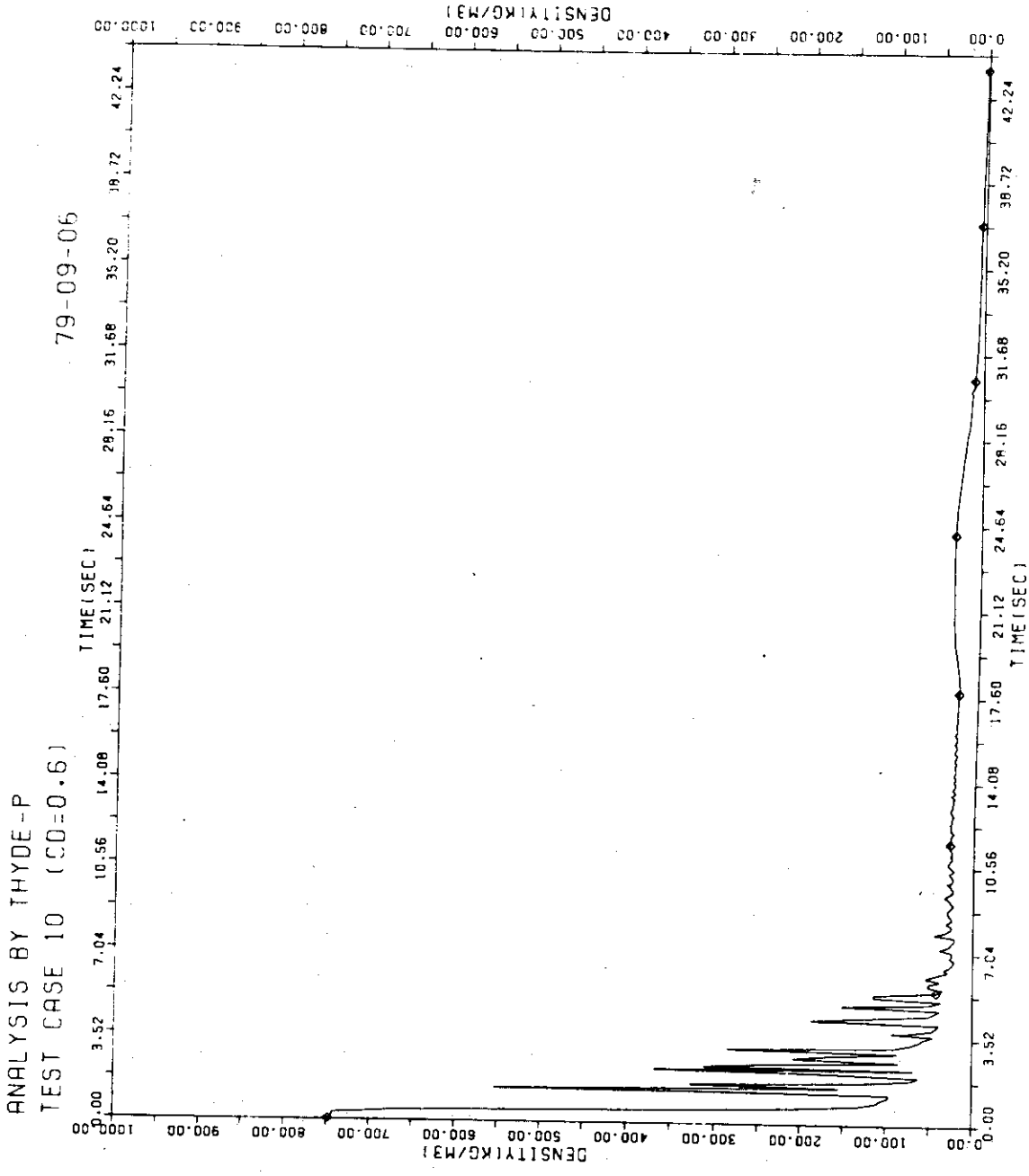

FIG. 7-73 DENSITY AT 22A

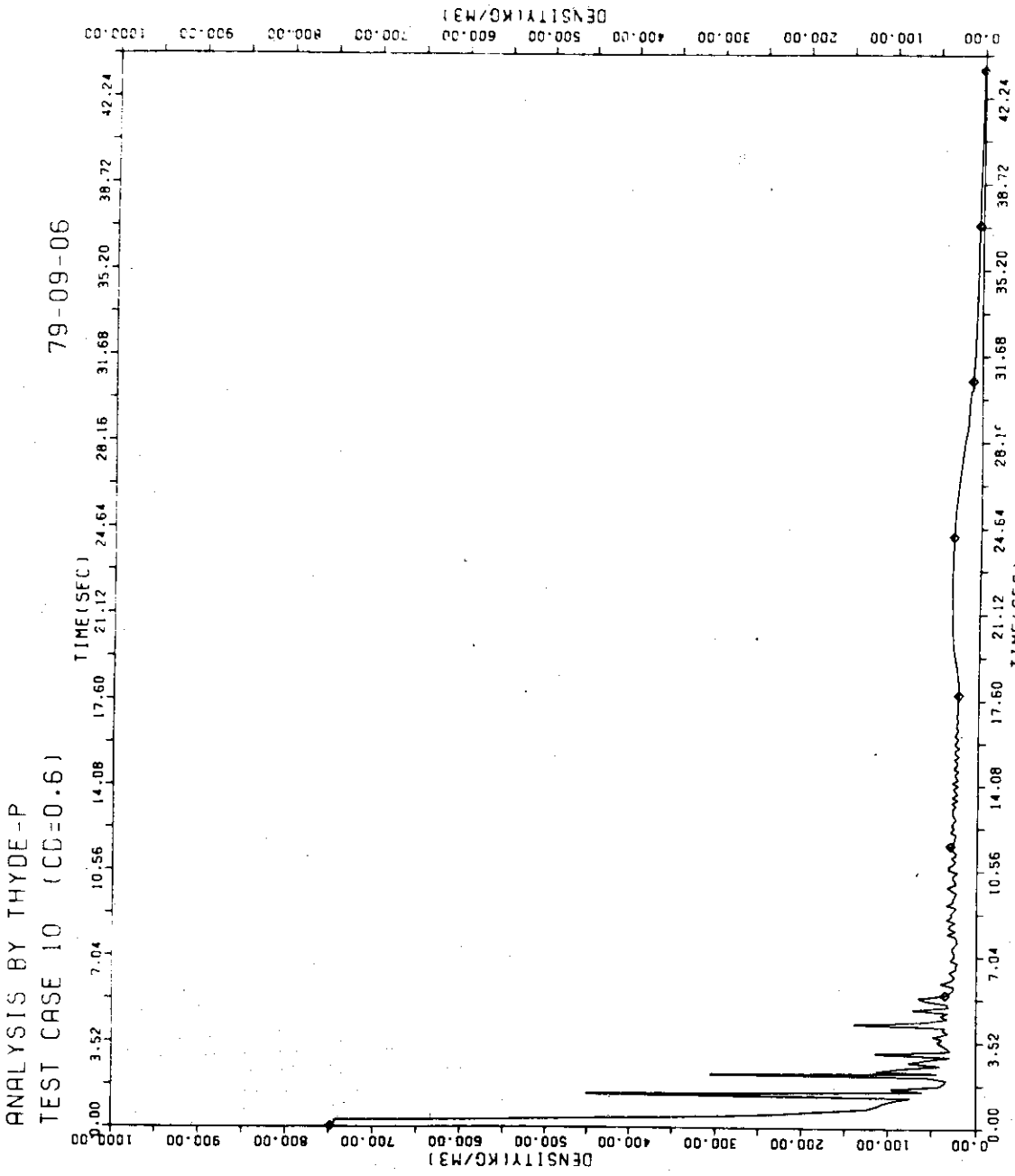

FIG. 7 - 74 DENSITY AT 23A

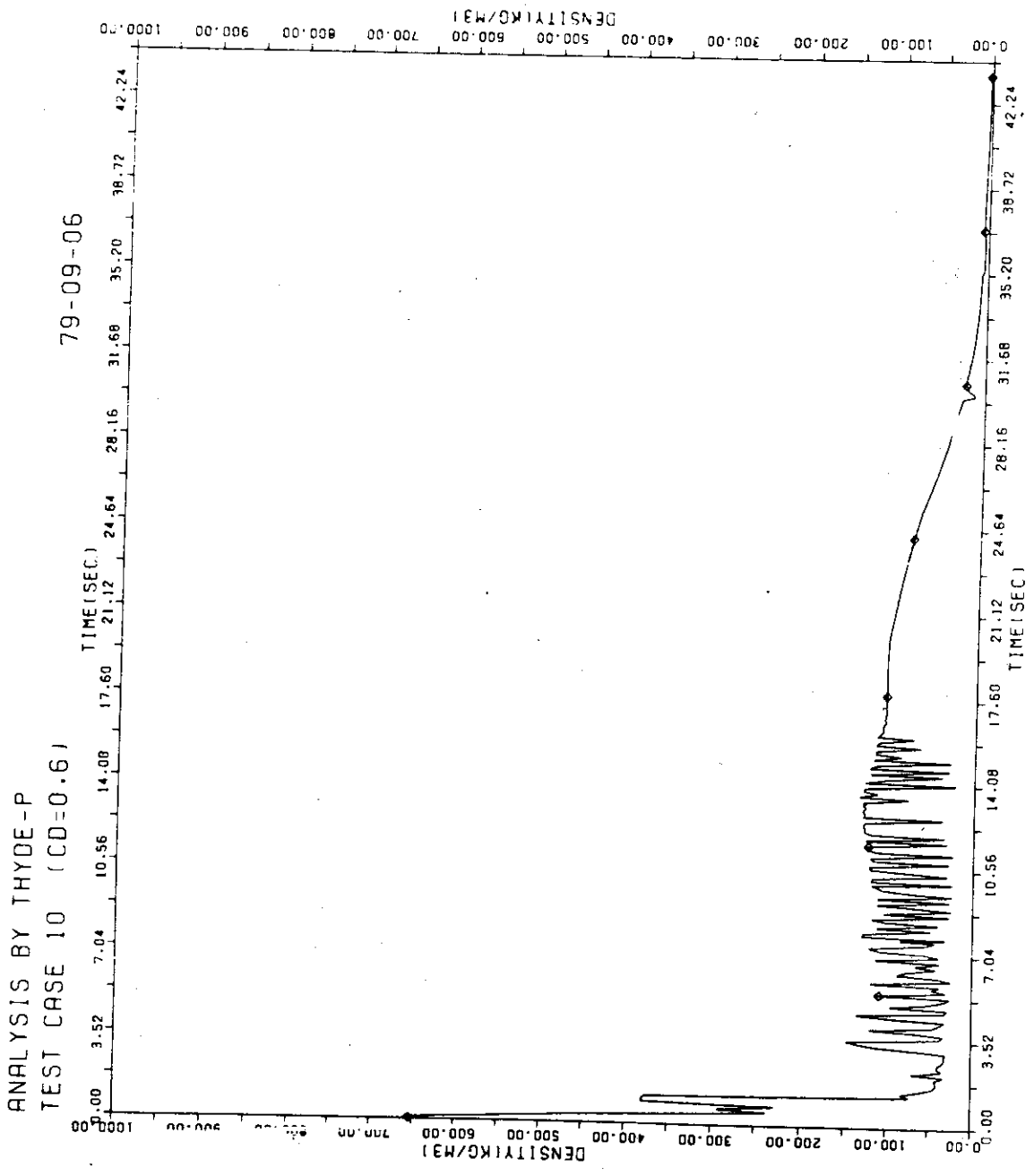
ANALYSIS BY THYDE-P
TEST CASE 10 (CD=0.6)
79-09-06
DENSITY AT 23E
TIME(SEC)
DENSITY(KG/M3)
0.00
3.52
7.04
10.56
14.08
17.60
21.12
24.64
28.16
31.68
35.20
38.72
42.24
0.00
100.00
200.00
300.00
400.00
500.00
600.00
700.00
800.00
900.00
1000.00

FIG. 7-75

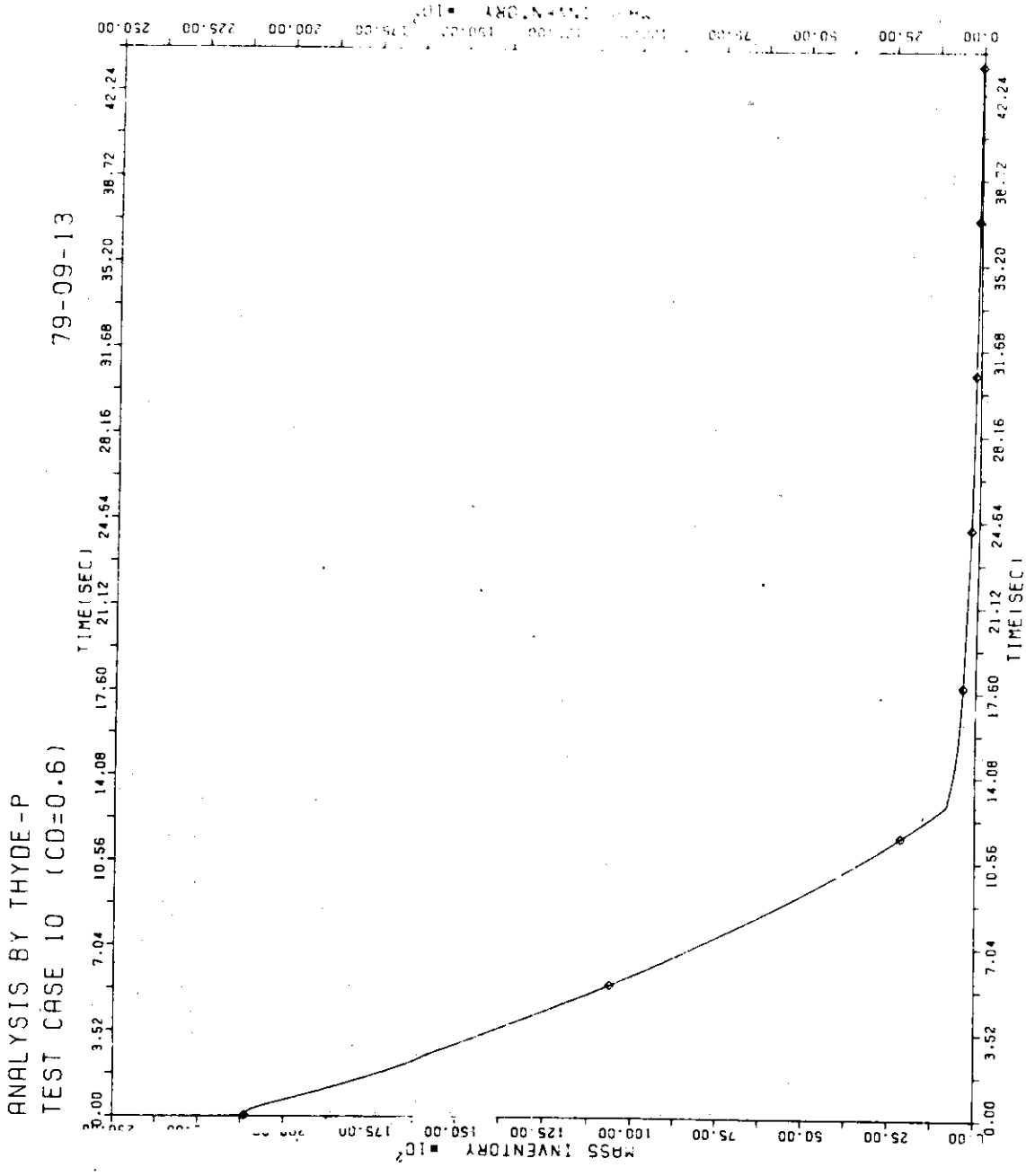

FIG. 7-76 MASS IN REG-2 OF PZR

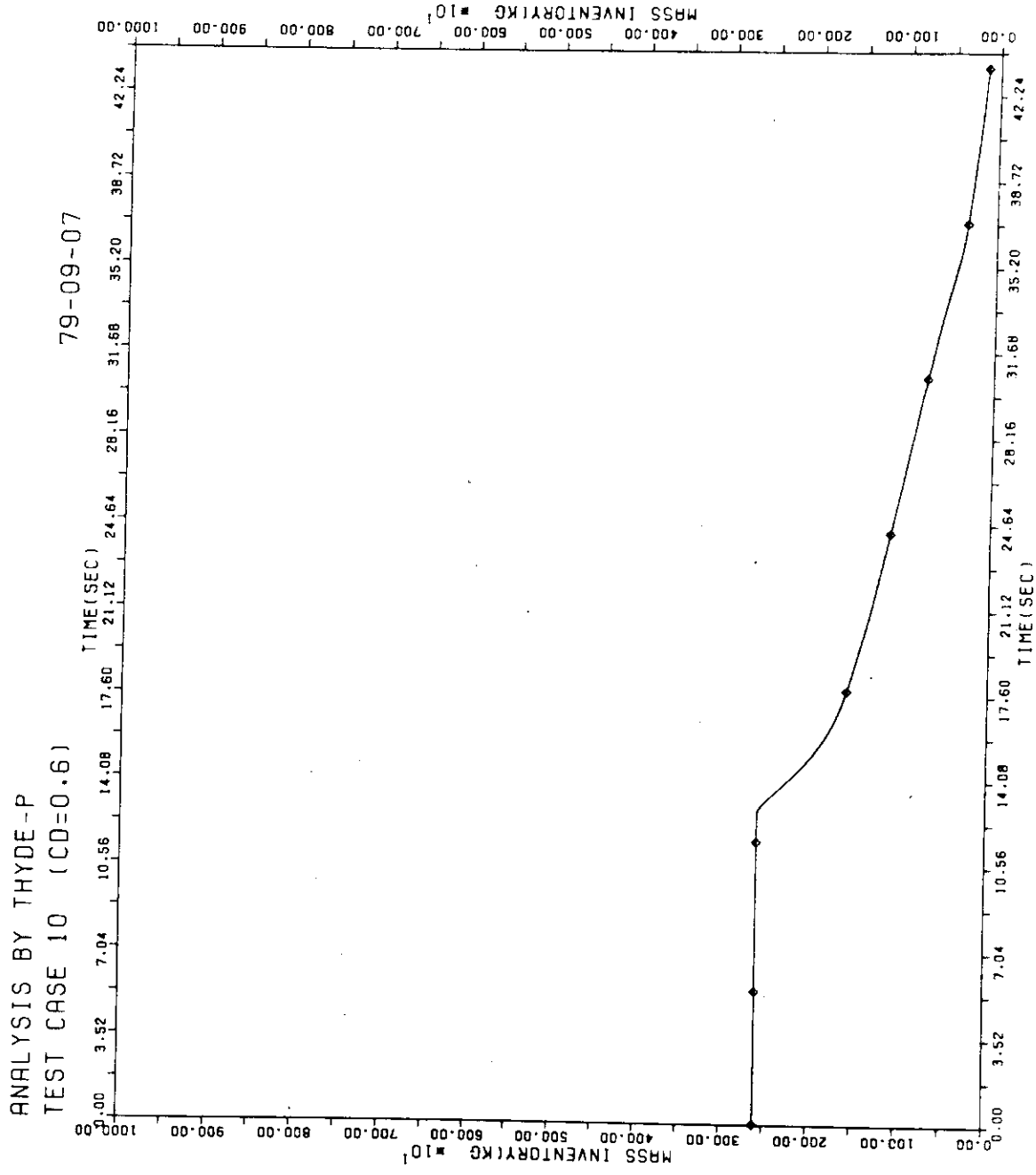
ANALYSIS BY THYDE-P
TEST CASE 10 (CD=0.6)
79-09-07
MASS IN REG-1 OF PZR
TIME(SEC)
MASS INVENTORY(KG) *10¹
0.00
3.52
7.04
10.56
14.08
17.60
21.12
24.64
28.16
31.68
35.20
38.72
42.24
100.00
200.00
300.00
400.00
500.00
600.00
700.00
800.00
900.00
1000.00

FIG. 7-77

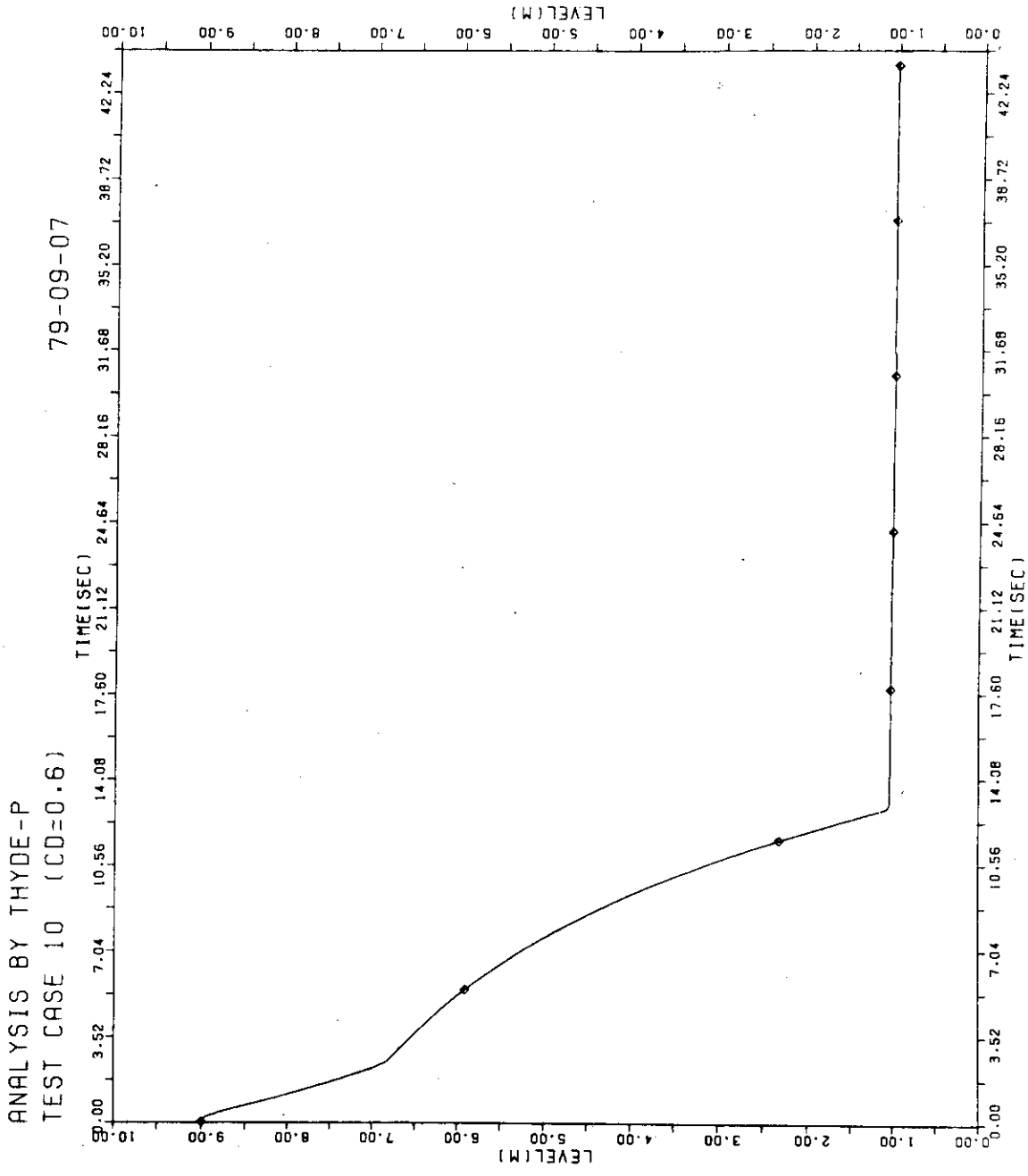

FIG. 7-78 REG-2 LEVEL IN PZR

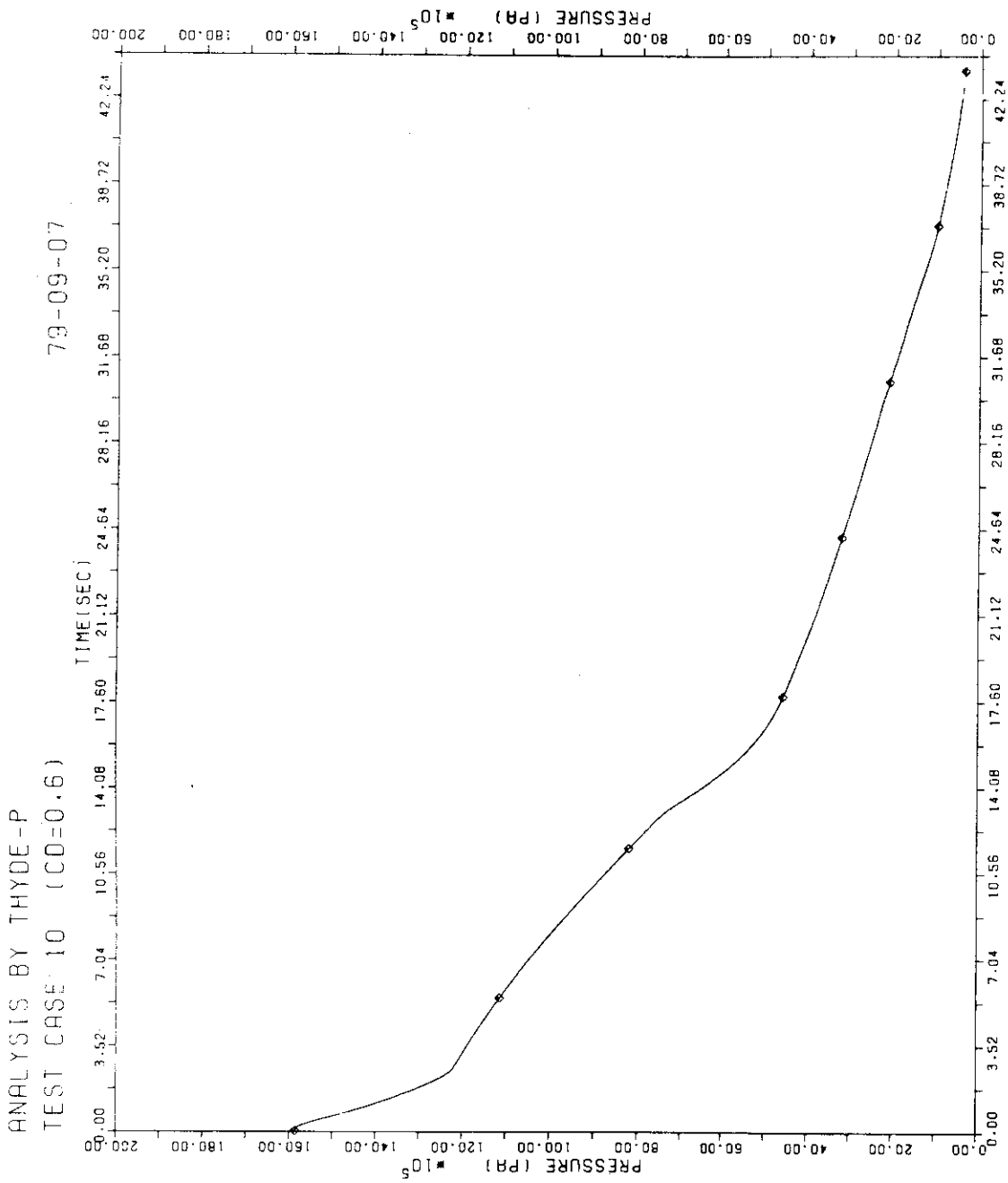

FIG. 7 - 79 PRESSURE IN PRESSURIZER

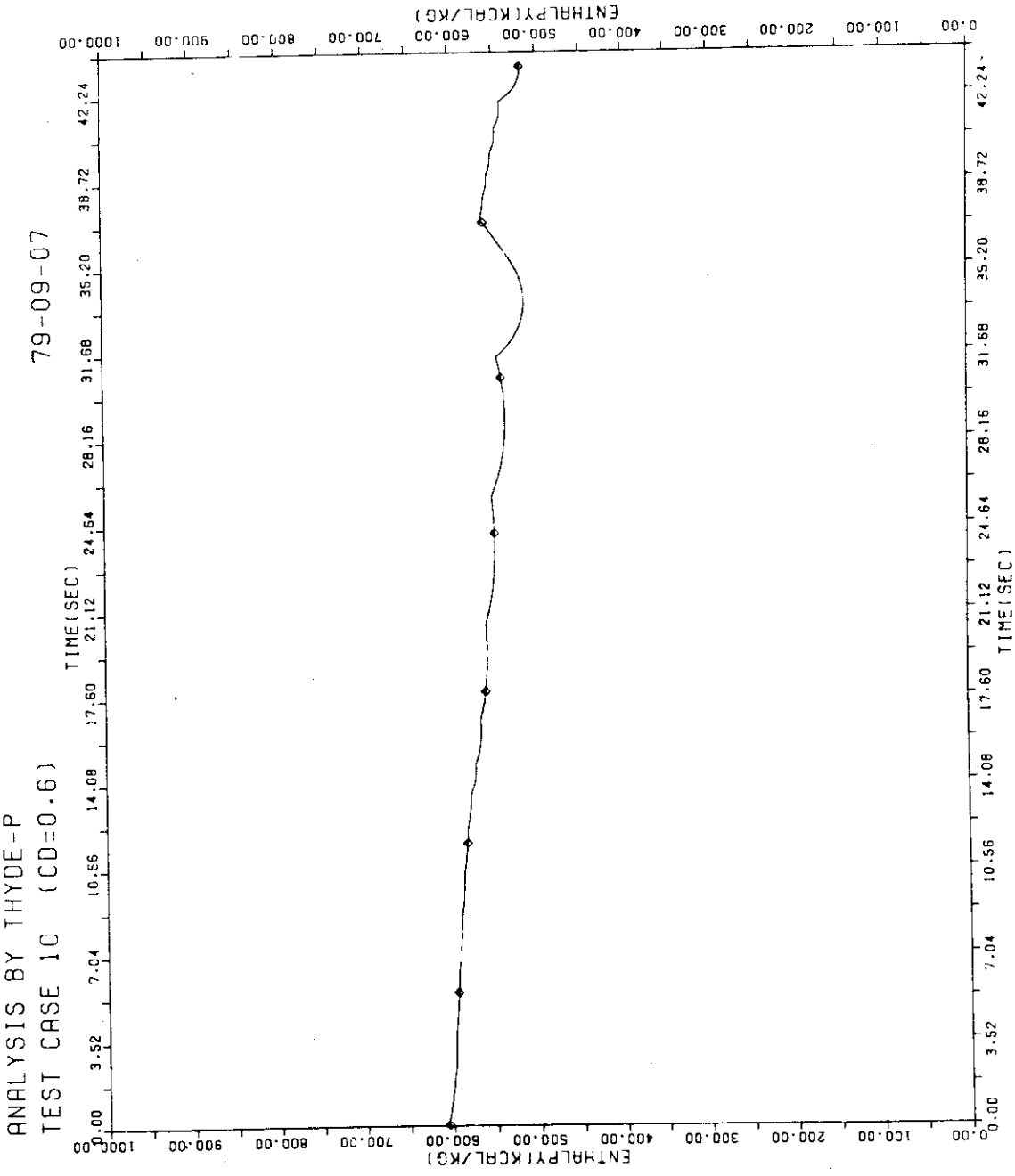

FIG. 7 - 80 ENTL OF REG-1 OF PZR

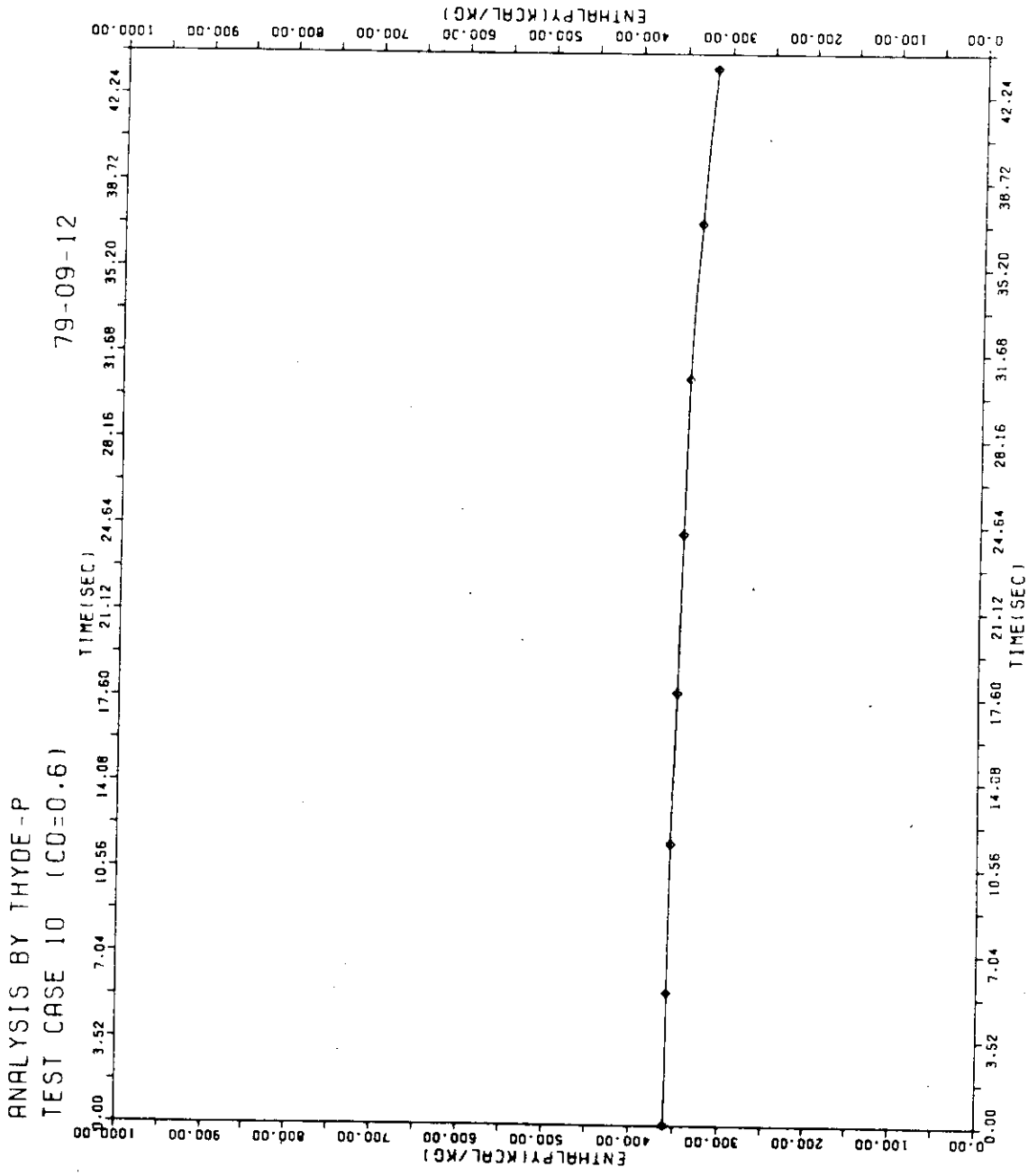

FIG. 7 - 81 ENTL OF REG-2 OF PZR

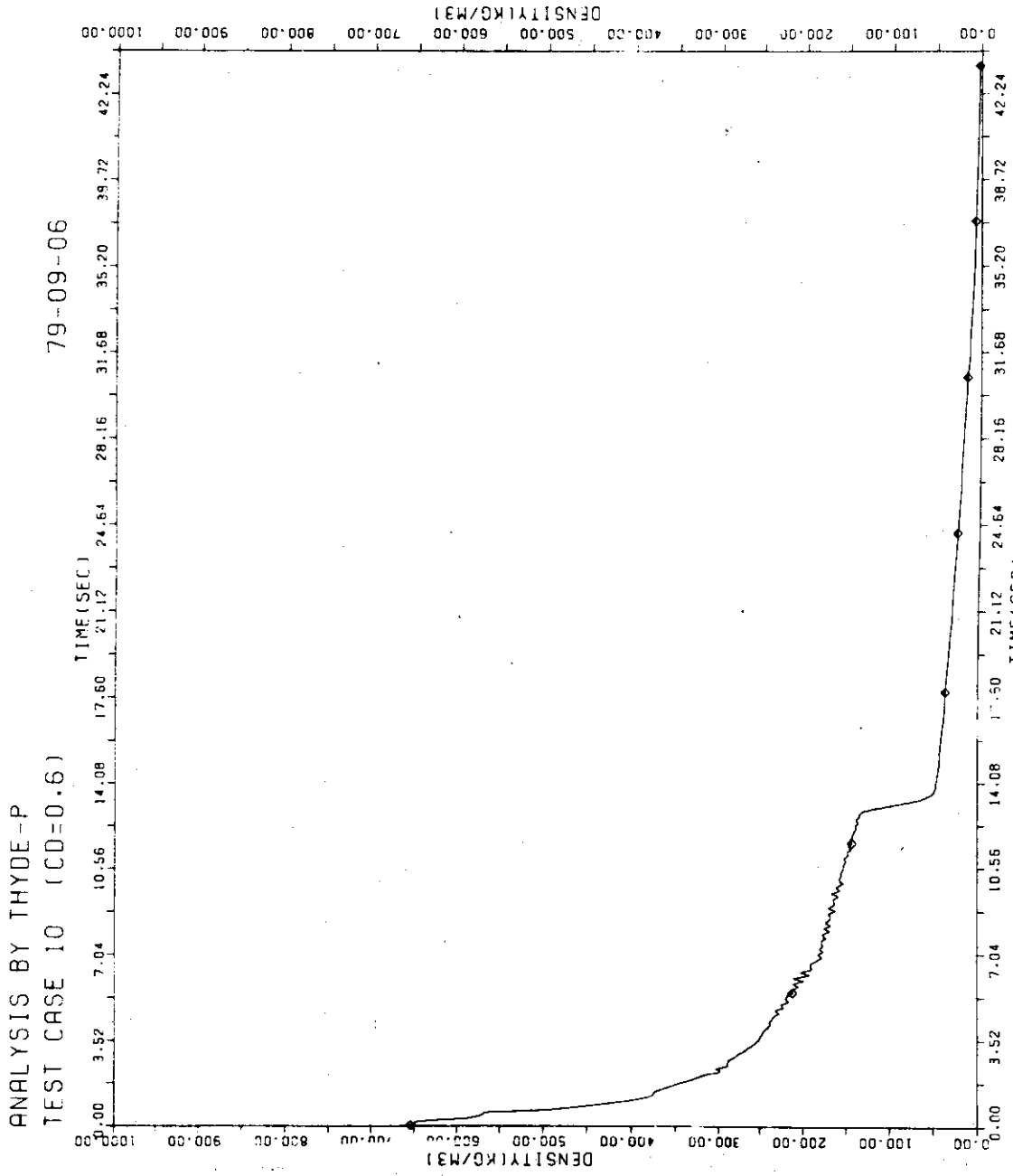
ANALYSIS BY THYDE-P
TEST CASE 10 (CD=0.6)
79-09-06
DENSITY AT 25A
TIME(SEC)
DENSITY(KG/M3)
0.00
3.52
7.04
10.56
14.08
17.60
21.12
24.64
28.16
31.68
35.20
39.72
42.24
0.0
100.00
200.00
300.00
400.00
500.00
600.00
700.00
800.00
900.00
1000.00

FIG. 7 - 82

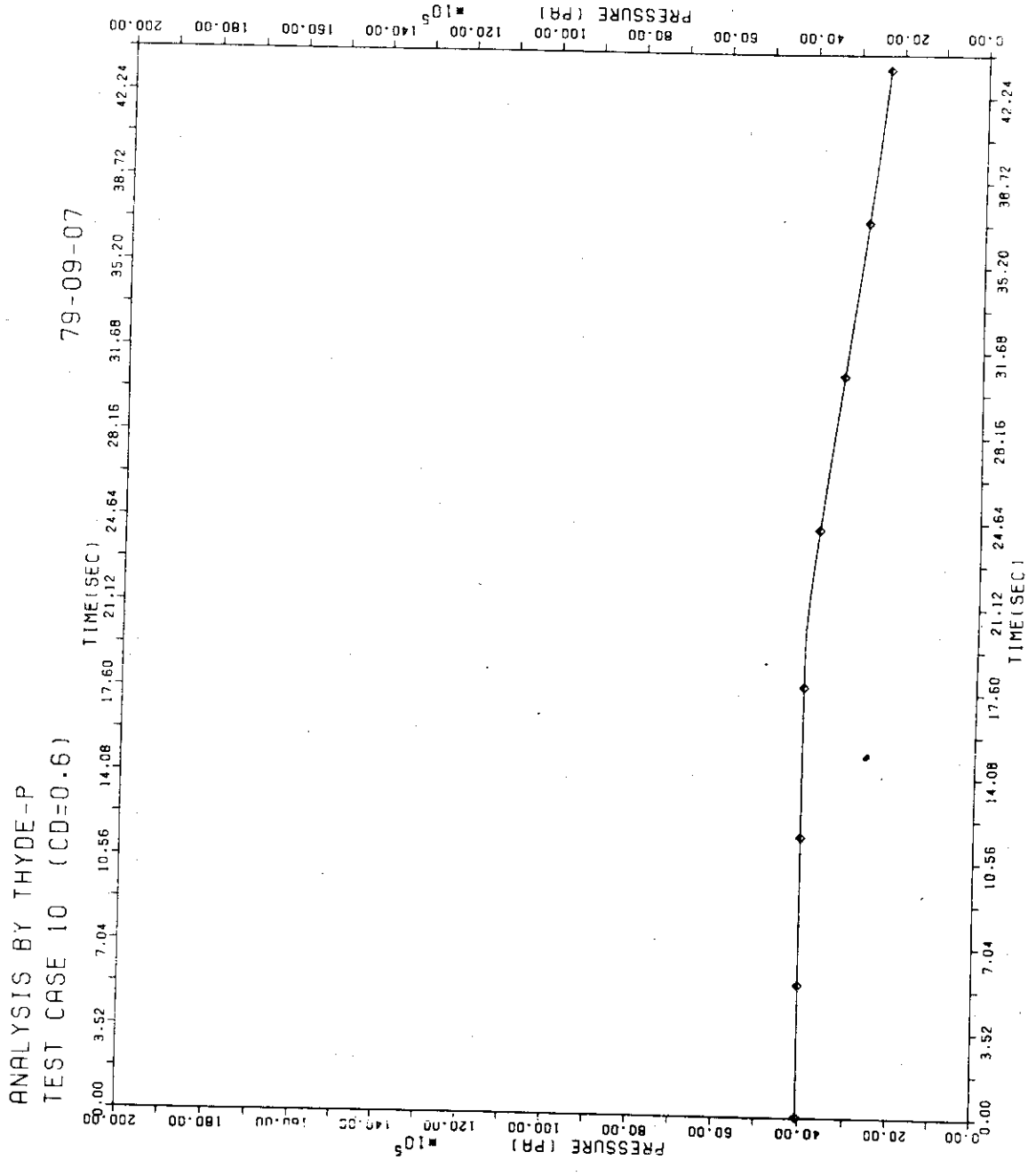

FIG. 7-83 PRESSURE IN ACC

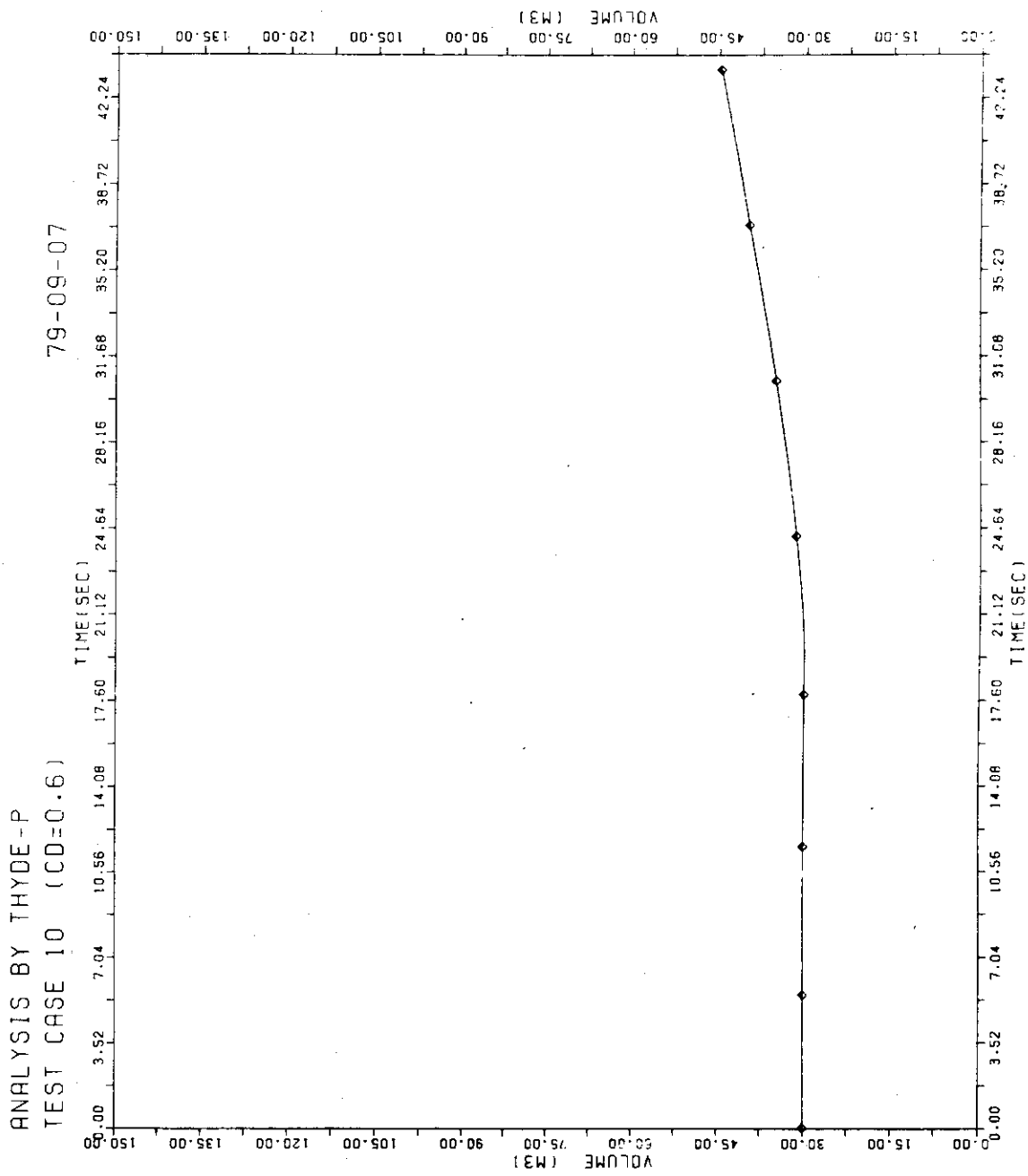

FIG. 7 - 84 GAS VOLUME IN ACC

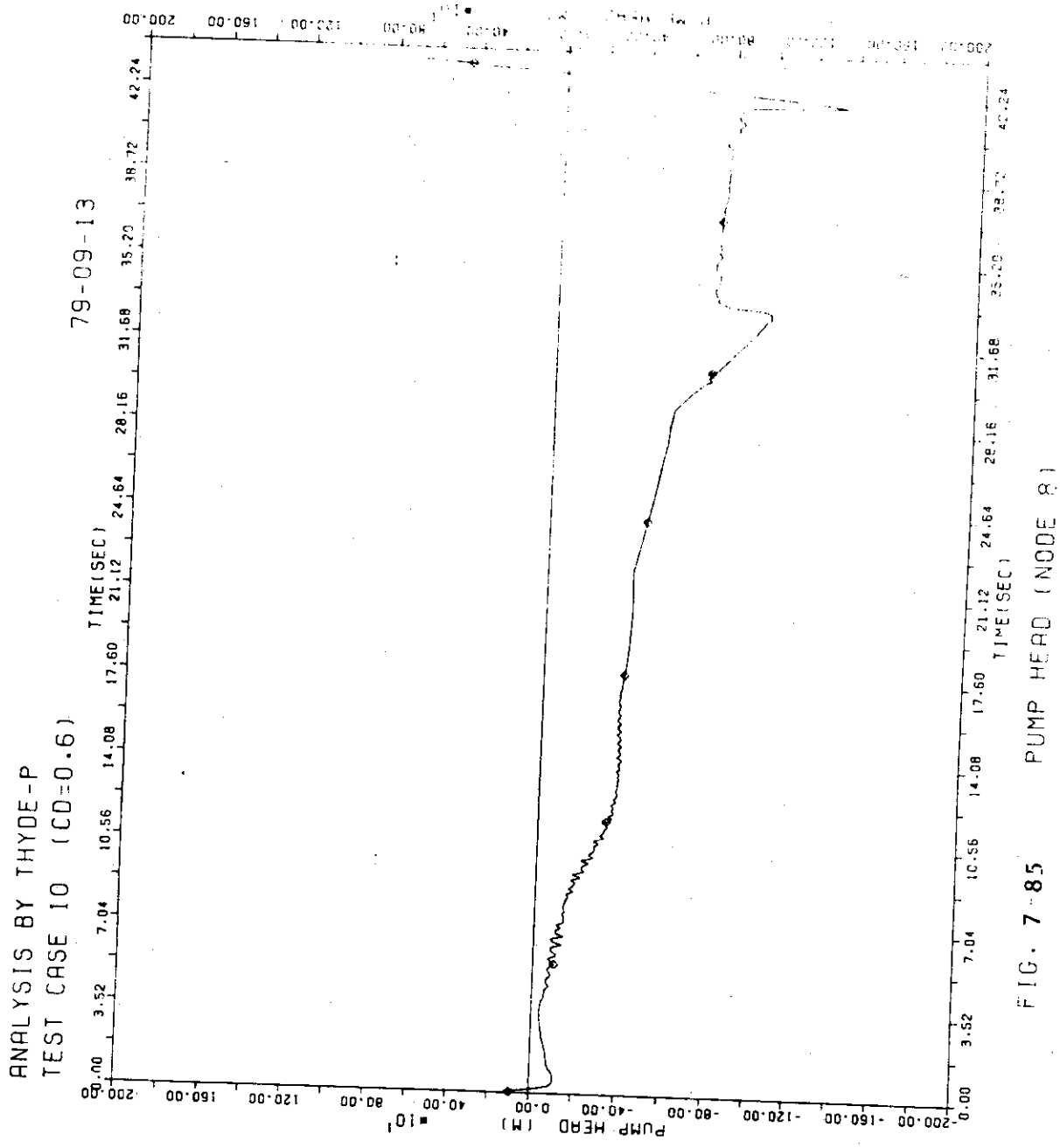

FIG. 7-85 PUMP HEAD (NODE 8)

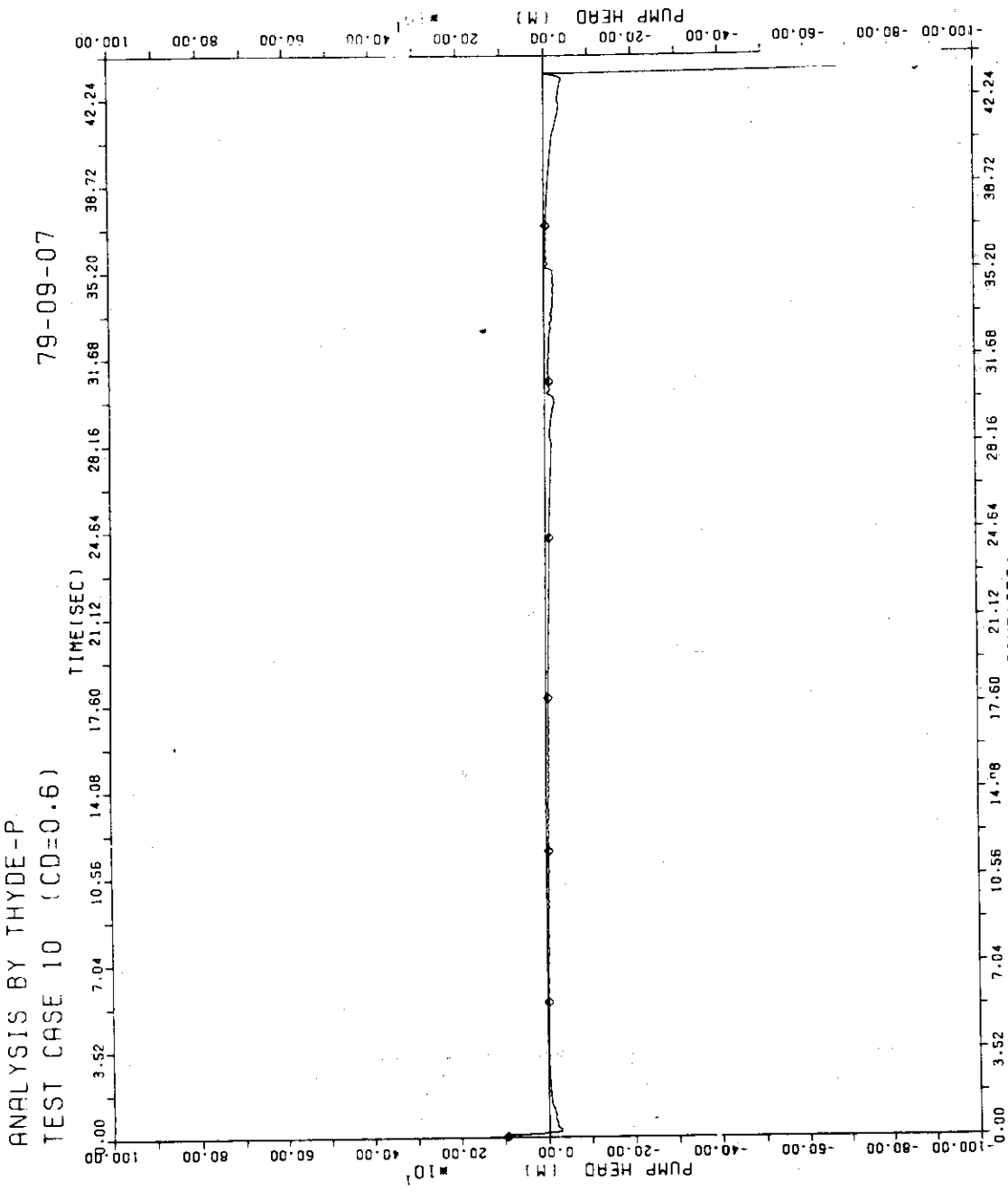

FIG. 7 - 86 PUMP HEAD (NODE 17)

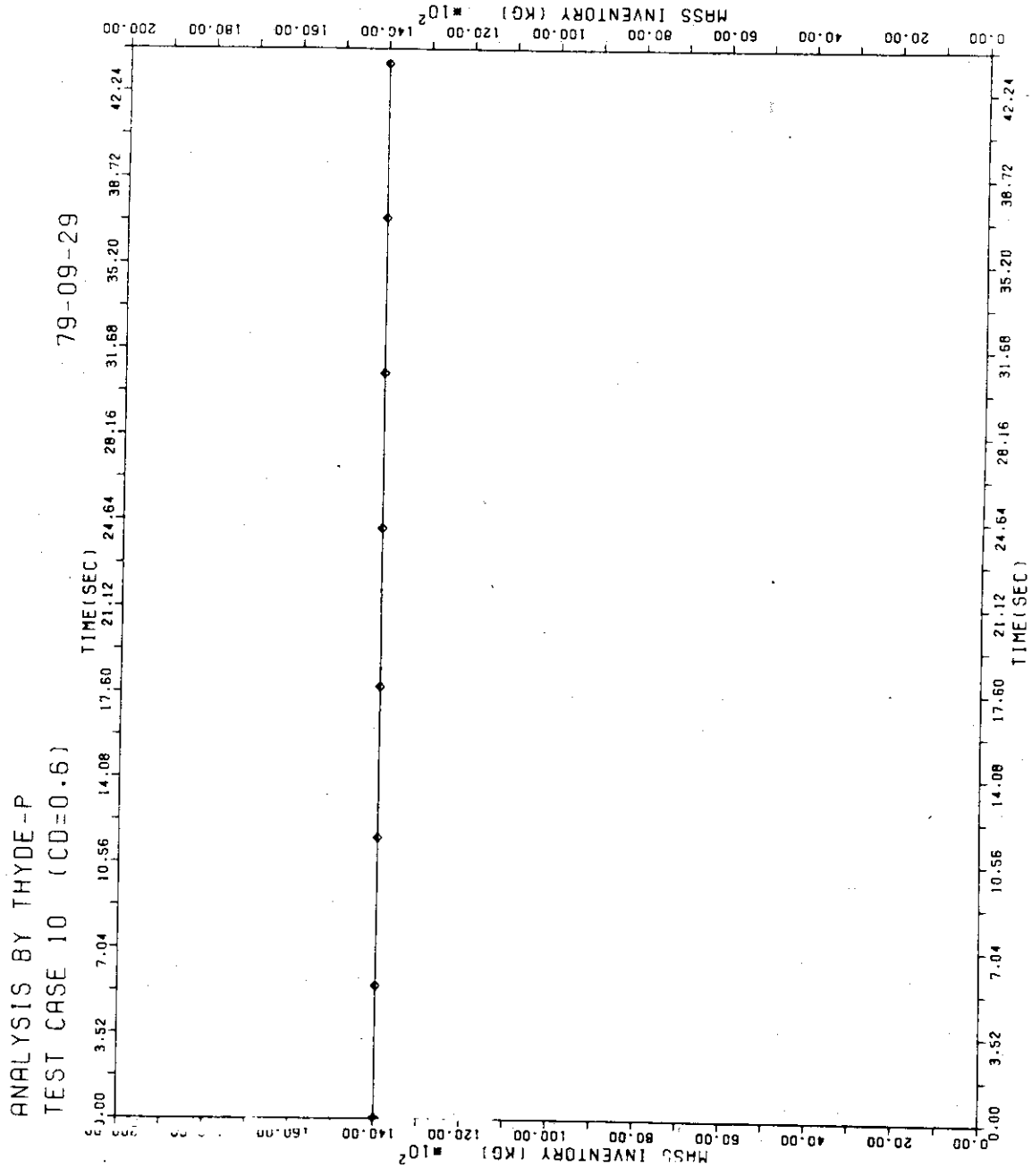

FIG. 7 - 87 REG-1 MASS IN NODE 30

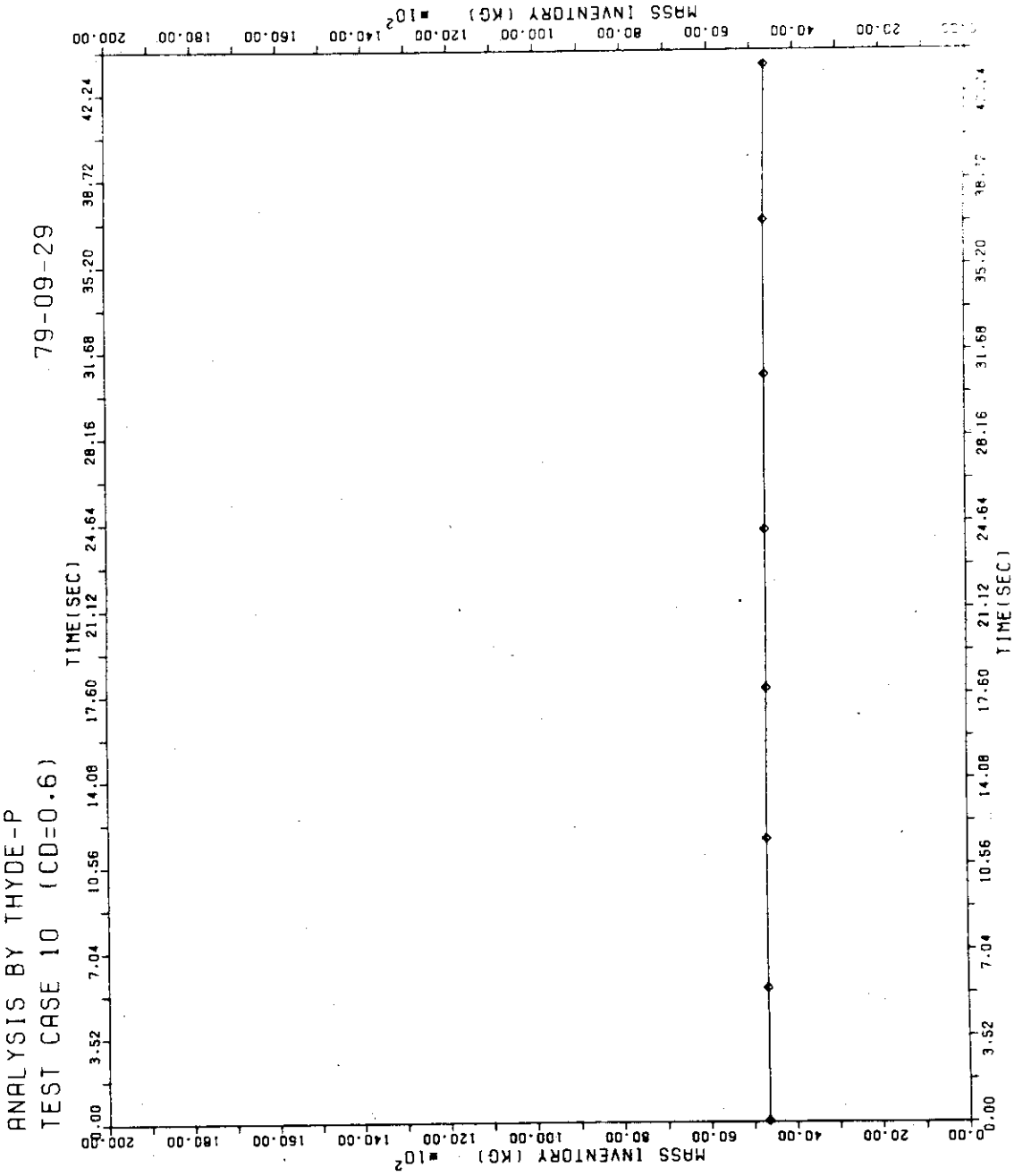

FIG. 7 - 88 REG-1 MASS IN NODE 29

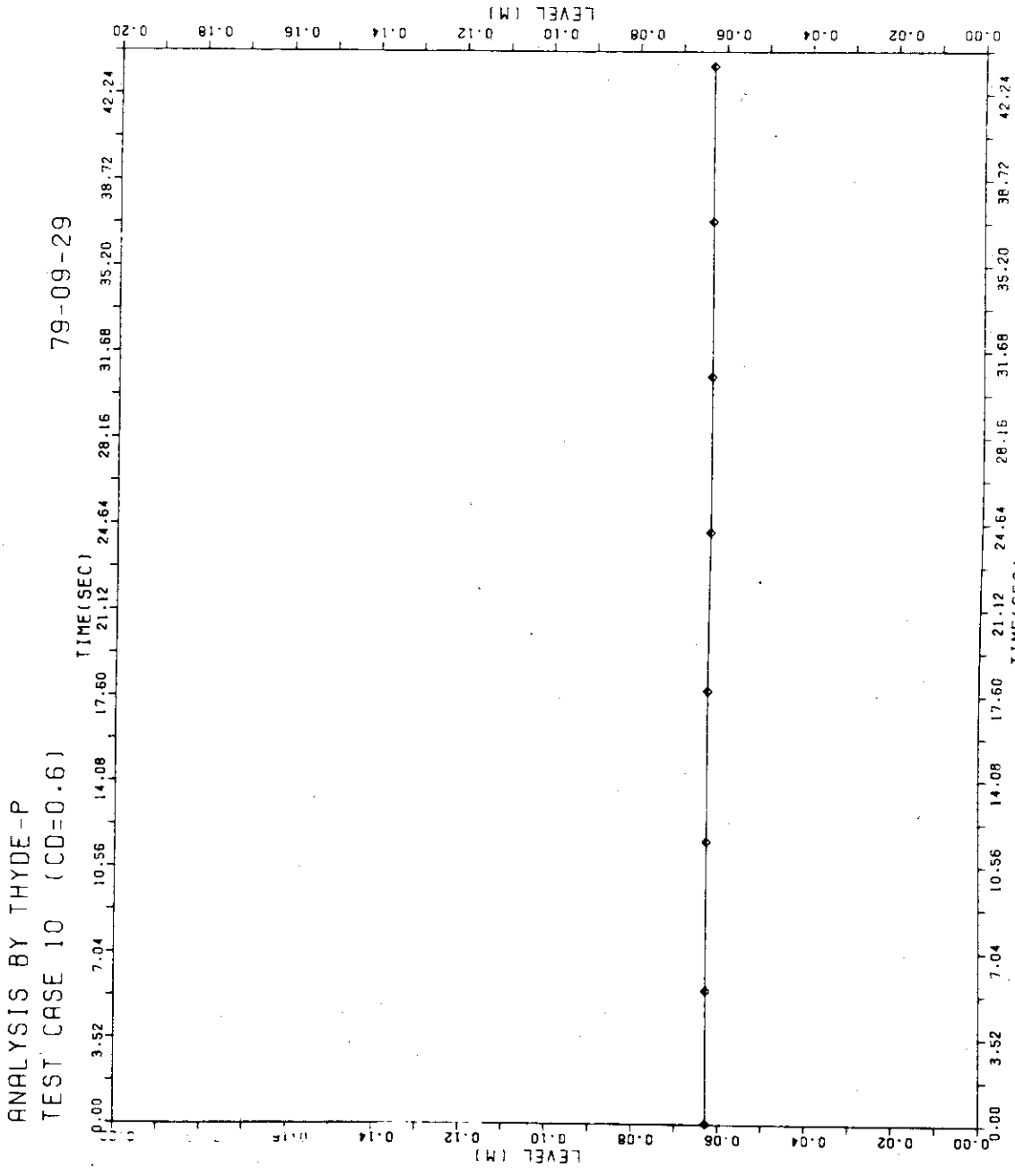

FIG. 7-89 REG-2 LEVEL IN NODE 29

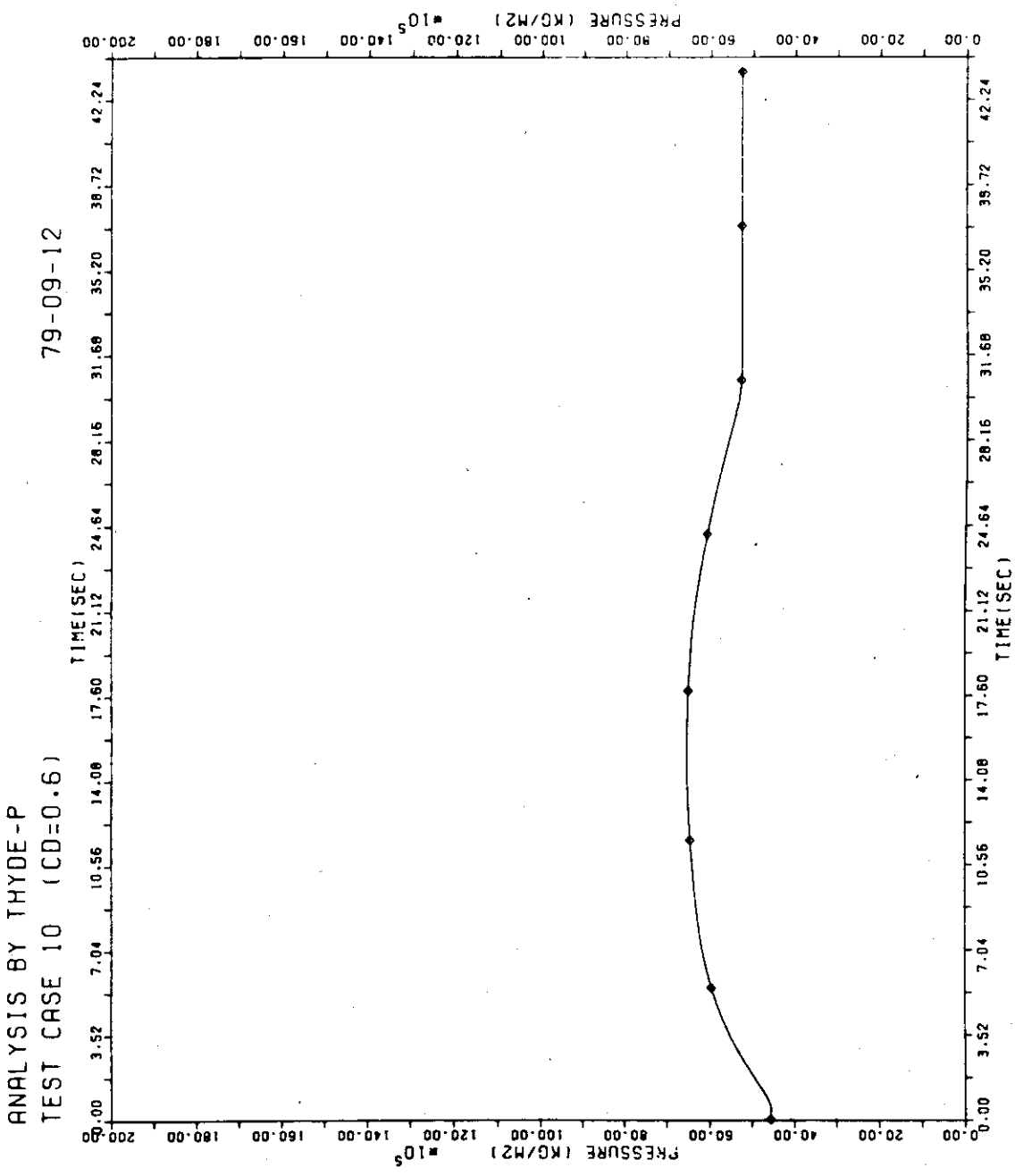

FIG. 7-90 PRESS IN SG (NODE 30)

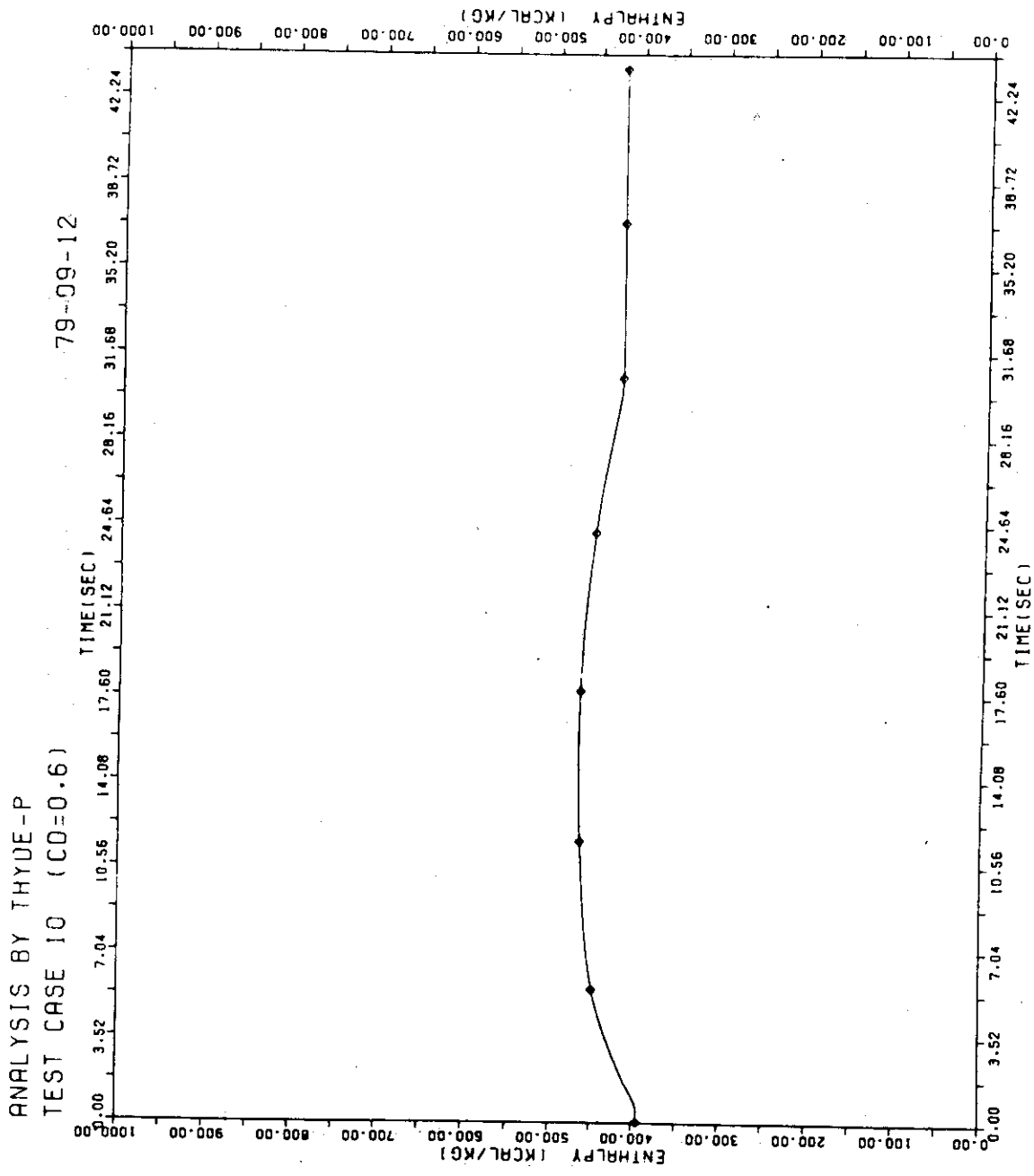

FIG. 7 - 91 ENT OF REG-1 IN NODE 30

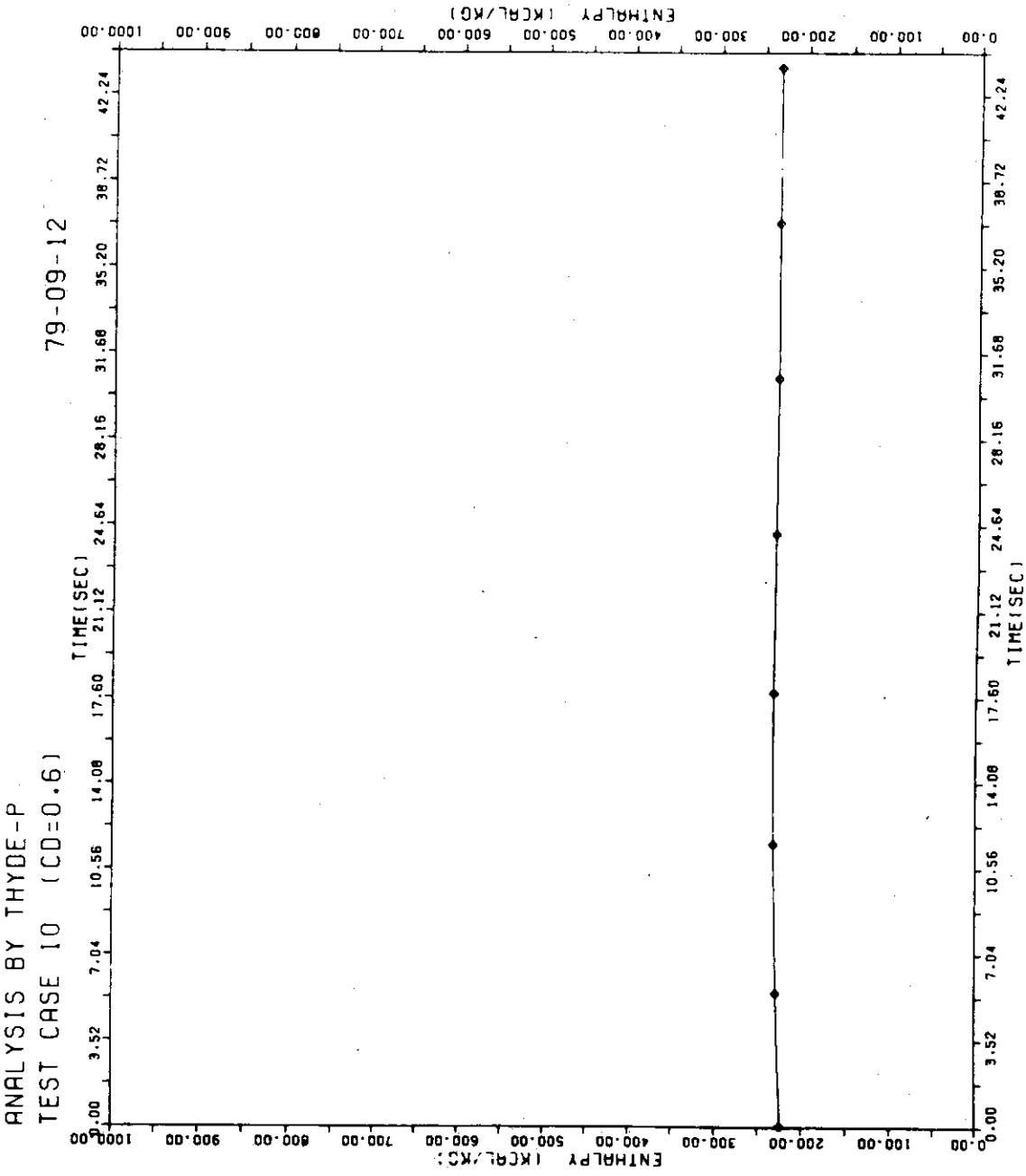

FIG. 7-92 ENT OF REG-2 IN NODE 30

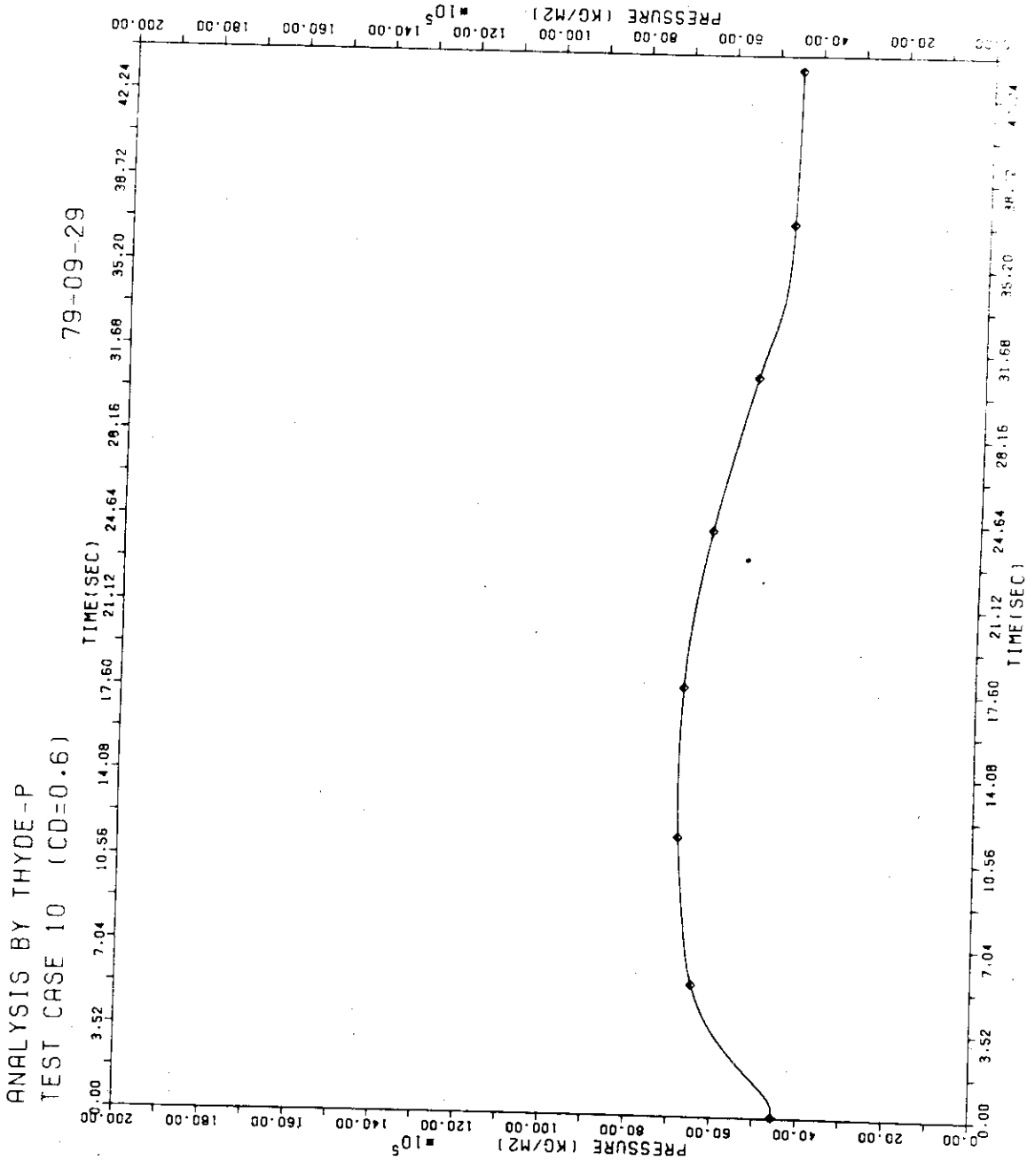

FIG. 7-93 PRESS IN SG (NODE 29)

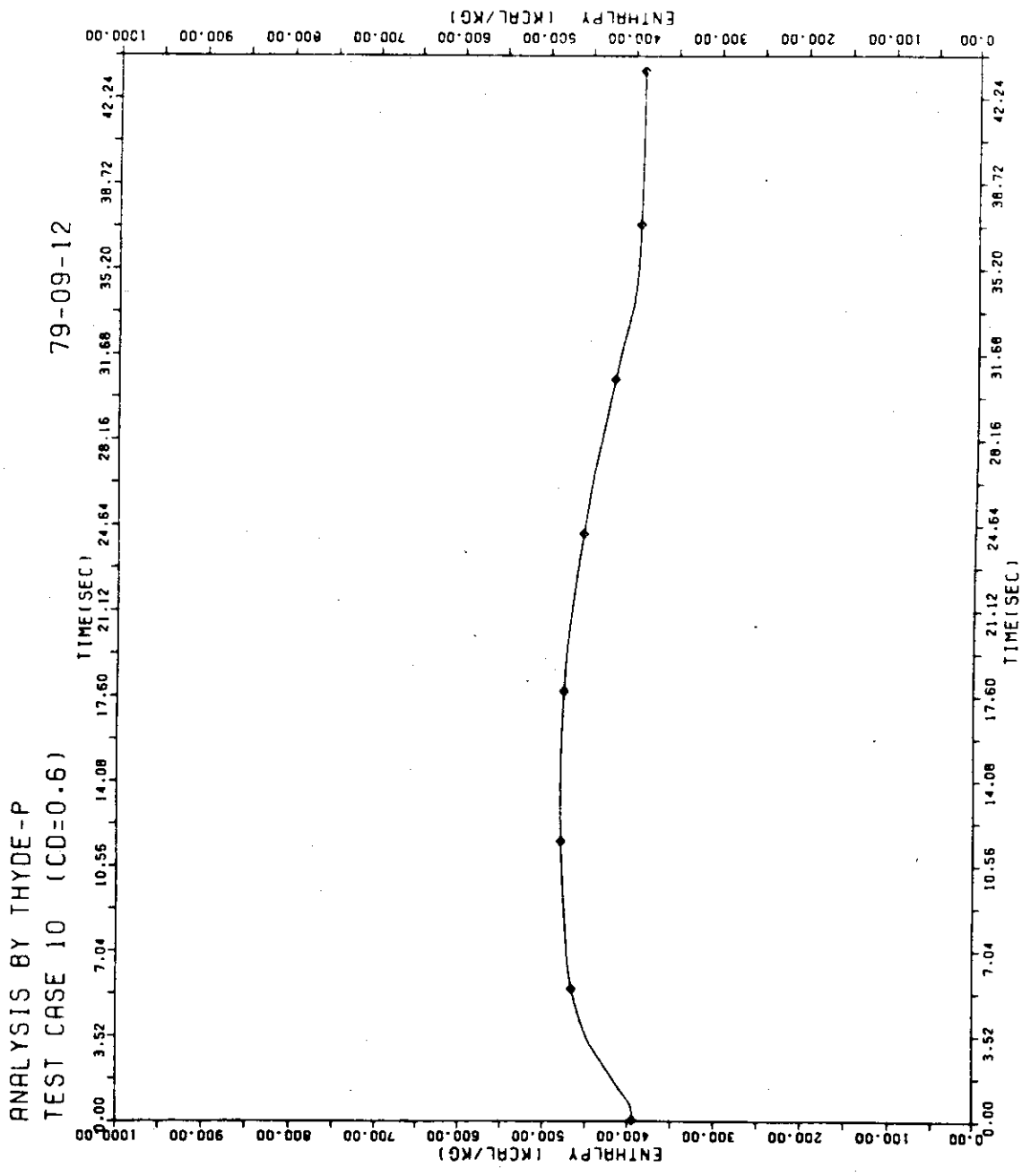

FIG. 7 - 94 ENT OF REG-1 IN NODE 29

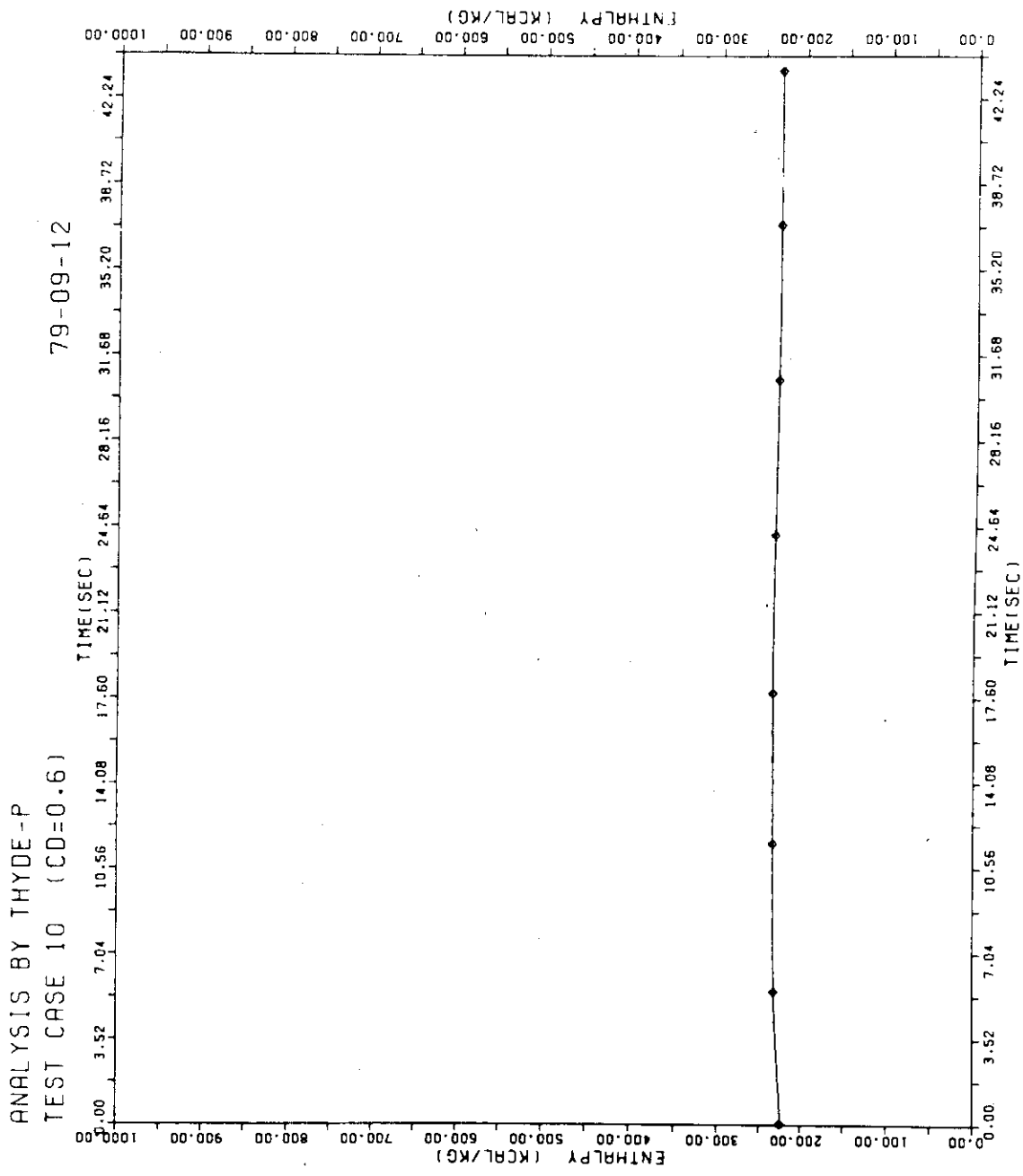

FIG. 7-95 ENT OF REG-2 IN NODE 29

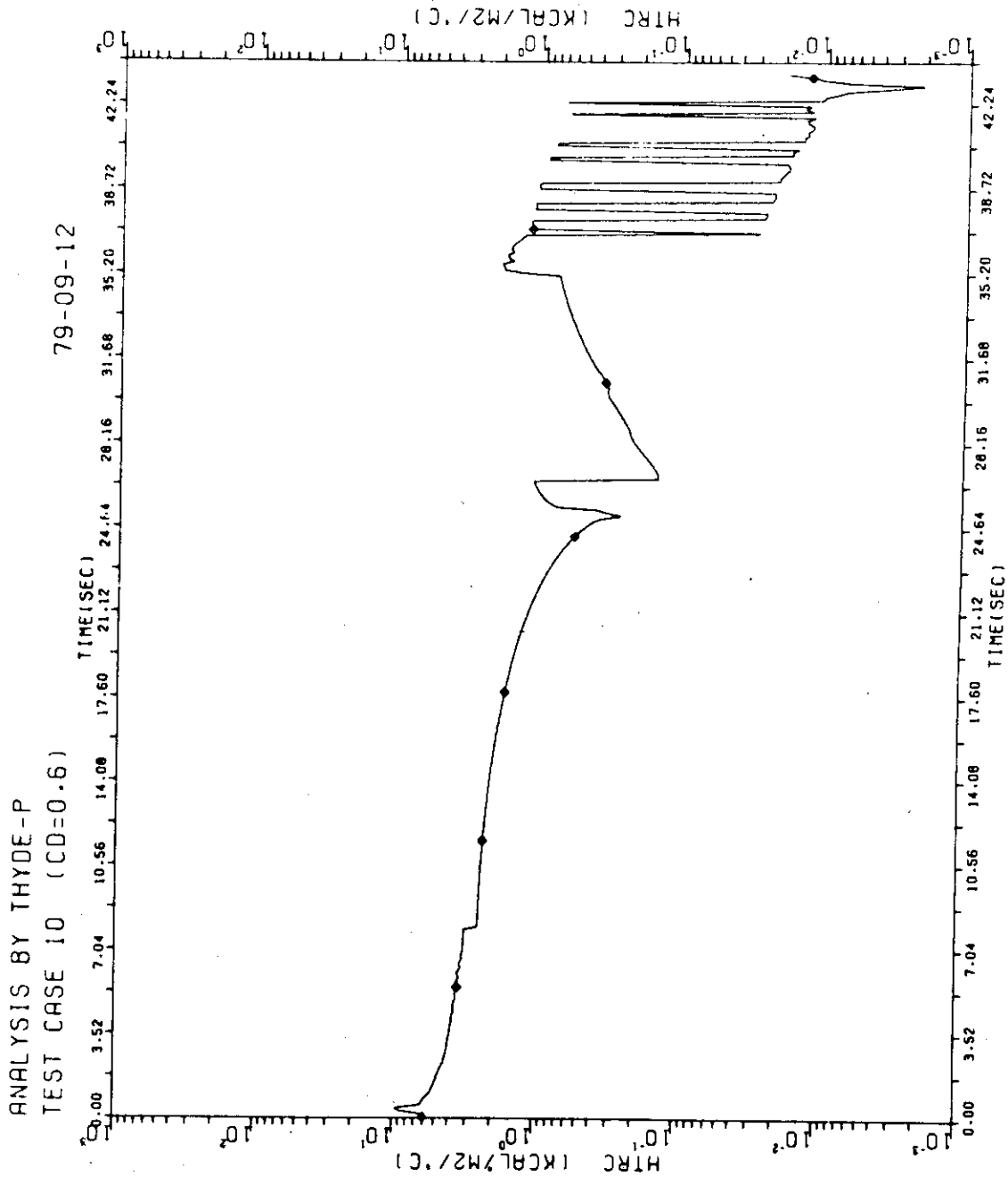

FIG. 7-96 HTRC(PRIMARY) OF NODE 3

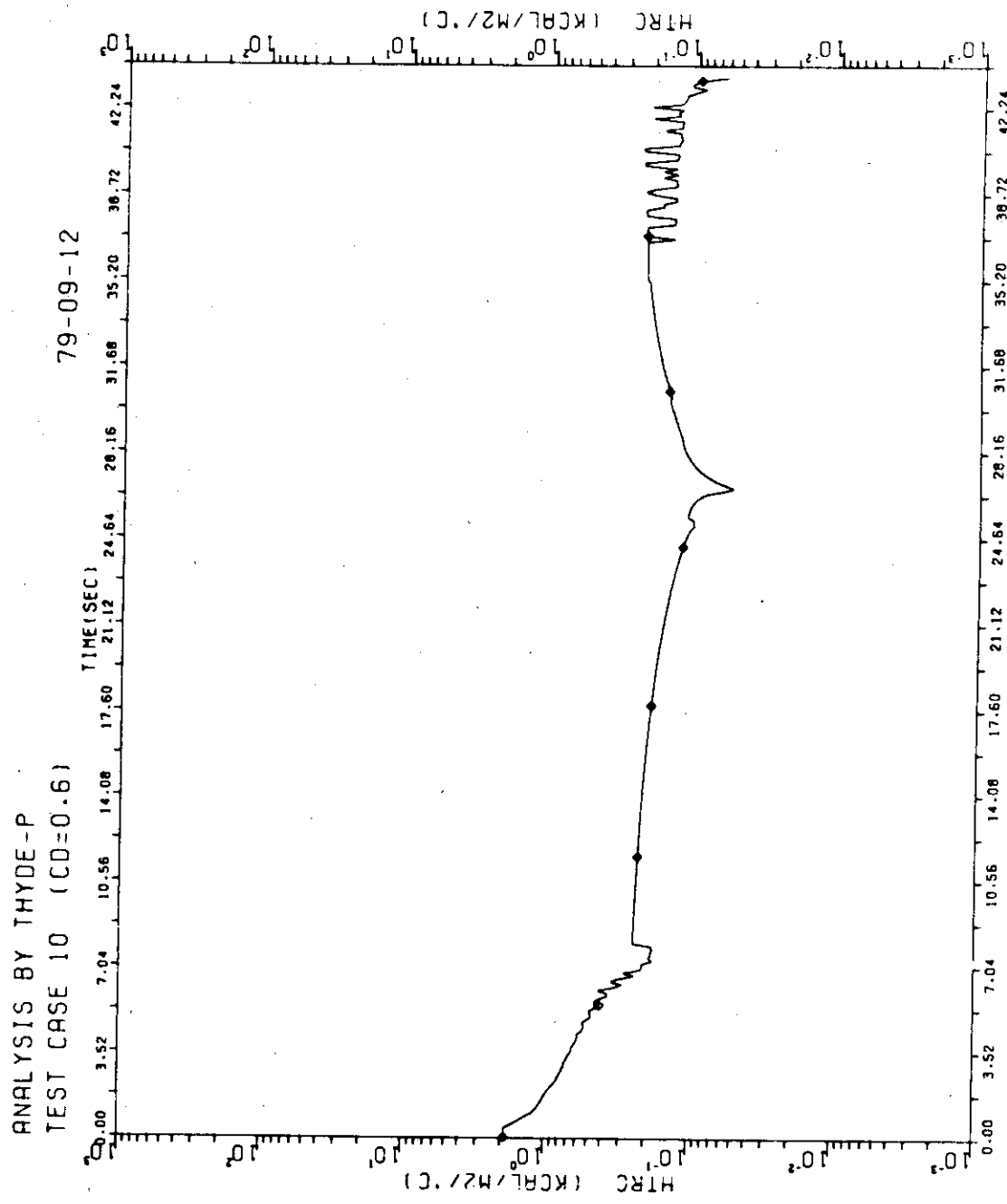

FIG. 7-97 HTRC(2NDRY) OF NODE 3

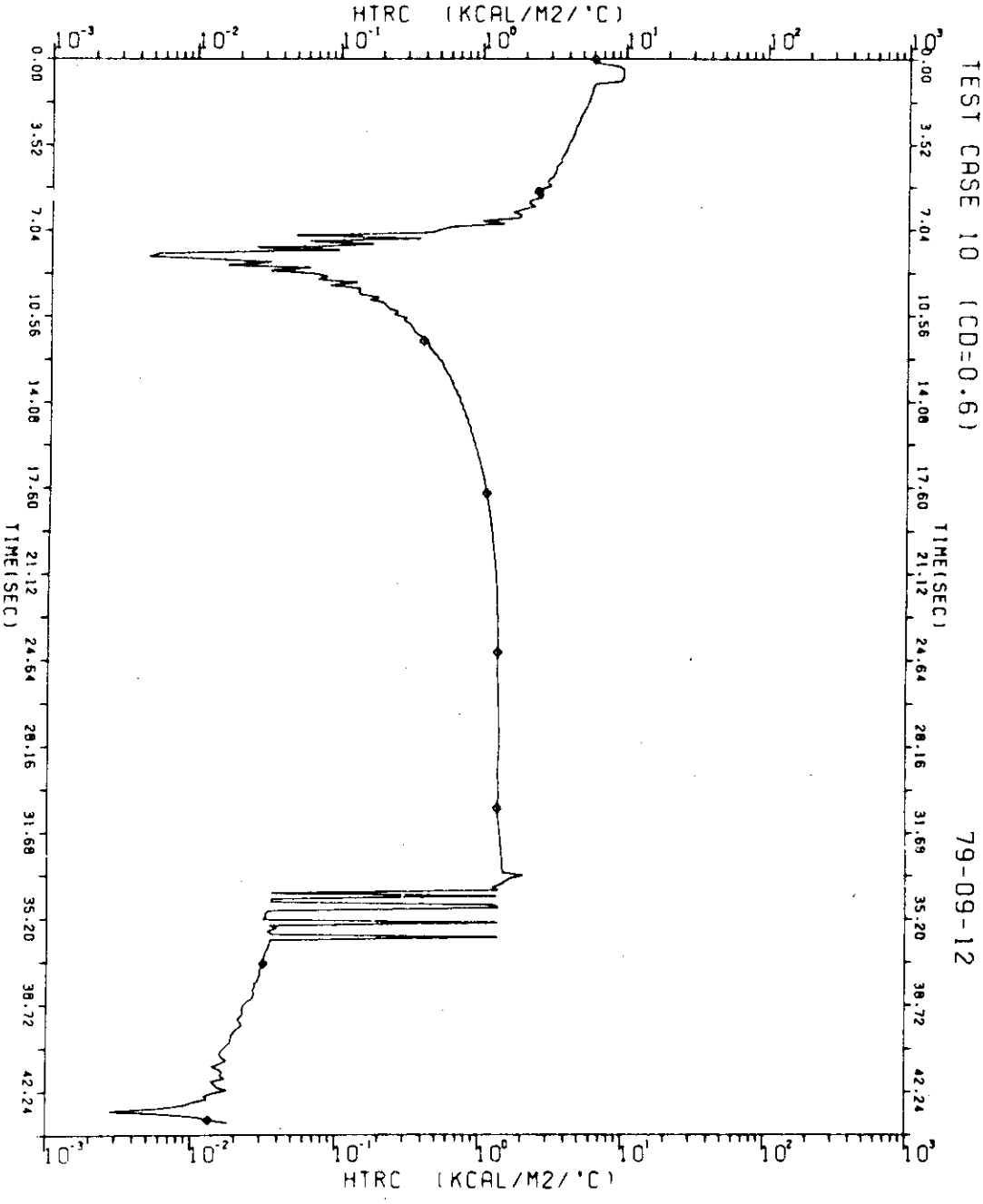

FIG. 7-98 HTRC(PRIMARY) OF NODE 4

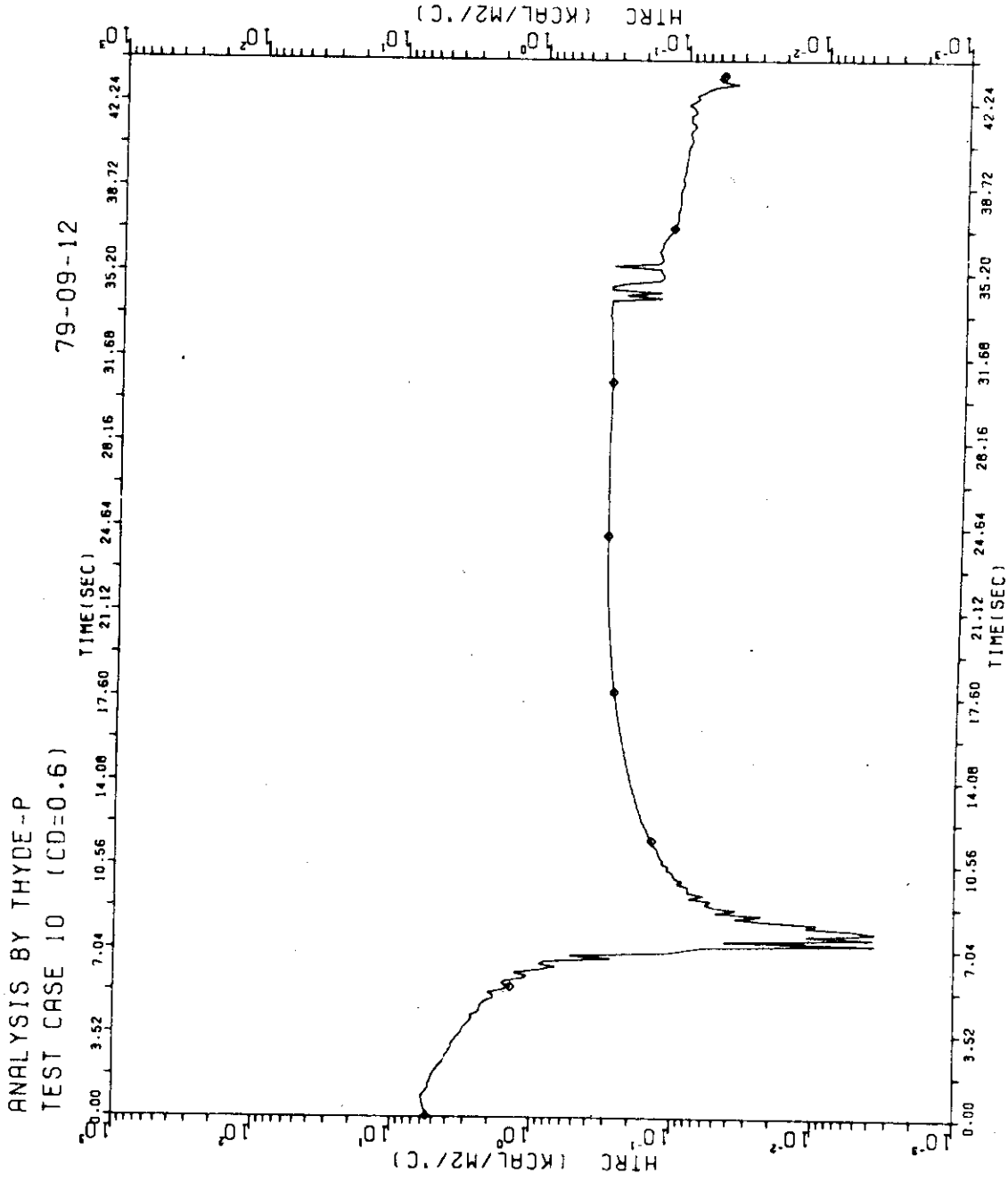

FIG. 7-99 HTRC(2NDRY) OF NODE 4

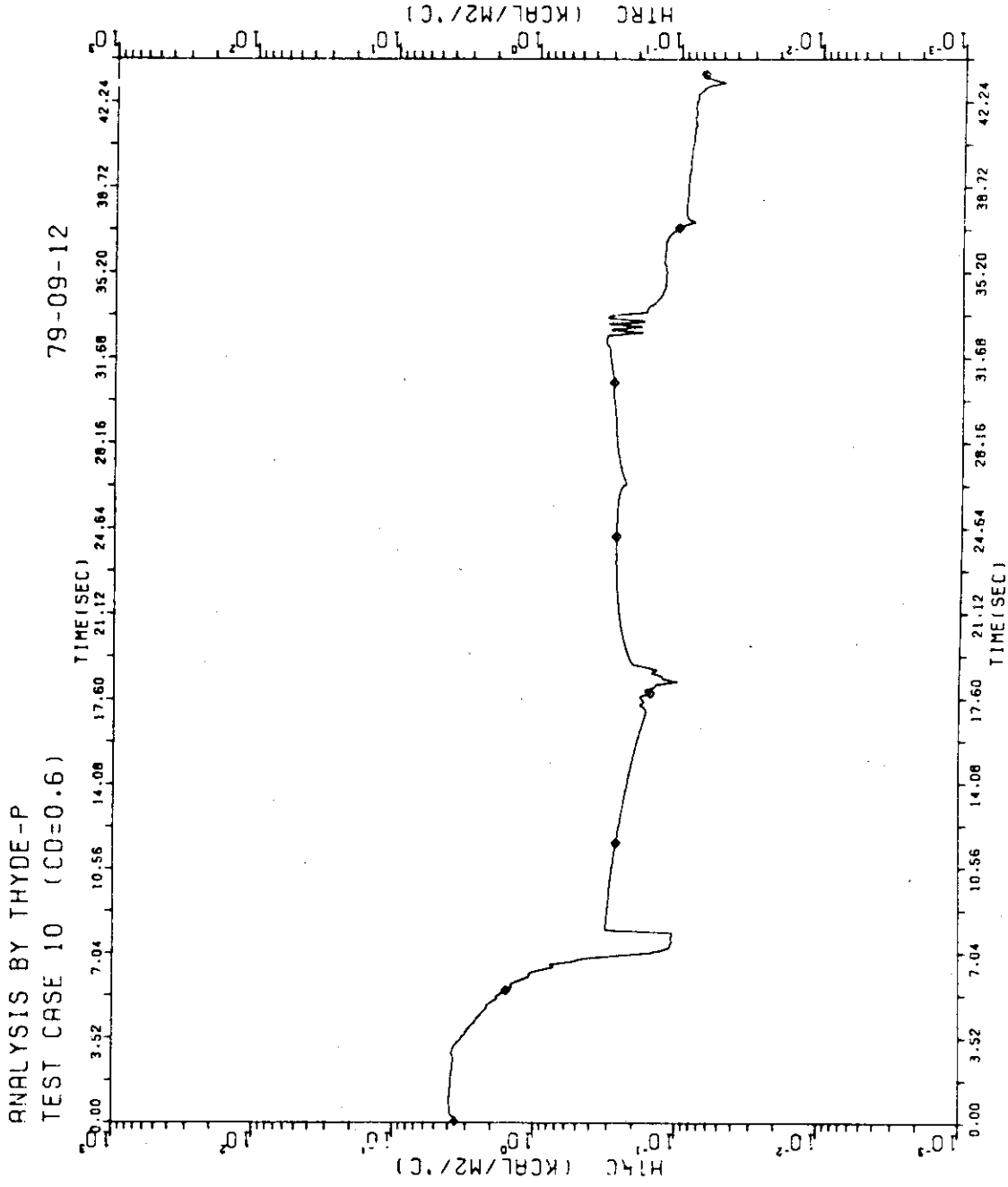

FIG. 7 - 100 HTRC(2NDRY) OF NODE 5

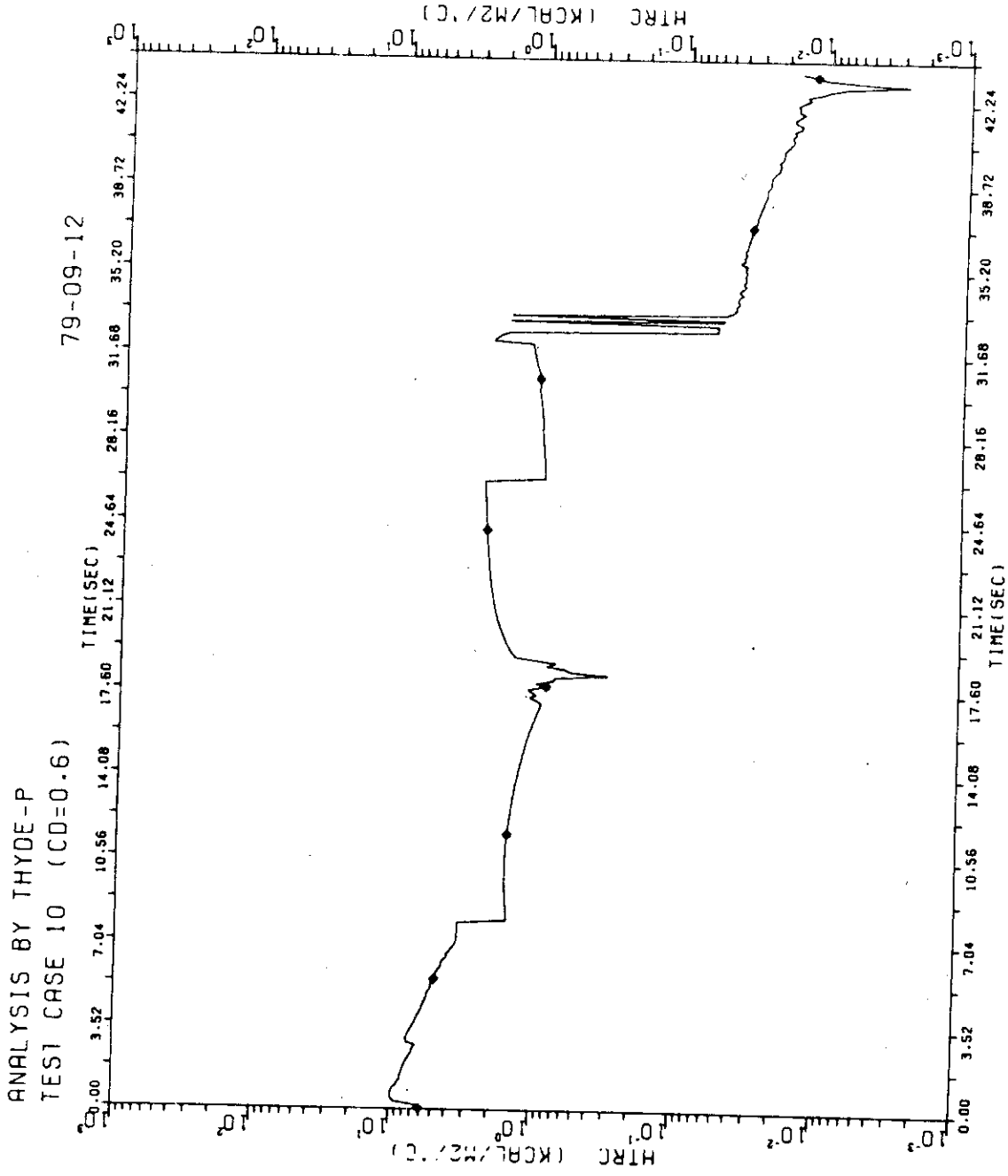

FIG. 7-101 HTRC(PRIMARY) OF NODE 5

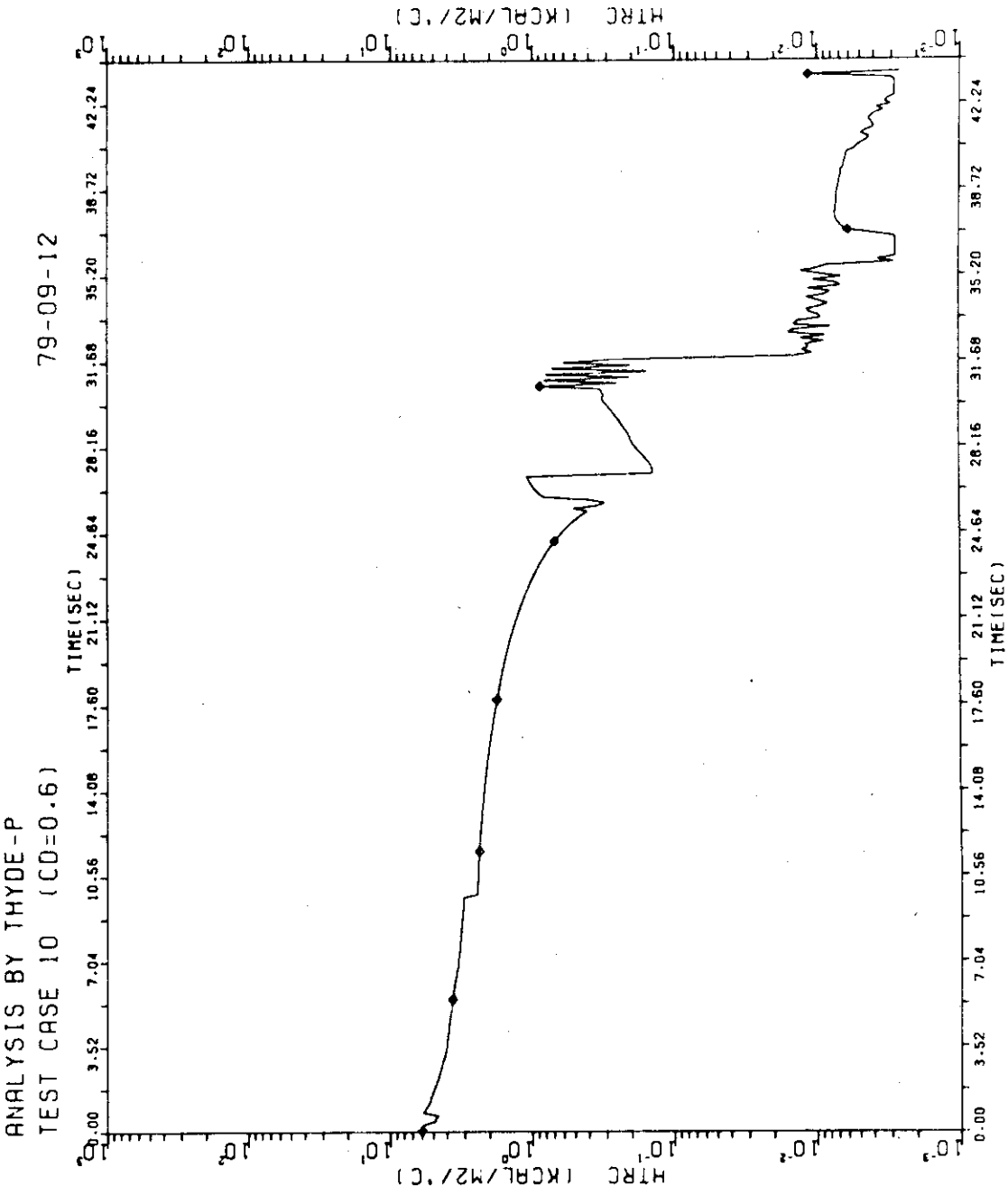

FIG. 7-102 HTRC(PRIMARY) OF NODE 12

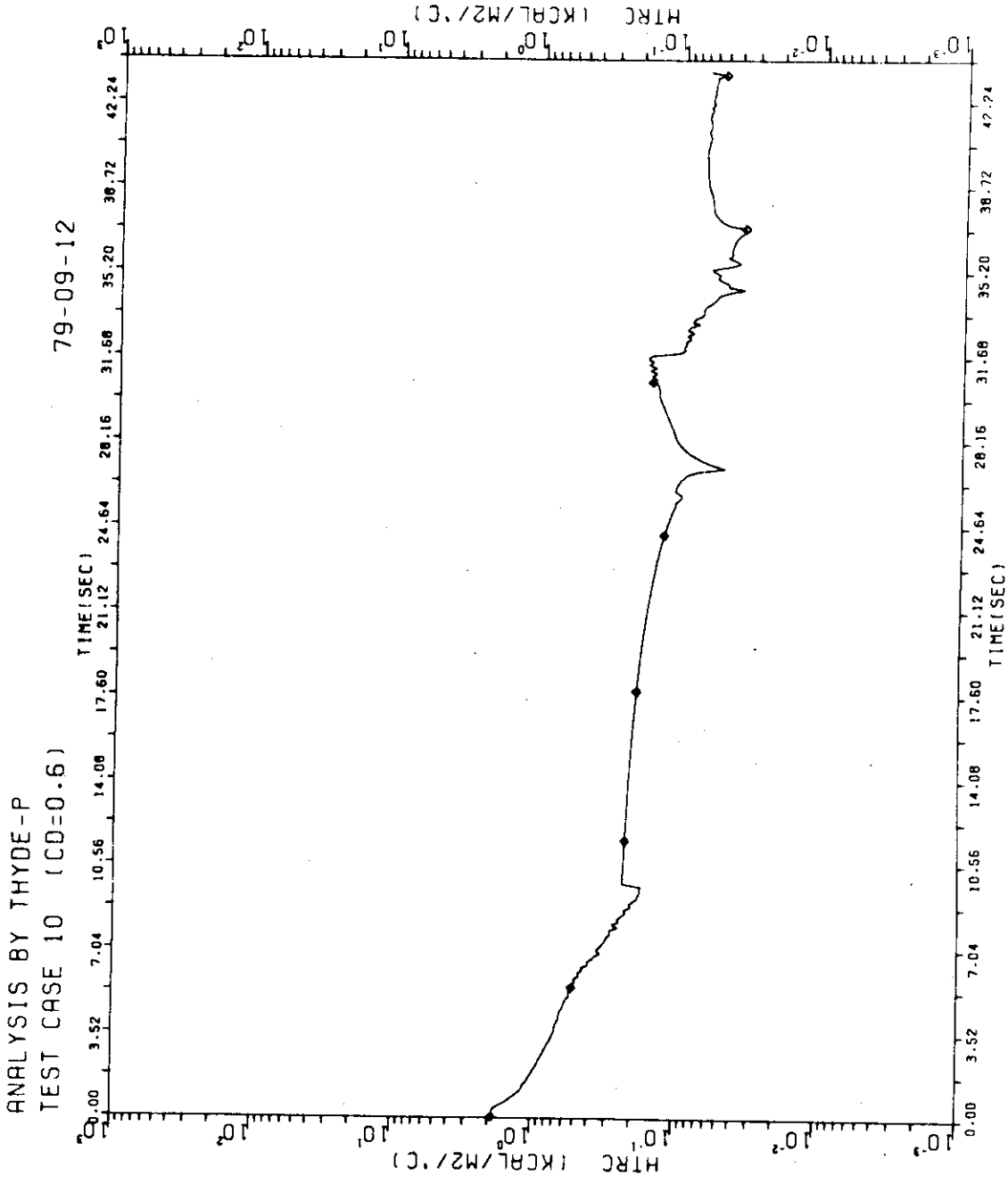

FIG. 7 - 103 HTRC(2NDRY) OF NODE 12

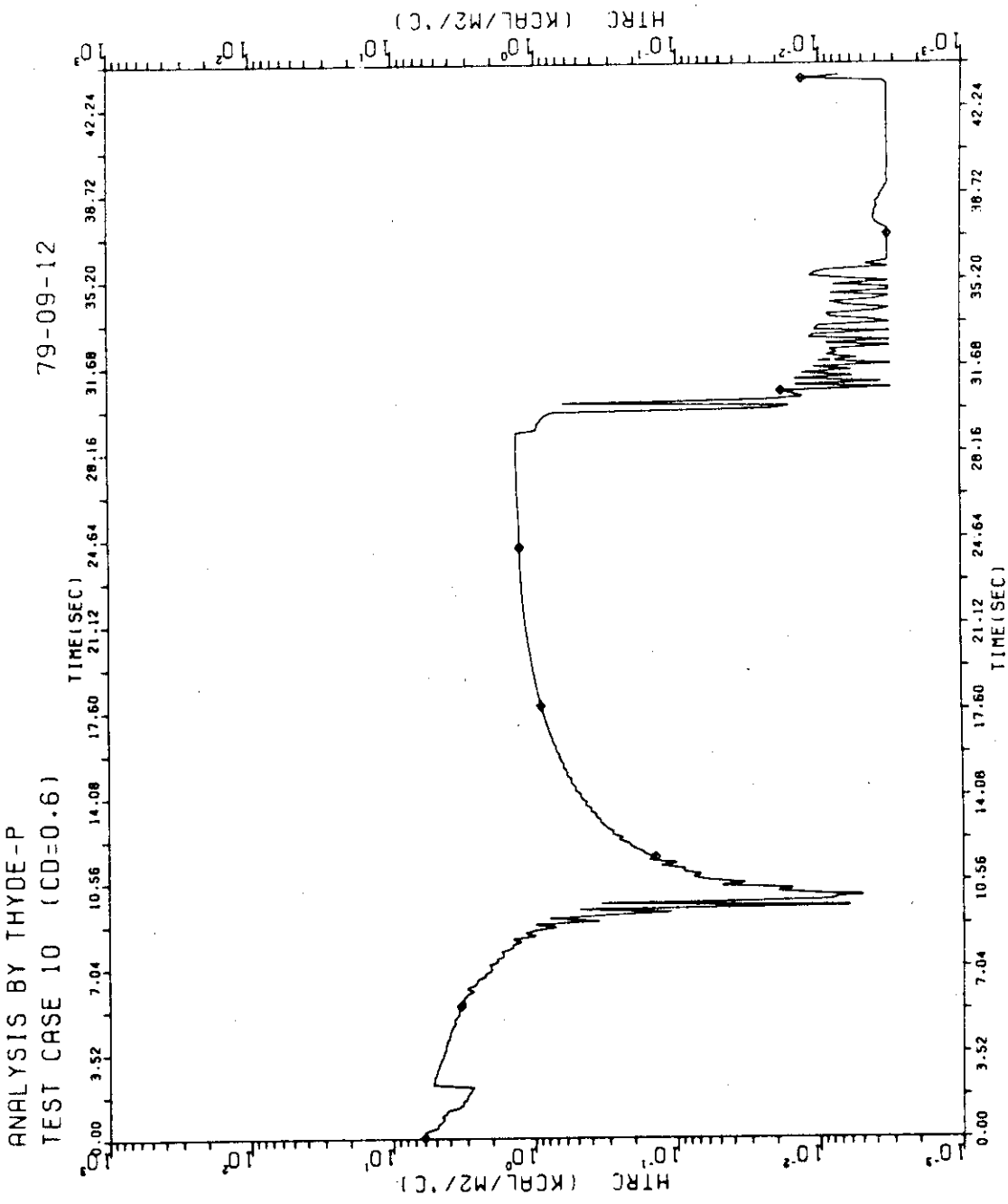

FIG. 7 - 104 HTRC(PRIMARY) OF NODE 13

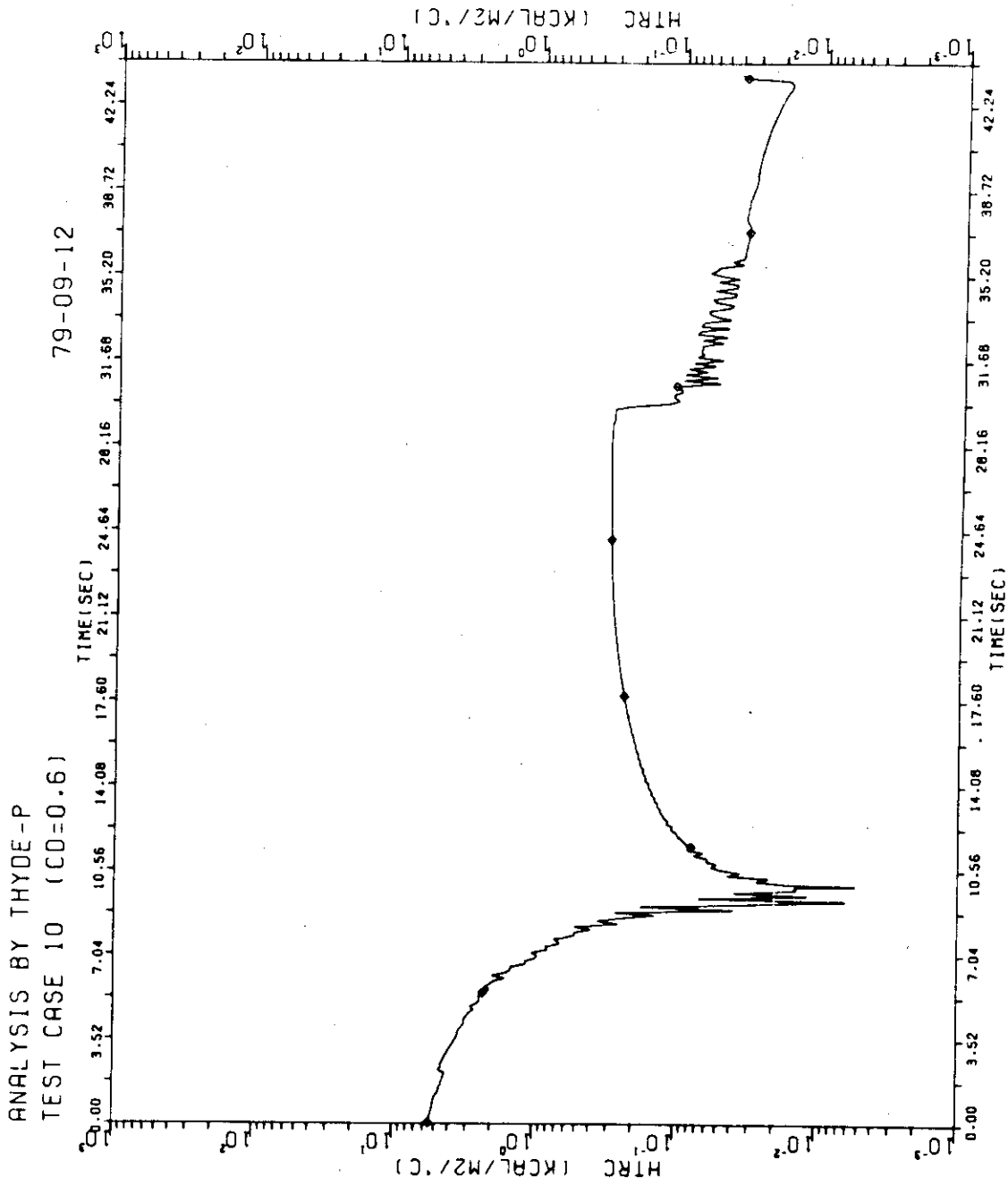

FIG. 7-105 HTRC(2NDRY) OF NODE 13

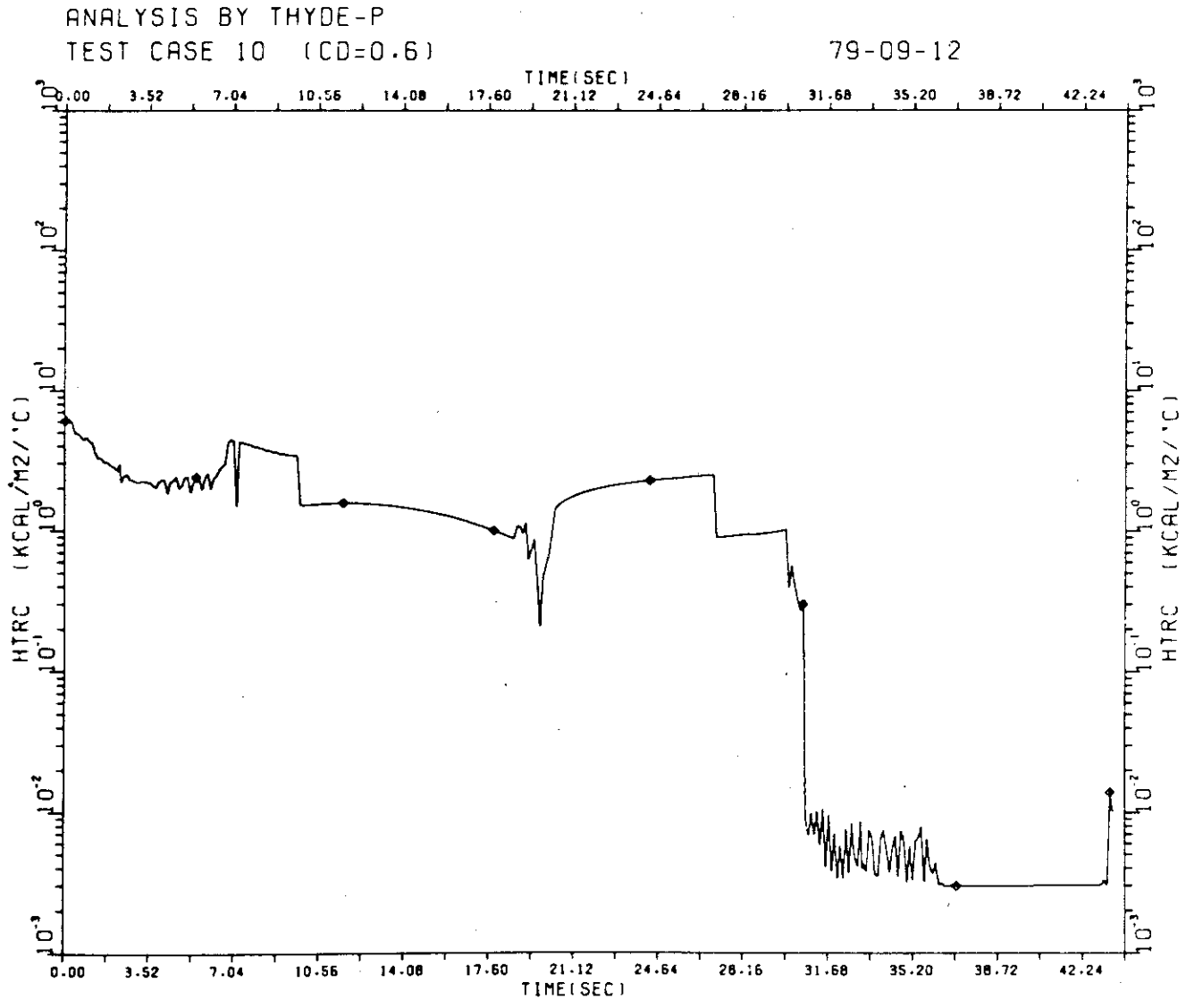

FIG. 7 - 106 HTRC(PRIMARY) OF NODE 14

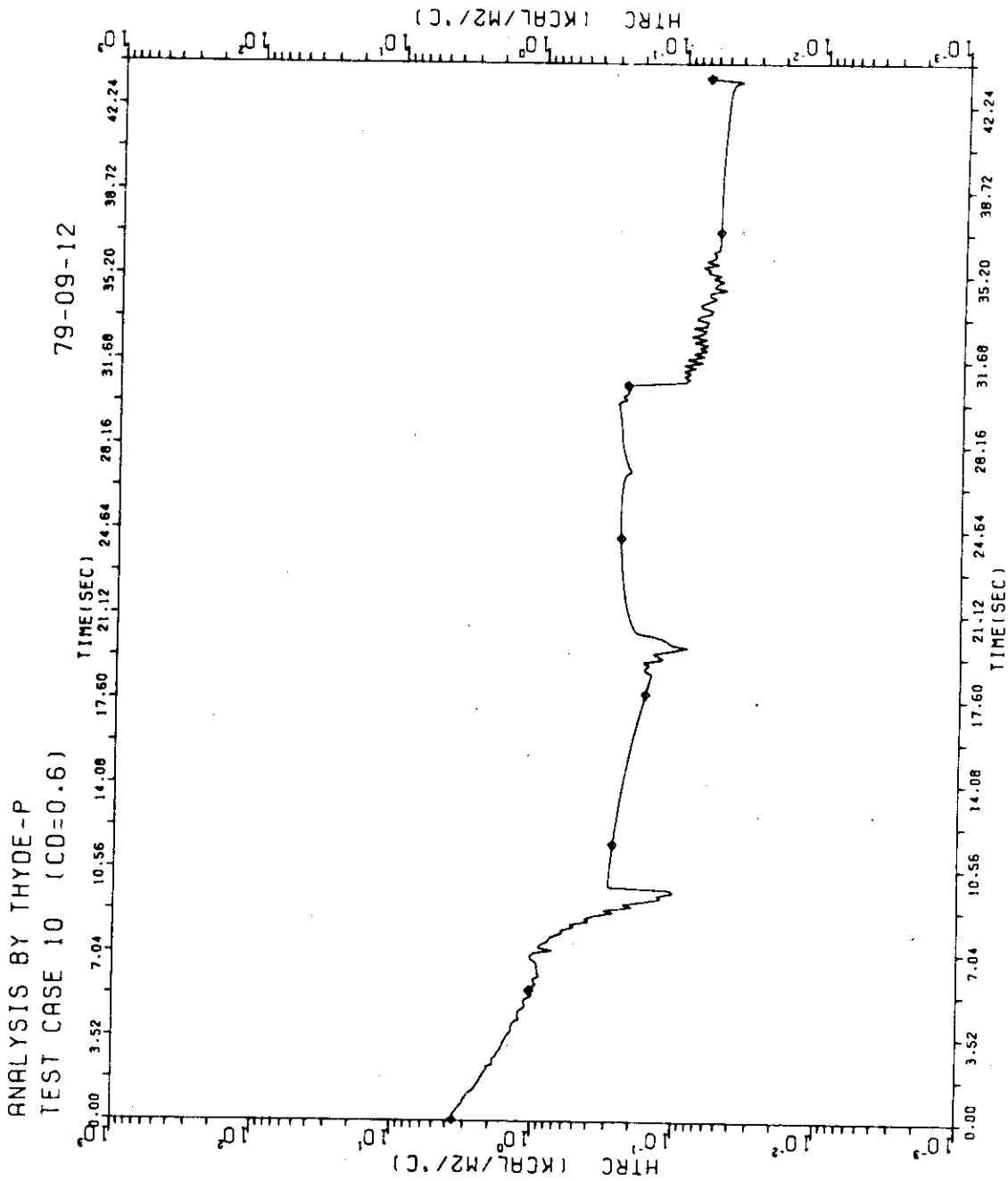

FIG. 7 - 107 HTRC(2NDRY) OF NODE 14

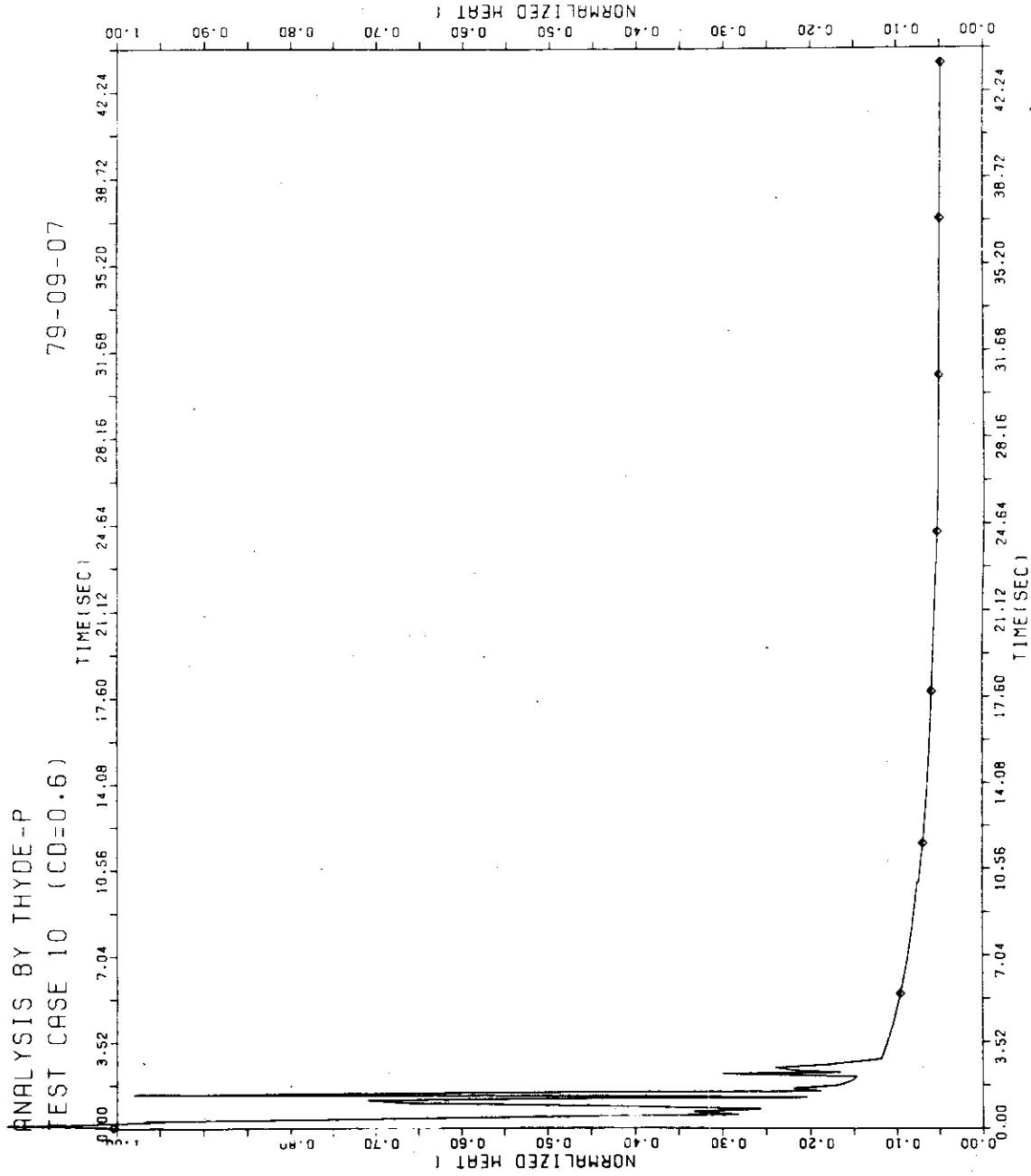

FIG. 7-108 HEAT IN CORE

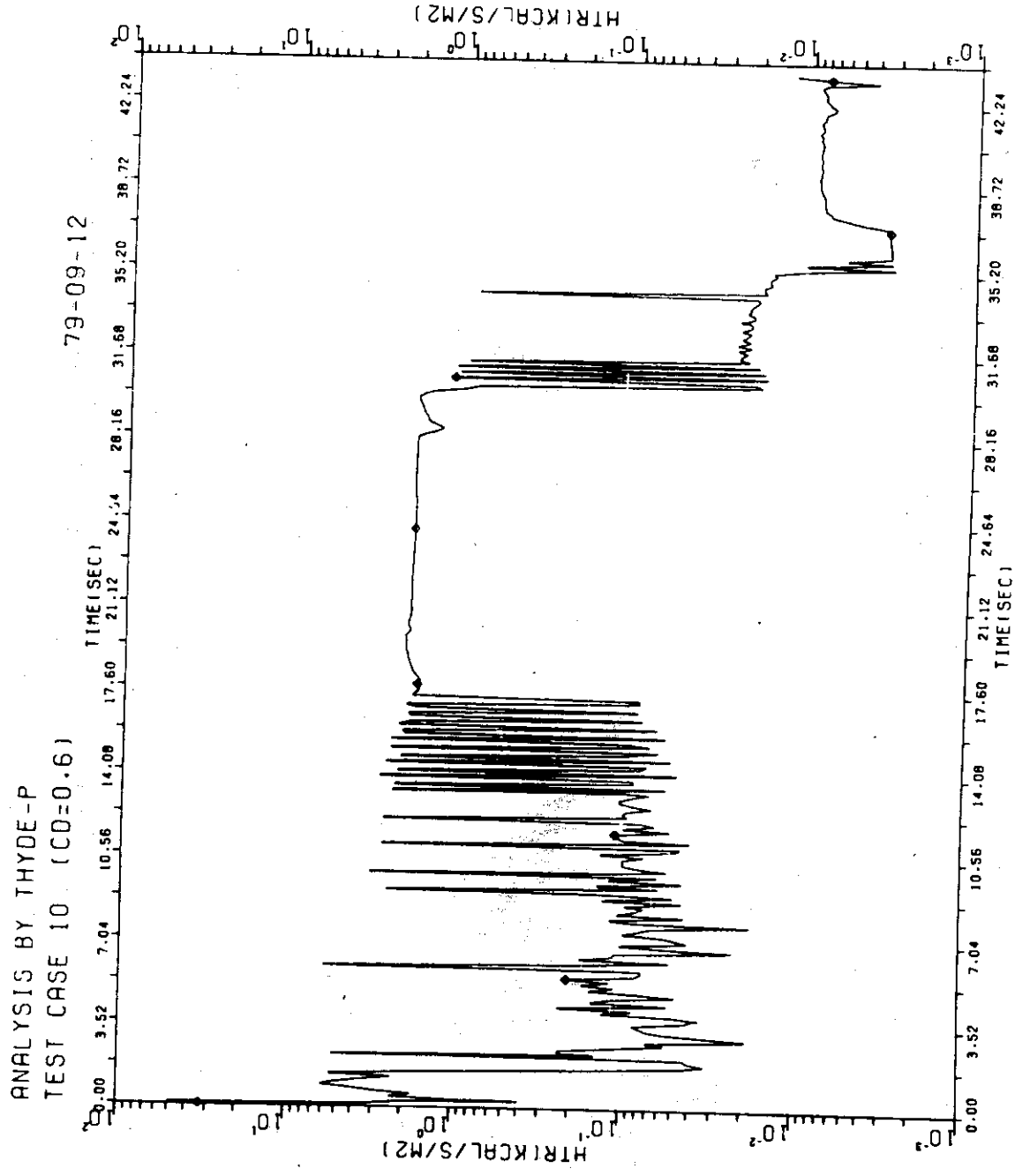
ANALYSIS BY THYDE-P
TEST CASE 10 (CD=0.6)
79-09-12
HTRC (NODE 23)
HTR(KCAL/S/M2)
TIME(SEC)
0.00
3.52
7.04
10.56
14.08
17.60
21.12
24.64
28.16
31.68
35.20
38.72
42.24

FIG. 7 - 109

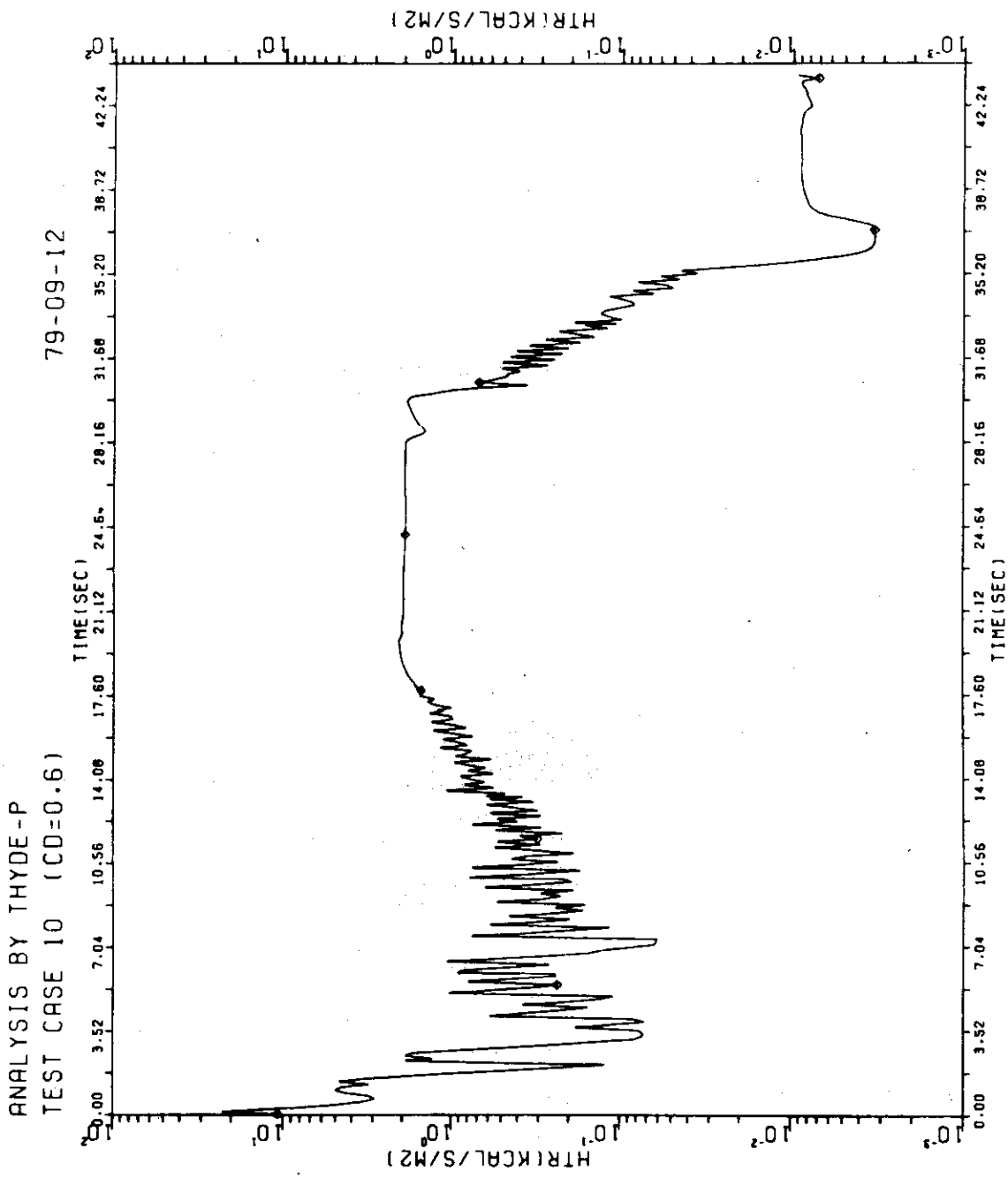

FIG. 7 - 110 HTRE (NODE 23)

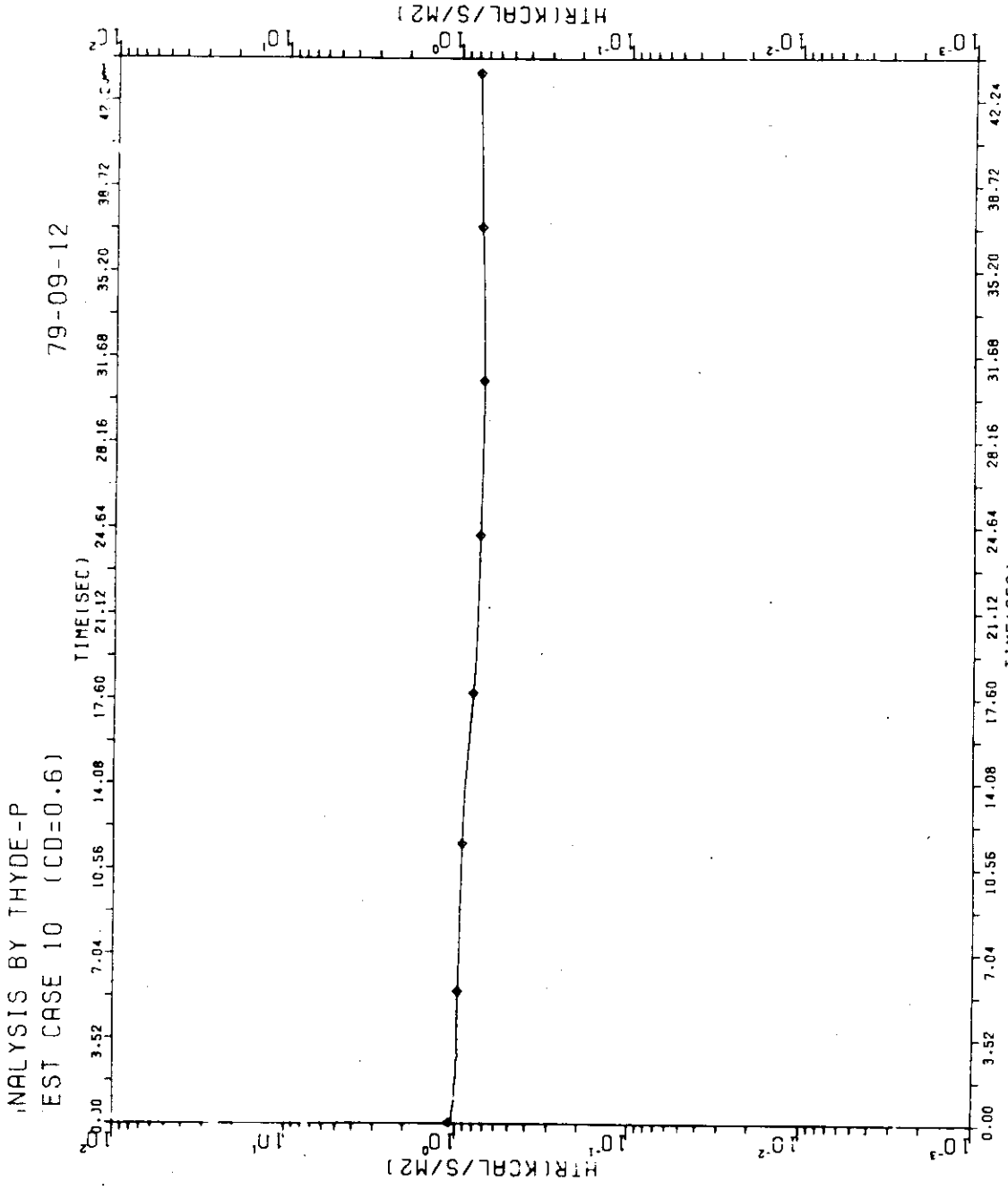

FIG. 7 - 111 HTR-GAP(NODE 23)

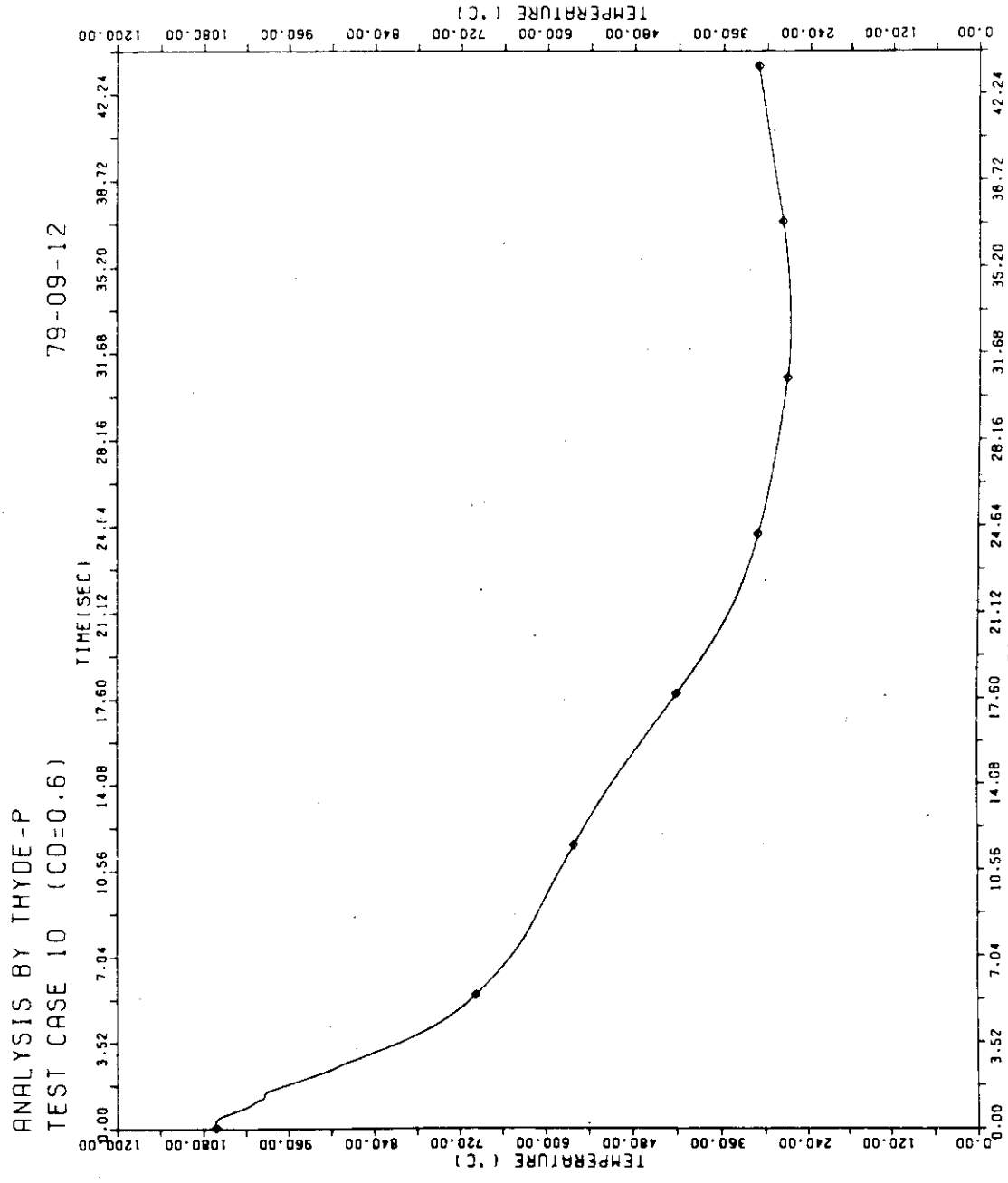

FIG. 7-112 FUEL CENT TEMP (NODE 23)

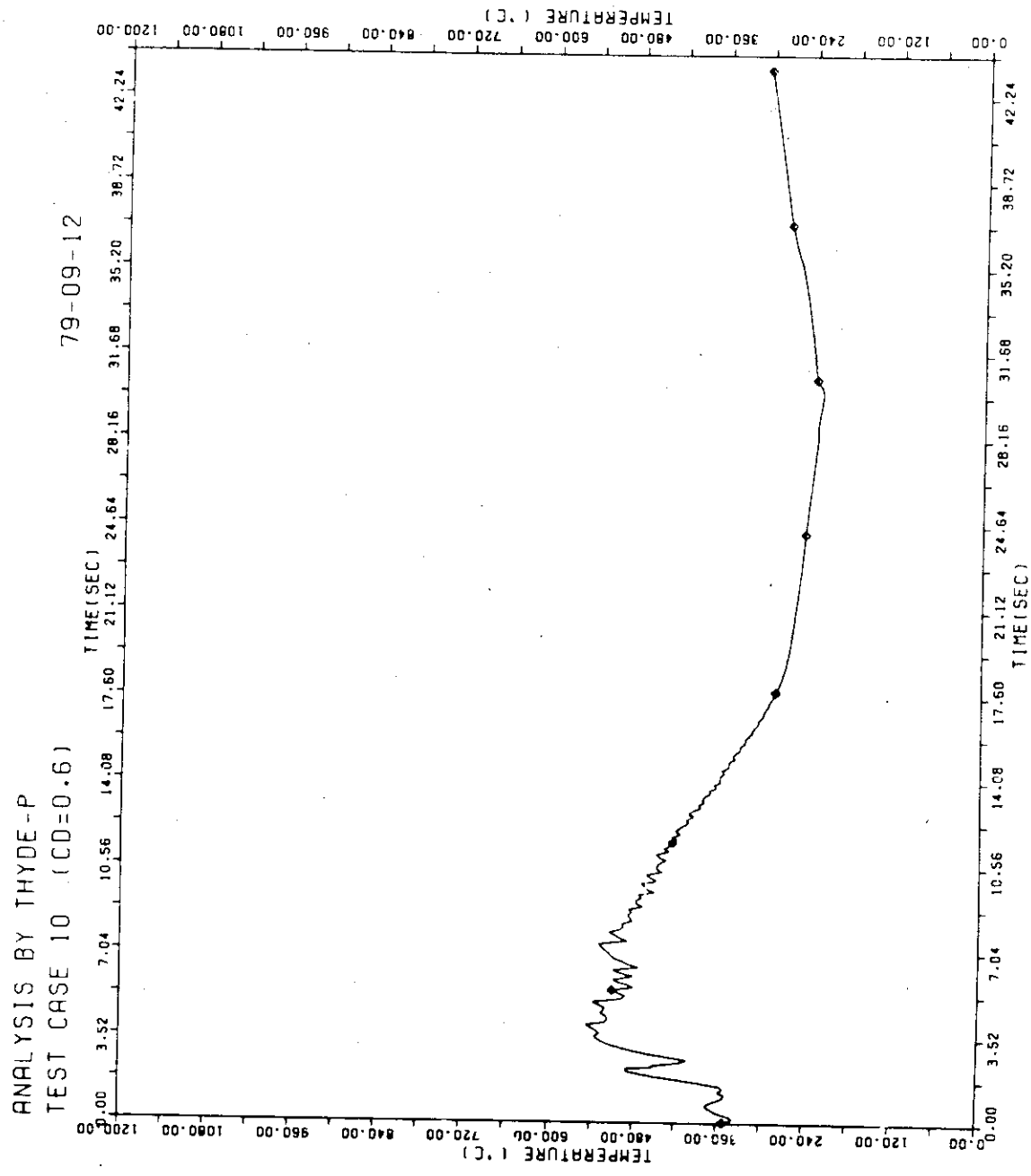

FIG. 7-113 SURFACE TEMP (NODE 23)

8. Needs for Code Modifications

In the following, 9 items for THYDE-P modifications yet to be made are cited, which have been found necessary in the course of this work and after publication of Ref.(1). As of Oct. 15, 1979, items (1), (2) and (7) has been resolved. Among the remainder, items (3), (4), (5), (8) and (9) may be easy or straightforward, but have not yet been implemented. Item (7) has been considered rather difficult and in fact is the reason why Run 10 failed at time 43 sec after end of blowdown.

Item (7) is the reason why one makes it a practice in existing LOCA analysis codes after end of blowdown either to calculate with a considerably high value of ECC water enthalpy or to ignore the time derivatives in the flow equations. To overcome this difficulty, we have implemented a new model in the THYDE-P code, which phenomenologically simulates the pressure recovery at low pressure. Implementation of such a model in the flow equation is not always possible. The reason why it was possible for THYDE-P is the new flow netework model incorporated in THYDE-P, which matches our phisical intuition.

(1) Irreversible Loss Coefficient at Expansion and Contraction of Flow Path

In the present version of THYDE-P, irreversible loss coefficient at expansion and contraction of flow path is not accounted for as such. Instead, we regard that it is included in the node loss coefficient. As a result, steady state adjustment gives rise to loss coefficients, some of which are very large. To correct this point, we will have to incorporate a friction loss term in node equation f_2 or f_3. We note that the kinetic energy term in f_2 or f_3 corresponds with the reversible portion of pressure loss at flow area change.

(2) SG Secondary Coolant and U-tube Wall Temperatures

As mentioned in section 6.2, there are at least three possible modifications needed with respect to SG secondary coolant and U-tube wall temperatures. The first is the refinement of the steam table especially of saturation temperature in the neighborhood of 65 ata. The second is the examination of the numerical technique for determination of the U-tube wall temperatures. The third is the implementation of an iterative technique for the steady state adjustment. After it is implemented, a reasonable value for the feed water flow

rate is expected to be obtained, provided that a suitable value for the initial subcooled water level is given.

(3) Steady State Adjustment of Primary Loop Pressure Distribution

If a suitable set of input data is provided, computer will automatically accomplish steady state adjustment. For most input data, empirical values will suffice for steady state adjustment, except for primary loop pressure distribution. The steady state adjustment for primary loop pressure distribution is rather subtle, and frequently requires a tedius procedure as described in section 4. It is expected, however, that is will be simplified to some extent by printing out some of the quantities involved in this procedure such as ζ_n and ξ_{nn}, in Eq.(3).

(4) Linkage Flow with a Dead or Break End and/or Mixing Junctions

A linkage flow with a dead or break end and/or mixing junctions is not presumed in the present version of THYDE-P. Those provisions are needed for THYDE-P, since such configurations are frequently found in experimental facilities. Moreover, the provision for a linkage flow with a break end is needed to analyze split break LOCA's.

(5) Heat Transfer between Coolant and Structure

Since structural material of a PWR plant is massive, energy initially stored in structure is substantial and may influence significantly the coolant behavior especially during refill and reflood phases.

(6) Solution Technique at Low Pressure

A number of quantities involved in the flow equations such as average density of two-phase mixture $\rho(p,h)$ and its derivatives are very sensitive to variations in p and h at low pressure, which occurs during refill and reflood phases of a LOCA. Such tendencies bring about a couple of difficulties inherent in low pressure.

In the formulation of THYDE-P, we utilize the relationship

$$d\rho = \frac{\partial \rho}{\partial h} dh + \frac{\partial \rho}{\partial p} dp \qquad (19)$$

in Eq.(10) to transform the flow equations. At low pressure, however, ρ, $\frac{\partial \rho}{\partial h}$ and $\frac{\partial \rho}{\partial p}$ change so drastically, especially near saturation enthalpy that Eq.(19) may break down and its inconsistency may be numerically

substantial, unless dh and dp are sufficiently made small. Neglecting the inconsistency, we may be able to continue the calculation, but then convergence of the solution of hydraulic network will be greatly deteriorated and will eventually fail due to the momentum flux term G^2/ρ in the momentum equation. To solve this problem, we may have to put a more strict restriction on the time step width control, at the expense of computer time which may then become so large as impractical.

(7) Flow Model at Low Pressure

As the system pressure drops below the saturation point, bubbles grow and, by increasing the specific volume of the coolant, reduce the rate at which the pressure drops. It is known, however, that if the calculation is continued with a realistic value of enthalpy for ECC water after end of blowdown, the pressure keeps dropping and finally the calculation fails. To avoid this, one makes it a practice in existing LOCA analysis codes after end of blowdown either to calculate with a considerably high value of ECC water enthalpy or to ignore the time derivatives in the flow equations. Since these assumptions are likely to lead to incorrect conclusions, it is needed that a LOCA code is capable of analysis with realistic values for ECC water enthalpy.

(8) Multiple Discharge Tank

Usually, a pressure suppression system is made of a series of discharge tanks. The present version of THYDE-P is not able to simulate such a system, but is equipped with a very simplified container model in terms of Pref(t) and two phase mixture of quality 0.1.

(9) Electric Heater

Electric heater models are needed to analyze behaviors of LOCA experimental facilities, since they are frequently equipped with an electric heater.

9. References

(1) Y. Asahi, "Description of THYDE-P Code (Preliminary Report of Methods and Models)", JAERI-M 7751, July 1978

(2) T. Shimooke, et al., private communication

(3) "WREM : Water Reactor Evaluation Model (Revision 1)", NUREG-75/056, USNRC, May 1975

(4) T.A. Porsching et al., "FLASH-4 : A Fully Implicit FORTRAN IV Program for the Digital Simulation of Transients in a Reactor Plant", WAPD-TM-840, Bettis Atomic Power Laboratory (March, 1969)

10. Acknowledgment

The authors would like to express their sincere thanks to Dr. K. Sato, Chief of Reactor Safety Code Development Laboratory, whose considerations have enabled the authors to conduct this work efficiently. Their thanks are also due to the members of Systems Section, Nuclear Energy Systems Development Department, FUJITSU LIMITED, who gave a number of proper suggestions in performing the computer calculation.

9. References

(1) Y. Asahi, "Description of THYDE-P Code (Preliminary Report of Methods and Models)", JAERI-M 7751, July 1978

(2) T. Shimooke, et al., private communication

(3) "WREM : Water Reactor Evaluation Model (Revision 1)", NUREG-75/056, USNRC, May 1975

(4) T.A. Porsching et al., "FLASH-4 : A Fully Implicit FORTRAN IV Program for the Digital Simulation of Transients in a Reactor Plant", WAPD-TM-840, Bettis Atomic Power Laboratory (March, 1969)

10. Acknowledgment

The authors would like to express their sincere thanks to Dr. K. Sato, Chief of Reactor Safety Code Development Laboratory, whose considerations have enabled the authors to conduct this work efficiently. Their thanks are also due to the members of Systems Section, Nuclear Energy Systems Development Department, FUJITSU LIMITED, who gave a number of proper suggestions in performing the computer calculation.

Appendix A THYDE-P Inputs Requirements

In the following, requirements for noding, control cards, data deck organization, input data cards and problem restart are presented.

A.1 Noding

When we intend to use THYDE-P, first of all we have to reticulate the plant by means of nodes and junctions according to the THYDE-P network theory[1]. It is required that the network has at least one mixing junction except for the core heatup calculation mode and that a normal node without heat source (or sink) must be placed at both the top and bottom ends of the core. After reticulating the plant, we have to number the nodes and junctions separately, strictly in numeric order in accordance with the following rules:

(a) Normal nodes (except linkage nodes) should be numbered in numeric order chain-wise from a mixing junction to a mixing junction according to the direction of the steady state chain flow.

(b) Linkage nodes should be numbered after all the other normal nodes and in numeric order from the corresponding mixing junction.

(c) Special nodes should be numbered after all the normal and linkage nodes.

(d) Normal and break junctions should be numbered first. Then mixing junctions should come. After them, injection junctions should be numbered.

(e) In the present version of THYDE-P, it is required that either of the hot leg nodes adjacent to the upper plenum mixing junction must be numbered as one and that the upper plenum should be numbered first among the mixing junctions.

A.2 Control Cards

Control cards for execution and tape manipulation are computer system dependent so that they will not be discussed in detail. General tape input and output needed are as follows.

Input File (Plot-Restart File):

This file contains information from a previous run that is to be

restarted. Restart information is presented in section A.5.

Output File:

The output file to be generated will be a plot-restart file if requested by the file control variable on the data block BB01 for the Problem Dimension Data.

A.3 Data Deck Organization

A THYDE-P data deck, ending with the terminator card, could contain more than one problem, each of which consists of a title card, data cards and the sub-terminator card. The terminator is a card whose first 4 columns are punched as BEND, while the subterminator is the identification card for dummy data block 99. A listing of the data cards is printed at the beginning of each THYDE-P problem.

A block identification card is placed for the top of each data block and is punched in the first 4 columns as BBXX, where XX indicates the data block number. If the block XX has more than one sub-block, a sub-block identification card must be placed at the top of each data sub-block and will be punched in the first 6 columns as BBXXYY where YY indicates the sub-block number starting with 01.

A.4 Data Card Summary

In the following description of the data cards, the data block number is given along with a descriptive title of the data block and the number of the sub-blocks. Then, the order of the data (1,2,.....), the variable name, the format (I,R or A) and the input data description are given where applicable. The format of the field, integer, real or floating, or alphanumeric is indicated by I, R, or A, respectively. Table data should be given as follows. First, the number of points must be given. Then as many sets of the independent and dependent variables as the point number must be inputted.

Reading input cards is performed solely by the free-format input routime REAG(2).

Data block number	(no block number)
Number of sub-blocks	
Descriptive title of data block	Problem Title

Order	Variable name	Format	Range	Input data description
1	ITITLE	A4		Problem title
				The problem title must be punched in columns 1 to 72 on an IBM card.

Data block number	BB01
Number of sub-blocks	1
Descriptive title of data block	Problem Dimension Data

Order	Variable name	Format	Range	Input data description
1	NMODL	I	0 ~ 2	Caculation mode (1)
2	LDMP	I	0 ~	File Control (2)
3	NEDI	I	0 ~ 9	Number of minor edit variables desired
4	NTC	I	1 ~ 20	Number of time step controls
5	NTRP	I	1 ~ 20	Number of trip controls
6	NVOL	I	1 ~ 100	Number of normal and special nodes
7	NJUNC	I	1 ~ 100	Number of junctions (including break and injection junctions)
8	NMIX	I	0 ~ 20	Number of mixing junctions
9	NPINJ	I	0 ~ 10	Number of pumped injection flows
10	NPUMP	I	0 ~ 4	Number of pumps
11	NACCUM	I	0 ~ 4	Number of accumulators
12	NSG	I	0 ~ 4	Number of steam generators
13	NSGT	I	0 ~ 10	Maximum number of SG nodes per unit
14	NCORE	I	3 ~ 50	Number of axial fuel nodes
15	NR	I	0 ~ 50	Number of radial fuel nodes
16	NF	I	0 ~ 50	Number of radial pellet nodes

(1) NMODL = 0 ; standard mode
1 ; core heatup mode
2 ; loop hydraulics mode

(2) LDMP = 0 ; no file used
N ; restart at restart number N using the file on FORTRAN Unit 3

Data block number	BB02
Number of sub-blocks	1
Descriptive title of data block	Minor Edit Variable Data

Order	Variable name	Format	Range	Input data description
1	AAA⌐XX	A4		
⎛	⎛	⎛		
NED1	BBB⌐YY	A4		

(a) Data block BB02 is required if NED1 is greater than zero. This data block specifies the variables to be edited in the minor edits. NED1 specifications must be inputted. Each specification consists of an alphanumeric entry and an integer entry as shown above, in which

AAA～BBB ; are variable symbols to be edited, and

XX～YY ; (1) is set equal to the number if the variable refers to a node except core nodes,

(2) is the number in numeric order from the bottom core node if the variable refers to a core node, and

(3) is the primary node number for HT1 and HT2.

(b) Symbols of available minor edit variables

Symbol	Variable (with reference to normal node)
PRA	Pressure at point A
PRE	Pressure at point E
GLA	Mass velocity at point A
GLE	Mass velocity at point E
HLA	Specific enthalpy at point A
HLE	Specific enthaopy at point E
RHA	Density at point A
RHE	Density at point E
XLA	Quality at point A
XLE	Quality at point E
ALA	Void fraction at point A
ALE	Void fraction at point E
QQQ	Power density
TMP	Temperature

Symbol	Variable (with reference to injection)
JMI	Injection flow rate

Symbol	Variable (with reference to pump)
HDP	Pump head
AAA	Relative pump speed
BBB	Relative pump torque
WWW	Relative volumetric flow rate
PEY	Pump eye pressure
XEY	Pump eye quality
HEY	Pump eye specific enthalpy

Symbol	Variable (with reference to accumulator)
PAC	Nitrogen pressure
GAJ	Mass flow rate
HAC	Water specific enthalpy
VAG	Nitrogen volume
VAL	Water volume
XAC	Phase indix

Symbol	Variable (with reference to SG secondary system)
PSG	Pressure
MUG	Feed water flow
MRG	Relief flow
MSG	Spray line flow
IVG	Phase index
HS1	Specific enthalpy of region I
HS2	Specific enthalpy of region II
MG1	Mass of region I
MG2	Mass of region II
HT1	Heat transfer coefficient of primary side
HT2	Heat transfer coefficient of secondary side

Symbol	Variable (with reference to pressurizer)
PPP	Pressure
GPR	Surge flow rate
MRP	Relief flow rate
MSP	Spray line flow
ISV	Phase index
HP1	Specific enthalpy of region I
HP2	Specific enthalpy of region II
MS1	Mass of region I
MS2	Mass of region II

Symbol	Variable (with reference to fuel)
QCR	Relative power
PG1	Gap pressure of rod 1
PG2	Gap pressure of rod 2
HC1	Heat transfer coefficient of rod 1
HC2	Heat transfer coefficient of rod 2
HG1	Gap conductivity of rod 1
HG2	Gap conductivity of rod 2
LI1	Thickness of zircaloy reacted at the clad inner surface of rod 1
LI2	Thickness of zircaloy reacted at the clad inner surface of rod 2
LO1	Thickness of zircaloy reacted at the clad outer surface of rod 1
LO2	Thickness of zircaloy reacted at the clad outer surface of rod 2
QM1	Metal-water heat production rate of rod 1
QM2	Metal-water heat production rate of rod 2
TS1	Fuel rod surface temperature of rod 1
TS2	Fuel rod surface temperature of rod 2
TC1	Fuel rod center temperature of rod 1
TC2	Fuel rod center temperature of rod 2

Data block number	BB 03
Number of sub-blocks	NTC
Descriptive title of data block	Time Step Control Sequence Data

Order	Variable name	Format	Range	Input data description
1	NMIN	I	1 ～ 1000	Number of DELTM's per minor edit
2	NMAJ	I	1 ～ 1000	Number of minor edits per major edit
3	NDMP	I	0 ～100	Number of major edits per restart file edit
4	NCHK	I	0, 1	Option for time step control NCHK = {0 time step control 1 no time step control
5	DELTM	R	0. ～	Maximum time step size (sec)
6	DTMIN	R	0.~DELTM	Minimum time step size (sec)
7	TLAST	R	0. ～	End of control by this subblock data
8	EPSMX	R	0. ～ 1.0	Maximum allowable relative increment except for G

Data block number	BB 04
Number of sub-blocks	NTRP
Descriptive title of data block	Trip Control Data

Order	Variable name	Format	Range	Input data description
1	IDTRP	I	-10 ～ -10	Action to be taken(1)
2	IZ	I	0 ～ NVOL	Location where action is to be taken(2)
3	IDSIG	I	±1 ～	Signal being compared to trigger the action(3)
4	IX	I	0～NVOL	Location where signal IDSIG belongs(4)
5	SETPT	R		Setpoint for signal IDSIG
6	DELAY	R	0.0 ～	Delay time for initiation of action after reaching setpoint (sec)

(1) IDTRP = ±1 ; end of problem
±2 ; locking of pump rotor
±3 ; scram
±4 ; pumped injection
±5 ; SG feedwater stop
±6 ; pressurizer heater off

If IDTRP is positive, the corresponding trip is in action.

Otherwise, it is out of action.

(2) IZ = { node number for |IDTRP| = 2 and 5
injection number NOPINJ (see BB09) for |IDTRP| = 4
heater number (see BB14) for |IDTRP| = 6

(3) IDSIG = { 1 ; time
2 ; pressure
3 ; temperature

(4) IX can not refer to any junction, but only to nodes.
IX is the node number where signal IDSIG belongs. IX is set equal to 0 when IDSIG = 1.

Data block number	BB05
Number of sub-blocks	1
Descriptive title of data block	Data for Steady State Adjustment of Loop Hydraulics

Order	Variable name	Format	Range	Input data description
1	IVOL	I	1～NLOOP	Node number (1)
2	G^A	R	0.0 ～	G at point A (Kg/m^2/sec)
3	h^A	R	0.0 ～	h at point A (Kcal/Kg)

(1) In the present version, it is imperative to set IVOL = 1.

Data block number	BB 06
Number of sub-blocks	NLOOP
Descriptive title of data block	Normal or Linkage Node Data

Order	Variable name	Format	Range	Input data description
1	NOV	I	1～NLOOP	Node number
2	IVTYP	I	1～9	Node type
3	IW1	I	1～NJUNC	From-junction number
4	IW2	I	1～NJUNC	To-junction number
5	IQ	I	0,1	With (IQ=1) and without (IQ=0) heat source or sink
6	P^A or k	R	0. ～	Initial pressure (ata) for IVTYP≠13 or loss coefficient for IVTYP=13
7	D_h	R	0. ～	Hydraulic diameter (m)
8	L	R	0. ～	Node length (m)
9	L_H	R	-50.～50.	Height of point E with reference to point A (m)

Note: (1) The input data D_h (order 7) for core normal nodes are dummy. They are set by data block BB16.

(2) Node type IVTYP should be given as follows:

IVTYP =
- 1 ; duct
- 2 ; core
- 3 ; core bypass
- 4 ; downcomer
- 5 ; lower plenum
- 6 ; upper head
- 7 ; SG primary duct (U-tube)
- 8 ; pump
- 9 ; orifice
- 13 ; linkage duct

Node types 3 to 6 may be 1, while node type 13 must be distingished from node type 1.

Data block number	BB 07
Number of sub-blocks	NJUNC
Descriptive title of data block	Junction Data

Order	Variable name	Format	Range	Input data description
1	NOJUNC	I	1～NJUNC	Junction number
2	IJTYP	I	1～7	Junction type(1)
3	VJUNC	R	0.～	Junction volume (m^3)

(1) IJTYP = 1 ; normal junction

2 ; upper plenum

3 ; downcomer top

4 ; mixing junction

5 ; accumulator injection junction

6 ; pressurizer injection junction

7 ; pumped injection junction

(IJTYP = 2 and 3 can be replaced by IJTYP = 4.)

Data block number	BB 08
Number of sub-blocks	NMIX
Descriptive title of data block	Mixing Junction Data

Order	Variable name	Format	Range	Input data description
1	NOMIX	I	1～NJUNC	Junction number
2	NOUT	I	1～4	Number of outgoing flows at steady state
3	JOUT1	I	1～NVOL	To-node number (1)
4	JOUT2	I	1～NVOL	To-node number (2)
5	JOUT3	I	1～NVOL	To-node number (3)
6	JOUT4	I	1～NVOL	To-node number (4)
7	OMAS1	R	0.～1.0	Fraction of rate of outgoing flow (1) at steady state
8	OMAS2	R	0.～1.0	Fraction of rate of outgoing flow (2) at steady state
9	OMAS3	R	0.～1.0	Fraction of rate of outgoing flow (3) at steady state
10	OMAS4	R	0.～1.0	Fraction of rate of outgoing flow (4) at steady state
				Note : Data (3,4,5,6) must correspond to data (7,8,9,10), respectively.

Data block number	BB 09
Number of sub-blocks	NPINJ
Descriptive title of data block	Pumped Injection Data

Order	Variable name	Format	Range	Input data description
1	NOPINJ	I	1∼NPINJ	Number of pumped injection
2	IJ	I	1∼NJUNC	Number of injection junction
3		R		dummy
4		R		dummy
5	h^{INJ}	R	0.0 ∼	Specific enthalpy of injected water (Kcal/Kg)
6	ρ^{INJ}	R	0.0 ∼	Density of injected water (Kg/m^3)
7	IPUMPI	I	1 ∼	Table points number for time vs. m^{INJ} curve
	(Feed IPUMPI pairs of the following inputs.)			
	t	R	0. ∼	time (sec.)
	m^{INJ}	R	0. ∼	Pumped injection flow (kg/sec)

Data block number	BB 10
Number of sub-blocks	NPUMP
Descriptive title of data block	Pump Data

Order	Variable name	Format	Range	Input data description
1	NOVOL	I	1～NVOL	Node number
2	IPTABL	I	1～NPUMP	Number of Table Group to be used
3	Ω_r	R	0. ～	Rated pump speed (rpm)
4	W_r	R	0. ～	Rated flow (m^3/sec)
5	$\mathcal{T}_r$	R	0. ～	Rated torque ($Kg \cdot m^2/sec^2/rad$)
6	H_{head_r}	R	0. ～	Rated head (m)
7	ρ_{f_r}	R	0. ～	Rated density (Kg/m^3)
8	$\Omega(0)$	R	0.～	Initial pump speed (rpm)
9	I_m	R	0. ～	Moment of inertia (kgm^2/rad^2)
10	k1	R	0. ～	Coefficient of angular momentum equation (See Eq.(2-3-51) in Ref.(1))
11	k2	R	0. ～	Coefficient of angular momentum equation (See Eq.(2-3-51) in Ref.(1))

Data block number	BB11 (contined)
Number of sub-blocks	less than or equal to NPUMP
Descriptive title of data block	Pump Characteristic Curves Data

Order	Variable name	Format	Range	Input data description
	w/a	R	-1.～ 1.	$W\Omega_r/(W_r\Omega)$
	$\mathcal{T}^F_\Omega$	R		Torque-discharge curve for positive speed
	$\mathcal{T}^R_\Omega$	R		Torque-discharge curve for negative speed
IV	IP4	I	1 ～	Table points number of torque-speed curves
	(Feed IP4 sets of the following inputs.)			
	a/w	R	-1.～1.	$\Omega W_r/(W\Omega_r)$
	$\mathcal{T}^F_W$	R		Torque-speed curve for forward flow
	$\mathcal{T}^F_W$	R		Torque-speed curve for reverse flow
V	IP5	I	1 ～	Table points number of time vs. electric torque
	(Feed IP5 sets of the following inputs.)			
	t	R	0. ～	time
	$\mathcal{T}_e/\mathcal{T}_r$	R		Electric torque relative to the rated value
VI	IP6	I	1 ～	Table points number of caviation effect curve
	(Feed IP6 pairs of the following inputs.)			
	x_{eye}	R	0.～1.	Eye quality

Data block number	BB 11 (continued)
Number of sub-blocks	less than or equal to NPUMP
Descriptive title of data block	Pump Characteristic Curves Data

Order	Variable name	Format	Range	Input data description
	σ	R	0.	Cavitation effect on pump head
VII	$(IP7)_a$	I	1 ~	Number of values considered for a in $NPSH_r$ table
	$(IP7)_w$	I	1 ~	Number of values considered for w in $NPSH_r$ table
	(First, feed the following $(IP7)_a$ data.)			
	a(1)	R		Values of relative pump speed for which $NPSH_r$ is to be given
	⟨	⟨		
	$a((IP7)_a)$	R		
	(Rpeat the following set of inputs for J = 1,2,...$(IP7)_w$.)			
	w(J)	R		Value of w for which $NPSH_r$ is given
	$NPSH_r$(w(J),a(1))	R		Required net positive suction head table as a function of a (= a(1), a(2),... a$(IP7)_a$) when w = w(J).
	⟨	⟨		
	$NPSH_r$(w(J),a($(IP7)_a$))	R		

Data block number	BB11
Number of sub-blocks	less than or equal to NPUMP
Descriptive title of data block	Pump Characteristic Curves Data

Order	Variable name	Format	Range	Input data description
1	NPTB	I	1～NPUMP	Table group number
I	IP1	I	1 ～	Table points number of head-discharge curves
	(Feed IP1 sets of the following inputs.)			
	w/a	R	-1.～1.	$W\Omega_r/(W_r\Omega)$
	H_Ω^F	R		Head-dischrge curve for positive speed
	H_Ω^R	R		Head-discharge curve for negative speed
II	IP2	I	1 ～	Table points number for head-speed curve
	(Feed IP2 sets of the following inputs.)			
	a/w	R	-1.～1.	$\Omega W_r/(W\Omega_r)$
	H_W^F	R		Head-speed curve for forward flow
	H_W^R	R		Head-speed curve for reverse flow
III	IP3	I	1 ～	Table points number of torque-discharge curve
	(Feed IP3 sets of the following inputs.)			

Data block number	BB 12
Number of sub-blocks	NACCUM
Descriptive title of data block	Accumulator Data

Order	Variable name	Format	Range	Input data description
1	NOV	I	1∼NVOL	Node number
2	IJUNC	I	1∼NJUNC	Injection junction number
3	$V_L(0)$	R	0. ∼	Initial water volume (m^3)
4	$V_G(0)$	R	0. ∼	Nitrogen gas volume (m^3)
5	$h_L(0)$	R	0. ∼	Initial specific enthalpy of water (Kcal/Kg)
6	$P_G(0)$	R	0. ∼	Initial pressure (ata)
7		R		dummy
8		R		dummy
9		R		dummy
10		R		dummy
11		R		dummy
12	c_{ACD}	R	0.11∼1.	$h_{ACD}(0)/h_{fs}(P_G(0))$
13	V_{ACD}	R	0. ∼	Dact volume from accumulator to check valve (m^3)

Data block number	BB 13
Number of sub-blocks	1
Descriptive title of data block	Break Description Data

Order	Variable name	Format	Range	Input data description
1	NBREAK	I	1∼NJUNC	Break junction number
2	TBRK	R	0. ∼	Break time (sec)
3	τ	R	0. ∼	Decay constant of pressure of break junction (sec)
4	C_2	R	0. ∼	See Eq.(2-1-35) of Ref.(1)
5	C_D	R	0. ∼	Discharge coefficient (critical flow)
6	C_{eff}	R	0. ∼	Discharge coefficient (inertial flow)
7	C_2	R	0.∼ 1.0	See Eq.(2-1-35) of Ref.(1)
8	C_D	R	0. ∼	Discharge coefficient (critical flow)
9	C_{eff}	R	0. ∼	Discharge coefficient (inertial flow)
10	IP	I	1 ∼	Table points number for time vs. container pressure curve
	(Feed IP pairs of the following inputs.)			
	t	R	0. ∼	Time (sec)
	P_{ref}	R	0. ∼	Container pressure (ata)

Note : Data 4 to 6 are associated with the from-junction of one of the two break nodes, while data 7 to 9 are associated with the to-junction of the other break nodes.

Data block number	BB 14
Number of sub-blocks	1
Descriptive title of data block	Pressurizer Data

Order	Variable name	Format	Range	Input data description
1	NOV	I	1∼NVOL	Node number
2	IJ	I	1∼NJUNC	Injection number
3	NSP	I	1∼NVOL	Number of node to which point L' (see Fig.2-3-3 of Ref.(1)) belongs
4	A_T	R	0. ∼	Pressurizer cross-section (m^2)
5	H_T	R	0. ∼	Pressurizer height (m)
6	A_{sp}	R	0.∼	Cross-section of spray line (m^2)
7	L_1	R	0. ∼	Length of heater 1 (m)
8	L_2	R	0. ∼	Length of heater 2 (m)
9	L_3	R	0. ∼	Length of heater 3 (m)
10	b_1	R	0. ∼	See Fig.3-2-2 of Ref.(1).
11	b_2	R	0. ∼	
12	b_3	R	0. ∼	
13	$Z_w(0)$	R	0. ∼	Initial water level (m)
14	$\alpha_1(0)$	R	0.∼1.0	Initial void fraction of region 1 (m)
15		R		dummy
16		R		dummy
17	P_{set}	R	0. ∼	Setpoint of relief valve (ata)
18		R		dummy
19	τ_{sub}	R	0. ∼	Heater time constant when coolant is subcooled (sec)

Data block number	BB 14 (continued)
Number of sub-blocks	1
Descriptive title of data block	Pressurizer Data

Order	Variable name	Format	Range	Input data description
20	τ_{sat}	R	0. ~	Heater time constant when coolant is saturated (sec)
21	τ_{sup}	R	0. ~	Heater time constant when coolant is superheated steam (sec)
22		R		dummy
23		R		
24		R		
25		R		
26		R		
27		R		
28		R		
29	L_{IN}	R	0. ~	Length of stand pipe (m)
30		R		dummy
31		R		
32	A_{re}	R	0. ~	Cross-sectional area of relief line (m^2)
33	IP	I	1 ~	Table points number for time vs heater outputs
	(Feed IP sets of the following inputs.)			
	t	R	0. ~	Time (sec)
	G_1	R	0. ~	Relative power input to heater 1
	G_2	R	0. ~	Relative power input to heater 2

Data block number	BB 14 (continued)
Number of sub-blocks	1
Descriptive title of data block	Pressurizer Data

Order	Variable name	Format	Range	Input data description
33	G_3	R	0. ~	Relative power input to heater 3

Note : Data (7,8,9) must correspond to data (10,11,12), respectively.

Data block number	BB 15
Number of sub-blocks	NSG
Descriptive title of data block	Steam Generator Data

Order	Variable name	Format	Range	Input data description
1	NOV	I	1∼NVOL	Node number
2	NTUBE	I	1∼2000	Number of U-tubes
3	NSGS	I	1∼NVOL	Number of inlet node for SG primary flow
4	NSGE	I	1∼NVOL	Number of outlet node for SG primary flow
5	NSGN	I	1∼NSGT	Number of SG primary nodes
6	NREF	I	1∼5	Numbers of relief values in turbine steam supply flow
7	A_T	R	0.∼	SG vessel cross-section (m^2)
8	H_T	R	0.∼	SG vessel height (m)
9	A_s-line	R	0.∼	Cross-sectional area of turbine steam supply line (m)
10		R		dummy
11	l_{pu}	R	0.∼	U-tube pitch
12	R_{SGou}	R	0.∼	U-tube outer radius (m)
13	l_{TSG}	R	0.	Wetted perimeter of SG vessel (m)
14	$Z_w(0)$	R	0.∼	Initial water level (m)
15	$h_{su}(0)$	R	0.∼	Initial specific enthalpy of feedwater (Kg/Kcal)
16		R		dummy
17		R		dummy

Data block number	BB 15 (continued)
Number of sub-blocks	NSG
Descriptive title of data block	Steam Generator Data

Order	Variable name	Format	Range	Input data description
18		R		dummy
19	P(0)	R		Initial pressure of SG secondary system (ata)
20		R		}
21		R		
22		R		} dummy
23		R		
24		R		}
25-1	$\phi_{SG}(1,0)$	R	(negative)	Initial heat flux of node NSGS ($Kcal/m^2/sec$)
25-2	$\phi_{SG}(2,0)$	R	(negative)	Initial heat flux of node NSGS+1 ($Kcal/m^2/sec$)
⌇	⌇	⌇	⌇	
⌇	⌇	⌇	⌇	
25-NSGN	$\phi_{SG}(NSGN,0)$	R	(negative)	Initial heat flux of node NSGE ($Kcal/m^2/sec$)
(Repeat the following data set for relief flow NREF times.)				
26-1	A_{re}	R	0. ~	Cross-sectional area of relief line (m^2)
26-2	P_{set}	R	0. ~	Setpoint for relief valve (ata)

Data block number	BB 15 (continued)
Number of sub-blocks	NSG
Descriptive title of data block	Steam Generator Data

Order	Variable name	Format	Range	Input data description
26-3	C_2	R	0.~1.0	See Eq.(2-1-27) of Ref.(1)
26-4	C_D	R	0. ~	Discharge coefficient (critical flow)
26-5	C_{eff}	R	0. ~	Discharge coefficient (inertial flow)
27	IP	I	1	Table points number of time vs. SG secondary flow
	(Feed IP sets of the following inputs.)			
	t	R	0. ~	Time (sec)
	$R_{m_{su}}$	R	0. ~	Relative feed water flow
	$R_{h_{su}}$	R	0. ~	Relative feed water specific enthalpy
		R		Dummy

Note : Input functions $R_{m_{su}}$ and $R_{h_{su}}$ (and a dummy function) describes the feed water behaviors up to container isolation. Since the time of container isolation is not known in advance, but depends on the situation, it would be necessary to give $R_{m_{su}}$ and $R_{h_{su}}$ for a sufficiently long time.

Data block number	BB 16
Number of sub-blocks	
Descriptive title of data block	Core Data

Order	Variable name	Format	Range	Input data description
1	NRODS	I	1～50000	Number of fuel rods
2	NCL	I	1～NVOL	Number of core bottom node
3	NCH	I	1～NVOL	Number of core top node
4	IEM	I	0, 1	Option for calculation mode IEM=0 Best estimate model =1 Evaluation model
5	T_o	R	0. ～	Reactor operating time before LOCA (hour)
6	r_{NF}	R	0.～1	Fuel rod outer radius (m)
7	$r_{NR}-r_{cl}^{in}$	R	0.～1	Clad thickness (m)
8	r_{NF}	R	0.～1	Pellet radius (m)
9	ℓ_p	R	0.～1	Fuel rod pitch (m)
10	BLMINI	R	0.～1	Minimum blockage
11	ℓ	R	0. ～	Neutron lifetime (sec)
12	λ_i	R	0. ～	Decay constant of delayed neutron precursor of i-th group (1/sec) (i=1,2 ・・・・・6)
13	β_i	R	0. ～	Delayed neutron fraction of i-th group
14	τ	R	0. ～	See below.
15	C_R	R	0. ～	Conversion ratio
16	λ_1	R	0. ～	Decay constant for U^{239} (1/sec)

Data block number	BB 16 (continued)
Number of sub-blocks	1
Descriptive title of data block	Core Data

Order	Variable name	Format	Range	Input data description
17	λ_2	R	0. ~	Decay constant for N_p^{239}
18	Σ_a/Σ_f	R	0. ~	See Eqs.(3-1-5) and (3-1-6) of Ref.(1)
19		R		Dummy
(Repeat inputs 20 to 22, NCORE times (J = NCL to NCH.))				
20	$\phi_0(J)$	R	0. ~	Initial heat flux (Kcal/m^2/sec)
21	$\ell_1(J)$	R	0. ~	Initial thickness of zircaloy reacted for rod 1 (m)
22	$\ell_2(J)$	R	0. ~	Initial thickness of zircaloy reacted for rod 2 (m)

Note: (1) After neutron density becomes sufficiently small, it will be made to vanish with a time constant, which is to be specified by τ (input order 14).

Data block number	BB17
Number of sub-blocks	1
Descriptive title of data block	Reactivity Data

Order	Variable name	Format	Range	Input data description
1	IP1	I	1 ~	Table points number for void fraction vs. void coefficient
	(Feed IP1 sets of the following inputs.)			
	α	R	0. ~	Void fraction
	γ_α	R		Void coefficient ($)
2	IP2	I	1 ~	Table poits number for temperature vs. temperature coefficient curve
	(Feed IP2 sets of the following inputs.)			
	T	R	0. ~	Temperature (°c)
	γ_T	R	0. ~	Temperature coefficient ($/°C)
3	IP3	I	1 ~	Table points number of time vs. external reactivity curve
	(Feed IP3 sets of the following inputs.)			
	t	R	0. ~	time (sec)
	R_{ex}	R		External reactivity ($)

Data block number	BB 18
Number of sub-blocks	1
Descriptive title of data block	Metal-water Leaction Data

Order	Variable name	Format	Range	Input data description
1	Δh_{reac}	R	0. ~	Heat of metal-water reaction (Kcal/Kg)
2	k_1	R	0. ~	Coefficient of Eq.(3-1-7) in Ref. (1) (m^2/sec)
3	k_2	R	0. ~	Coefficient of Eq.(3-1-7) in Ref.(1) (°k)

Data block number	BB 19
Number of sub-blocks	1
Descriptive title of data block	Gap Conductivity Data

Order	Variable name	Format	Range	Input data description
1	N	R	0. ~	Mols of gas in pin
2	P_{gc}	R	0. ~	Contact pressure (ata)
3	y_{He}	R	0. ~	Molecular fraction of helium in gap
4	y_{xe}	R	0. ~	Molecular fraction of xenon in gap
5	y_{kr}	R	0. ~	Molecular fraction of kripton in gap
6	y_{air}	R	0.	Molecular fraction of air in gap
7	y_{N_2}	R	0. ~	Molecular fraction of nitrogen in gap
8	y_{H_2}	R	0. ~	Molecular fraction of hydrogen in gap
9	y_{H_2O}	R	0. ~	Molecular fraction of water in gap
10	V_{pl}	R	0. ~	Plenum gas volume (m^3)
11		R		dummy
12		R		
13		R		
14	C_T	R	0. ~	Cons. in Eq.(3-3-29) in Ref.(1) (°C)
15	ε_{NF}	R	0. ~	Fuel pellet emissivity
16	ε_{cl}	R	0. ~	Fuel clad emissivity
17	FRASM	R	0. ~	Mean free path (m)

Data block number	BB 21
Number of sub-blocks	1
Descriptive title of data block	Clad Burst Description Data

Order	Variable name	Format	Range	Input data description
1	N_i	I		# of non-burst diagonal rods
2	M_i	I		# of non-burst off-diagonal rods
3	A	R		
4	C	R		
5	B	R		See Eq.(4-1-11) of Ref.(1)
6	D	R		
7	E	R		
8	A_0	R		
9	A_1	R		
10	A_2	R		See Eq.(4-1-14) of Ref.(1)
11	A_3	R		
12	A_4	R		
13	A	R		See Eq.(4-1-13) of Ref.(1)
14	B	R		

Data block number	BB 22
Number of sub-blocks	1
Descriptive title of data block	Miscellaneous Data

Order	Variable name	Format	Range	Input data description
1		R		dummy
2	γ_{H_2O}	R	0. ~	Isentopic exponent of water
3	γ_{N_2}	R	0. ~	Isentropic exponent of nitrogen
4	HTRCON	R	0. ~	Constant for reflood calculation

A.5 Input for Restarting

An old restart data file to be used must be mounted on FORTRAN Unit 3 and a blank file must be mounted on Unit 2. A new plot-restart file will be generated on Unit 50.

THYDE-P is used with the following input definitions.

Problem Dimension Data BB01

LDMP = a positive integer

NEDI ; can be changed.

NTC ; can be changed.

NTRP ; must be equal to the value at the previous run.

The others must be set equal to the values at the previous run.

Minor Edit Variable Data BB02

The quantities being edited on the new run need not have any relation to those of the original run. The same rules apply as for the original problem.

Time Step Control Sequence Data BB03

TLAST ; must be greater than the time at which the present run starts. The same rules as for the original problem apply to the rest of the variables.

Trip Control Data BB04

Data block BB04 must not be changed only with the following exception. For the sub-block corresponding to IDTRP = 1, the value for SETPT must be greater than that of the previous run.

The other data block need not be inputted except the terminator card and the dump card.

Appendix B. Input Data List of Run 10

```
 --  BLOWDOWN  AND  CORE REFLOOD TEST  (RUN 10) ---  APR.79( HIRANO )     DDD00010
BB01                                                                     DDD00020
     0    0    9   3   16   32   27   4   1   2   1   2   3   3   5   3  DDD00030
BB02                                                                     DDD00040
PRE-08  PRA-09  GLE-21  GLA-21  GLE-25  GLE-26  GLA-01  PRE-08  PRA-09   DDD00050
BB03                                                                     DDD00060
SB0301                                                                   DDD00070
       30    2   10    0    1.E-3    1.E-6      0.3    0.1               DDD00080
SB0305                                                                   DDD00090
       30    2   20    0    4.E-3    1.E-6     90.0    0.1               DDD00100
SB0308                                                                   DDD00110
       40    1    1    0    4.E-3    1.E-6   2000.0    0.1               DDD00120
BB04                                                                     DDD00130
SB0480                                                                   DDD00140
        1    0    1    0   1000.0    0.0                                 DDD00150
SB0481                                                                   DDD00160
        5   29    1    0     0.4     0.0                                 DDD00170
SB0482                                                                   DDD00180
        5   30    1    0     0.4     0.0                                 DDD00190
SB0483                                                                   DDD00200
        2    8    1    0     0.1     0.0                                 DDD00210
SB0484                                                                   DDD00220
        2   17    1    0     0.1     0.0                                 DDD00230
SB0485                                                                   DDD00240
        3    0    1    0     0.3     0.0                                 DDD00250
SB0486                                                                   DDD00260
        4    1    1    0    28.0     0.0                                 DDD00270
SB0487                                                                   DDD00280
       -4    1    1    0   1000.0    0.0                                 DDD00290
SB0490                                                                   DDD00300
        6    1   -3    1    240.0    0.005                               DDD00310
SB0491                                                                   DDD00320
        6    2   -3    1    250.0    0.0                                 DDD00330
SB0492                                                                   DDD00340
        6    3   -3    1    360.0    0.0                                 DDD00350
SB0493                                                                   DDD00360
       -6    1    3    1    350.0    0.0                                 DDD00370
SB0494                                                                   DDD00380
       -6    2    3    1    305.0    0.0                                 DDD00390
SB0495                                                                   DDD00400
       -6    3    3    1    380.0    0.0                                 DDD00410
SB0496                                                                   DDD00420
        6    2   -2    1    160.0    0.0                                 DDD00430
SB0497                                                                   DDD00440
       -6    2    2    1    190.0    0.0                                 DDD00450
BB05                                                                     DDD00460
        1  9000.0  360.0                                                 DDD00470
BB06                                                                     DDD00480
SB0601                                                                   DDD00490
        1    1   21    1    0   158.420   0.736    5.25    0.0           DDD00500
SB0602                                                                   DDD00510
        2    1    1    2    0   158.575   1.920    1.665   0.0           DDD00520
SB0603                                                                   DDD00530
        3    7    2    3    1   158.502   0.02     5.0     5.0           DDD00540
SB0604                                                                   DDD00550
        4    7    3    4    1   157.947   0.02     5.0     4.0           DDD00560
SB0605                                                                   DDD00570
        5    7    4    5    1   157.454   0.02     9.0    -9.0           DDD00580
SB0606                                                                   DDD00590
        6    1    5    6    0   157.814   1.9215   1.664  -1.0           DDD00600
SB0607                                                                   DDD00610
        7    1    6    7    0   157.476   0.787    7.33    0.0           DDD00620
```

```
SB0608                                                                  DDD00630
         8       8       7       8       0     154,872    0,4945    12,39      0,0    DDD00640
SB0609                                                                  DDD00650
         9       1       8      22       0     161,630     0,699     6,288     0,0    DDD00660
SB0610                                                                  DDD00670
        10       1      21      23       0     158,420    1,2748     4,857     0,0    DDD00680
SB0611                                                                  DDD00690
        11       1      23       9       0     158,575     3,327     1,665     0,0    DDD00700
SB0612                                                                  DDD00710
        12       7       9      10       1     158,502      0,02       5,0       5,0    DDD00720
SB0613                                                                  DDD00730
        13       7      10      11       1     157,947      0,02       5,0       4,0    DDD00740
SB0614                                                                  DDD00750
        14       7      11      12       1     157,454      0,02       9,0      -9,0    DDD00760
SB0615                                                                  DDD00770
        15       1      12      13       0     157,814    3,3281     1,664     -1,0    DDD00780
SB0616                                                                  DDD00790
        16       1      13      14       0     157,476    1,3631      7,33      0,0    DDD00800
SB0617                                                                  DDD00810
        17       8      14      15       0     154,872    0,8565     12,39      0,0    DDD00820
SB0618                                                                  DDD00830
        18       1      15      24       0     161,630    1,2107    2,7046     0,0    DDD00840
SB0619                                                                  DDD00850
        19       1      24      22       0     161,368    1,2107     3,144     0,0    DDD00860
SB0620                                                                  DDD00870
        20       4      22      16       0     161,575     1,777     4,577    -4,577  DDD00880
SB0621                                                                  DDD00890
        21       5      16      17       0     161,400     5,544      1,02       0,3    DDD00900
SB0622                                                                  DDD00910
        22       2      17      18       0     161,295       1,0       0,3       0,3    DDD00920
SB0623                                                                  DDD00930
        23       2      18      19       1     160,860       1,0       3,0       3,0    DDD00940
SB0624                                                                  DDD00950
        24       2      19      21       0     159,440       1,0       0,3       0,3    DDD00960
SB0625                                                                  DDD00970
        25      13      23      20       0         1,0       0,3      15,0      15,0    DDD00980
SB0626                                                                  DDD00981
        26      13      20      27       0         1,0       0,3      15,0      15,0    DDD00982
SB0627                                                                  DDD00983
        27      13      24      25       0        10,0    0,2447       1,0       1,0    DDD00984
SB0628                                                                  DDD00985
        28      13      24      26       0        10,0     0,223       1,0       1,0    DDD00986
BB07                                                                    DDD01230
         1       1     0.0                                              DDD01240
         2       1     0.0                                              DDD01250
         3       1     0.0                                              DDD01260
         4       1     0.0                                              DDD01270
         5       1     0.0                                              DDD01280
         6       1     0.0                                              DDD01290
         7       1     0.0                                              DDD01300
         8       1     0.0                                              DDD01310
         9       1     0.0                                              DDD01320
        10       1     0.0                                              DDD01330
        11       1     0.0                                              DDD01340
        12       1     0.0                                              DDD01350
        13       1     0.0                                              DDD01360
        14       1     0.0                                              DDD01370
        15       1     0.0                                              DDD01380
        16       1     0.0                                              DDD01390
        17       1     0.0                                              DDD01400
        18       1     0.0                                              DDD01410
        19       1     0.0                                              DDD01420
        20       1     0.0                                              DDD01430
        21       4    41.4                                              DDD01440
        22       4   9.068                                              DDD01450
        23       4     0.5                                              DDD01460
        24       4   0.504                                              DDD01470
        25       7      0.                                              DDD01480
        26       5      0.                                              DDD01490
        27       6      0.                                              DDD01500
```

```
BB08                                                                    DDD01600
SB0801                                                                  DDD01610
        21    2    1   10    0    0    0.25    0.75    0.    0.         DDD01620
SB0805                                                                  DDD01630
        22    1   20    0    0    0    1.0     0.0     0.    0.         DDD01640
SB0806                                                                  DDD01650
        23    2   11   25    0    0    1.0     0.0     0.    0.         DDD01660
SB0807                                                                  DDD01670
        24    3   19   27   28    0    1.0     0.0     0.    0.         DDD01680
BB09                                                                    DDD01710
SB0901                                                                  DDD01720
        1     25      0.0     0.047     50.0     1000.0                 DDD01730
        2                                                               DDD01740
        0.0   600.0   1000.0  600.0                                     DDD01750
BB10                                                                    DDD01760
SB1001                                                                  DDD01770
    8  1  1185.0  5.58   4.33E4  100.0  749.0  1150.0  3460.0 -0.5  0.0 DDD01780
SB1002                                                                  DDD01790
   17  1  1185.0 16.74   4.33E4  100.0  749.0  1150.0  3460.0 -0.5  0.0 DDD01800
BB11                                                                    DDD01810
SB1101                                                                  DDD01820
 1                                                                      DDD01830
 14                                                                     DDD01840
 -1.0  1.56  0.18  -0.85 1.33  0.34  -0.80 1.28  0.40  -0.72 1.30 0.48  DDD01850
 -0.62 1.35  0.556 -0.50 1.36  0.67  -0.34 1.34  0.77  -0.21 1.29 0.84  DDD01860
  0.75 1.07  1.62   1.0  0.98  1.94   0.25 1.16  1.16   0.50 1.13 1.35  DDD01870
 11                                                                     DDD01880
 -1.0  0.18  1.56  -0.75 -0.13 1.12  -0.50 -0.32 0.90  -0.32 -0.40 0.82 DDD01890
 -0.16 -0.42 0.76   0.0  -0.39 0.71   0.16 -0.28 0.71   0.32  0.16 0.76 DDD01900
  0.50  0.01 0.90   0.75 0.40  1.33   1.0   0.98 1.94                   DDD01910
 14                                                                     DDD01920
 -1.0  0.70 -1.42  -0.90 0.70 -1.32  -0.80 0.68 -1.23  -0.70 0.63 -1.14 DDD01930
 -0.60 0.53 -1.07  -0.50 0.47 -0.99  -0.40 0.46 -0.91  -0.30 0.45 -0.84 DDD01940
 -0.20 0.45 -0.77   0.0  0.48 -0.64   0.25 0.55 -0.49   0.50 0.66 -0.34 DDD01950
  0.75 0.83 -0.20   1.0  1.02 -1.10                                     DDD01960
   13                                                                   DDD01970
 -1.0 -1.42 0.70 -0.8 -1.12 0.5 -0.6 -0.82 0.4 -0.5 -0.68 0.39          DDD01980
 -0.4 -0.55 0.38 -0.2 -0.28 0.33 0.0 -0.08 0.28 0.11 0.0 0.25           DDD01990
  0.25 0.12 0.22  0.50 0.33 0.14 0.75 0.61 0.03 0.92 0.82 0.01          DDD02000
  1.0  1.02 -0.10                                                       DDD02010
  2                                                                     DDD02020
  0.0 1.0  1000.0  0.5                                                  DDD02030
  2                                                                     DDD02040
  -1.0  -50.0  1.0  50.0                                                DDD02050
  6  6                                                                  DDD02060
  0.0  0.2  0.4  0.6  0.8  1.0                                          DDD02070
  0.0  0.0  0.0  0.0  0.0  0.0  0.0                                     DDD02080
  0.2  0.0  3.065E-5  7.7239E-5  1.3263E-4  1.9460E-4  2.6207E-4       DDD02090
  0.4  0.0  4.866E-5  1.2261E-4  2.1053E-4  3.0996E-4  4.1602E-4       DDD02100
  0.6  0.0  6.376E-5  1.6066E-4  2.7587E-4  4.0485E-4  5.4514E-4       DDD02110
  0.8  0.0  7.7239E-5 1.9463E-4  3.3419E-4  4.9044E-4  6.6037E-4       DDD02120
  1.0  0.0  8.9628E-5 2.2585E-4  3.8780E-4  5.6910E-4  7.6631E-4       DDD02130
BB12                                                                    DDD02140
SB1201                                                                  DDD02150
       32   26   70.   30.   50.9   40.  0.  0.  0.  0.  0.            DDD02160
     0.9   3.0                                                          DDD02170
BB13                                                                    DDD02180
   8  2.001E-3  0.4  0.8  0.6  0.6  0.8  0.6  0.6                       DDD02190
   6                                                                    DDD02200
   0.0 1.0  7.5  2.7  15.  3.0  30.  3.0  60.  3.0  1000.  3.0          DDD02210
BB14                                                                    DDD02220
   31       27       19       3.58   15.56   0.1                      DDD02230
   0.915    0.915    0.915    1.525   3.05   4.58   9.0   0.99   157.0 DDD02240
   0.0     50.0   0.8   5.0   20.0  2.0  0.0  0.0  0.564  0.67  0.619  DDD02250
   0.47     0.    1.    10.   10.   1.0                                 DDD02260
   2                                                                    DDD02270
   0.       1.0  1.0   1.0  1000.  1.0  1.0  1.0                       DDD02280
                                                                        DDD02290
```

```
BB15                                                                    DDD02300
SB1501                                                                  DDD02310
   29    4000     3     5     3     1                                   DDD02320
   8.55  12.0  0.7  0.0001   3.0E-2  1.0E-2    10.4    4.0   180.  0.  DDD02330
   0.    0.05 45.0  0.1      0.564   0.619      0.47   0.963           DDD02340
 -60.  -65.  -70.                                                       DDD02350
   0.001      80.   0.5      0.5     0.5                               DDD02360
   3                                                                    DDD02370
   0.0  1.0  1.0  1.0  1.0  1.0  1.0  1.0  1000.0  1.0  1.0  0.0       DDD02380
SB1502                                                                  DDD02390
   30    12000  12   14    3     1                                     DDD02400
   25.65  12.0  2.1  0.0001   3.0E-2  1.0E-2    10.4    4.0   180.  0.  DDD02410
   0.     0.05 45.0  0.1      0.564   0.619      0.47   0.963           DDD02420
 -60.  -65.  -70.                                                       DDD02430
   0.003      80.   0.5      0.5     0.5                               DDD02440
   3                                                                    DDD02450
   0.0  1.0  1.0  1.0  1.0  1.0  1.0  1.0  1000.0  1.0  1.0  0.0       DDD02460
BB16                                                                    DDD02470
  40000  22          24          1                                     DDD02480
  9000.0  5.36E-3    0.620E-3  4.69E-3   1.42E-2    0.6   1.0E-4       DDD02490
  0.0124  0.0212E-02 0.0305    0.1402E-02                              DDD02500
  0.111   0.1254E-02 0.301     0.2529E-02                              DDD02510
  1.13    0.0736E-02 3.00      0.0269E-02                              DDD02520
  5.0     0.6        4.91E-04  3.41E-06  1.2        1.54E03           DDD02530
  0.0             2.08E02    0.0                                       DDD02540
  1.6122E-07      6.8E-07    1.622E-07                                 DDD02550
  1.6122E-07      6.8E-07    1.622E-07                                 DDD02560
BB17                                                                    DDD02570
    3                                                                   DDD02580
  0.0  0.0  0.5  -1.0  1.0  -5.0                                        DDD02590
    5                                                                   DDD02600
  20.0    0.1   300.0   0.0   1500.0   -0.1   2500.  -0.2   4500.  -1.0 DDD02610
    5                                                                   DDD02620
   0.0    0.0    1.0    -0.1    1.5.   -0.2   2.0   -3.0   1000.  -8.0 DDD02630
BB18                                                                    DDD02640
   1.54E03    0.775E-04     2.29E04                                     DDD02650
BB19                                                                    DDD02660
   0.0301     0.0  0.9495   0.0157   0.0028   0.0   0.032   0.0   0.0  DDD02670
   1.235E-05  0.0  0.0      0.0      0.0      0.6   0.6     0.0        DDD02680
BB21                                                                    DDD02690
  2  2   5.0E7     6.96E-08 2.87E4    2.86E-03  1.15E0   1.528E0        DDD02700
         1.49E-07  2.0E-08  1.25E-16  1.85E-01  8.0E09   3.3E-03        DDD02710
BB22                                                                    DDD02720
   0. 1.4  1.4  0.                                                      DDD02730
BEND                                                                    DDD09000
   0  0  0  0     0  0.                                                 DDD09010
```

Appendix C Appendices A and B References

(1) Y. Asahi, "Description of THYDE-P Code (Preliminary Report of Methods and Models)", JAERI-M 7751, July 1978

(2) K. Asai and K. Tsuchihashi, "A Subroutine Reading Data in Free Format (in Japanese)", JAERI-M 4458, May 1971